



Universiteit
Leiden
The Netherlands

Small changes for long term impact : optimization of structure kinetic properties : a case of CCR2 antagonists

Vilums, M.

Citation

Vilums, M. (2014, November 20). *Small changes for long term impact : optimization of structure kinetic properties : a case of CCR2 antagonists*. Retrieved from <https://hdl.handle.net/1887/29811>

Version: Corrected Publisher's Version

License: [Licence agreement concerning inclusion of doctoral thesis in the Institutional Repository of the University of Leiden](#)

Downloaded from: <https://hdl.handle.net/1887/29811>

Note: To cite this publication please use the final published version (if applicable).

Cover Page



Universiteit Leiden



The handle <http://hdl.handle.net/1887/29811> holds various files of this Leiden University dissertation.

Author: Vilums, Maris

Title: Small changes for long term impact : optimization of structure kinetic properties : a case of CCR2 antagonists

Issue Date: 2014-11-20

SMALL CHANGES FOR LONG TERM IMPACT

OPTIMIZATION OF STRUCTURE KINETIC PROPERTIES:

A CASE OF CCR2 ANTAGONISTS

Cover design: Māris Viļums
Thesis layout: Māris Viļums
Printed in the Netherlands

© Copyright, Māris Viļums, 2014

All rights reserved. No part of this book may be reproduced in any form or by any means without permission of the author.

SMALL CHANGES FOR LONG TERM IMPACT

OPTIMIZATION OF STRUCTURE KINETIC PROPERTIES:

A CASE OF CCR2 ANTAGONISTS

PROEFSHRIFT

ter verkrijging van

de graad van Doctor aan de Universiteit Leiden,
op gezag van Rector Magnificus prof. dr. C.J.J.M. Stolker,
volgens besluit van het College voor Promoties
te verdedigen op donderdag 20 November 2014
klokke 15.00 uur

door

Māris Viļums

geboren te Riga, Latvia
in 1985

PROMOTIECOMMISSIE

Promotor: Prof. Dr. A.P. IJzerman

Copromotor: Dr. L.H. Heitman

Overige leden: Prof. P. H. van der Graaf
Prof. G. van der Marel
Prof. G. Duburs (Latvian Institute of Organic Synthesis, Latvia)
Prof. H. van Vlijmen
Dr. John Saunders
Dr. Dean Stamos (Vertex Pharmaceuticals Inc., USA)

The research described in this thesis was performed at the Division of Medicinal Chemistry of the Leiden Academic Centre for Drug Research (formerly: Leiden/Amsterdam Centre for Drug Research), Leiden University (Leiden, The Netherlands). The research was financially supported by the Dutch Top Institute Pharma, project number D1-301.

*Man's mind,
once stretched by a new idea,
never regains its original dimensions.*
Oliver Wendell Holmes, Sr. (1809–1894)

to my children

CONTENTS

CHAPTER 1 GENERAL INTRODUCTION	9
CHAPTER 2 INDANES – PROPERTIES, PREPARATION, AND PRESENCE IN LIGANDS FOR G PROTEIN- COUPLED RECEPTORS	21
CHAPTER 3 STRUCTURE–KINETICS RELATIONSHIPS – AN OVERLOOKED PARAMETER IN HIT-TO-LEAD OPTIMIZATION: A CASE OF CYCLOPENTYLAMINES AS CCR2 ANTAGONISTS	63
CHAPTER 4 WHEN STRUCTURE–AFFINITY RELATIONSHIPS MEET STRUCTURE–KINETICS RELATIONSHIPS: 3-((INDEN-1-YL)AMINO)-1-ISOPROPYL-CYCLOPENTANE-1-CARBOXAMIDES AS CCR2 ANTAGONISTS	85
CHAPTER 5 EVALUATION OF (4-ARYLPIPERIDIN-1-YL)CYCLOPENTANECARBOXAMIDES AS HIGH AFFINITY AND LONG RESIDENCE TIME ANTAGONISTS FOR THE CCR2 RECEPTOR	119
CHAPTER 6 DESIGN AND SYNTHESIS OF NOVEL SMALL MOLECULE CCR2 ANTAGONISTS: EVALUATION OF 4-AMINOPIPERIDINE DERIVATIVES	143
CHAPTER 7 CONCLUSIONS AND FUTURE PERSPECTIVES	161
SUMMARY	175
SAMENVATTING	177
LIST OF PUBLICATIONS	181
AFTERWORD	183

CHAPTER 1

GENERAL INTRODUCTION

ABOUT THIS THESIS

This thesis focuses on a new approach in drug discovery, the so-called drug-target residence time. Next to more traditional drug discovery efforts, which are based on structure-affinity relationships, this thesis describes the use of an additional parameter – the structure-kinetic relationships. Knowledge of this additional parameter at the early stages of drug discovery may help the pharmaceutical industry to generate better drug candidates. Additionally, it could save big expenses in the later stages of drug discovery by minimizing the attrition rate of drug candidates due to efficacy problems. In more detail, this thesis focuses on the synthesis of new high affinity and long residence time small molecule antagonists for the chemokine receptor CCR2 - a potential target for the treatment of various inflammatory diseases.

THE BEGINNINGS OF DRUG DISCOVERY

Already in the early days of human civilization men used different plants as healing agents. These early drugs were most probably discovered through trial and error experimentation by observing the reactions of human and animal as a result of consumption of such products. Folk medicines derived from these “clinical trials” were the only available treatments until recent times. Scientific techniques in drug discovery started to emerge only in the late 1800s. Oswald Schmiedeberg was one of the first scientists to describe the correlation between the chemical structure of substances and their effectiveness.¹ It was an early attempt to describe structure-activity relationships (SAR). At the beginning of the 1900s chemical methods were developed to produce synthetic drugs, marking the beginnings of pharmaceutical industry.

DRUG DISCOVERY AND DEVELOPMENT

With the increasing knowledge and understanding of diseases, scientists started to hypothesize that modulation of a specific biological target may have therapeutic value in the treatment of a disease. This was the beginning of a paradigm shift in drug discovery from

“trial and error experiments” to “rational drug design”. In rational drug design, the biological target must fulfill two criteria. First, modulation of a given biological target must show evidence of therapeutic value. Second, the target must be “druggable”, i.e. the target is able to bind to a small molecule and the small molecule can modulate the target’s activity. When a suitable target is identified, the search for small molecules that bind to the target can begin. In pharmaceutical industry such small molecules (‘hit’ compounds) usually are found by screening libraries of potential drug compounds in high-throughput screening assays of the desired targets. Another option is to perform a virtual screening of libraries, if the structure of the target is available. Binding affinity is the main criterion in these screenings. Afterwards, the affinity of the initial hits is improved through further synthetic efforts and structure-affinity relationships are generated, a concept that was already used in the 19th century. After this ‘lead’ identification comes the lead optimization process in which a drug candidate is generated. Ideally, the drug candidate should not only have good binding affinity for the target, but also be “drug-like”. It should possess properties that are predicted to lead to adequate chemical and metabolic stability, oral bioavailability and minimal toxicity, which in turn would result in a safe and efficacious drug. However, these characteristics are still difficult to optimize using rational drug design techniques. So, often scientists are forced to return to the “trial and error” experimentation in the late stages of the drug development process. A survey of phase II clinical trials in 2008 - 2010 done by Thomson Reuters² revealed that less than a fifth (18%) of phase II clinical trials were successful. Half of the reported failures were due to insufficient efficacy and another fifth due to safety concerns (Figure 1). This indicates that more predictive models in earlier stages of drug development are still needed.

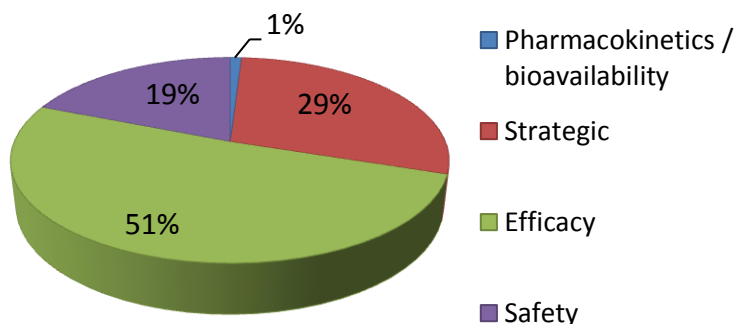


Figure 1. Phase II failures: 2008 – 2010. The failures are divided according to failure reasons. Adopted from Arrowsmith, 2011.²

RESIDENCE TIME IN DRUG DISCOVERY

As mentioned above, in current drug discovery the lead compounds are selected based on their affinity towards the desired target. Usually, affinity is determined using e.g., a radioligand displacement assay, which is an *in vitro* experiment based on binding equilibrium between a known radioligand and the compound in question. However, in the human body the concentrations of the drug and the endogenous competitor are constantly changing. Therefore, affinity that has been determined *in vitro* under equilibrium conditions does not necessarily translate in *in vivo* efficacy. To tackle the efficacy issue we need to improve and optimize the drug candidates on additional parameters. The past few years witnessed an increased interest in a new parameter, the so called drug-target residence time. More and more evidence suggests that drug efficacy may be associated with the time the drug remains on its target.^{3,4} Copeland et al⁵ already demonstrated that the drug–target residence time is, in some cases, a better predictor of *in vivo* efficacy than the binding affinity. However, it depends on the physiological context and the nature of drug–target interactions whether a long or short residence time is needed to yield a better drug. Thus the additional knowledge of drug-target residence time already at the early stage of drug development could help to

address the afore mentioned efficacy problem, thus potentially decreasing the attrition rate of drug candidates in the more expensive phase II clinical trials.

CHEMOKINES, CHEMOKINE RECEPTORS

Chemokines (chemoattractant cytokines) are a family of small and structurally similar proteins of 70-120 amino acids (MW = 8-14 kDa).⁶⁻⁸ They were first discovered in 1977⁹ and initially identified as controllers of immune cell migration.⁷ Chemokines are split into two main categories according to their biological actions – the inflammatory chemokines and homeostatic chemokines.¹⁰ The inflammatory chemokines are released under pathological conditions. The concentration gradient of chemokines recruits the immune cells towards the site of inflammation. Homeostatic chemokines are continuously produced and are involved in housekeeping functions such as recruiting leukocytes during hematopoiesis.

The chemokine receptors are members of the G protein-coupled receptor (GPCR) superfamily. This protein family has proven to be one of the most fruitful target classes for therapeutics. It constitutes a class of membrane-bound proteins, with a conserved transmembrane heptahelical fold, which respond to a whole spectrum of different endogenous and synthetic agonist ligands ranging from light and cations, biogenic amines, fragrances, pheromones and lipids to peptides and globular proteins. The whole GPCR family comprises three major classes, termed A, B and C. The chemokine receptors belong to class A GPCRs, also known as rhodopsin-like receptors (after the visual pigment) whose members form the largest group of GPCRs. The axis of chemokines and chemokine receptors mediates a vast number of physiological effects making the receptors of great interest as possible drug targets. However, the development of chemokine receptor antagonists has been very challenging. Only two compounds have successfully completed phase III clinical trials and are now marketed: maraviroc, a CCR5 antagonist for the treatment of HIV/AIDS, and plerixafor, a CXCR4 antagonist for the mobilization of stem cells prior to collection and subsequent transplantation after chemotherapy.

CHEMOKINE RECEPTOR 2 AND THE RATIONALE FOR TARGETING IT IN DISEASE

In the last decade there has been profound interest in the chemokine receptor 2 (CCR2) and its endogenous ligand CCL2 (also known as MCP-1). CCR2 is the only characterized high affinity receptor for CCL2, although CCR2 can be activated by other chemokines (e.g. CCL7, CCL8 and CCL13),¹¹ albeit with lower affinity. Studies of CCR2- and CCL2-deficient animals have revealed the critical role of this axis in monocyte recruitment in a number of inflammatory conditions such as delayed-type hypersensitivity reactions, antigen-induced granuloma formation, non-infectious peritonitis and also in infectious diseases.^{12, 13} Next to monocytes, CCR2 is located also on basophils, activated T cells, NK cells, and dendritic cells.^{11, 14, 15} However, most of the interest in CCR2 antagonism was due to the intention to inhibit monocytes/macrophages and their products, which are thought to be involved in damaging effects of inflammation in a number of disease states (e. g. rheumatoid arthritis (RA), multiple sclerosis (MS), atherosclerosis).¹⁶⁻¹⁸ Early studies showed TAK-779 (Figure 2), a small molecule CCR2 antagonist, inhibited collagen-induced arthritis.¹⁹ Additionally, use of the CCR2 antagonist INCB3344 (Figure 2) showed improvement in adjuvant-induced arthritis in rats.²⁰ Recently Lebre et al.²¹ described that blockade of CCR2 with an antibody prevented monocyte chemotaxis when it was induced by CCL2, however, it failed when chemotaxis was induced with synovial fluid, suggesting that CCR2 is the wrong target for the treatment of RA. Also in the case of MS, blockade of CCR2 drew a lot of enthusiasm. The preclinical data supported the role of the CCR2/CCL2 axis in a mouse model of MS with experimental autoimmune encephalitis.¹⁷ However, CCR2 antagonist MK-0812 (Figure 2), which worked in the murine model, failed in a phase II clinical trial due to lack of efficacy.

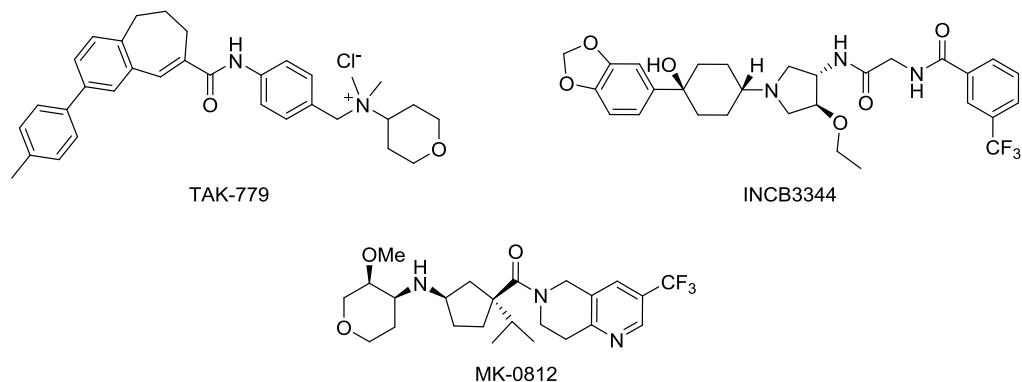


Figure 2. CCR2 antagonists.

Additionally, humanized anti-CCR2 antibody (MLN-1202) did not show efficacy in clinical trials of rheumatoid arthritis or multiple sclerosis.²² Another victim of the efficacy problem was AZD-2423 (a potent, orally bioavailable, non-competitive, negative allosteric modulator of the CCR2 chemokine receptor) which failed in a clinical trial of posttraumatic neuralgia.²³ However, many other preclinical studies indicated promise in asthma,²⁴ metabolic disease,²⁵ fibrosis, pain,^{26, 27} and COPD.²⁸ Hence, the development of new efficacious CCR2 antagonists is warranted.

AIM AND CONTENT

In the previous sections, a short history on the evolution of the drug discovery process was presented with a further emphasis on the more recent challenges in the development of efficacious treatments for CCR2-related diseases. Modern drug discovery has evolved tremendously to understand the molecular causes of different diseases and how these can be treated. However, the 21st century drug discovery of new treatments is still mostly based on the principles suggested in the 19th and 20th century, for example the strict focus on target affinity. This is a very important parameter indeed as a drug can be effective only when it is bound to its target. It is, however, not the only criterion to yield a successful drug. Several CCR2 antagonists, all with high binding affinity, were discussed as examples of failures due to efficacy issues. These are only a few out of many failures that we cannot afford to have,

especially in the late and costly clinical stages of the drug discovery process. We made a plea to consider at least one other parameter, i.e. residence time. Thus, the aim of this thesis is to develop a path towards high affinity and long residence time (RT) CCR2 antagonists in the very early stages of drug discovery, thus helping to proceed in the next phases of drug development with potentially better drug candidates.

In **chapter 2** we review the literature on a chemical substructure that proved to be important in our work. It is the indane ring system and we analyzed its properties, preparation, and presence in ligands for GPCRs. We then describe our subsequent discovery of new indane-containing CCR2 antagonists (**chapter 3**). The additional knowledge of the binding kinetics of several known CCR2 antagonists allowed us to reevaluate and choose a structure for further optimizations that other researchers had abandoned due to it having only modest binding affinity. The decision to determine in parallel both affinity and RT yielded the discovery of new high affinity and long residence time CCR2 antagonists. Furthermore (**chapter 4**), the indane containing CCR2 antagonists went into another cycle of optimization based on affinity and RT and yielded compounds with even longer RT.

Chapter 5 describes the structure-kinetic relationship for CCR2 receptor antagonists based on derivatives of MK-0483, a CCR2 antagonist from Merck, Inc. with slow binding kinetics. The structure of MK-0483 was altered step by step to reveal the crucial structural components that yield the long RT for the CCR2 receptor.

Chapter 6 describes our medicinal chemistry efforts to explore chemical space even more and develop CCR2 antagonists based on a new piperidinediamide scaffold. Series of new structures were synthesized to evaluate SAR of the substituents on the N-piperidinediamide moiety revealing the specificity of substituents and spacer types needed for affinity in the case of this scaffold.

Finally, a general discussion of the results of this thesis and a future outlook of CCR2 antagonists as potential treatments is presented, concluding this thesis.

REFERENCES

1. Schmiedeberg, O. *Grundriss der Arzneimittellehre*. Leipzig : F.C.W. Vogel: Leipzig, 1883.
2. Arrowsmith, J. Phase II failures: 2008-2010. *Nature Reviews Drug Discovery* **2011**, 10, 1-1.
3. Swinney, D. C. The role of binding kinetics in therapeutically useful drug action. *Curr Opin Drug Disc* **2009**, 12, 31-39.
4. Zhang, R. M.; Monsma, F. Binding kinetics and mechanism of action: toward the discovery and development of better and best in class drugs. *Expert Opin Drug Discov* **2010**, 5, 1023-1029.
5. Copeland, R. A. The dynamics of drug-target interactions: drug-target residence time and its impact on efficacy and safety. *Expert Opin Drug Discov* **2010**, 5, 305-310.
6. Onuffer, J. J.; Horuk, R. Chemokines, chemokine receptors and small-molecule antagonists: recent developments. *Trends in Pharmacological Sciences* **2002**, 23, 459-467.
7. Schwarz, M. K.; Wells, T. N. C. New therapeutics that modulate chemokine networks. *Nature Reviews Drug Discovery* **2002**, 1, 347-358.
8. Gao, Z. L.; Metz, W. A. Unraveling the chemistry of chemokine receptor ligands. *Chemical Reviews* **2003**, 103, 3733-3752.
9. Wu, V. Y.; Walz, D. A.; McCoy, L. E. Purification and Characterization of Human and Bovine Platelet Factor-4. *Prep Biochem* **1977**, 7, 479-493.
10. Wagner, W. G.; Roderburg, C.; Wein, F.; Diehlmann, A.; Frankhauser, M.; Schubert, R.; Eckstein, V.; Ho, A. D. Molecular and secretory profiles of human mesenchymal stromal cells and their abilities to maintain primitive hematopoietic progenitors. *Stem Cells* **2007**, 25, 2638-2647.
11. Viola, A.; Luster, A. D. Chemokines and their receptors: Drug targets in immunity and inflammation. *Annu Rev Pharmacol Toxicol* **2008**, 48, 171-197.
12. Kurihara, T.; Warr, G.; Loy, J.; Bravo, R. Defects in macrophage recruitment and host defense in mice lacking the CCR2 chemokine receptor. *Journal of Experimental Medicine* **1997**, 186, 1757-1762.
13. Boring, L.; Gosling, J.; Chensue, S. W.; Kunkel, S. L.; Farese, R. V.; Broxmeyer, H. E.; Charo, I. F. Impaired monocyte migration and reduced type 1 (Th1) cytokine responses in C-C chemokine receptor 2 knockout mice. *Journal of Clinical Investigation* **1997**, 100, 2552-2561.
14. van Helden, M. J. G.; Zaiss, D. M. W.; Sijts, A. J. A. M. CCR2 Defines a Distinct Population of NK Cells and Mediates Their Migration during Influenza Virus Infection in Mice. *Plos One* **2012**, 7.
15. Charo, I. F.; Ransohoff, R. M. The many roles of chemokines and chemokine receptors in inflammation. *The New England journal of medicine* **2006**, 354, 610-21.
16. Ogata, H.; Takeya, M.; Yoshimura, T.; Takagi, K.; Takahashi, K. The role of monocyte chemoattractant protein-1 (MCP-1) in the pathogenesis of collagen-induced arthritis in rats. *The Journal of pathology* **1997**, 182, 106-14.
17. Fife, B. T.; Huffnagle, G. B.; Kuziel, W. A.; Karpus, W. J. CC chemokine receptor 2 is critical for induction of experimental autoimmune encephalomyelitis. *The Journal of experimental medicine* **2000**, 192, 899-905.
18. Dawson, T. C.; Kuziel, W. A.; Osahar, T. A.; Maeda, N. Absence of CC chemokine receptor-2 reduces atherosclerosis in apolipoprotein E-deficient mice. *Atherosclerosis* **1999**, 143, 205-11.
19. Yang, Y. F.; Mukai, T.; Gao, P.; Yamaguchi, N.; Ono, S.; Iwaki, H.; Obika, S.; Imanishi, T.; Tsujimura, T.; Hamaoka, T.; Fujiwara, H. A non-peptide CCR5 antagonist inhibits collagen-induced arthritis by modulating T cell migration without affecting anti-collagen T cell responses. *Eur J Immunol* **2002**, 32, 2124-2132.
20. Brodmerkel, C. M.; Huber, R.; Covington, M.; Diamond, S.; Hall, L.; Collins, R.; Leffert, L.; Gallagher, K.; Feldman, P.; Collier, P.; Stow, M.; Gu, X.; Baribaud, F.; Shin, N.; Thomas, B.; Burn, T.; Hollis, G.; Yeleswaram, S.; Solomon, K.; Friedman, S.; Wang, A.; Xue, C. B.; Newton, R. C.; Scherle, P.; Vaddi, K. Discovery and pharmacological characterization of a novel rodent-active CCR2 antagonist, INCB3344. *Journal of immunology* **2005**, 175, 5370-8.
21. Lebre, M. C.; Vergunst, C. E.; Choi, I. Y. K.; Aarrass, S.; Oliveira, A. S. F.; Wyant, T.; Horuk, R.; Reedquist, K. A.; Tak, P. P. Why CCR2 and CCR5 Blockade Failed and Why CCR1 Blockade Might Still Be Effective in the Treatment of Rheumatoid Arthritis. *PLoS One* **2011**, 6.
22. Kalinowska, A.; Losy, J. Investigational C-C chemokine receptor 2 antagonists for the treatment of autoimmune diseases. *Expert Opin Inv Drug* **2008**, 17, 1267-79.
23. Kalliomaki, J.; Attal, N.; Jonzon, B.; Bach, F. W.; Huizar, K.; Ratcliffe, S.; Eriksson, B.; Janecki, M.; Danilov, A.; Bouhassira, D. A randomized, double-blind, placebo-controlled trial of a chemokine receptor 2 (CCR2) antagonist in posttraumatic neuralgia. *Pain* **2013**, 154, 761-7.

24. Kim, Y. K.; Oh, H. B.; Lee, E. Y.; Gho, Y. S.; Lee, J. E.; Kim, Y. Y. Association between a genetic variation of CC chemokine receptor-2 and atopic asthma. *Allergy* **2007**, *62*, 208-9.
25. Kang, Y. S.; Cha, J. J.; Hyun, Y. Y.; Cha, D. R. Novel C-C chemokine receptor 2 antagonists in metabolic disease: a review of recent developments. *Expert Opin Inv Drug* **2011**, *20*, 745-756.
26. Serrano, A.; Pare, M.; McIntosh, F.; Elmes, S. J. R.; Martino, G.; Jomphe, C.; Lessard, E.; Lembo, P. M. C.; Vaillancourt, F.; Perkins, M. N.; Cao, C. Q. Blocking spinal CCR2 with AZ889 reversed hyperalgesia in a model of neuropathic pain. *Mol Pain* **2010**, *6*.
27. Abbadie, C.; Bhangoo, S.; De Koninck, Y.; Malcangio, M.; Melik-Parsadaniantz, S.; White, F. A. Chemokines and pain mechanisms. *Brain Res Rev* **2009**, *60*, 125-134.
28. Belvisi, M. G.; Hele, D. J.; Birrell, M. A. New anti-inflammatory therapies and targets for asthma and chronic obstructive pulmonary disease. *Expert Opin Ther Tar* **2004**, *8*, 265-285.

CHAPTER 2

INDANES – PROPERTIES, PREPARATION, AND PRESENCE IN LIGANDS FOR G PROTEIN-COUPLED RECEPTORS

This chapter was based upon:

M. Vilums, J. Heuberger, L.H. Heitman, A.P. IJzerman.

(manuscript in preparation)

ABSTRACT

The indane (2,3-dihydro-1*H*-indene) ring system is an attractive scaffold for biologically active compounds due to the combination of aromatic and aliphatic properties fused together in one rigid system. This bicyclic structure provides a wide range of possibilities to incorporate specific substituents in different directionalities, thus being an attractive scaffold for medicinal chemists. Notably, many indane-based compounds are being used in the clinic to treat various diseases, such as indinavir, an HIV-1 protease inhibitor, indantadol, a potent MAO-inhibitor, the amine uptake inhibitor indatraline, and the ultra-long-acting β -adrenoceptor agonist indacaterol. Given the diversity of targets these drugs act on, one could argue that the indane ring system is a privileged substructure, just like indole, the nitrogen atom containing unsaturated version of it. In the present review the synthetic and medicinal chemistry of the indane ring system is described. In more detail, it contains a comprehensive overview of compounds bearing the indane substructure with G protein-coupled receptor (GPCR) activity, with particular emphasis on their structure–activity relationships (SAR).

INTRODUCTION

In the 1920's many compounds containing the 1,3-diketo-group or the enolic form of it were discovered to bear physiological activity, and combining this group with a phenol in the early 1930's resulted in a series of indan-1,3-diones showing bacteriostatic activity.¹ The compounds inhibited the proliferation of gram-positive bacteria and are very early representatives of pharmacologically active molecules based on the 2,3-dihydro-1*H*-indene structure **1** (also known as indane), which is also commonly found in indanones (such as indan-1-one **2**) or indandiones (such as indan-1,3-dione **3**) (Figure 1).

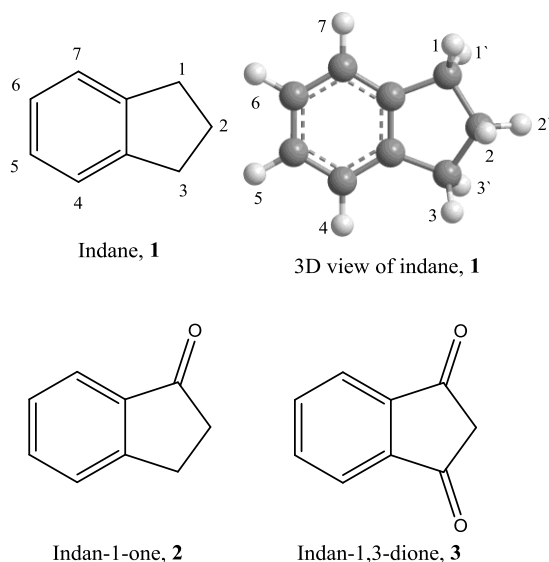


Figure 1. Chemical structures of indane ring system **1**, indan-1-one **2**, indan-1,3-dione **3**.

The indane ring system can be regarded as a fusion product of aromatic benzene and the aliphatic cyclopentane ring in one. This combination provides a broad diversity of chemical entities with indane as a core structure. Many different synthetic methods for the synthesis and diversification of indanes have been reported, which will be described below. Additionally, the ring system can accommodate substituents in six different directions on its aliphatic part and an additional four on the aromatic ring (see Figure 1, 3D view of indane) to add desired properties to such a molecule.

The indane substructure occurs in many natural products like pterosins,² or more hydrogenated forms of it in ionophores such as indanomycin,³ and stawamycin.⁴ This structural motif is also present in many marketed drugs, such as indinavir **4**,⁵ an HIV-1 protease inhibitor, indantadol **5**,⁶ a potent MAO-inhibitor, the amine uptake inhibitor indatraline **6**,⁷ the anti-inflammatory clidnac **7**, antiarrhythmic agent indecainide **8**,⁸ diuretic indacrinone **9**⁹ and the anticoagulant hedulin **10**¹⁰ (Figure 2). Given the big diversity of targets these drugs act on, one could argue that the indane ring system is a “privileged” substructure, just like indole, a nitrogen atom containing unsaturated version of it.¹¹ The activity of indane derivatives in biological systems and the wide variety of their actions make them an interesting moiety for medicinal chemistry.

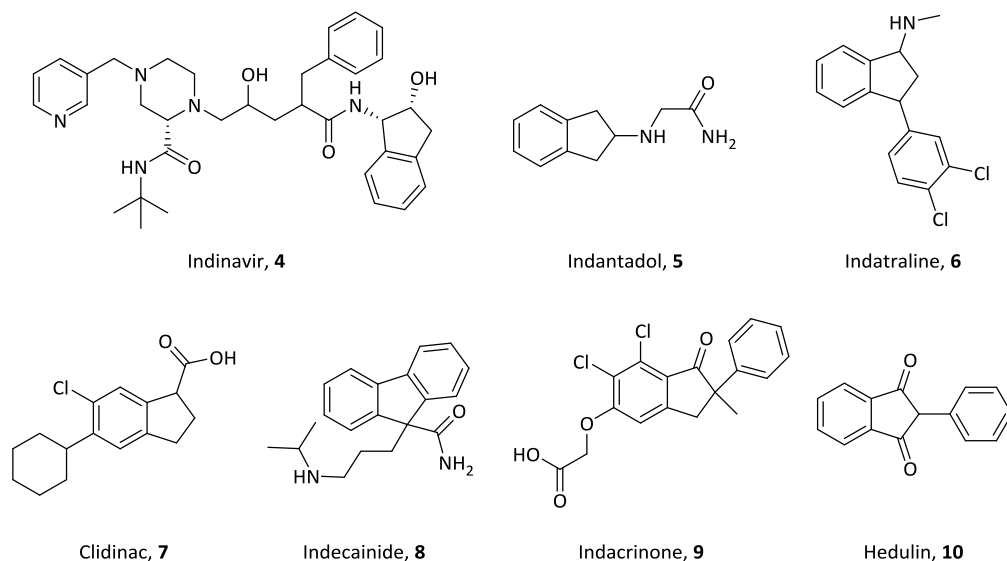


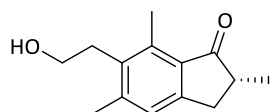
Figure 2. Examples of marketed drugs containing the indane ring system.

In this review, we aim to present the key chemical and pharmacological information on the indane ring system. In more detail, we will look at the activity of indanes on targets that have considerable importance in drug development – G protein-coupled receptors (GPCRs). The report is divided in the following sections: first the preservation and occurrence of the indane scaffold will be shown by discussing some of the natural products that contain this moiety. Additionally, synthetic routes to indanes are described as well as the possibilities of

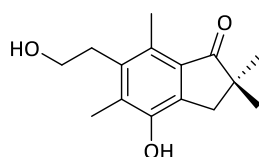
incorporating the indane system into a compound's chemical structure. Finally, an overview is given of compounds bearing the indane substructure with GPCR activity and inferences are made regarding their structure-activity relationships (SAR). This review excludes unsaturated indanes and polycyclic ring systems containing indane (e.g., 9*H*-fluorene, 1,2-dihydroacenaphthylene, indacenes and hydrogenated forms of these). SciFinder and Reaxys databases were used for a literature search based on the indane substructure. To retrieve the relevant literature on indanes with GPCR activity the following terms were used in different combinations as additional filters in the SciFinder database: *target*, *protein*, *G protein-coupled receptor*.

NATURAL OCCURRENCE OF INDANES

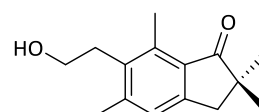
The indane scaffold is present across a wide range of species. One of the largest resources are *Pteridophyta* (ferns). Ferns produce more than 60 different structures that contain the indanone **2** scaffold, called pterosins. The structures and biological properties of these pterosins were first reviewed by Sychina and Semenov.¹² The first identified pterosin is pterosin B **11** (Figure 3) with antimicrobial properties. Other compounds from the pterosin family have also been reported to have biological activity such as cytotoxicity against cancer cell lines¹³ and antidiabetic activity.¹⁴ Some of the pterosins have been used for centuries in oriental medicine like onitin **12**. Ho et al.¹⁵ showed that onitin possesses smooth-muscle relaxant properties, suggested to take place through inhibition of a serotonin 5-HT receptor. More than a decade later Sheridan et al.¹⁶ proposed that pterosin Z **13** (the dehydroxylated form of onitin) is acting through the inhibition of extracellular calcium influx through calcium channels or by interference with the calcium/calmodulin cascade of reactions within the cell.



Pterosin B, **11**



Onitin, **12**



Pterosin Z, **13**

Figure 3. Indane derivatives found in *Pteridophyta*.

The indane system is also found in the stem bark of *Vatica pauciflora* as part of resveratrol oligomers (pauciflorol D and pauciflorol F)¹⁷ where it is formed by polymerization of resveratrol.¹⁸ Recently a new indanone containing compound has been isolated from the roots of *Uvaria afzelii*, named afzeliindanone **14** (Figure 4).¹⁹ Another source of naturally occurring indanes are fungi and bacteria. For example, the fomajorins D **15** and S **16** were isolated from the fungus *Heterobasidion annosum*. Tripartin **17** containing a dichlorinated methyl group and inhibiting histone H3 lysine 9 demethylase (KDM4) was isolated from a culture broth of a *Streptomyces* species associated with larvae of the dung beetle *Copris tripartitus*.²⁰

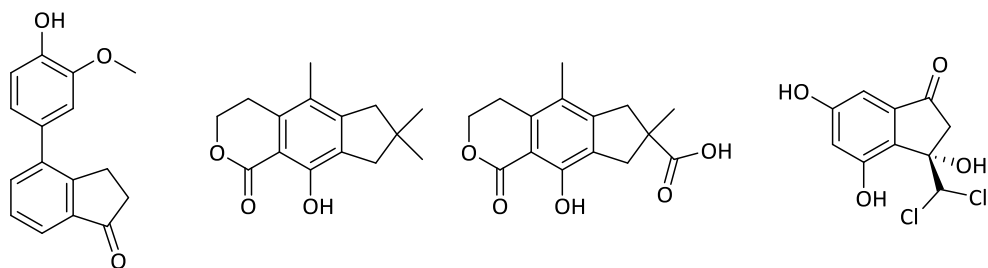
Azeliindanone, **14**Fomajorin D, **15**Fomajorin S, **16**Tripartin, **17**

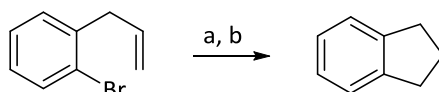
Figure 4. Indane derivatives found in *Uvaria afzelii* (afzeliindanone **14**), *Heterobasidion annosum* (fomajorins D **15** and S **16**), a culture broth of a *Streptomyces* species (tripartin **17**).

SYNTHESIS OF INDANE RING SYSTEM

As mentioned above the indane ring system is present in nature, but before it was identified in natural products, several synthetic routes had already been developed to produce indane-based structures. The first synthesis of an indandione, i.e. **3**, was described by Wislicenus in 1888²¹ and soon after the synthesis of indanone **2** by Gabriel and Hausmann²² and indane **1** by Kramer and Spilker²³ was reported. However, nowadays more recent synthetic approaches are used to obtain indane compounds. The methods described below show different routes how to synthesize, modify and incorporate various substituents on the desired location of the indane ring system.

The unsubstituted indane can be acquired using a palladium-catalyzed cross-coupling reaction with B-alkyl-9-borabicyclo[3.3.1]nonane (Scheme 1) as reported by Miyaura et al.²⁴ A more general method for the formation of different cyclic systems including indane (Scheme 2) was developed by Katritzky et al.²⁵

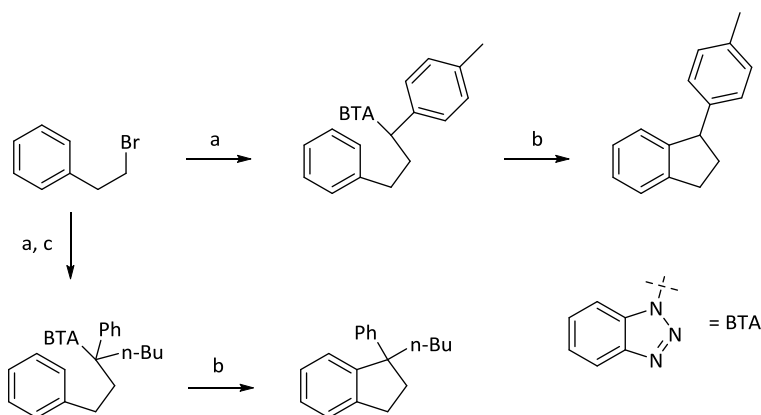
Scheme 1.



a) 9-BBN, THF, 0 °C-rt, 4h; b) PdCl₂(dppf), NaOH 3 equiv.

These authors used (benzotriazol-1-yl)-methanes to act as 1,1-dipole synthon equivalents. With this method 1-monosubstituted or 1,1-disubstituted indanes can be synthesized. However, a significant formation of alkenes was observed during five-membered ring annulations.

Scheme 2.



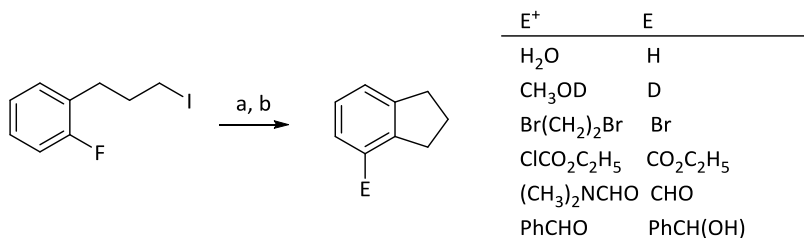
a) i) n-BuLi, 1-benzyl-1H-1,2,3-benzotriazole, THF, -78 °C, 3 h; ii) rt, overnight;

b) i) ZnBr₂, 130 °C, 12 h; ii) 160 °C, 24 h;

c) n-BuLi, n-BuLi, -78 °C, 3 h

Bailey and Longstaff²⁶ reported another method to arrive at the indane ring system and simultaneously incorporated a variety of different electrophiles selectively on the 4 position *via* an organolithium intermediate (Scheme 3).

Scheme 3.

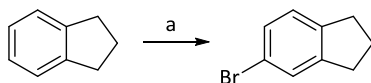


a) t-BuLi 3.2 equiv., n-pentane - Et₂O (4:1), -78 °C, 15 min; b) THF, warm, E⁺

Indanes with substitution on the 5 position are usually acquired either via a direct halogenation (used in the synthesis of mGluR2 modulators)²⁷ (Scheme 4a) or via deoxygenation of 5-substituted indanones (Scheme 4b).²⁸ Mathison et al.²⁹ developed another method (Scheme 5) which allows to introduce an aldehyde group directly on the indane ring where it can be modified further on. However, this method yields a mixture of 4- and 5-substituted indanes in a 1:4 ratio.

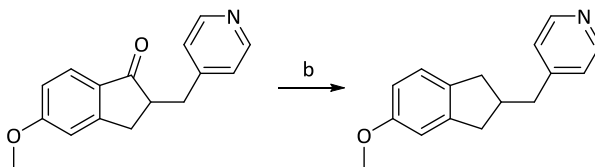
Scheme 4.

a)



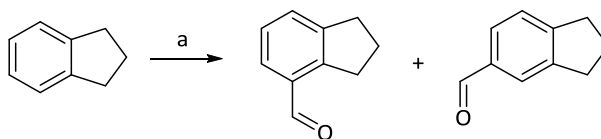
a) Al₂O₃, Br₂, 5 min, yield 33%

b)



b) i) KOH, H₂N-NH₂*H₂O, HO(CH₂)₂OH, reflux, 1.5 h, ii) 195°C, 4 h

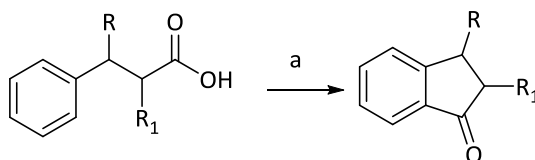
Scheme 5.



a) TiCl_4 , $\text{Cl}_2\text{CHOCH}_3$, 0°C , 30 min, yield: 84% (1:4 ratio)

The indanone structure **2** is much more versatile as a building block in medicinal chemistry. The ketone functional group can be directly used as the reactive center for different modifications or coupling reactions. A typical method for indan-1-one synthesis is based on intramolecular Friedel-Crafts acylation of phenylpropanoic acids. In this approach substituents on the propyl chain are translated into the corresponding 2- or 3-substituents on the indan-1-one. Recently Kangani and Day³⁰ reported conditions in which indan-1-ones are formed in high yields and short reaction times at room temperature in the presence of cyanuric chloride/pyridine/ AlCl_3 (Scheme 6).

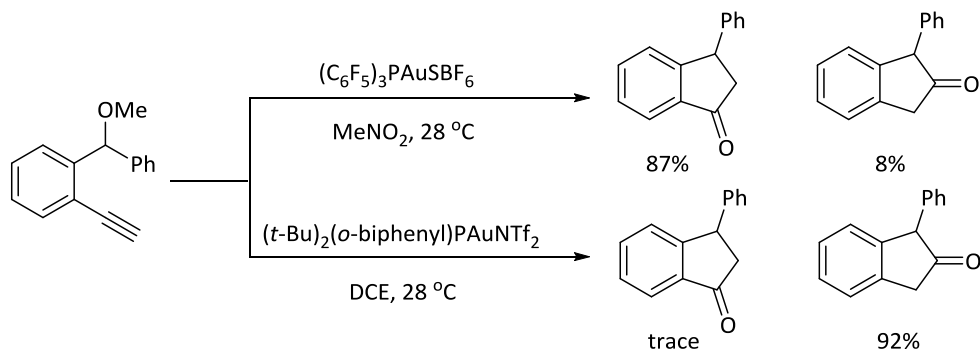
Scheme 6.



a) Cyanuric chloride, AlCl_3 , Py, rt, 25 min

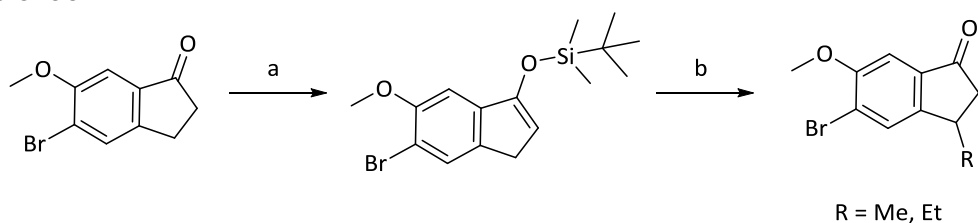
Very recently, Wang et al.³¹ described selective syntheses of indan-1-ones and indan-2-ones from 2-ethynylbenzyl ethers with suitable catalysts and solvents (Scheme 7). Using [tris(pentafluorophenyl)phosphine]gold hexafluoroantimonate $[(\text{C}_6\text{F}_5)_3\text{PAuSbF}_6]$ in nitromethane (MeNO_2) preferably yielded indan-1-ones whereas [(ortho-biphenyl)di(tert-butyl)phosphine]gold triflimide $[(t\text{-Bu})_2(o\text{-biphenyl})\text{PAuNTf}_2]$ in dichloroethane tended to form indan-2-one derivatives.

Scheme 7.



Another method worth mentioning is how to incorporate substituents on 3 position of already made indan-1-ones. Azemi et al. described that 3-(*t*-butyldimethylsilyloxy)indene (generated from indanone) can be selectively deprotonated with lithium diisopropylamide and then reacted with an alkylating agent.³² The silyl ether can be removed by quenching it with acid (Scheme 8). This approach was used by Vilums et al.³³ to generate the desired indanones as building blocks for CCR2 antagonists.

Scheme 8.



a) TBDMS-Cl, DBU, 0 °C-r.t.;

b) i) LDA, 1 h, -78 °C → -35 °C, → -78 °C, 1 h, corresponding alkyl iodide; ii) 12 M HCl.

Incorporation of substituents on the phenyl ring of the indane system is usually done via Friedel–Crafts acylation; however, it can result in mixtures of regioisomers.

INDANES AND G PROTEIN-COUPLED RECEPTORS

In a recent review Garland³⁴ discusses that 26% (437 of 1663) of marketed drugs that are listed in DrugBank are targeting G protein-coupled receptors. However, GPCRs or GPCR

related (e.g., receptor-activity modifying proteins or RAMPs) targets make only 7% (109 of 1479) of all the drugged targets. Apparently, GPCRs are privileged targets. GPCRs are very similar in overall structure, but the binding sites are tailored to accommodate their individual endogenous ligands, and, additionally, synthetic ligands, giving rise to ligand diversity. Ligands containing the indane substructure are among the ones with highest affinities for GPCRs and these are the subject of this review.

TARGETS IN DISEASES OF THE CENTRAL NERVOUS SYSTEM (CNS)

α_2 -Adrenoceptor

Alpha-2 adrenergic receptors (α_2 -adrenoceptors) are involved in several central and peripheral nervous system processes, such as alertness, heart rate regulation, vasomotor control and nociceptive processing. Recent studies suggest that α_2 -adrenoceptors are targets for the treatment of L-dopa-induced dyskinesia in Parkinson's disease. For example, fipamezole **18** (Figure 5) can be co-administered with the anti-parkinsonian drug L-dopa.³⁵ Fipamezole reduces the L-dopa-induced dyskinesia without affecting any other parkinsonian action of the drug; it even elongates the duration of L-dopa's action. It has high affinity for the human α_{2A} ($K_i = 9.2$ nM), α_{2B} ($K_i = 17$ nM), and α_{2C} ($K_i = 55$ nM) receptors, with lower affinity for the GPCRs histamine H_1 and H_3 and the non-GPCR serotonin transporter.³⁶ Its non-fluorinated analogue atipamezole **19**, which is used as an agent in reversing medetomidine-induced sedation-analgesia in veterinary practice, has an approximately 4-fold higher affinity for the α_{2A} ($K_i = 2.2$ nM), α_{2B} ($K_i = 3.9$ nM), and α_{2C} ($K_i = 12$ nM) receptors.

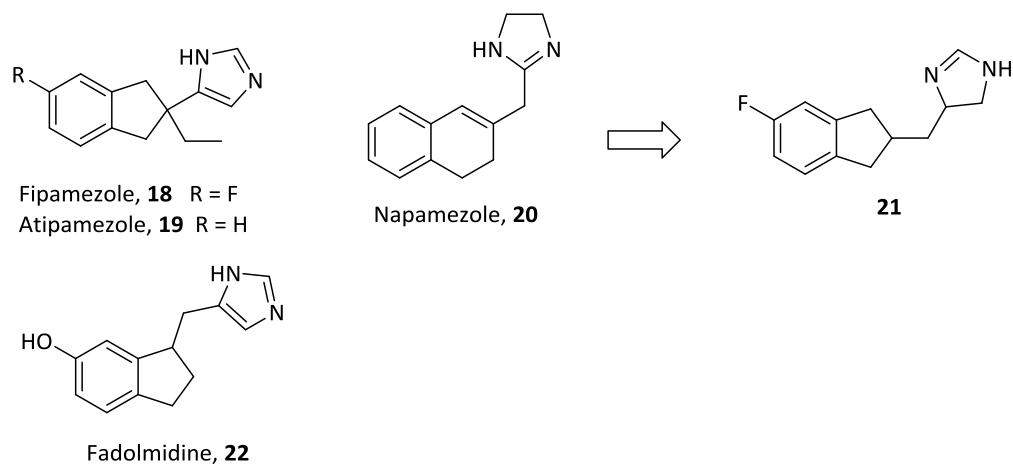


Figure 5. α_2 adrenoceptor ligands.

Another structurally similar α_2 adrenoceptor antagonist was designed to combine the properties of **18** with the monoamine uptake inhibition properties of napamezole **20**, thereby creating anti-depressant effects.³⁷ Compound **21** had the best balance between affinity for α_2 adrenoceptors and serotonin–norepinephrine reuptake inhibitor properties. The change from indane to indene affected only the α_2 adrenoceptors while a further change to benzofuran solely affected the serotonin reuptake inhibition. Additionally, the indane system displayed a much higher affinity (at least 8–fold) for the α_2 adrenoceptor compared to other bicyclic systems such as dihydronaphthalene, naphthalene and tetralin containing the same 4(5)-imidazole substituent.

In contrast to these antagonists, fadolmidine **22** is an agonist of α_2 adrenoceptors³⁸ being developed for post-operative pain treatment (currently phase IIb).³⁹ Structurally, this agonist is very similar to the antagonists with the indane system as a core. The main difference is the position of the imidazole/imidazoline on the cyclopentane ring. The affinity of the compound is similar to that of the antagonists, with 2.5 nM, 0.6 nM and 0.3 nM for the human α_{2A} , α_{2B} and α_{2C} receptors, respectively. Fadolmidine is also a full agonist for α_{1A} and α_{1B} adrenoceptors with EC_{50} values of 22 nM and 3.4 nM, respectively.⁴⁰

Thus, the indane system seems to be a preferred structure for α_2 adrenoceptor affinity and the location of imidazole/imidazoline rings determines the agonistic/antagonistic activity of the structures.

Dopamine Receptors

Central dopaminergic receptors are involved in many CNS diseases such as schizophrenia, depression and Parkinson's disease. The development of drugs targeting this receptor-type has therefore been a goal for several decades.

One of the earlier investigations was performed by Hacksell et al.⁴¹ identifying 4-hydroxy-2-(dipropylamino)indan **23** (Figure 6) as a potent dopamine receptor agonist. When its biochemical and behavioral effects in rats and emesis in dogs were measured, this compound was found to have similar potency compared to the known highly active dopamine agonist apomorphine, but it was considerably less potent than its tetralin analogue. In the indane series, potency was significantly reduced when the hydroxyl group was placed at the 6-position, or when a methyl-spacer was positioned between the indane and amine.

Another agonist, RDS-127 **24**, was identified to preferentially activate dopamine autoreceptors as opposed to the post-synaptic dopamine receptors (D_2).⁴² It was found to have a K_i of 10 nM when incubated with rat striatal membrane preparations, and was shown to be more potent than its tetralin analogue. Its structure is based on the core of **23**, only the 7-hydroxy substituent was replaced by a methoxy group and a 4-methoxygroup was added. This compound also has some serotonin (agonist) receptor activities.

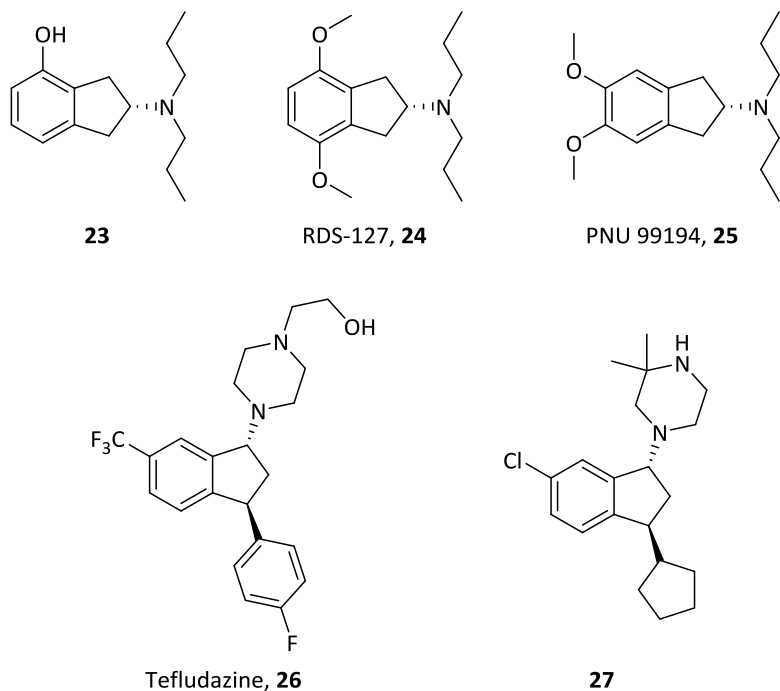


Figure 6. Dopamine receptor ligands.

When the methoxy groups were moved from the 4,7- to 5,6-positions the compound behaved as a postsynaptic dopamine receptor antagonist (PNU 99194) **25**.⁴³ This compound selectively binds to the D_3 receptor and thereby predominantly has an effect on locomotor activity. Its K_i value for this receptor is 78 nM, 20 fold lower than for the D_2 receptor (1572 nM).⁴⁴

A slightly bulkier molecule, tefludazine **26**, was found in a 1-piperazino-3-phenylindane series as a dopamine antagonist with high affinity.⁴⁵ These compounds have methyl phenidate and amphetamine antagonist activity and induce catalepsy in rats, indicating their antipsychotic activity, through D_1 and D_2 antagonism. Tefludazine has a K_i of 8.8 nM in rat striatal membranes, a binding affinity slightly higher than that of chlorpromazine, a known antipsychotic. Bogeso et al. showed that substituents such as chlorine, methyl or CF_3 and to a lesser extent fluorine at the indane 6-position are crucial for affinity. A variety of substituents on the piperazine moiety is tolerated, but the hydroxyethyl showed the best activity. The 4-fluoro substitution on the phenyl ring is important for the *in vivo* activity, most probably due

to increased metabolic stability. None of the *cis*-isomers were active dopamine antagonists, and only *trans*-isomers bound with high affinity to the dopamine receptor. At the same time it was found that many of the compounds in this series were potent dopamine uptake inhibitors and had high affinity for the 5HT₂ receptor as an antagonist **26** with a K_i of 8.6 nM while having only sub-micromolar affinity for the α_1 -adrenoceptor (IC_{50} = 670 nM).⁴⁶

Another series from the same research group showed high affinity for the D₁ and D₂ receptors, next to 5HT₂ and α -adrenoceptors.⁴⁷ In this series the *trans*-isomers were the active species. It was concluded that for the chiral center at the amine, one enantiomer contains the receptor blocking activity, whereas the other enantiomer is active as dopamine/norepinephrine uptake inhibitor. One of the most potent compounds in this series (**27**) was identified as a potential antipsychotic agent. D₁ and D₂ affinity were highest for small substituents on the 6-position of the indane moiety and much higher compared to 4-, 5- or 7-substituted structures. In addition, compounds with 6-fluoro and 6-chloro substituents preferred the D₁ receptor, whereas 6-CH₃ and 6-CF₃ favored the D₂ receptor. Exploration of the piperazine ring revealed that its optimal substituent is 3-Me. However, to avoid creating an additional chiral center, the 3 position was dimethylated, which yielded an increase in selectivity for the D₁ receptor. Formation of spirocycles at this position gave similar affinities, but a loss of selectivity for D₁/D₂. Larger substituents on the nitrogen atom such as *i*-propyl, hydroxy-ethyl and propyl did not markedly affect affinity for the dopamine receptors, in accordance with the tefludazine series. Finally, substitutions at the indane 3 position should be *trans*- oriented bulky groups, with the highest D₁ and D₂ affinity for the phenyl, 4-fluorophenyl and 3-thienyl moieties. Compound **27** had a K_i value of 0.84 nM and 7.1 nM for the D₁ and D₂ receptors, respectively. Affinities for the 5HT_{2A} (antagonist), 5HT_{2C} and α_1 -adrenoceptors were also high with 1.9 nM, 0.28 nM and 25 nM, respectively.

In summary, a typical high affinity dopamine receptor ligand based on the indane scaffold contains an amine on the pentane ring and on the phenyl ring an electron donating group (EDG) – in the case of agonists **23**, **24**, and an electron withdrawing group (EWG) – in the case

of antagonists **26**, **27**. The optimal distance between the two appears to be four carbon atoms.

Serotonin Receptors

The serotonin receptor family (5HT receptor) is involved in a wide range of CNS processes and is a target for several diseases including anxiety, depression, psychosis and cognitive impairment. Therefore, investigations to develop ligands for these receptors have produced a plethora of compounds with affinity for one or several of the subtypes 5HT₁ through 5HT₇.

Millan et al.⁴⁸ reported S15535 **28** (Figure 7) as a highly selective 5HT_{1A} receptor ligand which acts as weak partial agonist with high affinity ($K_i = 0.8$ nM). However, this compound was rapidly metabolized *in vivo* and more stable compounds were searched for. A decade later Peglion et al.⁴⁹ described 2-(arylcycloalkylamine)-indan-1-ols as ligands of the 5HT_{1A} receptor for treatment of anxiety. Additional substituents on the indane system improved selectivity and oral bioavailability while keeping the high affinity. Substitutions at the 6 position of the indane yielded the highest affinity. With a methoxy group a K_i value of 0.45 nM was obtained, two- to threefold better than 6-NO₂ or 6-F, or the 5-OMe analogue. However, the 5-OMe compound **29** ($K_i = 1$ nM) was selected for further investigations due to its better metabolic bioavailability. In the case of substituents on the 2 position a 4-substituted-piperidin-4-ol was deleterious for the affinity. However, piperazine or piperidine moieties substituted with benzodioxane or benzopyran maintained the high affinity for the receptor. Similar to dopamine receptor ligands **26** and **27** the *trans*-isomers were most active on the 5HT_{1A} receptor.

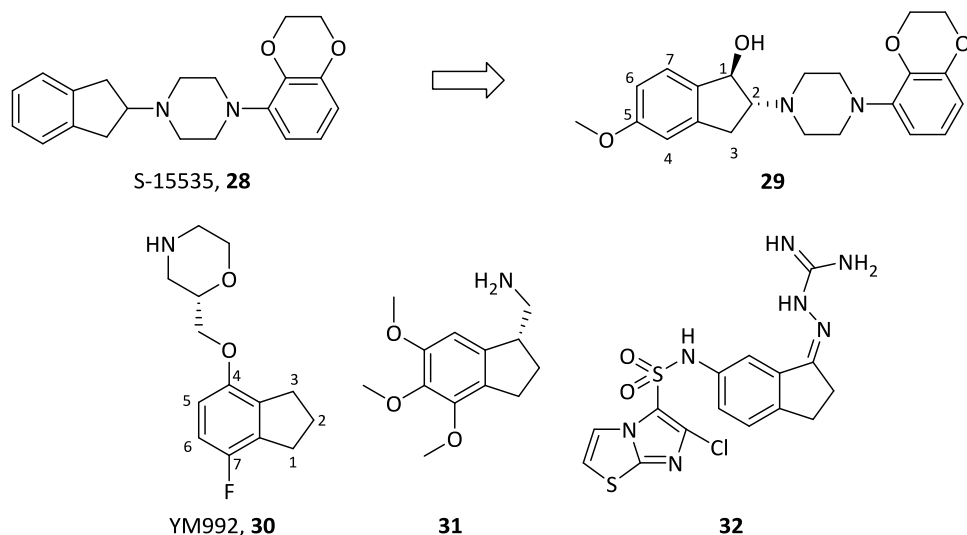


Figure 7. Serotonin receptor ligands.

YM992 **30** (Figure 7) was developed as a selective serotonin reuptake inhibitor (SSRI) with moderate ($K_i = 86$ nM) 5HT_{2A} affinity. Submicromolar ($K_i = 200$ nM and 680 nM) affinity was observed for the α_1 -adrenoceptor and 5HT_{2C} receptor, respectively.⁵⁰ The substitutions on the indane system are located on positions 4 and 7 compared to positions 1, 2 and 5 in **29**, potentially explaining the lower receptor affinities. Additionally, the basic nitrogen in compound **30** is located much further from the indane than in other serotonin receptor ligands described in this review.

A mescaline analogue was synthesized to develop a 5HT_{2A} receptor agonist, and the conformationally restricted **31** was found to have a K_i value of 69 nM at cloned human receptors.⁵¹ The more recently identified family of 5HT₆-receptors was investigated as a target for indenes/indanes.⁵² The SAR revealed compound **32** to have the highest affinity in the indane series for the human receptor ($K_i = 1.2$ nM). The 6-chloroimidazo[2,1-b][1,3]thiazole structural motif coupled to the sulfonamide in this compound was important for affinity, as the naphthyl and 4-methyl-3,4-dihydro-2H-1,4-benzoxazine analogues had over 20 fold lower affinity. The sulfonamide was preferentially located at the 5 or 6 position, as the

4 position abolished affinity. The guanylhydrazone could be replaced by an imidazolinyhydrazone group with only a marginal loss in affinity.

Melatonin Receptors

Melatonin (N-acetyl-5-methoxytryptamine) is a hormone that is secreted during darkness. It regulates the circadian rhythm and analogues of melatonin can be used to control diseases associated with circadian rhythm disorders.

Compounds **33** and **34** (Figure 8) were developed as melatonin analogues,⁵³ with binding affinities on chicken brain melatonin (MT) receptors of 16 nM and 7.6 nM, respectively. Their tetralin analogues had approximately 20 fold higher affinity, and the benzocycloheptane analogues had similar affinity, whereas the cyclobutane analogues had a lower affinity. Compounds with a butyramido substituent (such as **34**) had higher affinity than when substituted with a propionamido (**33**) or acetamido moiety, indicating the receptor favors longer lipophilic side chains. Moreover, as for the serotonin and dopamine receptors, the melatonin receptor has marked enantioselectivity for these compounds. The (+)-enantiomer of **33** had a K_i value of 3 nM, compared to 456 nM for the (-)-enantiomer. These features seem to be important for melatonin receptor affinity as an agonist, as will also become apparent in the next examples.

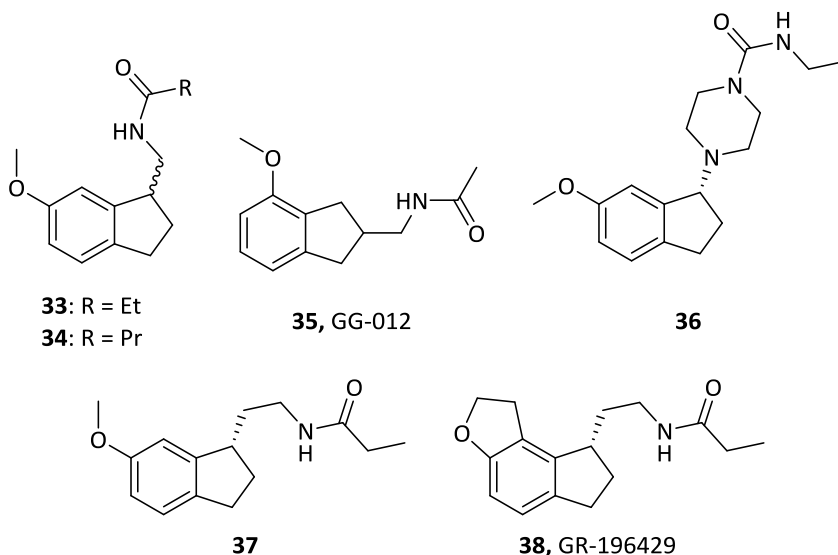


Figure 8. Melatonin receptor ligands.

Drijfhout et al. tested several compounds for melatonin receptor agonism.⁵⁴ GG-012 (compound **35**) was a partial agonist with high binding affinity ($K_i = 9.5$ nM) for the chicken retina melatonin receptors, 5-fold higher than its tetralin analogue. Additionally, in another paper,⁵⁵ a derivative of compound **35** that is lacking the methylene spacer between the indane and amide was found to have no affinity for the receptors, stressing the importance of the distance between the amide and methoxy group, equal to the distance seen in **33** and **34**.

Mattson et al. reported on piperazine amides attached to benzyl, indenyl and naphthalene groups as MT_2 receptor selective agents.⁵⁶ Compound **36** was reported to have high affinity and the best selectivity for the cloned human MT_2 receptor (h MT_1 , $IC_{50} = 200$ nM, h MT_2 , $IC_{50} = 1.7$ nM). The indanes in general had higher affinity than the more flexible benzyl or the bulkier tetralin and naphthyl analogues (20-30 fold). The compounds showed stereospecificity in their binding. Only R-enantiomers were active, whereas the S-enantiomers showed no activity at the MT receptors. The *n*-, *c*- and *i*-propyl substituents instead of ethylamine on the carbonyl piperazine yielded the highest affinity for the MT_2 receptor; however, the selectivity for the MT_1 receptor was decreased. Smaller substituents, such as methyl and ethyl, or larger substituents such as n-butyl reduced affinity.

Two other series of indanes were synthesized as therapeutic agents for sleep disorders, one describing the SAR of indane derivatives⁵⁷ the other the SAR of indeno-furans,⁵⁸ both yielding agonists with very high affinity. The K_i values on human melatonin receptors (MT_1) were 0.041 nM and 0.014 nM for **37** and **38**, respectively, even higher than that of melatonin itself (0.082 nM). Again, the geometry of substituents on the 1 position of the indane system plays an important role in binding affinity. The same configuration as in **36** is preferred for **37** and **38**.

In the indane series, the *S*-enantiomers had more than 100-fold higher affinity than the *R*-enantiomers. The indane system itself provided twofold higher affinity over a similar tetralin series, and more than 70-fold higher affinity than the 6,7,8,9-tetrahydro-5*H*-benzo[7]annulene derivative. The amide alkyl group should be ethyl or propyl, as seen before, whereas *iso*-propyl resulted in a decrease in affinity. Exchanging $-CH_3$ to $-CF_3$ on the amide led to a 5-fold increased affinity, yielding the most potent compound in the series with a K_i value of 0.012 nM. The length of the spacer between the indane and amide was also of importance, with optimal affinity provided by an ethyl spacer. Propyl and methyl spacers reduced affinity 20-fold and 1000-fold, respectively. Lastly, the methoxy group was substituted for ethoxy, propoxy and *iso*-propoxy groups, but this decreased affinity in this order. The 6-methoxy group yields a 7-fold increase in affinity. The authors argued that the H-bond can be formed only if the methyl group on the oxygen points towards the 7 position of the indane, giving access of the oxygen's lone pair for hydrogen bonding. It was concluded that substitution on the 7 position (but not the 5 position) prevents this conformation from occurring and therefore reduces affinity markedly.

Using this finding, Uchikawa et al. developed the second series of tricyclic indanes, such as compound **38**.⁵⁸ The methoxy group was fixed into the preferred position by incorporating it in a furan, 1,3-dioxolane, oxazole, pyran, morpholine, or 1,4-dioxane ring systems. In order to maintain affinity, the tricyclic system with the oxygen at the 6 position needed to be angular (6,7 position), not linear (5,6 position), underlining the hypothesis of the lone pair on the oxygen being accessible for hydrogen bonding as described before. The 1,6,7,8-tetrahydro-2*H*-indeno[5,4-*b*]furan ring system (compound **38**) resulted in the highest affinity. According

to the docking study,⁵⁸ an additional positive feature of compound **38** over melatonin is the indane system, which is located in the hydrophobic pocket at the bottom of the binding site, contributing to the high affinity of the MT₁ receptor.

Metabotropic Glutamate Receptor

There are three groups of metabotropic glutamate receptors, of which group one (mGluR1 and 5) is involved in increasing NMDA receptor activity while group two (mGluR2 and 3) and three (mGluR4, 6-8) inhibit neurotransmission. The mGluR1 is a potential target for neuroprotection via inhibition by an antagonist.⁵⁹ Pellicciari et al.⁶⁰ developed an mGluR1 selective antagonist called 1-aminoindan-1,5-dicarboxylic acid (AIDA, **39**) (Figure 9) which is a conformationally restricted analogue of the (carboxyphenyl) glycine derivatives. It inhibited glutamate-stimulated phosphoinositide hydrolysis in BHK cells expressing mGluR1 with an IC₅₀ of 7 μM. From the very limited SAR performed it became apparent that one of the two carboxylic acids should be at the 5 position of the indane in order to give the antagonistic effect on mGlu1. However, the compound showed also modest agonist action on mGlu5 receptors.

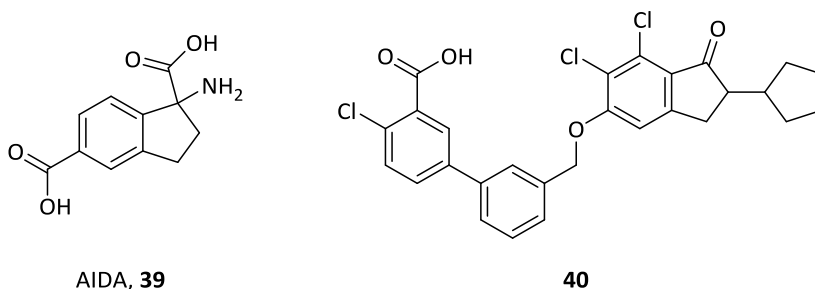


Figure 9. Metabotropic glutamate receptor ligands.

The group two receptors might act as a target for epilepsy, anxiety and schizophrenia treatment, especially through selective targeting of mGluR2.⁶¹ However, one of the main problems in the development of selective compounds for mGluR2 over mGluR3 is the high degree of sequence homology between group two mGluRs, especially at the (extracellular) glutamate binding site. Therefore, instead of targeting the orthosteric (glutamate) binding

site, emphasis these days is on allosteric modulators binding into the transmembrane domain of the receptor. Bonnefous et al. have reported a new class of selective mGluR2 positive allosteric modulators (PAM`s) based on biphenyl–indanones. Compound **40** was identified to have the highest potency for the human mGluR2, with an EC_{50} value of 5 nM.⁶² The indanone moiety provided receptor selectivity; for high potency there must be substitutions on the 6 and/or 7 position of the indanone and a cyclopentyl at the α -position of the ketone. Additionally, in the biphenyl system, the central phenyl and methylene group are best unsubstituted. The acid on the second phenyl is preferentially at the *meta*-position, and electron–withdrawing substituents on the *para* position improve affinity additionally.

Vasoactive Intestinal Polypeptide Receptor 2

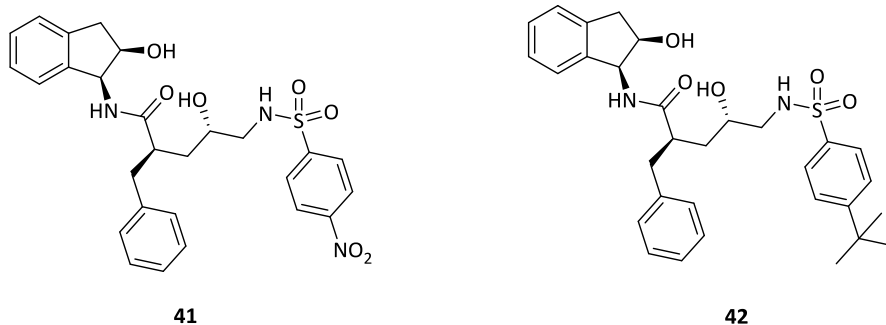


Figure 10. Vasoactive intestinal polypeptide receptor 2 ligands.

Vasoactive intestinal polypeptide receptor 2 (VAPC₂) is a member of the secretin receptor family (class B GPCRs). VAPC₂ is involved in sustaining circadian rhythm,⁶³ regulation of immune responses,⁶⁴ schizophrenia^{65, 66} and upregulation of basal metabolic rate.⁶⁷ Thus far there are only two known small molecule ligands for the VAPC₂ receptor discovered by Chu et al.⁶⁸ Compound **41** (Figure 10) was the only hit from a high-throughput screen of 1.67 million compounds. After a structure similarity search another analog, compound **42**, was found. Both compounds showed antagonistic activity on the VAPC₂ receptor. Compound **41** was the more potent inhibitor with an IC_{50} value of 2.3 μ M and selective towards the VAPC₂ receptor. The change of the electron–withdrawing nitro group to the lipophilic, electron–donating *t*-

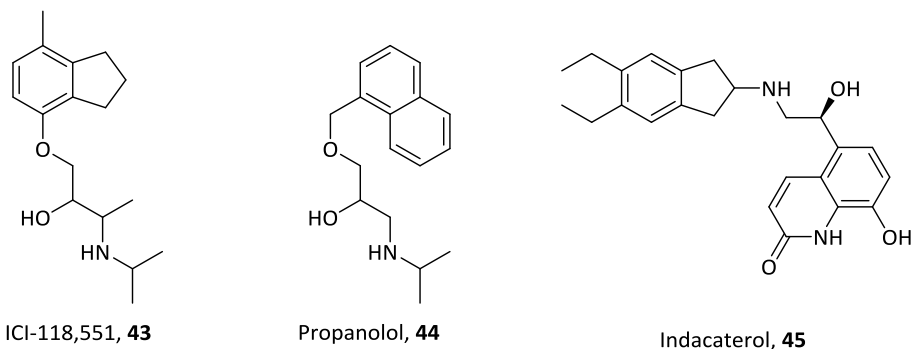
butyl group in **42** led to a small degree of activation of VAPC₁ receptors at higher concentrations, while maintaining the antagonist activity on the VAPC₂ receptor.

INFLAMMATORY DISEASE TARGETS

β_2 -Adrenergic Receptor

One of the beta-adrenergic receptors is the β_2 -adrenoreceptor, involved in smooth-muscle relaxation, blood vessel dilation, control of the heart rate and the digestive system among others. It is especially of interest in asthma and COPD as a target for bronchodilation.

In 1980 indane derivative ICI-118,551 **43** (Figure 11) was identified as a selective antagonist for the β_2 -adrenoreceptor, and has mostly served as a research tool ever since as β_2 -adrenoreceptor blockade is not regarded as therapeutically useful.⁶⁹ **43** is quite similar to propranolol, a non-selective beta blocker, and is the indane analogue of α -methyl substituted propranolol (**44**). It is thought that the structure gets its selectivity and potency through three aspects. Firstly, **43** is as potent as its naphthalene analogue α -methylpropranolol, but is five times more selective for the β_2 -adrenoreceptor. The indane ring therefore must give a preference to the β_2 -adrenoreceptor over the β_1 -adrenoreceptor. Secondly, the oxymethylene bridge between the ring and the propanolamine is of importance for potency as the same structure is seen in propranolol and other potent beta-blockers, but not in the less potent ethanolamine compounds H35/25 and butoxamine. Lastly, selectivity for the β_2 -adrenoreceptor is enhanced through the additional methyl group in the propanolamine moiety, as α -methylpropranolol, H35/25 and butoxamine are more selective than propranolol and contain this feature too.

Figure 11. β_2 adrenergic receptor ligands.

Recently, a potent and selective agonist for the β_2 -adrenoreceptor was developed (indacaterol **45**).^{70, 71} It is marketed as an inhaled ultra-long acting bronchodilator, and is especially aimed at asthma and COPD treatment. It has the highest affinity for the β_2 -adrenoreceptor in the series, however, the affinity values vary in different reports ($K_i = 76$ and 16 nM).^{70, 71} The indane scaffold was chosen for this compound in order to easily substitute the phenyl in the indane to regulate lipophilicity (for long-term activity *via* possible membrane binding causing a high local concentration around the receptor). This part of the molecule allows big variations due to the remote position from the key epinephrine mimicking part. The di-ethyl substitution pattern was chosen to keep the indane part symmetrical and a-chiral for simplicity. The SAR can then be broken down into three parts, when compared to the non-selective β_2 -agonist epinephrine. Compound **45** has a 8-hydroxyquinolinone catechol mimetic, as a replacement for the catechol moiety of epinephrine and an ethanolamine linking group, which remained unchanged. These are the crucial parts for agonist activity at the β_2 -receptor. The third part is the amino substituent, in which the N-methyl group of epinephrine is replaced by a 5,6-diethyl indanyl moiety. The 5,6-disubstitutions led to higher affinity than 4,7-disubstitutions. Dimethyl substitution decreased affinity compared to the unsubstituted indane, whereas diethyl substitution gave the highest affinity, slightly higher than di-*n*-propyl and di-*n*-butyl. Lastly, introduction of a methyl group at the 2 position of the indane ring increased affinity by 10 fold compared to **45**, however, β_1 -affinity was increased even more, and thereby selectivity was lost.

Chemokine Receptor 2

Chemokines are a class of chemoattractant cytokines, and their main action is to control the activation and trafficking of leukocytes and other cell types in a range of inflammatory and non-inflammatory conditions. One of these, chemokine ligand 2 (CCL2), acts on memory T cells, monocytes, and basophils.⁷² It creates a chemotactic gradient and activates the movement of immune cells to the site of inflammation by binding to its cell-surface receptor, chemokine receptor 2 (CCR2).⁷³ Pre-clinical models of inflammatory diseases (e.g., atherosclerosis,⁷⁴ asthma,⁷⁵ multiple sclerosis,⁷⁶ rheumatoid arthritis,⁷⁷ neuropathic pain⁷⁸) have pointed to a critical role of the CCR2 and CCL2.

Recently, Vilums et al.⁷⁹ reported a new approach in hit-to-lead optimization for CCR2 antagonists. This report suggests that next to SAR, one should also use structure-kinetic relationships (SKR) to yield compounds with good affinity and optimal drug-target binding kinetics already at the early stages of the drug discovery cycle. It was discovered that the constrained indane system yielded better affinity than more flexible alkyl linkers, but the affinity was worse than that of aliphatic heterocycles. However, in the SKR study the indane derivative showed the longest residence time and was used for further optimization which yielded compound **46** (Figure 12) with high affinity and long residence time ($K_i = 3.6$ nM, RT = 135 min). Substituents on the 5 position improved affinity in general, but only halogens like Cl and Br also prolonged the residence time.

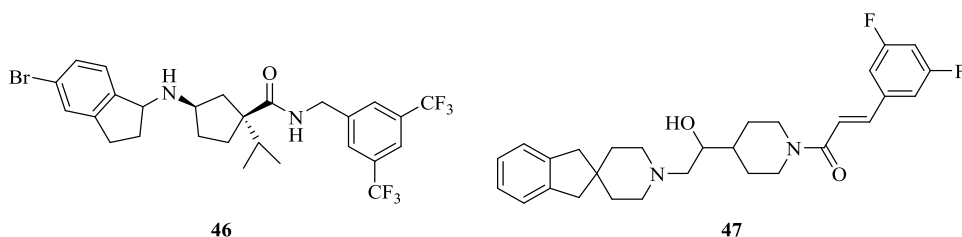


Figure 12. Chemokine receptor 2 antagonists.

In a patent application⁸⁰ Bristol-Myers Squibb disclosed several CCR2 antagonists with indene and indane (**47**) structures. Not much has been published yet about these compounds,

however, it is anticipated that they will have high affinities due to their resemblance to other CCR2 antagonists, such as reported in several GSK patents.^{81, 82} The indene/indane group would fill the needed hydrophobic space of the 'end group', which requires at least one aromatic ring for affinity at the receptor.

Protease-Activated Receptor 2

Four protease-activated receptors (PAR's) are among the most unusual receptors in the vast super-family of GPCR's due to their manner of activation. There are no known endogenous extracellular ligands for these receptors. Instead, they are activated via proteolytic cleavage of their *N*-terminus by serine proteases. The remainder of the *N*-terminus folds back onto the receptor and induces intramolecular activation of the PAR.⁸³ The PAR₁ subtype has been most investigated, because it is activated by thrombin, suggesting it as a potential target in cardiovascular diseases. In contrast, PAR₂ is resistant to thrombin, but can be activated by trypsin, tryptase or cathepsin G and has been linked to inflammatory and proliferative disorders.^{83, 84}

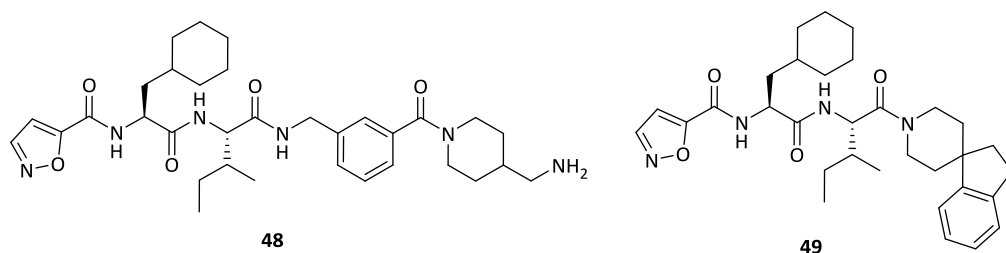


Figure 13. Protease-activated receptor 2 ligands.

Recently, Barry et al reported the discovery of selective agonists and antagonists of PAR₂.⁸⁵ The authors truncated the known PAR₂ agonist SLIGRL-NH₂ by three amino acids and derivatized both ends of the tripeptide to yield agonist **48** (Figure 13) with sub-micromolar potency (EC₅₀ = 0.28 μM). The removal of the primary amine on the piperidine ring altered the agonistic effect into antagonism of PAR₂. A spiroindanepiperidine group coupled directly to the terminal amide group of the tripeptide yielded the most potent antagonist **49**.

CARDIOVASCULAR DISEASE TARGETS

Endothelin Receptor

The endothelin receptors ET_A, ET_B and ET_C are mainly involved in the cardiovascular system regulating vasoconstriction and -dilation. They are used as a target in hypertension⁸⁶ and renal failure⁸⁷.

In the 1990's a research group from SmithKline Beecham Pharmaceuticals developed several antagonists for the ET_A and ET_B receptor with an indane core structure.^{88, 89} Through molecular modeling of the peptide endothelin-1 (ET-1), the natural ligand of these receptors, important side chains for binding were identified. The 1 and 3 positions on the indane ring are substituted with phenyl groups, possibly mimicking two aromatic side chains of ET-1. Additionally, the carboxylic acid at position 2 plays an important role in binding as the corresponding methyl ester had no measurable affinity for the ET receptors. Introduction of electron-donating substituents on the 1- and 3-phenyl groups improved affinity, with both phenyls *para*-substituted with methoxy groups giving a marked increase in affinity. A 3,4-methylenedioxy instead of one of these methoxy groups improved the affinity even more, as did substitutions at the 6 position of the indane. To mimic the C-terminal carboxylic acid of ET-1, a carboxylic acid was introduced with a methylenoxy spacer to the *ortho*-position of one of the phenyl rings. This resulted in structure **50** (SB 209670) (Figure 14), the (+)-enantiomer being more potent than the (-)-enantiomer, with a K_i value on human ET_A and ET_B receptors of 0.43 nM and 15 nM, respectively. However, despite its high affinity, a shortcoming with this compound was its limited bioavailability. Therefore compound **51** (enrasentan) was developed, changing only the oxyacetic acid at the 2 position of the phenyl ring into an alcohol. This slightly reduced the affinity for ET_A, but improved the selectivity over the ET_B receptor by 10 fold and also improved bioavailability, resulting in binding affinities of 1.1 nM and 111 nM for ET_A and ET_B receptors, respectively.

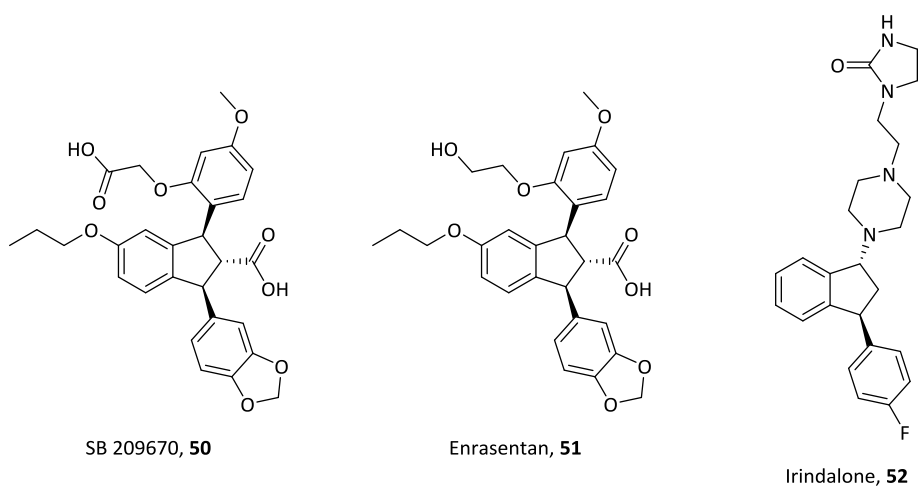


Figure 14. Endothelin receptor ligands **50**, **51** and serotonin receptor ligand **52**.

Serotonin Receptor

Apart from serotonin receptors in the brain as discussed above, there are also peripheral receptors, such as peripheral 5HT₂ receptors. These receptors could be used as antihypertensive targets when blocked with an antagonist.

As described for the compounds targeting serotonin receptors in the CNS, several features are crucial for affinity to these receptors. All these elements are present in the dopamine and 5HT₂ antagonist tefludazine **26**. One of its characteristics, the substitution on the 6 position of the indane, is less important for serotonin receptor affinity. Hence, Bogeso et al.⁹⁰ used tefludazine without its 6-CF₃ substitution as a starting point to target selectively the peripheral 5HT₂ receptors. Additionally, their compounds had some α_1 -adrenoceptor antagonistic affinity, although less than for 5HT₂. These combined effects may be responsible for the antihypertensive effects of these drugs. The SAR showed that the 4-fluoro substituent on the phenyl is crucial for activity of the compounds, as in tefludazine, since other substituents, including hydrogen, yielded inactive compounds. Substitutions at the piperazine ring were important for tuning central and peripheral activity, to the extent that a 1-ethyl-2-imidazolidinone moiety abolished neuroleptic activity and kept peripheral activity indicated

by the compound's antihypertensive effects in rats. Additionally, the (+)-enantiomer was found to be much more active resulting in compound **52** (irindalone) (Figure 14), with IC_{50} values of 3.4 nM, 400 nM and 26 nM for $5HT_2$, dopamine (DA) and α_1 -receptors, respectively.

TARGETS OF METABOLIC DISEASES

Melanin Concentrating Hormone Receptor

The melanin concentrating hormone receptor exists as two subtypes in humans, MCH-R1 and MCH-R2 and is involved in feeding behaviour and energy homeostasis. Inhibition of this receptor could therefore be a new way of treating obesity and metabolic syndromes.^{91, 92}

An indane-derived chemical class was identified as a promising lead for an antagonist of the MCH-R1⁹³ and its optimization was published recently.⁹⁴ The indane moiety was found to be superior for receptor selectivity over cyclopentyl, cyclobutyl, cyclopropylmethyl and dihydrobenzofuran. A bromine or CN at the 6 position of the indane gave higher affinity for the MCH-R1, with the CN group giving the highest potency and selectivity. This group was then linked to a benzimidazole group by several linkers, the *cis*-4-methyleneaminocyclohexane giving the best results. This investigation showed that the *cis*-conformation was highly preferred over the *trans*- conformation and that the methylene spacer between the indane and NH is important for activity. The selected compound **53** (Figure 15) has a K_i value of 3 nM for the human MCH-R1, but was not further developed because of potent hERG inhibition, activities which could not be dissociated.

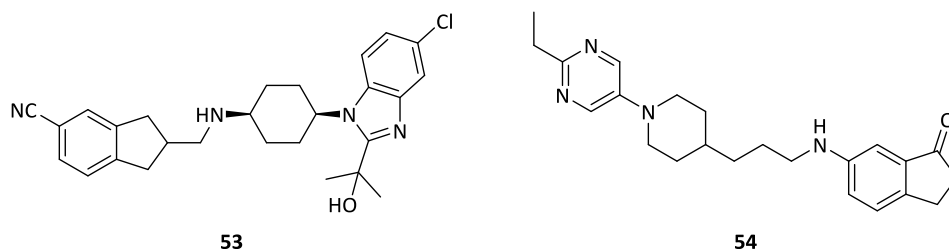


Figure 15. Melanin concentrating hormone receptor antagonist **53** and GPR119 agonist **54**.

GPR119

A relatively new GPCR termed GPR119 has been identified as a potential target for the treatment of obesity and diabetes. An agonist for this receptor was discovered and after optimization indanone **54** was found to have the desired effect of plasma glucose control in rodents.⁹⁵ Different bicyclic scaffolds were investigated and the indanone scaffold was identified as giving the highest affinity for GPR119. The nitrogen on the 6 position of the indanone was important for agonist activity. In addition, a propyl-spacer to the piperidine gave the best affinities. The EC₅₀ value of the most potent compound **54** for human GPR119 was 51 nM.

GPR40

GPR40 (also known as free fatty acid receptor 1) is highly expressed in the pancreas and is a potential therapeutic target for diabetes. Itoh et al.⁹⁶ described that long-chain free fatty acids (FFAs) are the endogenous ligands for GPR40. Furthermore, by activating GPR40 FFAs amplify glucose-stimulated insulin secretion from pancreatic β cells. Takeda Pharmaceuticals developed fasiglifam **55** (Figure 16), a GPR40 agonist that showed significant glucose-lowering effects in patients with type 2 diabetes by stimulating glucose-dependent insulin secretion.⁹⁷ However, recently Takeda announced termination of fasiglifam development due to liver safety concerns.⁹⁸ Boehringer Ingelheim has filed a patent application that describes more potent indanyl analogues of fasiglifam as GPR40 agonists. Compound **56** showed the best potency in the series having an EC₅₀ value of 1 nM⁹⁹ (compared to fasiglifam's EC₅₀ = 14 nM).¹⁰⁰

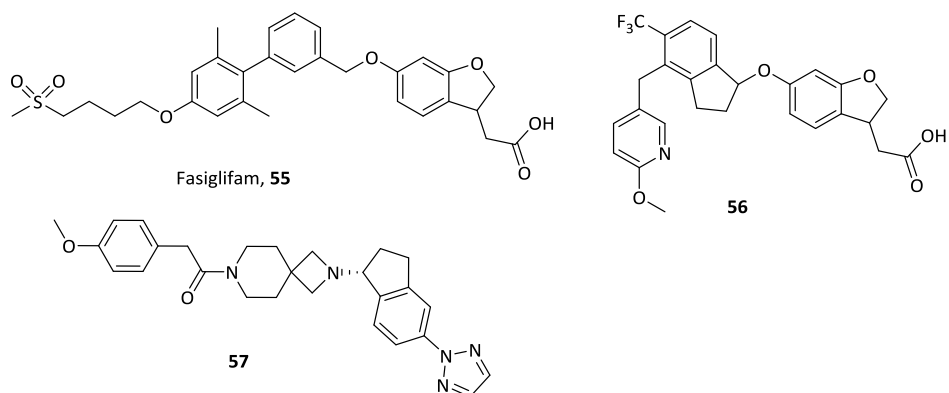


Figure 16. GPR40 agonists **55**, **56** and growth hormone secretagogue receptor inverse agonist **57**.

Growth Hormone Secretagogue Receptor

Growth hormone secretagogue receptor (GHSR) and its endogenous ligand ghrelin are expressed in pancreas where they are involved in regulation of glucose-induced insulin release. Blockade of the GHSR/ghrelin axis results in enhancement of glucose-induced insulin release from perfused pancreas, whereas addition of exogenous ghrelin suppresses it.¹⁰¹ This suggests that antagonism of the ghrelin receptor enhances insulin release thereby normalizing the glycemic control in high-fat diet-induced obesity and counteracting the progression of type 2 diabetes. Pfizer has developed a series of small-molecule inverse agonists for GHSR based on a 2,3-dihydro-1H-inden-1-yl-2,7-diazaspiro[3.6]nonane scaffold as potential treatment of type 2 diabetes.¹⁰² Compound **57** (Figure 16) had the best affinity in the series ($K_i = 3.1$ nM). This scaffold tolerates a wide variety of different chemical groups on the acetamide side, while substituents on the indenyl ring should be aromatic rings with at least a nitrogen atom on the 2 position.

MISCELLANEOUS TARGETS

α_1 -Adrenoceptor

The α_1 -adrenoceptors have several subtypes that are very similar in structure. The α_{1A} , α_{1B} and α_{1D} receptors are all acting mainly on smooth muscle cells leading to vasoconstriction,

bronchospasms and decreased motility in the GI-tract. Subtype α_{1A} receptor selective agonists have been shown to be efficacious in *in vivo* models of stress urinary incontinence (SUI).¹⁰³ However, full α_{1A} receptor agonists possess a slender therapeutic index over α_{1A} induced cardiovascular effects. Therefore partial agonism and organ specificity are desired characteristics in SUI treatment.

In the search for a compound with these features, indanes and tetrahydronaphthalenes coupled to a 2-imidazole were investigated.¹⁰⁴ The tetrahydronaphthalene derivative **58** (Figure 17) had an attractive pharmacological profile, combining good potency, low E_{max} , good selectivity and *in vitro* metabolic stability. However, according to Conlon et al.¹⁰⁵ α_{1A} partial agonists mediate their effect *via* a central pathway rather than directly on the urethral smooth muscle, thus CNS penetrant partial agonists are desired for *in vivo* efficacy. Compound **58** has a high total polar surface area (TPSA = 83 Å²) with an associated P-glycoprotein-mediated efflux, which could have a negative impact on the crossing of the blood–brain barrier (BBB).¹⁰⁶ As the indane derivatives were found to be more potent than the tetrahydronaphthalene congeners, it was decided to continue with the indane core and decrease the TPSA value by exchanging the sulfonamide group to an isostere with smaller TPSA penalty. After thorough SAR evaluation compound **59** (PF-3774076) was generated bearing a 4-methylenemethoxy group (EC_{50} = 31 nM, TPSA = 38 Å²) instead of sulfonamide. Additionally, the chlorine substituent on the 5 position of the indane reduced the compound's E_{max} value and gave the wanted partial agonism. Unfortunately, **59** did not offer the necessary degree of selectivity over cardiovascular events when assessed in *in vivo* models of cardiovascular function.

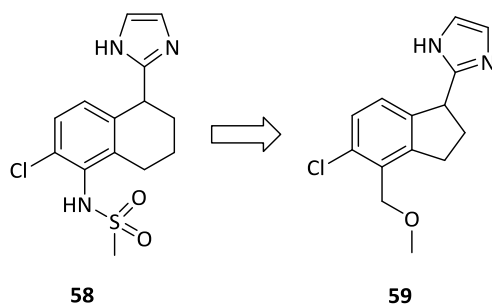


Figure 17. α_1 -Adrenoceptor ligands.

The structure of **59** bears resemblance to some of the α_{2A} , dopamine, serotonin and melatonin ligands. Fadolmidine **22** for example has the same location for the imidazole on the 1 position of the indane, only with an additional methyl-spacer. This α_2 -receptor agonist is also a α_1 receptor full agonist and the selectivity of **59** compared to **22** seems to be due to the bulk of the substitution on position 4.

Prostaglandin F Receptor

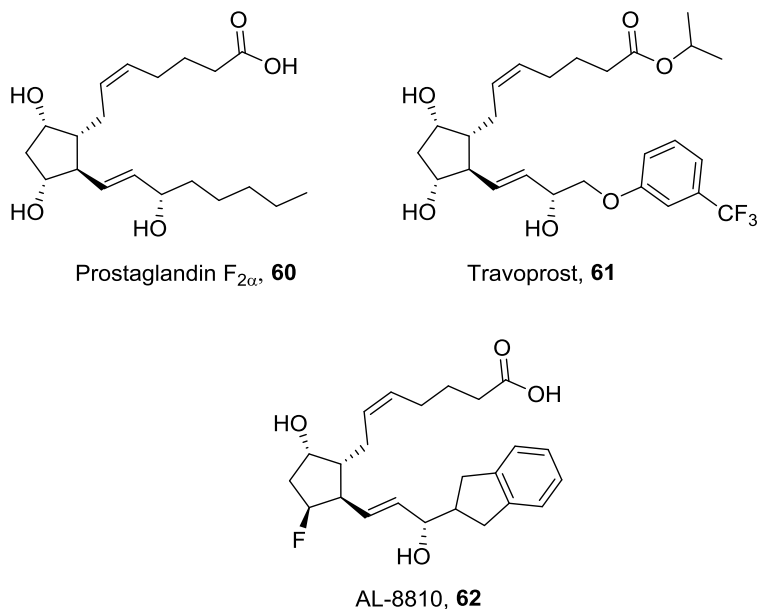


Figure 18. Prostaglandin F receptor ligands.

The endogenous ligand of the prostaglandin F receptor (FP receptor) is prostaglandin $F_{2\alpha}$ (PGF $_{2\alpha}$, **60**). It is involved in many physiological responses, such as the regulation of parturition (including luteolysis),¹⁰⁷ intraocular pressure,¹⁰⁸ cardiac hypertrophy¹⁰⁹ and kidney function.¹¹⁰ The FP receptor agonist travoprost **61** (analogue of prostaglandin $F_{2\alpha}$, **60**) (Figure 18) is used to treat glaucoma and ocular hypertension. However, the 2-indane analogue of prostaglandin $F_{2\alpha}$ (AL-8810, **62**) is a low-efficacy FP receptor agonist and can be used as selective functional antagonist.¹¹¹ Although AL-8810 has low potency, it proved useful in studying PGF $_{2\alpha}$ -mediated up-regulation of the nerve growth factor IB.¹¹²

CONCLUSIONS

In the above sections, we summarized the major targets of the GPCR protein superfamily where the indane system is used as the core structure in the development of high affinity ligands for these targets. Compounds containing this structure are used in the treatment of a wide variety of diseases through an even wider variety of mechanisms of action. Some of these compounds show very high affinities towards Class A and Class C GPCRs, possibly in part because of the good fit of the indane moiety itself. Additionally, the distinct shape of the indane, due to the fused aromatic and aliphatic rings, makes it a useful scaffold to orient substituents on it. On top of that, the scaffold can be used to mimic constrained alkyl linkers between the phenyl ring and other substituents on the 1 and 2 positions of indane. Apparently these features can be very well accommodated by many GPCRs, suggesting the indane moiety is a privileged structure. Last but not least, using the indane system as the core structure provides 'freedom to operate' to the medicinal chemist. It allows to introduce substituents in ten different directions to find the "perfect-fit" for every substituent, generating very selective and high affinity ligands for GPCRs.

ACKNOWLEDGMENTS

This project was financially supported by the Dutch Top Institute Pharma (Project D1-301).

REFERENCES

1. Robinson, F. A.; Suthers, A. J.; Walker, T. K. Some new antiseptics related to indan-1:3-dione. *Biochemical Journal* **1932**, 26, 1890 - 1901.
2. Bardouille, V.; Mootoo, B. S.; Hirotsu, K.; Clardy, J. Sesquiterpenes from *Pityrogramma-Calomelanos*. *Phytochemistry* **1978**, 17, 275-277.
3. Li, C.; Roege, K. E.; Kelly, W. L. Analysis of the indanomycin biosynthetic gene cluster from *Streptomyces antibioticus* NRRL 8167. *Chembiochem* **2009**, 10, 1064-72.
4. Miao, S. C.; Anstee, M. R.; Baichwal, V.; Park, A. Stawamycin, a New Pyrroloketoindane Natural Product from the Cultures of *Streptomyces* Sp. *Tetrahedron Lett* **1995**, 36, 5699-5702.
5. Dorsey, B. D.; Levin, R. B.; Mcdaniel, S. L.; Vacca, J. P.; Guare, J. P.; Darke, P. L.; Zugay, J. A.; Emini, E. A.; Schleif, W. A.; Quintero, J. C.; Lin, J. H.; Chen, I. W.; Holloway, M. K.; Fitzgerald, P. M. D.; Axel, M. G.; Ostovic, D.; Anderson, P. S.; Huff, J. R. L-735,524 - the Design of a Potent and Orally Bioavailable Hiv Protease Inhibitor. *Journal of Medicinal Chemistry* **1994**, 37, 3443-3451.
6. Villetti, G.; Bregola, G.; Bassani, F.; Bergamaschi, M.; Rondelli, I.; Pietra, C.; Simonato, M. Preclinical evaluation of CHF3381 as a novel antiepileptic agent. *Neuropharmacology* **2001**, 40, 866-78.
7. Yu, H.; Kim, I. J.; Folk, J. E.; Tian, X.; Rothman, R. B.; Baumann, M. H.; Dersch, C. M.; Flippen-Anderson, J. L.; Parrish, D.; Jacobson, A. E.; Rice, K. C. Synthesis and pharmacological evaluation of 3-(3,4-dichlorophenyl)-1-indanamine derivatives as nonselective ligands for biogenic amine transporters. *Journal of medicinal chemistry* **2004**, 47, 2624-34.
8. Nestico, P. F.; Morganroth, J.; Horowitz, L. N.; Mulhern, C. Efficacy of oral and intravenous indecainide in ventricular arrhythmias. *The American journal of cardiology* **1987**, 59, 1332-6.
9. Woltersdorf, O. W., Jr.; deSolms, S. J.; Stokker, G. E.; Cragoe, E. J., Jr. (Acylaryloxy)acetic acid diuretics. 5. [(2-Alkyl- and 2,2-disubstituted-1,3-dioxo-5-indanyl)oxy]acetic acids. *Journal of medicinal chemistry* **1984**, 27, 840-5.
10. Fisher, M. M.; Wilensky, N. D.; Griffith, R. W.; Drumm, A.; Diefenbach, A. E.; Frankel, G. J. Hedulin (phenindione), a new anticoagulant; a comparison of the anticoagulant action of Hedulin and combinations of Hedulin and Dicumarol. *N Y State J Med* **1954**, 54, 778-83.
11. Welsch, M. E.; Snyder, S. A.; Stockwell, B. R. Privileged scaffolds for library design and drug discovery. *Curr Opin Chem Biol* **2010**, 14, 347-61.
12. Syrchina, A. I.; Semenov, A. A. Natural Indanones. *Khim Prir Soedin* **1982**, 3-14.
13. Chen, Y. H.; Chang, F. R.; Lu, M. C.; Hsieh, P. W.; Wu, M. J.; Du, Y. C.; Wu, Y. C. New benzoyl glucosides and cytotoxic pterisin sesquiterpenes from *Pteris ensiformis* burm. *Molecules* **2008**, 13, 255-266.
14. Hsu, F. L.; Huang, C. F.; Chen, Y. W.; Yen, Y. P.; Wu, C. T.; Uang, B. J.; Yang, R. S.; Liu, S. H. Antidiabetic effects of pterisin A, a small-molecular-weight natural product, on diabetic mouse models. *Diabetes* **2013**, 62, 628-38.
15. Ho, S. T.; Yang, M. S.; Wu, T. S.; Wang, C. H. Studies on the Taiwan Folk Medicine .3. A Smooth-Muscle Relaxant from *Onychium-Siliculosum*, Onitin. *Planta Med* **1985**, 51, 148-150.
16. Sheridan, H.; Frankish, N.; Farrell, R. Smooth muscle relaxant activity of pterisin Z and related compounds. *Planta Med* **1999**, 65, 271-272.
17. Ito, T.; Tanaka, T.; Inuma, M.; Nakaya, K.; Takahashi, Y.; Sawa, R.; Murata, J.; Darnaedi, D. Three new resveratrol oligomers from the stem bark of *Vatica pauciflora*. *Journal of Natural Products* **2004**, 67, 932-937.
18. Kopp, P. Resveratrol, a phytoestrogen found in red wine. A possible explanation for the conundrum of the 'French paradox'? *European Journal of Endocrinology* **1998**, 138, 619-620.
19. Okpekon, T.; Millot, M.; Champy, P.; Gleye, C.; Yolou, S.; Bories, C.; Loiseau, P.; Laurens, A.; Hocquemiller, R. A novel 1-indanone isolated from *Uvaria afzelii* roots. *Natural Product Research* **2009**, 23, 909-915.
20. Kim, S. H.; Kwon, S. H.; Park, S. H.; Lee, J. K.; Bang, H. S.; Nam, S. J.; Kwon, H. C.; Shin, J.; Oh, D. C. Tripartin, a Histone Demethylase Inhibitor from a Bacterium Associated with a Dung Beetle Larva. *Organic Letters* **2013**, 15, 1834-1837.
21. Wislicenus. Einwirkung von Essigester auf Phtalsäureester. *Justus Liebigs Annalen der Chemie* **1888**, 246, 347 - 355.
22. Gabriel, S.; Hausmann, J. Einwirkung des o-Cyanbenzylchlorids auf Natracetessigester. *Berichte der deutschen chemischen Gesellschaft* **1889**, 22, 2017 - 2019.
23. Kramer, G.; Spilker, A. Ueber das Inden und Styrol im Steinkohlentheer. *Berichte der deutschen chemischen Gesellschaft* **1890**, 23, 3276 - 3283.

24. Miyaura, N.; Ishiyama, T.; Sasaki, H.; Ishikawa, M.; Satoh, M.; Suzuki, A. Palladium-Catalyzed Intermolecular and Intramolecular Cross-Coupling Reactions of B-Alkyl-9-Borabicyclo[3.3.1]Nonane Derivatives with 1-Halo-1-Alkenes or Haloarenes - Syntheses of Functionalized Alkenes, Arenes, and Cycloalkenes Via a Hydroboration Coupling Sequence. *Journal of the American Chemical Society* **1989**, *111*, 314-321.
25. Katritzky, A. R.; Wang, X. J.; Xie, L. H.; Toader, D. Functionalized (benzotriazol-1-yl)methanes as 1,1-dipole synthon equivalents in diverse annulations to aromatic and heteroaromatic rings. *Journal of Organic Chemistry* **1998**, *63*, 3445-3449.
26. Bailey, W. F.; Longstaff, S. C. Generation and cyclization of a benzyne-tethered alkyllithium: Preparation of 4-substituted indans. *Journal of Organic Chemistry* **1998**, *63*, 432-433.
27. George, P.; Hall, D.; Hartung, R.; Kosley, R. W.; Scotese, A. C. Substituted Para-Biphenyloxymethyl dihydro oxazolopyrimidinones, Preparation and use thereof. 2011.
28. Hartmann, R. W.; Bayer, H.; Grun, G. Aromatase Inhibitors - Syntheses and Structure-Activity Studies of Novel Pyridyl-Substituted Indanones, Indans, and Tetralins. *Journal of Medicinal Chemistry* **1994**, *37*, 1275-1281.
29. Mathison, I. W.; Solomons, W. E.; Jones, R. H. Synthesis of Cyclopentano-1,2,3,4-Tetrahydroisoquinolines - Novel Heterocyclic-Systems. *Journal of Organic Chemistry* **1974**, *39*, 2852-2855.
30. Kangani, C. O.; Day, B. W. Mild, efficient Friedel-Crafts acylations from carboxylic acids using cyanuric chloride and AlCl₃. *Organic letters* **2008**, *10*, 2645-8.
31. Wang, C. D.; Hsieh, Y. F.; Liu, R. S. Gold-Catalyzed Carboalkoxylations of 2-Ethynylbenzyl Ethers to form 1- and 2-Indanones Chemoselectively: Effects of Ligands and Solvents. *Advanced Synthesis & Catalysis* **2014**, *356*, 144 - 152.
32. Azemi, T.; Kitamura, M.; Narasaka, K. Transformation of 1,5- and 1,6-dienes to carbocycles by hydrozirconation and oxidation with cerium(IV) compounds. *Tetrahedron* **2004**, *60*, 1339-1344.
33. Vilums, M.; Zweemer, A. J. M.; Barmare, F.; Gracht, A. M. F.; Bleeker, D. C. T.; Yu, Z.; Vries, H.; Gross, R.; Clemens, J.; Krenitsky, P.; Brussee, J.; Stamos, D.; Saunders, J.; Heitman, L. H.; Ijzerman, A. P. When Structure-Affinity Relationships Meet Structure-Kinetics Relationships: An Example of 3-((Inden-1-yl)amino)-1-isopropyl-cyclopentane-1-carboxamides as CCR2 Antagonists. *Prepared Manuscript*.
34. Garland, S. L. Are GPCRs Still a Source of New Targets? *Journal of Biomolecular Screening* **2013**, *18*, 947-966.
35. LeWitt, P. A.; Hauser, R. A.; Lu, M.; Nicholas, A. P.; Weiner, W.; Coppard, N.; Leinonen, M.; Savola, J. M. Randomized clinical trial of fipamezole for dyskinesia in Parkinson disease (FJORD study). *Neurology* **2012**, *79*, 163-169.
36. Savola, J. M.; Hill, M.; Engstrom, M.; Merivuori, H.; Wurster, S.; McGuire, S. G.; Fox, S. H.; Crossman, A. R.; Brotchie, J. M. Fipamezole (JP-1730) is a potent alpha(2) adrenergic receptor antagonist that reduces levodopa-induced dyskinesia in the MPTP-lesioned primate model of Parkinson's disease. *Movement Disord* **2003**, *18*, 872-883.
37. Cordi, A. A.; Berque-Bestel, I.; Persigand, T.; Lacoste, J. M.; Newman-Tancredi, A.; Audinot, V.; Millan, M. J. Potential antidepressants displayed combined alpha(2)-adrenoceptor antagonist and monoamine uptake inhibitor properties. *Journal of medicinal chemistry* **2001**, *44*, 787-805.
38. Karjalainen, A.; Huhtala, P.; Savola, J. M.; Wurster, S.; Eloranta, M.; Hillila, M.; Saxlund, R.; Cockcroft, V.; Karjalainen, A. Imidazole derivatives having affinity for alpha2 receptors. Nov.6, 2001, 2001.
39. RecroPharma Pipeline. (11/26/2013).
40. Lehtimaki, J.; Leino, T.; Koivisto, A.; Viitamaa, T.; Lehtimaki, T.; Haapalinna, A.; Kuokkanen, K.; Virtanen, R. In vitro and in vivo profiling of fadolmidine, a novel potent alpha(2)-adrenoceptor agonist with local mode of action. *European Journal of Pharmacology* **2008**, *599*, 65-71.
41. Hacksell, U.; Arvidsson, L. E.; Svensson, U.; Nilsson, J. L. G.; Wikstrom, H.; Lindberg, P.; Sanchez, D.; Hjorth, S.; Carlsson, A.; Paalzow, L. Monophenolic 2-(Dipropylamino)Indans and Related-Compounds - Central Dopamine-Receptor Stimulating Activity. *Journal of Medicinal Chemistry* **1981**, *24*, 429-434.
42. Arneric, S. P.; Long, J. P.; Williams, M.; Goodale, D. B.; Mott, J.; Lakoski, J. M.; Gebhart, G. F. Rds-127 (2-Di-Normal-Propylamino-4,7-Dimethoxyindane) - Central Effects of a New Dopamine Receptor Agonist. *Journal of Pharmacology and Experimental Therapeutics* **1983**, *224*, 161-170.
43. Cannon, J. G.; Perez, J. A.; Bhatnagar, R. K.; Long, J. P.; Sharabi, F. M. Conformationally Restricted Congeners of Dopamine Derived from 2-Aminoindan. *Journal of Medicinal Chemistry* **1982**, *25*, 1442-1446.
44. Waters, N.; Svensson, K.; Haadsmasvensson, S. R.; Smith, M. W.; Carlsson, A. The Dopamine D3-Receptor - a Postsynaptic Receptor Inhibitory on Rat Locomotor-Activity. *J Neural Transm-Gen* **1993**, *94*, 11-19.

45. Bogeso, K. P. Neuroleptic Activity and Dopamine-Uptake Inhibition in 1-Piperazino-3-Phenylindans. *Journal of Medicinal Chemistry* **1983**, *26*, 935-947.
46. Svendsen, O.; Arnt, J.; Boeck, V.; Bogeso, K. P.; Christensen, A. V.; Hyttel, J.; Larsen, J. J. The Neuropharmacological Profile of Tefludazine, a Potential Antipsychotic Drug with Dopamine and Serotonin Receptor Antagonistic Effects. *Drug Develop Res* **1986**, *7*, 35-47.
47. Bogeso, K. P.; Arnt, J.; Frederiksen, K.; Hansen, H. O.; Hyttel, J.; Pedersen, H. Enhanced D-1 Affinity in a Series of Piperazine Ring-Substituted 1-Piperazino-3-Arylindans with Potential Atypical Antipsychotic Activity. *Journal of Medicinal Chemistry* **1995**, *38*, 4380-4392.
48. Millan, M. J.; Rivet, J. M.; Canton, H.; Lejeune, F.; Gobert, A.; Widdowson, P.; Bervoets, K.; Brocco, M.; Peglion, J. L. S-15535 - a Highly Selective Benzodioxopiperazine 5-HT_{1A} Receptor Ligand Which Acts as an Agonist and an Antagonist at Presynaptic and Postsynaptic Sites Respectively. *European Journal of Pharmacology* **1993**, *230*, 99-102.
49. Peglion, J. L.; Goument, B.; Despau, N.; Charlot, V.; Giraud, H.; Nisole, C.; Newman-Tancredi, A.; Dekeyne, A.; Bertrand, M.; Genissel, P.; Millan, M. J. Improvement in the selectivity and metabolic stability of the serotonin 5-HT_{1A} ligand, S 15535: A series of cis- and trans-2-(arylcycloalkylamine) 1-indanols. *Journal of Medicinal Chemistry* **2002**, *45*, 165-176.
50. Hatanaka, K.; Nomura, T.; Hidaka, K.; Takeuchi, H.; Yatsugi, S.; Fujii, M.; Yamaguchi, T. Biochemical profile of YM992, a novel selective serotonin reuptake inhibitor with 5-HT_{2A} receptor antagonistic activity. *Neuropharmacology* **1996**, *35*, 1621-1626.
51. McLean, T. H.; Chambers, J. J.; Parrish, J. C.; Braden, M. R.; Marona-Lewicka, D.; Kurrasch-Orbaugh, D.; Nichols, D. E. C-(4,5,6-trimethoxyindan-1-yl)methanamine: A mescaline analogue designed using a homology model of the 5-HT_{2A} receptor. (vol 49, pg 4270, 2006). *Journal of Medicinal Chemistry* **2006**, *49*, 7558-7558.
52. Mesquida, N.; Lopez-Perez, S.; Dinares, I.; Frigola, J.; Merce, R.; Holenz, J.; Perez, R.; Burgueno, J.; Alcalde, E. Identification of Novel Indanylsulfonamide Guanylylhydrazones as Potent 5-HT₆ Serotonin Receptor Antagonists. *Journal of Medicinal Chemistry* **2009**, *52*, 6153-6157.
53. Kloubert, S.; Mathe-Allainmat, M.; Andrieux, J.; Sicsic, S.; Langlois, M. Synthesis of benzocycloalkane derivatives as new conformationally restricted ligands for melatonin receptors. *Bioorganic & Medicinal Chemistry Letters* **1998**, *8*, 3325-3330.
54. Drijfhout, W. J.; de Vries, J. B.; Homan, E. J.; Brons, H. F.; Copinga, S.; Gruppen, G.; Beresford, I. J. M.; Hagan, R. M.; Grol, C. J.; Westerink, B. H. C. Novel non-indolic melatonin receptor agonists differentially entrain endogenous melatonin rhythm and increase its amplitude. *European Journal of Pharmacology* **1999**, *382*, 157-166.
55. Jansen, J. M.; Copinga, S.; Gruppen, G.; Molinari, E. J.; Dubocovich, M. L.; Grol, C. J. The high affinity melatonin binding site probed with conformationally restricted ligands .1. Pharmacophore and minireceptor models. *Bioorgan Med Chem* **1996**, *4*, 1321-1332.
56. Mattson, R. J.; Catt, J. D.; Keavy, D.; Sloan, C. P.; Epperson, J.; Gao, Q.; Hodges, D. B.; Iben, L.; Mahle, C. D.; Ryan, E.; Yocca, F. D. Indanyl piperazines as melatonergic MT₂ selective agents. *Bioorganic & Medicinal Chemistry Letters* **2003**, *13*, 1199-1202.
57. Fukatsu, K.; Uchikawa, O.; Kawada, M.; Yamano, T.; Yamashita, M.; Kato, K.; Hirai, K.; Hinuma, S.; Miyamoto, M.; Ohkawa, S. Synthesis of a novel series of benzocycloalkene derivatives as melatonin receptor agonists. *Journal of Medicinal Chemistry* **2002**, *45*, 4212-4221.
58. Uchikawa, O.; Fukatsu, K.; Tokunoh, R.; Kawada, M.; Matsumoto, K.; Imai, Y.; Hinuma, S.; Kato, K.; Nishikawa, H.; Hirai, K.; Miyamoto, M.; Ohkawa, S. Synthesis of a novel series of tricyclic indan derivatives as melatonin receptor agonists. *Journal of Medicinal Chemistry* **2002**, *45*, 4222-4239.
59. Pellegrini-Giampietro, D. E.; Cozzi, A.; Peruginelli, F.; Leonardi, P.; Meli, E.; Pellicciari, R.; Moroni, F. 1-aminoindan-1,5-dicarboxylic acid and (S)-(+)-2-(3'-carboxybicyclo[1.1.1] pentyl)-glycine, two mGlu₁ receptor-preferring antagonists, reduce neuronal death in vitro and in vivo models of cerebral ischaemia. *European Journal of Neuroscience* **1999**, *11*, 3637-3647.
60. Pellicciari, R.; Luneia, R.; Costantino, G.; Marinozzi, M.; Natalini, B.; Jakobsen, P.; Kanstrup, A.; Lombardi, G.; Moroni, F.; Thomsen, C. 1-Aminoindan-1,5-Dicarboxylic Acid - a Novel Antagonist at Phospholipase C-Linked Metabotropic Glutamate Receptors. *Journal of Medicinal Chemistry* **1995**, *38*, 3717-3719.
61. Conn, P. J.; Jones, C. K. Promise of mGluR_{2/3} activators in psychiatry. *Neuropsychopharmacology* **2009**, *34*, 248-249.

62. Bonnefous, C.; Vernier, J. M.; Hutchinson, J. H.; Gardner, M. F.; Cramer, M.; James, J. K.; Rowe, B. A.; Daggett, L. P.; Schaffhauser, H.; Kamenecka, T. M. Biphenyl-indanones: Allosteric potentiators of the metabotropic glutamate subtype 2 receptor. *Bioorganic & Medicinal Chemistry Letters* **2005**, *15*, 4354-4358.
63. Harmar, A. J.; Marston, H. M.; Shen, S. B.; Spratt, C.; West, K. M.; Sheward, W. J.; Morrison, C. F.; Dorin, J. R.; Piggins, H. D.; Reubi, J. C.; Kelly, J. S.; Maywood, E. S.; Hastings, M. H. The VPAC(2) receptor is essential for circadian function in the mouse suprachiasmatic nuclei. *Cell* **2002**, *109*, 497-508.
64. Goetzl, E. J.; Voice, J. K.; Shen, S. B.; Dorsam, G.; Kong, Y.; West, K. M.; Morrison, C. F.; Harmar, A. J. Enhanced delayed-type hypersensitivity and diminished immediate-type hypersensitivity in mice lacking the inducible VPAC(2) receptor for vasoactive intestinal peptide. *P Natl Acad Sci USA* **2001**, *98*, 13854-13859.
65. Levinson, D. F.; Duan, J. B.; Oh, S.; Wang, K.; Sanders, A. R.; Shi, J. X.; Zhang, N.; Mowry, B. J.; Olincy, A.; Amin, F.; Cloninger, C. R.; Silverman, J. M.; Buccola, N. G.; Byerley, W. F.; Black, D. W.; Kendler, K. S.; Freedman, R.; Dudbridge, F.; Pe'er, I.; Hakonarson, H.; Bergen, S. E.; Fanous, A. H.; Holmans, P. A.; Gejman, P. V. Copy Number Variants in Schizophrenia: Confirmation of Five Previous Findings and New Evidence for 3q29 Microdeletions and VIPR2 Duplications. *Am J Psychiat* **2011**, *168*, 302-316.
66. Vacic, V.; McCarthy, S.; Malhotra, D.; Murray, F.; Chou, H. H.; Peoples, A.; Makarov, V.; Yoon, S.; Bhandari, A.; Corominas, R.; Iakoucheva, L. M.; Krastoshevsky, O.; Krause, V.; Larach-Walters, V.; Welsh, D. K.; Craig, D.; Kelsoe, J. R.; Gershon, E. S.; Leal, S. M.; Aquila, M. D.; Morris, D. W.; Gill, M.; Corvin, A.; Insel, P. A.; McClellan, J.; King, M. C.; Karayiorgou, M.; Levy, D. L.; DeLisi, L. E.; Sebat, J. Duplications of the neuropeptide receptor gene VIPR2 confer significant risk for schizophrenia. *Nature* **2011**, *471*, 499-503.
67. Asnicar, M. A.; Koster, A.; Heiman, M. L.; Tinsley, F.; Smith, D. P.; Galbreath, E.; Fox, N.; Ma, Y. L.; Blum, W. F.; Hsiung, H. M. Vasoactive intestinal polypeptide/pituitary adenylate cyclase-activating peptide receptor 2 deficiency in mice results in growth retardation and increased basal metabolic rate. *Endocrinology* **2002**, *143*, 3994-4006.
68. Chu, A.; Caldwell, J. S.; Chen, Y. A. Identification and characterization of a small molecule antagonist of human VPAC2 receptor. *Mol. Pharmacol.* **2010**, *77*, 95-101.
69. Odonnell, S. R.; Wanstall, J. C. Evidence That ICI 118, 551 Is a Potent, Highly Beta2-Selective Adrenoceptor Antagonist and Can Be Used to Characterize Beta-Adrenoceptor Populations in Tissues. *Life Sciences* **1980**, *27*, 671-677.
70. Baur, F.; Beattie, D.; Beer, D.; Bentley, D.; Bradley, M.; Bruce, I.; Charlton, S. J.; Cuenoud, B.; Ernst, R.; Fairhurst, R. A.; Faller, B.; Farr, D.; Keller, T.; Fozard, J. R.; Fullerton, J.; Garman, S.; Hatto, J.; Hayden, C.; He, H. D.; Howes, C.; Janus, D.; Jiang, Z. J.; Lewis, C.; Loeuillet-Ritzler, F.; Moser, H.; Reilly, J.; Steward, A.; Sykes, D.; Tedaldi, L.; Trifilieff, A.; Tweed, M.; Watson, S.; Wissler, E.; Wyss, D. The Identification of Indacaterol as an Ultralong-Acting Inhaled beta(2)-Adrenoceptor Agonist. *Journal of Medicinal Chemistry* **2010**, *53*, 3675-3684.
71. Beattie, D.; Beer, D.; Bradley, M. E.; Bruce, I.; Charlton, S. J.; Cuenoud, B. M.; Fairhurst, R. A.; Farr, D.; Fozard, J. R.; Janus, D.; Rosethorne, E. M.; Sandham, D. A.; Sykes, D. A.; Trifilieff, A.; Turner, K. L.; Wissler, E. An investigation into the structure-activity relationships associated with the systematic modification of the beta(2)-adrenoceptor agonist indacaterol. *Bioorganic & Medicinal Chemistry Letters* **2012**, *22*, 6280-6285.
72. Charo, I. F.; Ransohoff, R. M. The many roles of chemokines and chemokine receptors in inflammation. *The New England journal of medicine* **2006**, *354*, 610-21.
73. Serbina, N. V.; Pamer, E. G. Monocyte emigration from bone marrow during bacterial infection requires signals mediated by chemokine receptor CCR2. *Nat Immunol* **2006**, *7*, 311-317.
74. Dawson, T. C.; Kuziel, W. A.; Osahar, T. A.; Maeda, N. Absence of CC chemokine receptor-2 reduces atherosclerosis in apolipoprotein E-deficient mice. *Atherosclerosis* **1999**, *143*, 205-11.
75. Kim, Y. K.; Oh, H. B.; Lee, E. Y.; Gho, Y. S.; Lee, J. E.; Kim, Y. Y. Association between a genetic variation of CC chemokine receptor-2 and atopic asthma. *Allergy* **2007**, *62*, 208-9.
76. Fife, B. T.; Huffnagle, G. B.; Kuziel, W. A.; Karpus, W. J. CC chemokine receptor 2 is critical for induction of experimental autoimmune encephalomyelitis. *The Journal of experimental medicine* **2000**, *192*, 899-905.
77. Ogata, H.; Takeya, M.; Yoshimura, T.; Takagi, K.; Takahashi, K. The role of monocyte chemoattractant protein-1 (MCP-1) in the pathogenesis of collagen-induced arthritis in rats. *The Journal of pathology* **1997**, *182*, 106-14.
78. White, F. A.; Feldman, P.; Miller, R. J. Chemokine Signaling and the Management of Neuropathic Pain. *Molecular Interventions* **2009**, *9*, 188-195.
79. Vilums, M.; Zweemer, A. J.; Yu, Z.; de Vries, H.; Hillger, J. M.; Wapenaar, H.; Bollen, I. A.; Barmare, F.; Gross, R.; Clemens, J.; Krenitsky, P.; Brussee, J.; Stamos, D.; Saunders, J.; Heitman, L. H.; Ijzerman, A. P. Structure-

Kinetic Relationships-An Overlooked Parameter in Hit-to-Lead Optimization: A Case of Cyclopentylamines as Chemokine Receptor 2 Antagonists. *Journal of Medicinal Chemistry* **2013**, 56, 7706-7714.

80. Carter, P. H. Spiroindenes and spiroindanes as antagonists of CC chemokine receptor 2: WO 2009023754. *Expert Opin Ther Pat* **2010**, 20, 283-289.

81. Budzik, B. W.; Bury, M. J.; Gu, M.; Liu, R.; Ren, F.; Sehon, C. A.; Wang, G. Z.; Zhang, J. Spiroindenes and spiroindanes as modulators of chemokine receptors. WO2009023754, **2009**.

82. Budzik, B. W.; Haile, P. A.; Hughes, T. V.; Sehon, C. A.; Wang, G. Z. Spirodihydrobenzofurans as modulators of chemokine receptors WO2009061881, **2009**.

83. Steinhoff, M.; Buddenkotte, J.; Shpacovitch, V.; Rattenholl, A.; Moormann, C.; Vergnolle, N.; Luger, T. A.; Hollenberg, M. D. Proteinase-activated receptors: Transducers of proteinase-mediated signaling in inflammation and immune response. *Endocr Rev* **2005**, 26, 1-43.

84. Ossovskaya, V. S.; Bunnett, N. W. Protease-activated receptors: Contribution to physiology and disease. *Physiol Rev* **2004**, 84, 579-621.

85. Barry, G. D.; Suen, J. Y.; Le, G. T.; Cotterell, A.; Reid, R. C.; Fairlie, D. P. Novel Agonists and Antagonists for Human Protease Activated Receptor 2. *J. Med. Chem.* **2010**, 53, 7428-7440.

86. Weber, M. A.; Black, H.; Bakris, G.; Krum, H.; Linas, S.; Weiss, R.; Linseman, J. V.; Wiens, B. L.; Warren, M. S.; Lindholm, L. H. A selective endothelin-receptor antagonist to reduce blood pressure in patients with treatment-resistant hypertension: a randomised, double-blind, placebo-controlled trial. *Lancet* **2009**, 374, 1423-1431.

87. Cristol, J. P.; Warner, T. D.; Thiemermann, C.; Vane, J. R. Mediation Via Different Receptors of the Vasoconstrictor Effects of Endothelins and Sarafotoxins in the Systemic Circulation and Renal Vasculature of the Anesthetized Rat. *Brit J Pharmacol* **1993**, 108, 776-779.

88. Elliott, J. D.; Lago, M. A.; Cousins, R. D.; Gao, A. M.; Leber, J. D.; Erhard, K. F.; Nambi, P.; Elshourbagy, N. A.; Kumar, C.; Lee, J. A.; Bean, J. W.; Debrosse, C. W.; Eggleston, D. S.; Brooks, D. P.; Feuerstein, G.; Ruffolo, R. R.; Weinstock, J.; Gleason, J. G.; Peishoff, C. E.; Ohlstein, E. H. 1,3-Diarylindan-2-Carboxylic Acids, Potent and Selective Nonpeptide Endothelin Receptor Antagonists. *Journal of Medicinal Chemistry* **1994**, 37, 1553-1557.

89. Ohlstein, E. H.; Nambi, P.; Lago, A.; Hay, D. W. P.; Beck, G.; Fong, K. L.; Eddy, E. P.; Smith, P.; Ellens, H.; Elliott, J. D. Nonpeptide endothelin receptor antagonists .6. Pharmacological characterization of SE 217242, a potent and highly bioavailable endothelin receptor antagonist. *Journal of Pharmacology and Experimental Therapeutics* **1996**, 276, 609-615.

90. Bogeso, K. P.; Arnt, J.; Boeck, V.; Christensen, A. V.; Hyttel, J.; Jensen, K. G. Antihypertensive Activity in a Series of 1-Piperazino-3-Phenylindans with Potent 5-Ht2-Antagonistic Activity. *Journal of Medicinal Chemistry* **1988**, 31, 2247-2256.

91. Kowalski, T. J.; McBriar, M. D. Therapeutic potential of melanin-concentrating hormone-1 receptor antagonists for obesity the treatment of obesity. *Expert Opin Inv Drug* **2004**, 13, 1113-1122.

92. Handlon, A. L.; Zhou, H. Q. Melanin-concentrating hormone-1 receptor antagonists for the treatment of obesity. *Journal of Medicinal Chemistry* **2006**, 49, 4017-4022.

93. Erickson, S. D.; Banner, B.; Berthel, S.; Conde-Knape, K.; Falcioni, F.; Hakimi, I.; Hennessy, B.; Kester, R. F.; Kim, K.; Ma, C.; McComas, W.; Mennona, F.; Mischke, S.; Orzechowski, L.; Qian, Y.; Salari, H.; Teng, J.; Thakkar, K.; Taub, R.; Tilley, J. W.; Wang, H. Potent, selective MCH-1 receptor antagonists. *Bioorganic & Medicinal Chemistry Letters* **2008**, 18, 1402-1406.

94. Qian, Y. M.; Conde-Knape, K.; Erickson, S. D.; Falcioni, F.; Gillespie, P.; Hakimi, I.; Mennona, F.; Ren, Y. L.; Salari, H.; So, S. S.; Tilley, J. W. Potent MCH-1 receptor antagonists from cis-1,4-diaminocyclohexane-derived indane analogs. *Bioorganic & Medicinal Chemistry Letters* **2013**, 23, 4216-4220.

95. Sakairi, M.; Kogami, M.; Torii, M.; Kataoka, H.; Fujieda, H.; Makino, M.; Kataoka, D.; Okamoto, R.; Miyazawa, T.; Okabe, M.; Inoue, M.; Takahashi, N.; Harada, S.; Watanabe, N. Synthesis and SAR studies of bicyclic amine series GPR119 agonists. *Bioorganic & Medicinal Chemistry Letters* **2012**, 22, 5123-5128.

96. Itoh, Y.; Kawamata, Y.; Harada, M.; Kobayashi, M.; Fujii, R.; Fukusumi, S.; Ogi, K.; Hosoya, M.; Tanaka, Y.; Uejima, H.; Tanaka, H.; Maruyama, M.; Satoh, R.; Okubo, S.; Kizawa, H.; Komatsu, H.; Matsumura, F.; Noguchi, Y.; Shinobara, T.; Hinuma, S.; Fujisawa, Y.; Fujino, M. Free fatty acids regulate insulin secretion from pancreatic beta cells through GPR40. *Nature* **2003**, 422, 173-176.

97. Takeda http://www.takeda.com/news/2013/20130516_5780.html [accessed January 7th 2014].

98. Takeda http://www.takeda.com/news/2013/20131227_6117.html [accessed January 8th 2014].

99. Himmelsbach, F.; Eckhardt, M.; Langkopf, E.; Peters, S. Preparation of indanyloxydihydrobenzofuranylacetic acids as GPR40 modulators for treatment of metabolic disease. *US20130289074A1*, **2013**.
100. Kaku, K. Fasiglifam as a new potential treatment option for patients with type 2 diabetes. *Expert Opin Pharmacol* **2013**, *14*, 2591-2600.
101. Dezaki, K.; Sone, H.; Koizumi, M.; Nakata, M.; Kakei, M.; Nagai, H.; Hosoda, H.; Kangawa, K.; Yada, T. Blockade of pancreatic islet-derived ghrelin enhances insulin secretion to prevent high-fat diet-induced glucose intolerance. *Diabetes* **2006**, *55*, 3486-3493.
102. Bhattacharya, S. K.; Cameron, K. O. K.; Fernando, D. P.; Kung, D. W.-S.; Londregan, A. T.; McClure, K. F.; Simila, S. T. M. 2,3-Dihydro-1H-inden-1-yl-2,7-diazaspiro[3.6]nonane derivatives as ghrelin receptor antagonists or inverse agonists and their preparation and use for the treatment of ghrelin receptor-mediated diseases. *WO2011114271A1*, **2011**.
103. Brune, M. E.; O'Neill, A. B.; Gauvin, D. M.; Katwala, S. P.; Altenbach, R. J.; Brioni, J. D.; Hancock, A. A.; Sullivan, J. P. Comparison of alpha 1-adrenoceptor agonists in canine urethral pressure profilometry and abdominal leak point pressure models. *J Urology* **2001**, *166*, 1555-1559.
104. Whitlock, G. A.; Conlon, K.; McMurray, G.; Roberts, L. R.; Stobie, A.; Thurlow, R. J. Novel 2-imidazoles as potent and selective alpha(1A) adrenoceptor partial agonists. *Bioorganic & Medicinal Chemistry Letters* **2008**, *18*, 2930-2934.
105. Conlon, K.; Christy, C.; Westbrook, S.; Whitlock, G.; Roberts, L.; Stobie, A.; McMurray, G. Pharmacological Properties of 2-((R-5-Chloro-4-methoxymethylindan-1-yl)-1H-imidazole (PF-3774076), a Novel and Selective alpha 1(A)-Adrenergic Partial Agonist, in Vitro and in Vivo Models of Urethral Function. *Journal of Pharmacology and Experimental Therapeutics* **2009**, *330*, 892-901.
106. Roberts, L. R.; Bryans, J.; Conlon, K.; McMurray, G.; Stobie, A.; Whitlock, G. A. Novel 2-imidazoles as potent, selective and CNS penetrant alpha(1A) adrenoceptor partial agonists. *Bioorganic & Medicinal Chemistry Letters* **2008**, *18*, 6437-6440.
107. Makino, S.; Zaragoza, D. B.; Mitchell, B. F.; Robertson, S.; Olson, D. M. Prostaglandin F-2 alpha and its receptor as activators of human decidua. *Semin Reprod Med* **2007**, *25*, 60-68.
108. Lee, P. Y.; Shao, H.; Xu, L.; Qu, C. K. The Effect of Prostaglandin-F2-Alpha on Intraocular-Pressure in Normotensive Human-Subjects. *Invest Ophthalmol Vis Sci* **1988**, *29*, 1474-1477.
109. Lai, J.; Jin, H. K.; Yang, R. H.; Winer, J.; Li, W.; Yen, R.; King, K. L.; Zeigler, F.; Ko, A.; Cheng, J.; Bunting, S.; Paoni, N. F. Prostaglandin F-2 alpha induces cardiac myocyte hypertrophy in vitro and cardiac growth in vivo. *Am J Physiol-Heart C* **1996**, *271*, H2197-H2208.
110. Bryer, M. D.; Breyer, R. M. G protein-coupled prostanoid receptors and the kidney. *Annu Rev Physiol* **2001**, *63*, 579-605.
111. Griffin, B. W.; Klimko, P.; Crider, J. Y.; Sharif, N. A. AL-8810: A novel prostaglandin F-2 alpha analog with selective antagonist effects at the prostaglandin F-2 alpha (FP) receptor. *Journal of Pharmacology and Experimental Therapeutics* **1999**, *290*, 1278-1284.
112. Liang, Y. B.; Li, C.; Guzman, V. M.; Chang, W. W.; Evinger, A. J.; Pablo, J. V.; Woodward, D. F. Upregulation of orphan nuclear receptor Nur77 following PGF(2 alpha), Bimatoprost, and Butaprost treatments. Essential role of a protein kinase C pathway involved in EP2 receptor activated Nur77 gene transcription. *Brit J Pharmacol* **2004**, *142*, 737-748.

CHAPTER 3

STRUCTURE–KINETICS RELATIONSHIPS – AN OVERLOOKED PARAMETER IN HIT-TO-LEAD OPTIMIZATION: A CASE OF CYCLOPENTYLAMINES AS CCR2 ANTAGONISTS

This chapter was based upon:

M. Vilums, A.J.M. Zweemer, Z. Yu, H. de Vries, J.M. Hillger, H. Wapenaar, I.A.E. Bollen, F. Barmare, R. Gross, J. Clemens, P. Krenitsky, J. Brussee, D. Stamos, J. Saunders, L.H. Heitman, A. P. IJzerman. *Journal of Medicinal Chemistry* 2013, 56 (19), pp 7706–7714

ABSTRACT

Preclinical models of inflammatory diseases (e.g. neuropathic pain, rheumatoid arthritis and multiple sclerosis) have pointed to a critical role of the chemokine receptor CCR2 and chemokine ligand 2 (CCL2). However, one of the biggest problems of high affinity inhibitors of CCR2 is their lack of efficacy in clinical trials. We report a new approach for the design of high affinity and long residence time CCR2 antagonists. We developed a new competition association assay for CCR2, which allows us to investigate the relation of the structure of the ligand and its receptor residence time [i.e. structure–kinetic relationship (SKR)] next to a traditional structure–affinity relationship (SAR). By applying combined knowledge of SAR and SKR we were able to re-evaluate the hit-to-lead process of cyclopentylamines as CCR2 antagonists. Affinity-based optimization yielded compound **1** with good binding ($K_i = 6.8$ nM), but very short residence time (2.4 min). However, when the optimization was also based on residence time, the hit-to-lead process yielded compound **22a** – a new high affinity CCR2 antagonist (3.6 nM) with a residence time of 135 min.

INTRODUCTION

Chemokines are a class of chemoattractant cytokines and their main action is to control the trafficking and activation of leukocytes and other cell types for a range of inflammatory and noninflammatory conditions. One of these, monocyte chemoattractant protein-1 [MCP-1/chemokine ligand 2 (CCL2)], acts on monocytes, memory T cells, and basophils.¹ It creates a chemotactic gradient and activates the movement of immune cells to the site of inflammation by binding to its cell-surface receptor, CC chemokine receptor-2 (CCR2).² This CCL2/CCR2 pair is overexpressed in several inflammatory conditions in which excessive monocyte recruitment is observed. CCR2 and CCL2 knockout mice and CCR2 or CCL2 antibody-treated rodents show decreased recruitment of monocytes and produce considerably decreased inflammatory responses.³ This indicates CCR2 as potential target for treatment of several immune-based inflammatory diseases and conditions, such as multiple sclerosis,⁴ atherosclerosis,⁵ rheumatoid arthritis,⁶ diabetes,⁷ asthma,⁸ and neuropathic pain.⁹

In the past decade there has been an increasing interest in the development of small-molecule antagonists of the CCR2 receptor resulting in the disclosure of many different chemical classes. However, there are still no selective CCR2 antagonists on the market for the treatment of inflammatory diseases. Clinical trials so far have failed mostly due to lack of efficacy, including the one for the CCR2 antagonist MK-0812 (Figure 1).¹⁰

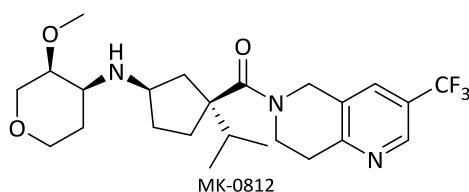


Figure 1. CCR2 antagonist MK-0812.

It has been suggested that binding kinetics, especially the lifetime of the ligand-receptor complex can be used as a predictor for drug efficacy and safety.^{11, 12} The concept of binding kinetics is often overlooked in the early phase of drug discovery, however, incorporation of this parameter could help to decrease the attrition rate in later stages of drug development.¹³

In this concept of kinetics an additional pharmacological parameter – the ligand-receptor residence time (RT, the reciprocal of the dissociation rate constant k_{off}) is defined,¹⁴ which is a measure for the duration that a ligand is bound to its target.

In this study we first evaluated several reference CCR2 antagonists using a recently developed competition association assay for CCR2 that yielded the respective association and dissociation rate constants. As our starting point we chose compound **1** which was also the lead compound in the process that led to the development of MK-0812 by the Merck group.¹⁰ The determination of the binding kinetics of several known structures with this particular scaffold subsequently allowed us to generate a new series of high affinity and long residence time CCR2 antagonists based on structure **2**, which was previously abandoned by other groups in optimization steps due to its modest binding affinity (Figure 2).¹⁵

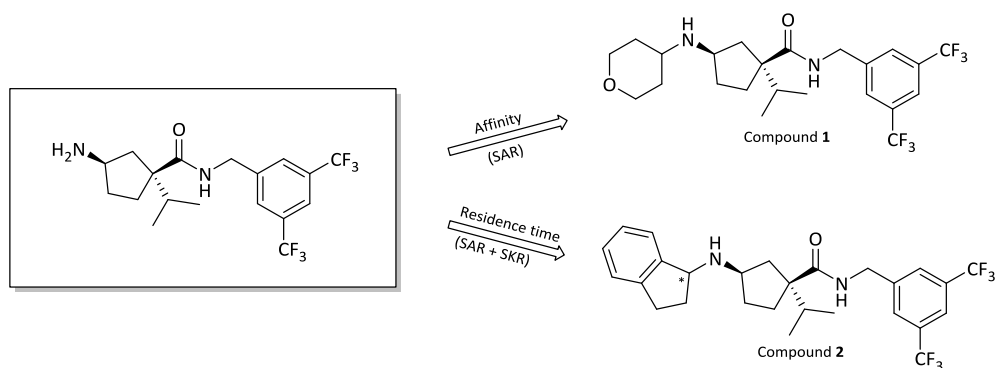


Figure 2. Residence time and affinity values are both pharmacological parameters that may, however, suggest different lead structures.

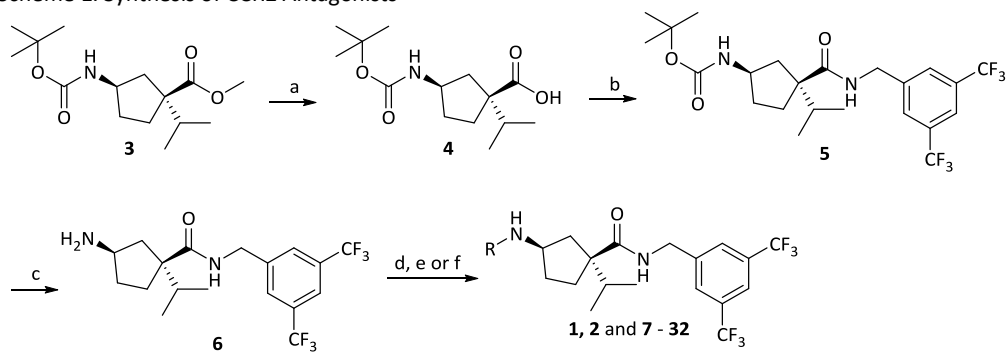
RESULTS AND DISCUSSION

Chemistry

Synthesis of (1*S*,3*R*)-methyl-3-((*tert*-butoxycarbonyl)amino)-1-isopropylcyclopentane carboxylate **3** was achieved following the synthetic approach reported by Kothandaraman et al.¹⁵ The desired *N*-Boc protected ester **3** was saponified to yield acid **4**. Subsequently acid **4** was used in peptide coupling reaction with 3,5-bis(trifluoromethyl)benzylamine to yield

amide **5** under bromo-tris-pyrrolidino phosphoniumhexafluorophosphate (PyBroP) conditions.¹⁶ Removal of the *N*-Boc group with trifluoroacetic acid (TFA) in DCM produced amine **6**. Reductive amination with different ketones under NaBH(OAc)₃ conditions afforded the desired products **1, 2**, and **11, 12**. Compounds **7 – 9** were synthesized by alkylating amine **6** with different alkylating agents. Compounds **10** and **13 – 32** were generated from amine **6** and an array of different ketones with 5-ethyl-2-methylpyridine borane complex (PEMB) under conditions reported by Burkhardt and Coleridge (Scheme 1).¹⁷

Scheme 1. Synthesis of CCR2 Antagonists^a



^aReagents and conditions: a) 4M LiOH aq., MeOH, reflux, 4h, 91%; b) 3,5-Bis(trifluoromethyl)benzylamine, PyBroP, DIPEA, DMAP, DCM, r.t., 24h, 83%; c) TFA, DCM, r.t., 1h, 85%; d) corresponding ketone, (AcO)₃BHNa, AcOH, DCE, r.t., 18h, 21-86% (compounds **1, 2**, and **11, 12**); e) corresponding alkylating agent, DiPEA, CH₃CN, 60 °C, 2h, 14-54% (compounds **7 – 9**); f) for array synthesis - corresponding ketone, 5-ethyl-2-methylpyridine borane (PEMB), AcOH, NMP, 65 °C, 24h, (compounds **10** and **13 – 32**).

Biology

To determine the binding affinity all compounds were tested in a ¹²⁵I-CCL2 displacement assay on human bone osteosarcoma (U2OS)-CCR2 membrane preparations as described previously by our group.¹⁸ Several methods can be used to determine ligand binding kinetics [e.g. a kinetic radioligand binding assay,¹⁹ surface plasmon resonance (SPR),²⁰ “two-step” competition binding assay,²¹ and “Tag-lite” Cisbio²²]. Most of these assays require special modifications of the target protein or the ligand. Therefore, we chose to use the competition association assay, as this assay allowed us to determine the kinetics of unlabeled ligands to the receptor expressed in membrane preparations. In our hands this is the most robust and accurate assay in order to measure kinetics of unlabeled ligands.

Validation of the [³H]INCB3344 Competition Association Assay for CCR2

A competition association assay was set up to determine the kinetic parameters of unlabeled ligands.²³ For this assay we used the radiolabeled small molecule CCR2 antagonist [³H]INCB3344²⁴ instead of the endogenous agonist protein radioligand ¹²⁵I-CCL2. Because of the large size of CCL2 (8600 Da) there is at best only a partial overlap in binding site with small molecule antagonists. Because the theoretical model of the competition association assay is based on the assumption that unlabeled and radiolabeled ligands should compete for the same binding site, we decided to use [³H]INCB3344 in our assay. This radioligand bears considerable chemical resemblance to the compounds reported in this study. We first validated this method by measuring the competition association of [³H]INCB3344 in the absence and presence of three different concentrations of INCB3344 (1-, 3- and 10-fold its *K_i*) (Figure 3).

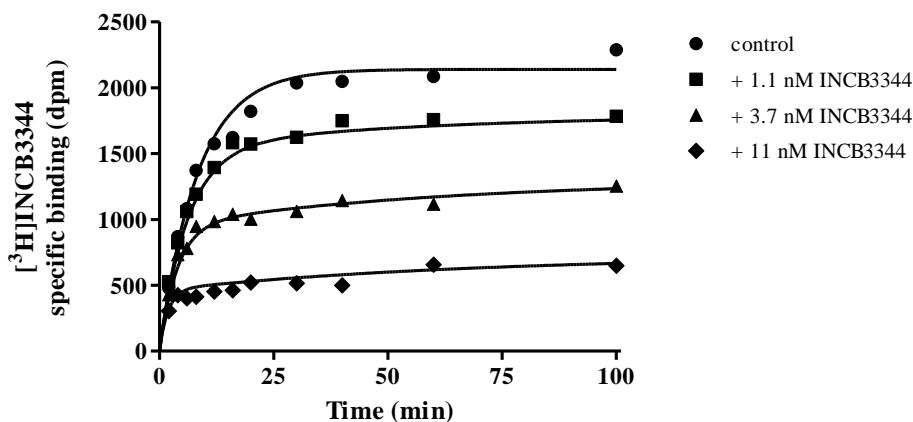


Figure 3. Competition association assay with [³H]INCB3344 at 25 °C in the absence or presence of 1.1, 3.7 and 11 nM of unlabeled INCB3344.

This resulted in a k_{on} and k_{off} values for unlabeled INCB3344 of $0.035 \pm 0.010 \text{ nM}^{-1} \cdot \text{min}^{-1}$ and $0.024 \pm 0.002 \text{ min}^{-1}$, respectively, at 25 °C (Table 1). The corresponding residence time was $43 \pm 2 \text{ min}$. These results were in good agreement with k_{on} and k_{off} values of [³H]INCB3344 binding from ‘traditional’ association and dissociation experiments, $0.054 \pm 0.002 \text{ nM}^{-1} \text{ min}^{-1}$ and 0.013 ± 0.002 respectively¹⁷ (Table 1).

Table 1. Comparison of equilibrium binding and kinetic parameters of INCB3344 determined using different methods.

Assay	K_D/K_i (nM)	k_{on} ($nM^{-1} min^{-1}$)	k_{off} (min^{-1})
Saturation binding ^a	0.90 ± 0.03	NA	NA
Displacement ^b	1.2 ± 0.1	NA	NA
Association and dissociation ^c	0.23 ± 0.04	0.054 ± 0.002	0.013 ± 0.002
Competition association ^d	0.72 ± 0.19	0.035 ± 0.010	0.024 ± 0.002

Data are presented as means \pm S.E.M. of three independent experiments performed in duplicate.

NA, not applicable

^aSaturation binding of 1- 45 nM [³H]INCB3344 to CCR2 at 25°C

^bDisplacement of 3.5 nM [³H]INCB3344 from CCR2 at 25°C

^cAssociation and dissociation of [³H]INCB3344 measured in standard kinetic assays at 25°C

^dAssociation and dissociation of INCB3344 measured in competition association assays at 25°C

Screening of CCR2 Antagonists Using the Dual-Point Competition Association Assay

The competition association assay described above is laborious and time consuming, and hence we developed a so-called dual point competition association assay for CCR2, according to principles we recently established for the adenosine A₁ receptor.²⁵ To this end we co-incubated [³H]INCB3344 with unlabeled antagonists at a concentration equal to their K_i value that was determined in the ¹²⁵I-CCL2 displacement assay. The so-called kinetic rate index (KRI) was calculated by dividing the specific radioligand binding at 50 min (t_1) by the binding at 240 min. (t_2). In this assay antagonists with a slower dissociation rate, and therefore a longer residence time than [³H]INCB3344 would result in a KRI > 1 (Figure 4).

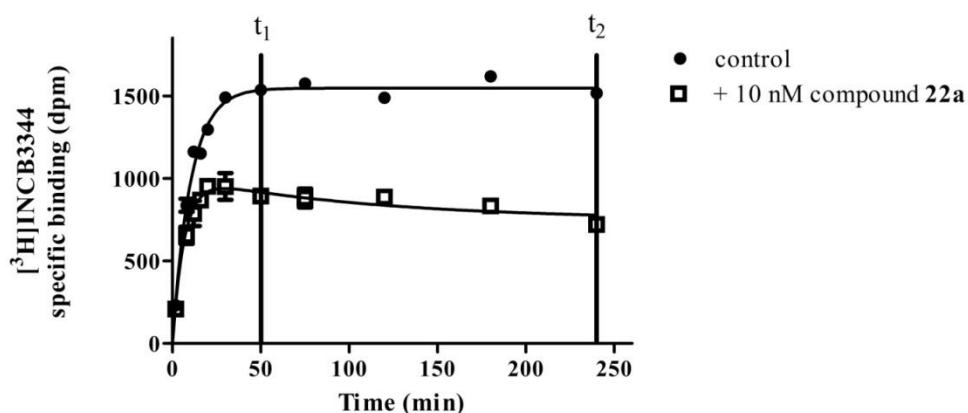


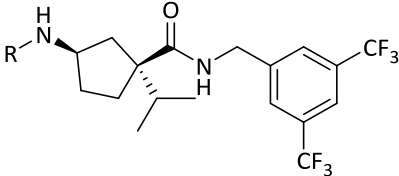
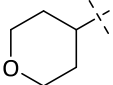
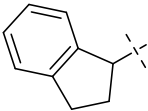
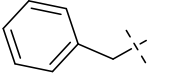
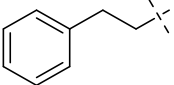
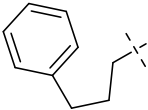
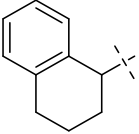
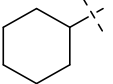
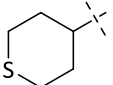
Figure 4. Representative competition association assay curves of control and long residence time compound **22a**. B_{t_1} : specific radioligand binding at the first time point ($t_1 = 50$ min); B_{t_2} : specific

radioligand binding at the second time point ($t_2 = 240$ min). Kinetic rate index (KRI) is defined as B_{t1}/B_{t2} , which equaled to 1.2 for compound **22a**.

Structure – Affinity Relationships Vs Structure – Residence Time Relationships

The 3-amino-1-isopropylcyclopentanecarboxamide scaffold has been extensively evaluated based on binding affinities for CCR2 and selectivity against other chemokine receptors and the hERG channel.^{15,26,27} Therefore, we decided to resynthesize several reported derivatives of compound **1**^{15,28} and determined their binding affinity in radioligand displacement assays (Table 2). Introduction of benzyl group yielded compound **7** with affinity of 437nM. When the spacer length between phenyl ring and basic nitrogen was extended to ethyl, binding was almost lost (compound **8** $K_i = 2400$ nM). Prolonging the chain to propyl allowed us to regain affinity (compound **9** $K_i = 134$ nM). Combining the knowledge of compounds **7** and **9** in one structure yielded the indane derivative compound **2** with even more improved affinity ($K_i = 50$ nM). Expanding the ring system to tetrahydronaphthalene resulted in additional increase in affinity (compound **10**, $K_i = 33$ nM). Removal of aromatics yielded compound **11** with cyclohexane ring which showed decrease in affinity ($K_i = 110$ nM), but incorporation of heteroatoms in 4- position regained affinity (compound **1** and **12**, $K_i = 6.8$ nM and $K_i = 31$ nM, respectively) as it was described by Kothandaraman et al.¹⁵ Based on affinity alone, compound **1** would be the logical choice for lead optimization which yielded the clinical candidate MK-0812 in the case of the Merck research group.¹⁰ However, the kinetic evaluation of these known structures in a competition association assay allowed us to utilize an additional parameter – residence time (RT). In this assay the best affinity compound **1** had a RT of 2.4 min, while compound **2** had a 4-fold longer RT of 9.5 min (Table 2). Structurally closely related compound **10** had a RT of 5.6 min, which convinced us to continue with compounds **2** and **10**, as they had longer RT.

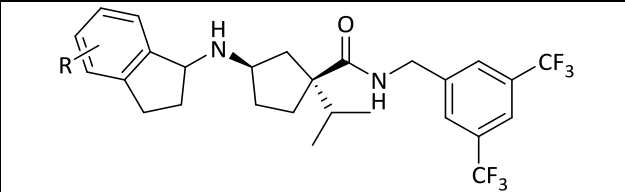
Table 2. Binding affinities and residence time (RT) of compounds **1**, **2**, **7** – **12**.

			
Nr.	R	K_i (nM) \pm SEM (n=3)	RT (min)
1		6.8 ± 2.2	2.4 ± 0.2
2		50 ± 8	9.5 ± 1.5
7		437 ± 62	-
8		2400 ± 900	-
9		134 ± 35	-
10		33 ± 2	5.6 ± 0.5
11		110 ± 13	1.9 ± 0.4
12		31 ± 9	4.3 ± 1.4

Using a number of commercially available indanones we introduced different substituents on the indane ring (Table 3) to cover chemical space as broadly as possible. The SAR exploration on the 4- position showed that H-bond accepting and hydrophilic groups are tolerated. The 4-NH₂ group led to a minor increase (compound **13**, $K_i = 43$ nM), but 4-OH and 4-CN groups showed a decrease in affinity (compound **14**, $K_i = 86$ nM and compound **15**, $K_i = 70$ nM). 4-Me (compound **16**) and 4-MeO (compound **17**) were not tolerated on this position (26% and 30%

displacement at 1 μM , respectively). On the 5- position methoxy and hydroxyl groups improved the affinity, which had also been suggested for other CCR2 antagonists.^{27,29} The methoxy group (compound **18**) showed an 8 fold increase in affinity (6.1 nM) while the hydroxyl group (compound **19**) displayed a less than 2-fold increase compared to the unsubstituted indenyl derivative (29 nM and 50 nM, respectively). On the contrary, the introduction of fluorine, which was previously reported as best substituent in arylpiperidine analogs by Pasternak et al,²⁷ resulted in a dramatic decrease in affinity in case of the indenyl derivative (compound **20**, 30% displacement at 1 μM). 5-Cl substitution yielded better affinity than 5-F (compound **21**, 18 nM) and 5-Br was better than 5-Cl (compound **22**, 7.2 nM). 6-Cl (compound **23**) led to a dramatic decrease in affinity (28% displacement at 1 μM). However, 6-Me and 6-CN groups were tolerated having similar affinities to unsubstituted indane ring (compound **24**, $K_i = 55$ nM and compound **25**, $K_i = 54$ nM).

Table 3. Binding affinities and Kinetic rate index (KRI) of indenyl derivatives **2** and **13 – 28**.

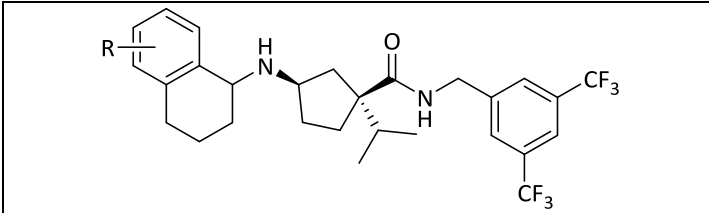
			
Nr.	R	K_i (nM) \pm SEM (n=3)	KRI (n=2)
2	H	50 \pm 8	0.7 (0.7/0.7)
13	4-NH ₂	43 \pm 7	0.8 (0.7/0.8)
14	4-OH	86 \pm 8	0.6 (0.5/0.8)
15	4-CN	70 \pm 11	0.8 (0.7/0.8)
16	4-Me	26 % ^a	-
17	4-OMe	30 % ^a	-
18	5-OMe	6.1 \pm 0.7	0.6 (0.6/0.6)
19	5-OH	29 \pm 2	0.7 (0.7/0.8)
20	5-F	30 % ^a	-
21	5-Cl	18 \pm 1	1.1 (1.1/1.2)
22	5-Br	7.2 \pm 0.5	1.1 (1.0/1.1)
23	6-Cl	28 % ^a	-
4	6-Me	55 \pm 2	0.8 (0.8/0.8)
25	6-CN	54 \pm 4	0.6 (0.6/0.6)
26	4;5-di OMe	130 \pm 6	-
27	5;6-di OMe	3.9 \pm 0.3	0.7 (0.7/0.7)
28	5;6-($-\text{OCH}_2\text{O}-$)	6.3 \pm 0.8	0.6 (0.6/0.7)

^a% displ. at 1 μM ¹²⁵I-CCL2

We continued the investigation with the analysis of disubstitution, learning that the combination of 4,5- substitution resulted in more than 2-fold decrease in affinity (compound **26**, $K_i = 130$ nM). On the contrary, the 5,6-dimethoxy group yielded compound **27** with a high affinity of 3.9 nM. Connecting the dimethoxy groups into a dioxolane ring yielded a small decrease in affinity (compound **28**, $K_i = 6.3$ nM).

Using the knowledge of the best position for substitution we continued the investigation on the 1,2,3,4-tetrahydronaphthalene ring by introducing substituents on the 5-position (Table 4). Electron donating groups showed very similar results to what we found for the indenyl moiety. Compounds **29** and **30** showed good affinity (27 nM and 35 nM, respectively), while electron withdrawing groups showed a decrease or complete lack of affinity (compounds **31** and **32**).

After SAR evaluation, the higher affinity compounds were screened in our kinetic assay to determine their KRI value (Guo et al.²⁵, see also Figure 2). A KRI value < 1 indicates that the residence time of a tested compound is shorter than the residence time of the radioligand (less than 43 min in this particular case). A KRI value > 1 reflects a residence time of more than 43 min.

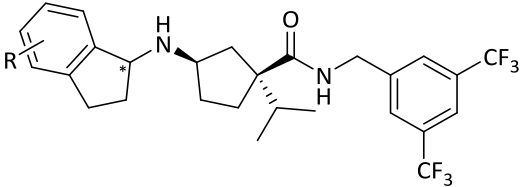
Table 4. Binding affinities and Kinetic rate index (KRI) of tetrahydronaphthalene derivatives **10** and **29** – **32**.


Nr.	R	K_i (nM) \pm SEM (n=3)	KRI
10	H	33 \pm 2	0.6 (0.6/0.5)
29	5-OMe	27 \pm 1	0.7 (0.7/0.8)
30	5-OH	35 \pm 2	0.8 (0.7/0.8)
31	5-Br	48% ^a	-
32	5-COOH	0% ^a	-

^a% displ. at 1 μ M ¹²⁵I-CCL2

Compound **2** in the screen showed a KRI value of 0.7 (RT = 9.5 min). However, compounds **21** and **22** had higher KRI values (1.1 for both compounds). These compounds were tested in a full competition association assay to determine their association and dissociation rate constant (Table 5). Increasing the size of the substituent – change from 5-Cl to 5-Br (compound **21** Vs compound **22**) also yielded longer residence times (56 min and 94 min, respectively). Compound **22** was separated in two diastereomers by preparative supercritical fluid chromatography (SFC) using Phenomenex Lux-4 column (Phenomenex Inc.). The first compound to elute (**22a**) had an affinity of 3.6 nM. However, the second compound (**22b**) to elute had a 100-fold decreased affinity (K_i = 289 nM). These separated diastereomers had very similar k_{off} rates (Table 5) which translated in similar residence times (**22a** RT = 135 min and **22b** RT = 77 min), but a significant difference was observed for their k_{on} rates. Apparently, the stereochemistry of the indane ring system has a major impact on compound association rate to the receptor while the dissociation is not affected.

Table 5. Kinetic data of compounds **21**, **22**, **22a** and **22b**.

					
Nr.	R	K_i (nM) \pm SEM (n=3)	k_{on} (nM ⁻¹ min ⁻¹)	k_{off} (min ⁻¹)	RT (min)
21	5-Cl	18 \pm 1	0.0027 \pm 0.0006	0.020 \pm 0.004	56 \pm 14
22	5-Br	7.2 \pm 0.5	0.010 \pm 0.002	0.011 \pm 0.0002	94 \pm 3
22a	5-Br	3.6 \pm 0.9	0.0053 \pm 0.0007	0.0074 \pm 0.0004	135 \pm 8
22b	5-Br	289 \pm 94	0.00030 \pm 0.00007	0.015 \pm 0.004	77 \pm 18

CONCLUSIONS

We have demonstrated that next to affinity, additional knowledge of residence time is useful for selecting and developing new CCR2 antagonists. The (1S, 3R)-N-(3,5-bis(trifluoromethyl)benzyl)-3-((5-bromo-2,3-dihydro-1H-inden-1-yl)amino)-1-isopropylcyclopentanecarboxamide (**22a**) had a RT of 135 min. In comparison to the best affinity compound from the first SAR screening, i.e. compound **1** (Table 1), **22a** had a 56-fold increased residence time, while having similar affinity. This indicates that affinity and residence time do not correlate; moreover, while SAR driven hit-to-lead optimizations often fail in later stages of drug development due to lack of efficacy (e.g. MK-0812), it has been shown on other targets that residence time is linked to the duration of the *in vivo* antagonist effect.³⁰⁻³² Compound **22a** may thus be a useful tool to test whether prolonged blockade of CCR2 has a beneficial effect on CCR2 related disorders, such as neuropathic pain.

EXPERIMENTAL SECTION

Chemistry

All solvents and reagents were purchased from commercial sources and were of analytical grade. Demineralised water is simply referred to as H₂O, as it was used in all cases unless stated otherwise (i.e. brine). ¹H and ¹³C NMR spectra were recorded on a Bruker AV 400 liquid spectrometer (¹H NMR, 400 MHz; ¹³C NMR, 100 MHz) or using a Bruker 500 MHz Avance III NMR spectrometer (compound **22a** and **22b**) at ambient temperature. Chemical shifts are reported in parts per million (ppm), are designated by δ and are downfield to the internal standard tetramethylsilane (TMS). Coupling-constants are reported

in Hz and are designated as *J*. Analytical purity of the final compounds was determined by high-performance liquid chromatography (HPLC) with a Phenomenex Gemini 3 μ m C18 110A column (50 x 4.6 mm, 3 μ m), measuring UV absorbance at 254 nm. Sample preparation and HPLC method for compounds **1**, **2**, **7** – **9** and **11**, **12** were as follows: 0.3-0.8 mg of compound was dissolved in 1 mL of a 1:1:1 mixture of CH₃CN/H₂O/*t*-BuOH and eluted from the column within 15 minutes at flow rate of 1.0 mL. Elution method was set up as follows: 1 – 4 min isocratic system of H₂O/CH₃CN/1% TFA in H₂O, 80/10/10, from 4th min a gradient was applied 80/10/10 to 0/90/10 within 9 min, followed by one minute of equilibration at 0/90/10 and one minute at 80/10/10. All compounds showed a single peak at the designated retention time and are at least 95% pure. High Resolution Mass spectral analyses (HRMS) were performed on LTQ-Orbitrap FTMS operated in a positive ionization mode with an ESI source. Mobile phase A: 0.1% formic acid in water. B: 0.08% formic acid in CH₃CN. Gradient: 10% B to 80% B in 26 min. Flow rate: 0.4 mL/min. Preparative HPLC's (for compounds **10**, **13** – **32**) were performed on a Waters AutoPurification HPLC-UV system with a diode array detector using a Luna C18 Phenomenex column (75mm x 30mm, 5 μ m), and a linear gradient from 1 to 99% of mobile phase B was applied. Mobile phase A consisted of 5 mM HCl solution and mobile phase B consisted of acetonitrile. Flow rate was 50 mL/min. LC-MS analyses were performed using an Onyx C18 monolithic column (50mm x 4.6mm, 5 μ m), and a linear gradient from 1 to 99% mobile phase B was applied. Mobile phase A consisted of 0.05% TFA in water and mobile phase B consisted of 0.035% TFA in acetonitrile. Flow rate was 12 mL/min. Separations of enantiomers were accomplished using chiral SFC. The column was Phenomenex Lux-4 (250 x 10 mm), 5 μ m. The mobile phase condition of 10% MeOH with 20 mM NH₃ and 90% CO₂ was applied at a flow rate of 10.0 mL/min. Thin-layer chromatography (TLC) was routinely consulted to monitor the progress of reactions, using aluminium-coated Merck silica gel F²⁵⁴ plates. Purification by column chromatography was achieved by use of Grace Davison DAVISIL silica column material (LC60A 30-200 micron). The procedure for a series of similar compounds is given as a general procedure for all within that series, annotated by the numbers of the compounds.

Synthesis of (1*S*,3*R*)-methyl-3-((*tert*-butoxycarbonyl)amino)-1-isopropylcyclopentanecarboxylate (**3**) was achieved following the synthetic approach reported by Kothandaraman S. et al.¹⁵

(1*S*,3*R*)-3-((*tert*-butoxycarbonyl)amino)-1-isopropylcyclopentanecarboxylic acid (**4**). A solution of ester **3** (4.20 g, 14.72 mmol) in EtOH (30 mL) and 4 M aqueous lithium hydroxide (LiOH_{aq}, 40 mL) was refluxed for 4 hours. After concentration in vacuum, the solution was acidified with aqueous hydrochloric acid and extracted with DCM/H₂O. The organic layer was dried over MgSO₄ and after concentration in vacuum, yielded the desired product as a yellow powder (3.62 g, 91%). ¹H NMR (400 MHz, CDCl₃): δ : 10.75 (s, 1H), 6.53^{*a*} (s, 0.5H), 5.05^{*b*} (s, 0.5H), 3.98 – 3.78 (m, 1H), 2.25 – 1.50 (m, 7H), 1.40 (d, *J* = 16.8 Hz, 9H), 0.86 (d, *J* = 6.8 Hz, 6H); ¹³C NMR (100 MHz, CDCl₃): δ : 182.9^{*a*}, 181.7^{*b*}, 157.6^{*b*}, 155.6^{*a*}, 80.4^{*b*}, 79.1^{*a*}, 56.9, 52.8^{*b*}, 51.7^{*a*}, 38.6^{*b*}, 38.2^{*a*}, 35.0^{*b*}, 34.5^{*a*}, 33.2^{*a*}, 32.9^{*b*}, 32.1^{*a*}, 31.8^{*b*}, 28.3, 18.7, 18.2^{*b*}, 18.0^{*a*}. *a* and *b* is indicated for different rotamers.

Tert-butyl(3-((3,5-bis(trifluoromethyl)benzyl)carbamoyl)-3-isopropylcyclopentyl) carbamate (**5**). Compound **4** (1.53 g, 5.65 mmol) was dissolved in 50 ml DCM. To this mixture 3,5 bis(trifluoromethyl) benzylamine (1.89 g, 5.65 mmol) was added with DiPEA (2.95 mL, 16.9 mmol), PyBrOP (2.64 g, 5.65 mmol) and DMAP (0.55 g, 4.5 mmol). The reaction mixture was stirred for 24 hours at room temperature. The product was extracted with DCM/citric acid solution in water and then with DCM/1M NaOH. The organic layer was dried with MgSO₄ and evaporated. The product was purified by column chromatography (0-100% ethyl acetate in DCM) to give the product as a yellow oil (2.33 g, 83%). ¹H NMR (400 MHz, CDCl₃): δ : 7.69 (s, 3H), 7.25 (br.s, 1H), 5.17 (br.s, 1H), 4.51 – 4.49 (m, 2H), 3.81 (br.s, 1H), 1.99-1.90 (m, 4H), 1.69-1.72 (m, 2H), 1.50-1.58 (m, 1H), 1.36 (s, 9H), 0.74-0.77 (m, 6 H). ¹³C NMR (100 MHz, CDCl₃): δ : 178.6, 155.6, 142.1, 132.2, 131.8, 131.5, 131.2, 127.4, 127.3, 124.5, 121.8, 121.0, 119.1, 78.9, 57.6, 51.6, 42.8, 36.3, 34.6, 33.3, 32.6, 28.2, 18.7, 17.5.

3-amino-N-(3,5-bis(trifluoromethyl)benzyl)-1-isopropylcyclopentanecarboxamide (6). Trifluoroacetic acid (20 mL) was added to a solution of compound **5** (2.33 g 4.6 mmol) in 50 mL DCM. The reaction mixture was stirred for 1 hour at room temperature. The reaction mixture was neutralized with 1M NaOH and extracted with DCM. The organic layer was dried with MgSO₄, filtered and evaporated to give the product as a yellow crystals (1.55 g, 85%). ¹H NMR (400 MHz, CDCl₃): δ: 9.16 (br.s, 1H), 7.70-7.67 (m, 3H), 4.50-4.39 (m, 2H), 3.61-3.60 (m, 1H), 2.22-2.15 (m, 1H), 2.02-1.95 (m, 1H), 1.85-1.64 (m, 3H), 1.42-1.37 (m, 2H), 0.82-0.80 (m, 6H). ¹³C NMR (100 MHz, CDCl₃): δ: 179.4, 142.5, 131.8, 131.5, 131.2, 130.9, 127.3, 127.2, 124.6, 121.9, 120.4, 119.2, 57.3, 52.2, 42.4, 39.7, 35.3, 33.9, 33.6, 18.8, 16.9.

General procedure for the synthesis of compounds 1, 2, and 11, 12.

Amine **6** was dissolved in 4 mL dichloroethane in a 5 mL reaction tube and the corresponding ketone (1 eq.) was added. Sequentially acetic acid (1 eq.) and sodium triacetoxyborohydride (1.5 eq.) were added. The reaction mixture was stirred for 18 hours at room temperature and then washed with 1M NaOH and H₂O. The organic layer was dried with MgSO₄, filtered and evaporated. The product was purified by column chromatography (0-100% ethyl acetate in DCM) to give the desired product.

(1S,3R)-N-(3,5-bis(trifluoromethyl)benzyl)-1-isopropyl-3-((tetrahydro-2H-pyran-4-yl)amino)cyclopentanecarboxamide (1). Yield = 21%. ¹H NMR (400 MHz, CDCl₃): δ: 9.16 (s, 1H), 7.76-7.73 (m, 3H), 4.56-4.53 (m, 2H), 3.98-3.89 (m, 2H), 3.57-3.53 (m, 1H), 3.43-3.28 (m, 2H), 2.66-2.61 (m, 1H), 2.36-2.30 (m, 1H), 2.03-1.80 (m, 2H), 1.78 – 1.6 (m, 5H), 1.49-1.40 (m, 1H), 1.31-1.20 (m, 3H), 0.93-0.89 (m, 6H); ¹³C NMR (400 MHz, CDCl₃): δ: 179.1, 142.4, 131.8, 131.54, 131.2, 130.9, 127.7, 127.3, 124.6, 121.8, 121.0, 119.2, 66.9, 66.9, 57.5, 54.8, 51.9, 42.6, 37.1, 35.1, 34.3, 33.7, 33.6, 33.3, 19.5, 17.0; LC/MS: 481⁺; t_R = 7.01 min

(1S,3R)-N-(3,5-bis(trifluoromethyl)benzyl)-3-((2,3-dihydro-1H-inden-1-yl)amino)-1-isopropylcyclopentanecarboxamide (2). Yield = 25% (mixture of diastereomers). ¹H NMR (400 MHz, CDCl₃): δ: 9.48 (s, 1H), 7.76-7.74 (m, 3H), 7.22 - 7.05 (m, 4H), 4.60-4.50 (m, 2H), 4.28-4.22 (m, 1H), 3.70-3.60 (m, 1H), 3.00-2.90 (m, 1H), 2.87-2.78 (m, 1H), 2.70-2.34 (m, 3H), 2.1-1.53 (m, 6H), 0.93-0.89 (m, 6H); ¹³C NMR (400 MHz, CDCl₃): δ: 179.4, 144.5, 144.4, 144.6, 131.8, 131.5, 127.9, 127.6, 126.3, 126.2, 125.0, 123.5, 123.5, 122.0, 121.9, 61.3, 58.0, 56.6, 42.6, 37.2, 36.0, 34.5, 33.9, 33.7, 33.4, 19.6, 17.0; LC/MS: 513⁺; t_R = 8.12 min

(1S,3R)-N-(3,5-bis(trifluoromethyl)benzyl)-3-(cyclohexylamino)-1-isopropylcyclopentane-1-carboxamide (11). Yield = 76%. ¹H NMR (400 MHz, CDCl₃): δ: 9.77 (br.s, 1H), 7.73 (s, 3H), 4.58-4.43 (m, 2H), 3.53-3.50 (m, 1H), 2.43-2.30 (m, 2H), 2.00-1.40 (m, 12H), 1.25-1.10 (m, 3H), 0.93-0.89 (m, 8H); ¹³C NMR (400 MHz, CDCl₃): δ: 179.55, 142.64, 132.12, 131.79, 131.46, 131.13, 127.74, 127.63, 124.66, 121.95, 120.81, 119.10, 57.30, 55.36, 54.48, 42.49, 36.95, 35.41, 34.12, 33.74, 33.37, 32.97, 25.83, 25.02, 19.48, 16.80; LC/MS: 479⁺; t_R = 7.31 min.

(1S,3R)-N-(3,5-bis(trifluoromethyl)benzyl)-1-isopropyl-3-((tetrahydro-2H-thiopyran-4-yl)amino)cyclopentane-1-carboxamide (12). Yield = 86%. ¹H NMR (400 MHz, CDCl₃): δ: 9.12 (br.s, 1H), 7.76 (s, 1H) 7.75 (s, 2H), 4.56-4.50 (m, 2H), 2.60-2.57 (m, 4H), 2.42-2.38 (m, 1H), 2.34-2.30 (m, 1H), 2.20-1.70 (m, 7H), 1.48 – 1.27 (m, 4H), 0.93-0.89 (m, 6H); ¹³C NMR (400 MHz, CDCl₃): δ: 179.08, 142.41, 131.83, 131.54, 131.16, 130.86, 127.75, 127.31, 124.53, 121.94, 121.05, 119.22, 57.50, 54.85, 53.92, 42.58, 37.28, 35.21, 35.08, 34.62, 33.53, 33.30, 27.93, 19.49, 17.01; LC/MS: 497⁺; t_R = 7.51 min.

General procedure for the synthesis of compounds 7 – 9.

Amine **6** (1 eq.) was dissolved in 4 mL of acetonitrile and corresponding alkylating agent (1.2 eq.) was added. Sequentially DiPEA (1.2 eq.) The reaction mixture was stirred in microwave for 2 hours at 60°C and purified with column chromatography (60% ethylacetate, 20 % DCM, 20% petroleum ether and 0-3% triethylamine in ethyl acetate).

(1S,3R)-3-(benzylamino)-N-(3,5-bis(trifluoromethyl)benzyl)-1-isopropylcyclopentane-1-carboxamide (7). Yield = 27% (as HCl salt). ¹H NMR (400 MHz, CDCl₃): δ: 9.40 (br.s, 1H), 7.73 (s, 1H), 7.66 (s, 2H), 7.30 – 7.24 (m, 3H), 7.16 – 7.13 (m, 2H), 4.44 (d, J = 4.8 Hz, 2H), 3.73 (d, J = 2.4 Hz, 2H), 3.46 – 3.41 (m, 1H),

2.41 – 2.33 (m, 1H), 2.02 – 1.90 (m, 4H), 1.85 – 1.78 (m, 2H), 1.59 – 1.52 (m, 1H), 0.91 (dd, $J = 10.8$ Hz, $J^2 = 6.8$ Hz, 6H). ^{13}C NMR (100 MHz, CDCl_3) δ : 179.4, 142.6, 139.0, 132.0, 131.7, 131.3, 131.0, 128.6, 127.8, 127.5, 127.3, 124.6, 121.9, 120.8, 58.8, 58.7, 57.3, 51.9, 42.5, 35.3, 33.5, 33.1, 19.5, 16.9; LC-MS: 487⁺; t_{R} : 7.40 min

(1*S*,3*R*)-*N*-(3,5-bis(trifluoromethyl)benzyl)-1-isopropyl-3-(phenethylamino)cyclopentane-1-carboxamide (**8**). Yield = 14% (as HCl salt). ^1H NMR (400 MHz, MeOD) δ : 8.01 – 7.84 (m, 3H), 7.43 – 7.23 (m, 5H), 4.53(dd, $J = 22.4$ Hz, $J^2 = 15.2$ Hz, 2H), 3.70 – 3.59 (m, 1H), 3.28 – 3.15 (m, 2H), 3.06 – 2.94 (m, 2H), 2.30 – 1.97 (m, 5H), 1.97 – 1.79 (m, 1H), 1.60 – 1.46 (m, 1H), 0.90 (dd, $J = 29.0$, $J^2 = 6.7$ Hz, 6H); ^{13}C NMR (101 MHz, MeOD) δ : 178.60, 142.70, 136.26, 131.49, 131.16, 131.06, 130.66, 128.80, 128.64, 128.40, 127.96, 127.88, 127.28, 126.92, 124.57, 121.86, 120.47, 118.59, 58.13, 57.98, 48.24, 48.03, 47.82, 47.60, 47.39, 47.18, 46.97, 42.32, 32.82, 32.44, 32.20, 32.03, 28.94, 17.83, 16.32; LC/MS: 501⁺; t_{R} = 6.51 min.

(1*S*,3*R*)-*N*-(3,5-bis(trifluoromethyl)benzyl)-1-isopropyl-3-((3-phenylpropyl)amino)cyclopentane-1-carboxamide (**9**). Yield = 54% (as HCl salt). ^1H NMR (400 MHz, CDCl_3) δ : 9.49 (br.s, 1H), 7.75 (s, 3H), 7.28 (t, $J = 7.6$ Hz, 2H), 7.20 (t, $J = 7.6$ Hz, 1H), 7.08 (d, $J = 7.6$ Hz, 2H), 4.56 – 4.45 (m, 2H), 3.33 – 3.27 (m, 1H), 2.6 – 2.54 (m, 4H), 2.39 – 2.32 (m, 1H), 2.00 – 1.45 (m, 10H), 0.91 (dd, $J = 10.8$ Hz, $J^2 = 6.8$ Hz, 6H). ^{13}C NMR (100 MHz, CDCl_3) δ : 179.4, 142.5, 141.4, 132.0, 131.7, 131.4, 131.1, 128.3, 128.1, 127.4, 125.9, 124.6, 121.9, 120.7, 59.1, 57.2, 47.5, 42.5, 36.2, 35.2, 33.5, 33.4, 31.6, 19.4, 16.8; LC/MS: 515⁺; t_{R} = 7.94 min.

General procedure for the synthesis of compounds 10 and 13 – 32.

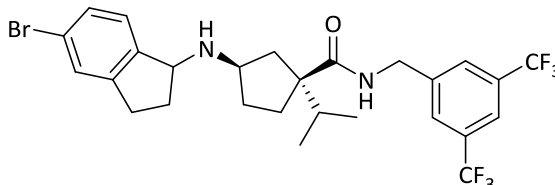
To a series of 1.5 mL glass tubes was added amine **6** in *N*-methyl-2-pyrrolidone (NMP) (0.95 M, 0.095 mmol) followed by solutions of different ketones (0.5 M, 0.1 mmol) in NMP and these mixtures were subsequently treated with acetic acid (0.1 mmol) followed by 5-ethyl-2-methyl-pyridine borane (PEMB) (0.2 mmol). The reaction mixture was heated at 65 °C on a reaction block for 24 h. The reaction mixtures were purified directly using an automated mass-guided reverse phase-HPLC, and product containing fractions were concentrated to give final products >90% purity as judged by LC-MS (average of 220 nm and 254 nm traces).

Purity, M^+ and retention times of compounds **10**, **13** – **32**.

Nr.	R	% Purity (Average of 220 and 254 nm)	Mol wt	M^+	Retention time (min)
10	H	95.8	526.6	527.3	1.79
13	4-NH ₂	99.7	527.5	528.3	1.48
14	4-OH	97.4	528.5	529.2	1.64
15	4-CN	96.4	537.2	538.2	1.69
16	4-Me	90.4	526.6	527.3	1.81
17	4-OMe	90.9	542.6	543.2	1.79
18	5-OMe	95.8	542.6	543.2	1.77
19	5-OH	95.1	528.5	529.2	1.71
20	5-F	93.4	530.5	531.3	1.79
21	5-Cl	94.9	546.9	547.0	1.85
22	5-Br	92.0	591.4	591.0	1.80
22a	5-Br	99.5 (99.0% de)	591.4	591.3	1.83
22b	5-Br	98.5 (96.9% de)	591.4	591.3	1.87
23	6-CN	97.1	537.5	538.2	1.71
24	6-Me	93.3	526.6	527.3	1.76

25	6-Cl	95.2	546.9	547.0	1.83
26	4;5-di OMe	94.6	572.6	573.2	1.67
27	5;6-di OMe	97.2	572.6	573.2	1.64
28	5;6-(-OCH ₂ O-)	94.8	556.5	557.2	1.68
29	5-OMe	95.7	556.6	557.2	1.78
30	5-OH	93.1	542.6	543.1	1.68
31	5-Br	90.6	605.5	605.1	1.90
32	5-COOH	94.7	570.6	571.2	1.65

(1*R*,3*S*)-*N*-[[3,5-bis(trifluoromethyl)phenyl]methyl]-3-[(5-bromoindan-1-yl)amino]-1-isopropylcyclopentanecarboxamide (**22a**)



¹H NMR (500 MHz, DMSO-*d*₆) δ: 8.56 (t, *J* = 6.0 Hz, 1H), 7.94 (d, *J* = 4.5 Hz, 3H), 7.38 (d, *J* = 1.9 Hz, 1H), 7.26 (dd, *J* = 8.0, 1.9 Hz, 1H), 7.12 (d, *J* = 8.0 Hz, 1H), 4.50 (dd, *J* = 15.6, 5.9 Hz, 1H), 4.43 (dd, *J* = 15.6, 5.9 Hz, 1H), 4.03 (t, *J* = 6.9 Hz, 1H), 3.19 (q, *J* = 6.7 Hz, 1H), 2.88 (ddd, *J* = 16.1, 8.4, 4.3 Hz, 1H), 2.69 (dt, *J* = 15.9, 7.9 Hz, 1H), 2.29 (m, 1H), 2.13 (ddd, *J* = 13.1, 7.3, 4.1 Hz, 1H), 2.12 (m, 1H), 1.87 (m, 2H), 1.81 (dtd, *J* = 10.4, 6.8, 3.9 Hz, 1H), 1.66 (dq, *J* = 12.3, 7.8 Hz, 1H), 1.64 (dq, *J* = 12.3, 7.8 Hz, 1H), 1.32 (m, 1H), 0.80 (d, *J* = 6.1 Hz, 3H), 0.76 (d, *J* = 6.1 Hz, 3H).

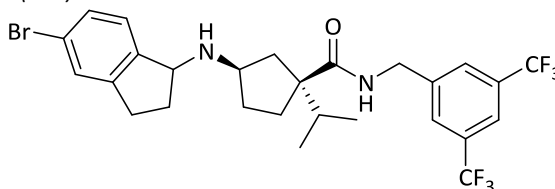
¹⁹F NMR (376 MHz, CDCl₃) δ: -62.87.

¹³C NMR (125 MHz, DMSO-*d*₆) δ: 177.97, 146.42, 145.85, 144.56, 130.77 (d, *J*_{C-F} = 32.6 Hz), 130.25 (d, *J*_{C-F} = 32.6 Hz), 129.06, 128.36, 128.36, 127.74, 126.32, 123.77 (q, *J*_{C-F} = 222.65 Hz), 123.77 (q, *J*_{C-F} = 222.65 Hz), 120.72, 120.32, 60.93, 57.27, 56.97, 42.63, 40.13, 34.53, 33.13, 32.90, 30.82, 30.17, 18.83, 18.32.

HRMS calc. for (C₂₇H₂₉BrF₆N₂O) [M + H]⁺ 591.1440, found 591.1444.

SFC chiral purity: 99.5 (99.0% de), [α]_D²⁰ = + 12.2 (c = 0.23, CHCl₃).

(1*R*,3*S*)-*N*-[[3,5-bis(trifluoromethyl)phenyl]methyl]-3-[(5-bromoindan-1-yl)amino]-1-isopropylcyclopentanecarboxamide (**22b**)



¹H NMR (500 MHz, DMSO-*d*₆) δ: 8.56 (t, *J* = 6.0 Hz, 1H), 7.94 (bs, 2H), 7.92 (bs, 1H), 7.38 (d, *J* = 1.9 Hz, 1H), 7.26 (dd, *J* = 8.0, 1.9 Hz, 1H), 7.12 (d, *J* = 8.0 Hz, 1H), 4.50 (dd, *J* = 15.6, 5.9 Hz, 1H), 4.43 (dd, *J* = 15.6, 5.9 Hz, 1H), 4.13 (t, *J* = 6.9 Hz, 1H), 3.19 (q, *J* = 6.7 Hz, 1H), 2.88 (ddd, *J* = 16.1, 8.4, 4.3 Hz, 1H), 2.69 (dt, *J* = 15.9, 7.9 Hz, 1H), 2.29 (m, 1H), 2.13 (ddd, *J* = 13.1, 7.3, 4.1 Hz, 1H), 2.12 (m, 1H), 1.82 - 2.00 (m, 2H), 1.81 (dtd, *J* = 10.4, 6.8, 3.9 Hz, 1H), 1.66 (dq, *J* = 12.3, 7.8 Hz, 1H), 1.64 (dq, *J* = 12.3, 7.8 Hz, 1H), 1.32 (m, 1H), 0.80 (d, *J* = 6.1 Hz, 3H), 0.76 (d, *J* = 6.1 Hz, 3H).

¹⁹F NMR (376 MHz, CDCl₃) δ: -62.89.

¹³C NMR (125 MHz, DMSO-*d*₆) δ : 177.97, 146.42, 144.56, 144.50, 130.77 (d, J_{C-F} = 32.6 Hz), 130.25 (d, J_{C-F} = 32.6 Hz), 129.06, 128.36, 128.36, 127.74, 126.32, 123.77 (q, J_{C-F} = 222.65 Hz), 123.77 (q, J_{C-F} = 222.65 Hz), 120.72, 120.32, 60.93, 57.27, 56.97, 42.63, 38.42, 34.53, 33.13, 32.90, 30.82, 30.17, 18.83, 18.32.

HRMS calc. for (C₂₇H₂₉BrF₆N₂O) [M + H]⁺ 591.1440, found 591.1437

SFC chiral purity: 98.5 (96.9% de), $[\alpha]_D^{20}$ = - 31.2 (c = 0.17, CHCl₃).

Biology

Chemicals and reagents. ¹²⁵I-CCL2 (2200 Ci/mmol) was purchased from Perkin-Elmer (Waltham, MA). INCB3344 was synthesized as described previously.^{33,34} [³H]INCB3344 (specific activity 32Ci mmol⁻¹) was custom-labeled by Vitrox (Placentia, CA) for which a dehydrogenated precursor of INCB3344 was provided. TangoTM CCR2-*bla* U2OS cells stably expressing human CCR2 were obtained from Invitrogen (Carlsbad, CA).

Cell culture and membrane preparation. U2OS cells stably expressing the human CCR2 receptor (Invitrogen, Carlsbad, CA) were cultured in McCoy5a medium supplemented with 10% fetal calf serum, 2 mM glutamine, 0.1 mM non-essential amino acids (NEAA), 25 mM HEPES, 1 mM sodium pyruvate, 100 IU/ml penicillin, 100 μ g/ml streptomycin, 100 μ g/ml G418, 50 μ g/ml hygromycin and 125 μ g/ml zeocin in a humidified atmosphere at 37°C and 5% CO₂. Cell culture and membrane preparation were performed as described previously.¹⁸

¹²⁵I-CCL2 displacement assay. Binding assays were performed as described previously.¹⁸

[³H]INCB3344 competition association assay. The kinetic parameters of unlabelled ligands at 25°C were determined using the competition association assay described by Motulsky and Mahan.²³ At different time points 10 μ g U2OS-CCR2 membranes were added to 1.8 nM [³H]INCB3344 in a total volume of 100 μ L assay buffer in the absence or presence of competing ligand. To validate the assay three concentrations of INCB3344 (1-, 3- and 10-fold its K_i value of [³H]INCB3344 displacement) were used. This validation showed that using a single concentration (that equals the K_i) of unlabeled ligand was sufficient to accurately measure k_{on} and k_{off} . Incubation was terminated by dilution with ice-cold 50 mM Tris-HCl buffer supplemented with 0.05% CHAPS. Separation of bound from free radioligand was performed by rapid filtration through a 96-well GF/B filter plate pre-coated with 0.25% PEI using a Perkin Elmer Filtermate-harvester (Perkin Elmer, Groningen, the Netherlands). Filters were washed ten times with ice-cold wash buffer. 25 μ L of Microscint scintillation cocktail (Perkin-Elmer, Waltham, MA) was added to each well and the filter-bound radioactivity was determined by scintillation spectrometry using the P-E 1450 Microbeta Wallac Trilux scintillation counter (Perkin Elmer). Kinetic parameters of unlabeled ligands were calculated by using equation (3) as mentioned below in "Data analysis".

[³H]INCB3344 dual point competition association assay. Kinetic rate index (KRI) values of unlabeled ligands were determined using the dual-point competition association assay as described previously, in which radioligand binding was determined at two different time points.²⁵ Time point t_1 represents the time at which radioligand binding reached 99.5% of total binding at equilibrium,

$$t_1 = 8 \cdot t_{1/2, \text{association}} \quad (1)$$

The second time point (t_2) was arbitrarily set at 4 hrs where little, but reliably measureable, specific binding remained. 10 μ g of U2OS-CCR2 membranes were incubated for 50 min (t_1) or 240 min (t_2) in a total volume of 100 μ L of assay buffer with 1.8 nM [³H]INCB3344 in the absence or presence of unlabeled ligands at 25°C. The amount of radioligand bound to the receptor was measured after co-incubation of the unlabeled ligands at 1-fold their respective K_i value in the ¹²⁵I-CCL2 displacement assay. Incubations were terminated and samples were obtained as described under "competition association assay". KRI values of unlabeled ligands were calculated by using equation (2) as mentioned below in "data analysis".

Data analysis. All experiments were analyzed using the non-linear regression curve fitting program Prism 5 (GraphPad, San Diego, CA, U.S.A.). For radioligand displacement data K_i values were calculated from IC₅₀ values using the Cheng and Prusoff equation.³²

Data of the dual point competition association assay was analyzed as described previously.²⁵

KRI values were calculated by dividing the specific radioligand binding measured at t_1 (B_{t1}) by its binding at t_2 (B_{t2}) in the presence of unlabeled competing ligand as follows:

$$KRI = B_{t1} / B_{t2}. \quad (2)$$

Association and dissociation rates for unlabeled ligands were determined by non-linear regression analysis of the competition association data as described by Motulsky and Mahan:²³

$$K_A = k_1[L] + k_2$$

$$K_B = k_3[I] + k_4$$

$$S = \sqrt{(K_A - K_B)^2 + 4 \cdot k_1 \cdot k_3 \cdot L \cdot I \cdot 10^{-18}}$$

$$K_F = 0.5(K_A + K_B + S) \quad (3)$$

$$K_S = 0.5(K_A + K_B - S)$$

$$Q = \frac{B_{\max} \cdot k_1 \cdot L \cdot 10^{-9}}{K_F - K_S}$$

$$Y = Q \cdot \left(\frac{k_4 \cdot (K_F - K_S)}{K_F \cdot K_S} + \frac{k_4 - K_F}{K_F} e^{(-K_F \cdot X)} - \frac{k_4 - K_S}{K_S} e^{(-K_S \cdot X)} \right)$$

where X is the time (min), Y is the specific binding (DPM), k_1 the k_{on} ($M^{-1} \cdot min^{-1}$) of [³H]INCB3344 predetermined in association experiments, k_2 the k_{off} (min^{-1}) of [³H] INCB3344 predetermined in dissociation experiments, L the concentration of [³H]INCB3344 used (nM), B_{\max} the total binding (DPM) and I the concentration of unlabeled ligand (nM). Fixing these parameters into equation (3) allows the following parameters to be calculated: k_3 is the k_{on} ($M^{-1} \cdot min^{-1}$) of the unlabeled ligand and k_4 is the k_{off} (min^{-1}) of the unlabeled ligand. The association and dissociation rates were used to calculate the 'kinetic K_D ' as follows:

$$K_D = k_{off} / k_{on} \quad (4)$$

The residence time was calculated according to the formula $RT = 1/k_{off}$.

Abbreviations

Boc, tert-Butyloxycarbonyl; CCL2, chemokine ligand 2; CCR2, chemokine receptor 2; CHAPS, 3-[(3-cholamidopropyl)dimethylammonio]-1-propanesulfonate; DCM, dichloromethane; DiPEA, N,N-Diisopropylethylamine; DMAP, N,N-Dimethylaminopyridine; DPM, disintegrations per minute; HEPES, 4-(2-Hydroxyethyl)piperazine-1-ethanesulfonic acid; hERG, human Ether-à-go-go-Related Gene; HPLC, High-performance liquid chromatography; HRMS, High Resolution Mass spectral analyses; KRI, kinetic rate index NEAA, non-essential amino acids; NMP, N-methylpyrrolidone; NMR, Nuclear magnetic resonance; PEI, Polyethylenimine; PyBrOP, Bromo-tris-pyrrolidino phosphoniumhexafluorophosphate; RT, residence time; SAR, structure-affinity relationships; SFC, SKR, structure-kinetic relationships; TFA, trifluoroacetic acid; TLC, thin layer chromatography; Tris, tris(hydroxymethyl)aminomethane; U2OS, Human Bone Osteosarcoma Cells.

ACKNOWLEDGEMENT

This study was financially supported by the Dutch Top Institute Pharma, project number D1-301. We thank Dr. Julien Louvel and Jacobus van Veldhoven for their input in analytical data analysis. We acknowledge Dong Guo and Prof. Dr. Martine Smit (Vrije Universiteit, Amsterdam, The Netherlands) for helpful comments and suggestions.

REFERENCES

1. Charo, I. F.; Ransohoff, R. M. The many roles of chemokines and chemokine receptors in inflammation. *New Engl. J. Med.* **2006**, *354*, 610 – 621.
2. Serbina, N. V.; Pamer, E. G. Monocyte emigration from bone marrow during bacterial infection requires signals mediated by chemokine receptor CCR2. *Nat. Immunol.* **2006**, *7*, 311 – 317.
3. Leuschner, F.; Dutta, P.; Gorbатов, R.; Novobrantseva, T. I.; Donahoe, J. S.; Courties, G.; Lee, K. M.; Kim, J. I.; Markmann, J. F.; Marinelli, B.; Panizzi, P.; Lee, W. W.; Iwamoto, Y.; Milstein, S.; Epstein-Barash, H.; Cantley, W.; Wong, J.; Cortez-Retamozo, V.; Newton, A.; Love, K.; Libby, P.; Pittet, M. J.; Swirski, F. K.; Kotliansky, V.; Langer, R.; Weissleder, R.; Anderson, D. G.; Nahrendorf, M. Therapeutic siRNA silencing in inflammatory monocytes in mice. *Nat. Biotechnol.* **2011**, *29*, 1005 – 1010.
4. Fife, B. T.; Huffnagle, G. B.; Kuziel, W. A.; Karpus, W. J. CC chemokine receptor 2 is critical for induction of experimental autoimmune encephalomyelitis. *J. Exp. Med.* **2000**, *192*, 899 – 905.
5. Dawson, T. C.; Kuziel, W. A.; Osahar, T. A.; Maeda, N. Absence of CC chemokine receptor-2 reduces atherosclerosis in apolipoprotein E-deficient mice. *Atherosclerosis* **1999**, *143*, 205 – 211.
6. Ogata, H.; Takeya, M.; Yoshimura, T.; Takagi, K.; Takahashi, K. The role of monocyte chemoattractant protein-1 (MCP-1) in the pathogenesis of collagen-induced arthritis in rats. *The J. Pathol.* **1997**, *182*, 106 – 114.
7. Kanda, H.; Tateya, S.; Tamori, Y.; Kotani, K.; Hiasa, K.; Kitazawa, R.; Kitazawa, S.; Miyachi, H.; Maeda, S.; Egashira, K.; Kasuga, M. MCP-1 contributes to macrophage infiltration into adipose tissue, insulin resistance, and hepatic steatosis in obesity. *J. Clin. Invest.* **2006**, *116*, 1494 – 1505.
8. Kim, Y. K.; Oh, H. B.; Lee, E. Y.; Gho, Y. S.; Lee, J. E.; Kim, Y. Y. Association between a genetic variation of CC chemokine receptor-2 and atopic asthma. *Allergy* **2007**, *62*, 208 – 209.
9. White, F. A.; Feldman, P.; Miller, R. J. Chemokine signaling and the management of neuropathic pain. *Mol. Interv.* **2009**, *9*, 188 – 195.
10. Struthers, M.; Pasternak, A. CCR2 antagonists. *Curr. Top. Med. Chem.* **2010**, *10*, 1278 – 1298.
11. Swenney, D. C. Biochemical mechanisms of drug action: what does it take for success? *Nat. Rev. Drug Discov.* **2004**, *3*, 801 – 808.
12. Copeland, R. A.; Pompliano, D. L.; Meek, T. D. Drug-target residence time and its implications for lead optimization. *Nat. Rev. Drug Discov.* **2006**, *5*, 730 – 739.
13. Zhang, R. M.; Monsma, F. Binding kinetics and mechanism of action: toward the discovery and development of better and best in class drugs. *Expert Opin. Drug. Dis.* **2010**, *5*, 1023-1029.
14. Copeland, R. A. Evaluation of enzyme inhibitors in drug discovery. A guide for medicinal chemists and pharmacologists. *Method. Biochem. Anal.* **2005**, *46*, 1-265.
15. Kothandaraman, S.; Donnelly, K. L.; Butora, G.; Jiao, R.; Pasternak, A.; Morriello, G. J.; Goble, S. D.; Zhou, C.; Mills, S. G.; Maccoss, M.; Vicario, P. P.; Ayala, J. M.; Demartino, J. A.; Struthers, M.; Cascieri, M. A.; Yang, L. Design, synthesis, and structure-activity relationship of novel CCR2 antagonists. *Bioorg. Med. Chem. Lett.* **2009**, *19*, 1830 – 1834.
16. Frerot, E.; Coste, J.; Pantaloni, A.; Dufour, M. N.; Jouin, P. Pybop and Pybrop - 2 Reagents for the Difficult Coupling of the Alpha,Alpha-Dialkyl Amino-Acid, Aib. *Tetrahedron* **1991**, *47*, 259 – 270.
17. Burkhardt, E. R.; Coleridge, B. M. Reductive amination with 5-ethyl-2-methylpyridine borane. *Tetrahedron Lett.* **2008**, *49*, 5152 – 5155.
18. Zweemer, A. J. M.; Nederpelt, I.; Vrieling, H.; Hafith, S.; Doornbos, M. L. J.; de Vries, H.; Abt, J.; Gross, R.; Stamos, D.; Saunders, J.; Smit, M. J.; Ijzerman, A. P.; Heitman, L. H. Multiple binding sites for small molecule antagonists at the chemokine receptor CCR2. *Mol. Pharmacol.* **2013** Oct;*84*(4):551-61.
19. Casarosa, P.; Kollak, I.; Kiechle, T.; Ostermann, A.; Schnapp, A.; Kiesling, R.; Pieper, M.; Sieger, P.; Gantner, F. Functional and Biochemical Rationales for 24-Hour Long Duration of Action of Olodaterol. *J. Pharmacol. Exp. Ther.* **2011**, *337*, 600-609.

20. Rich, R. L.; Hoth, L. R.; Geoghegan, K. F.; Brown, T. A.; LeMotte, P. K.; Simons, S. P.; Hensley, P.; Myszka, D. G. Kinetic analysis of estrogen receptor / ligand interactions. *PNAS*. **2002**, *99*, 13, 8562-8567.
21. Packeu A.; Wennerberg, M.; Balendran, A.; Vauquelin, G. Estimation of the Dissociation Rate of Unlabelled Ligand-Receptor Complexes by a 'Two-Step' Competition Binding Approach. *Br. J. Pharmacol.* **2010**, *161*, 1311-1328.
22. <http://www.htrf.com/tag-lite-technology>
23. Motulsky, H. J.; Mahan, L. C. The kinetics of competitive radioligand binding predicted by the law of mass action. *Mol. Pharmacol.* **1984**, *25*, 1-9.
24. Shin, N.; Baribaud, F.; Wang, K.; Yang, G.; Wynn, R.; Covington, M. B.; Feldman, P.; Gallagher, K. B.; Leffet, L. M.; Lo, Y. Y.; Wang, A.; Xue, C. B.; Newton, R. C.; Scherle, P. A. Pharmacological characterization of INCB3344, a small molecule antagonist of human CCR2. *Biochem. Biophys. Res. Co.* **2009**, *387*, 251 – 255.
25. Guo, D.; van Dorp, E. J.; Mulder-Krieger, T.; van Veldhoven, J. P.; Brussee, J.; Ijzerman, A. P.; Heitman, L. H. Dual-Point Competition Association Assay: A Fast and High-Throughput Kinetic Screening Method for Assessing Ligand-Receptor Binding Kinetics. *J. Biomol. Screen.* **2013**, *18*, 3, 309 – 320.
26. Yang, L.; Butora, G.; Jiao, R. X.; Pasternak, A.; Zhou, C.; Parsons, W. H.; Mills, S. G.; Vicario, P. P.; Ayala, J. M.; Cascieri, M. A.; MacCoss, M. Discovery of 3-piperidinyl-1-cyclopentanecarboxamide as a novel scaffold for highly potent CC chemokine receptor 2 antagonists. *J. Med. Chem.* **2007**, *50*, 2609 – 2611.
27. Pasternak, A.; Goble, S. D.; Vicario, P. P.; Di Salvo, J.; Ayala, J. M.; Struthers, M.; DeMartino, J. A.; Mills, S. G.; Yang, L. Potent heteroaryl piperidine and carboxyphenyl piperidine 1-alkyl-cyclopentane carboxamide CCR2 antagonists. *Bioorg. Med. Chem. Lett.* **2008**, *18*, 994 – 998.
28. Goble, S. D.; Yang, L.; Zhou, C.; Kothandaraman, S.; Guideen, D.; Butora, G.; Pasternak, A.; Mills, S. G. Alkylamino, arylamino, and sulfonamido cyclopentyl amide modulators of chemokine receptor activity. *U.S. Patent 2007/117797*, May 24, **2007**.
29. Zhang, X.; Hufnagel, H.; Markotan, T.; Lanter, J.; Cai, C.; Hou, C.; Singer, M.; Opas, E.; McKenney, S.; Crysler, C.; Johnson, D.; Sui, Z. Overcoming hERG activity in the discovery of a series of 4-azetidiny-1-aryl-cyclohexanes as CCR2 antagonists. *Bioorg. Med. Chem. Lett.* **2011**, *21*, 5577 – 5582.
30. Van Liefde, I.; Vauquelin, G. Sartan-AT1 receptor interactions: in vitro evidence for insurmountable antagonism and inverse agonism. *Mol. Cell Endocrinol.* **2009**, *302*, 237 – 243.
31. Casarosa, P.; Bouyssou, T.; Germeyer, S.; Schnapp, A.; Gantner, F.; Pieper, M. Preclinical evaluation of long-acting muscarinic antagonists: comparison of tiotropium and investigational drugs. *J. Pharmacol. Exp. Ther.* **2009**, *330*, 660 – 668.
32. Anthes, J. C.; Gilchrest, H.; Richard, C.; Eckel, S.; Hesk, D.; West, R. E., Jr.; Williams, S. M.; Greenfeder, S.; Billah, M.; Kreutner, W.; Egan, R. E. Biochemical characterization of desloratadine, a potent antagonist of the human histamine H(1) receptor. *Eur. J. Pharmacol.* **2002**, *449*, 229 – 237.
33. Xue, C. B.; Metcalf, B.; Feng, H.; Cao, G.; Huang, T.; Zheng, C. S.; Robinson, D. J.; Han, A. Q. 3-Aminopyrrolidine derivatives as modulators of chemokine receptors. *Patent WO2004050024*, June 17, **2004**.
34. Brodmerkel, C. M.; Huber, R.; Covington, M.; Diamond, S.; Hall, L.; Collins, R.; Leffet, L.; Gallagher, K.; Feldman, P.; Collier, P.; Stow, M.; Gu, X.; Baribaud, F.; Shin, N.; Thomas, B.; Burn, T.; Hollis, G.; Yeleswaram, S.; Solomon, K.; Friedman, S.; Wang, A.; Xue, C. B.; Newton, R. C.; Scherle, P.; Vaddi, K. Discovery and pharmacological characterization of a novel rodent-active CCR2 antagonist, INCB3344. *J. Immunol.* **2005**, *175*, 5370 – 5378.
35. Cheng, Y.; Prusoff, W. H. Relationship between the inhibition constant (K1) and the concentration of inhibitor which causes 50 per cent inhibition (I50) of an enzymatic reaction. *Biochem. Pharmacol.* **1973**, *22*, 3099 – 3108.

CHAPTER 4

WHEN STRUCTURE–AFFINITY RELATIONSHIPS MEET STRUCTURE–KINETICS RELATIONSHIPS: 3- ((INDEN-1-YL)AMINO)-1-ISOPROPYL- CYCLOPENTANE-1-CARBOXAMIDES AS CCR2 ANTAGONISTS

This chapter was based upon:

M. Vilums, A.J.M. Zweemer, F. Barmare, A.M.F. van der Gracht, D.C.T. Bleeker, Z. Yu, H. de Vries, R. Gross, J. Clemens, P. Krenitsky, J. Brussee, D. Stamos, J. Saunders, L.H. Heitman, A. P. IJzerman.

(manuscript in preparation)

ABSTRACT

Chemokine ligand 2 (CCL2) mediates chemotaxis of monocytes to inflammatory sites *via* interaction with its G protein–coupled receptor CCR2. Preclinical animal models suggest that the CCL2-CCR2 axis has a critical role in the development and maintenance of inflammatory disease states (e.g., multiple sclerosis, atherosclerosis, insulin resistance, restenosis, and neuropathic pain), which can be treated through inhibition of the CCR2 receptor. However, in clinical trials high-affinity inhibitors of CCR2 have often demonstrated a lack of efficacy. We have previously described a new approach for the design of high–affinity CCR2 antagonists, by taking their residence time (RT) on the receptor into account. Here, we report our findings on both structure–affinity relationship (SAR) and structure–kinetic relationship (SKR) studies for a series of 3-((inden-1-yl)amino)-1-isopropyl-cyclopentane-1-carboxamides as CCR2 antagonists. SAR studies showed that this class of compounds tolerates a vast diversity of substituents on the indenyl ring with only small changes in affinity. However, the SKR is affected greatly by minor modifications of the structure. The combination of SAR and SKR in the hit-to-lead process resulted in the discovery of a new high–affinity and long–residence–time CCR2 antagonist (compound **15a**, $K_i = 2.4$ nM; RT = 714 min).

INTRODUCTION

Chemokines are a class of endogenous pro-inflammatory proteins that act through activation and recruitment of leukocytes and other cell types in a range of inflammatory and non-inflammatory conditions. However, inappropriate overexpression of such proteins is implicated in a variety of disease conditions.¹ Both C-C Chemokine Ligand 2 (CCL2) and its cognate receptor C-C Chemokine Receptor 2 (CCR2) are involved in various autoimmune or inflammation-associated diseases. Blockade of the CCL2-CCR2 axis via either genetic or pharmacologic intervention has proven efficacious in animal models of multiple sclerosis, atherosclerosis, insulin resistance, restenosis, and neuropathic pain.²⁻⁴

Fuelled by such promising preclinical data, there has been an increasing interest in advancing antagonists of CCR2 into clinical trials. However, till now all small molecules tested have failed in clinical trials because of lack of efficacy, e.g., MK-0812 (orthosteric CCR2 antagonist for the treatment of rheumatoid arthritis and multiple sclerosis)⁵ and AZD-2423 (potent, orally bioavailable, non-competitive, negative allosteric modulator of the CCR2 chemokine receptor for treatment of neuropathic pain).⁶ A humanized anti-CCR2 antibody (MLN-1202) did not show efficacy either in patients with rheumatoid arthritis and multiple sclerosis.⁷ However, administration of the antibody reduced the numbers of circulating monocytes in peripheral blood.⁸ Moreover, a study of MNL-1202 in patients with risk factors for atherosclerosis demonstrated that treatment was able to reduce C-reactive protein levels.⁹ This shows that CCR2 antagonism can have important biological effects in humans.

Apparently, to be efficacious in treatment of CCR2-related diseases, high-affinity antagonism is not enough. Moreover, blockade of CCR2 can cause an increase in endogenous CCL2 levels⁸ which will compete again with the administered drug. To be able to withstand this increasing concentration of endogenous ligand, the drug should be slowly dissociating.

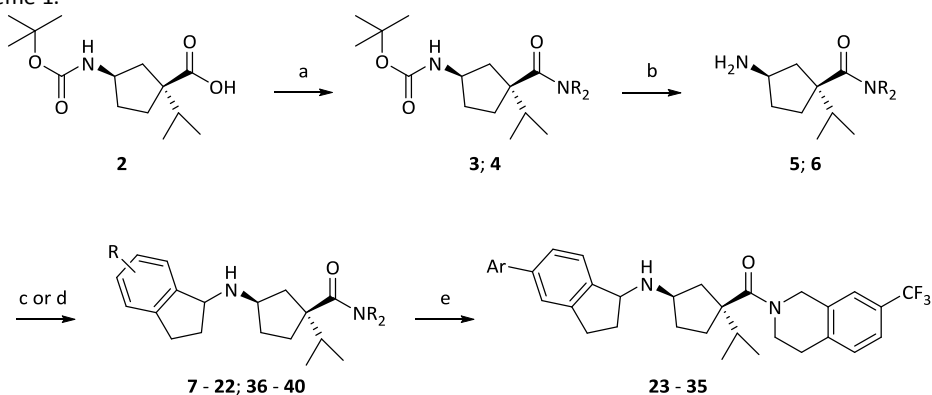
Previously we reported that by using an additional parameter in drug design, the so-called residence time (RT) on the receptor, we generated high-affinity and longer-residence-time CCR2 antagonists based on a (1*S*,3*R*)-3-amino-*N*-(3,5-bis(trifluoromethyl)benzyl)-1-

isopropylcyclopentane-1-carboxamide scaffold.¹⁰ We explored different substituents and ring systems on the 3-amino group of the scaffold and observed that the longest residence time was found with an indane ring system. Although potent and long-residence-time compounds were identified in that study, we now sought to prolong the RT and define more detailed structure-kinetics relationships for the CCR2 receptor. In the present study we evaluated different amide groups for the 3-((inden-1-yl)amino)-1-isopropyl-cyclopentane-1-carboxamide scaffold based on their RT and explored a broad chemical space around the indane ring system to define the SAR and SKR for 3-((inden-1-yl)amino)-1-isopropyl-cyclopentane-1-carboxamides as CCR2 antagonists.

RESULTS AND DISCUSSION

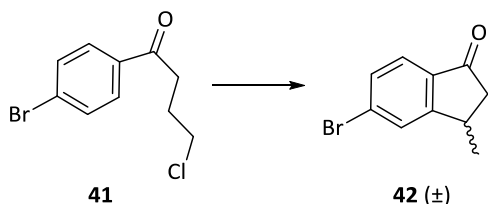
Chemistry

The synthesis of *N*-(3,5-bis(trifluoromethyl)benzyl)-3-((2,3-dihydro-1*H*-inden-1-yl)amino)-1-isopropylcyclopentane-1-carboxamide **1** and (1*S*,3*R*)-3-((tert-butoxycarbonyl)amino)-1-isopropylcyclopentane-1-carboxylic acid **2** was achieved following the approach reported earlier by our group.¹⁰ From acid **2** and 1-(4-(trifluoromethyl)pyridin-2-yl)piperazine or 7-(trifluoromethyl)-1,2,3,4-tetrahydroisoquinoline hydrochloride via a peptide coupling reaction were generated amides **3** and **4** under bromo-tris-pyrrolidino phosphoniumhexafluorophosphate (PyBroP) conditions.¹¹

Scheme 1.^a

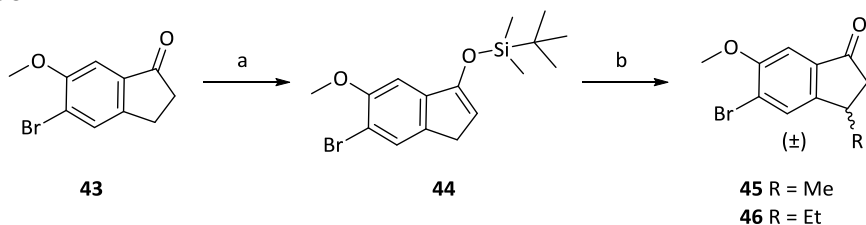
^aReagents and conditions: a) 1-(4-(trifluoromethyl)pyridin-2-yl)piperazine or 7-(trifluoromethyl)-1,2,3,4-tetrahydroisoquinoline hydrochloride, PyBrOP, DIPEA, DMAP, DCM, room temperature, 24 h, 82 - 90%; b) TFA, DCM, room temperature, 1 h, 90 - 98%; c) for array synthesis – corresponding indanone (1.05 equiv), 5-ethyl-2-methylpyridine borane (PEMB) (2.1 equiv), AcOH (1.05 equiv), NMP, 65 °C, 24 h, (compounds **7**; **9** – **13** and **17** – **22**); d) i) corresponding indanone (1,1 eq.), Ti(*O*-*i*-Pr)₄ (3 eq.), THF, 48 h, ii) NaBH₄, EtOH 16 h, room temperature, 8 – 41% (compounds **8**; **14** – **16** and **36** – **40**); e) array synthesis - compound **15**, corresponding aryl boronic acid, Na₂CO₃, Pd(PPh₃)₄, toluene/NMP/H₂O, 80°C, 24 h, (compounds **23**–**35**).

Subsequently, a solution of TFA in DCM (1:1) was used to remove the *N*-Boc protecting group which yielded amines **5** and **6**. Compounds **7**, **9** – **13** and **17a** – **22** were generated from amines **5** and **6** using an array of different indanones with the 5-ethyl-2-methylpyridine borane complex (PEMB) under conditions reported by Burkhardt and Coleridge (Scheme 1).¹² In the case of the 5-CF₃ derivative (compound **17**) diastereomers were separated during the purification, however, only the first diastereomer to elute (**17a**) had a sufficient purity to be tested in bioassays. Compounds **8**, **14** – **16** and **36** – **40** were synthesized from **6** in a Ti(*O*-*i*-Pr)₄ promoted reductive amination reaction with different indanones. Compounds **23** – **35** were synthesized via Suzuki–coupling of compound **15** with the corresponding arylboronic acids. The synthesis of 3-Me; 5-Br indanone **42** was achieved by intramolecular cyclization of commercially available 1-(4-bromophenyl)-4-chlorobutan-1-one **41** following a procedure reported in patent literature (Scheme 2).¹³

Scheme 2.^a

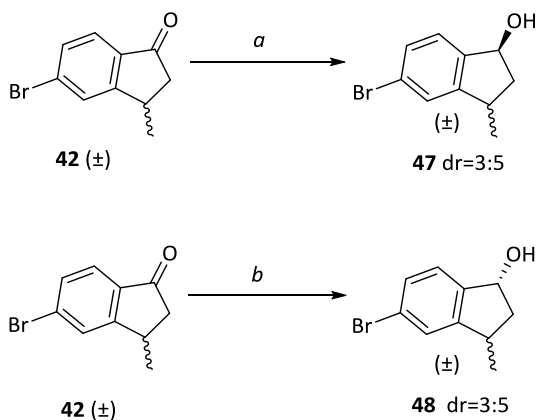
^aReagents and conditions: a) i) NaCl, AlCl₃, melt at 130 °C, ii) 4'-bromo-4-chloro-butyrophenone, 180 °C, 30 min, 91%.

The 3-alkyl; 5-Br; 6-OMe indanones were synthesized as shown in Scheme 3. The reaction of 5-Br; 6-OMe indanone **43** with *tert*-butyldimethylchlorosilane and DBU in benzene gave ((6-bromo-5-methoxy-1*H*-inden-3-yl)oxy)(*tert*-butyl)dimethylsilane (**44**). Deprotonation of **44** with *n*-BuLi and reaction of the lithium salt with methyl iodide or ethyl iodide in THF and subsequent quenching of the reaction mixture with 12 M HCl resulted in 5-bromo-6-methoxy-3-alkyl-indanones (**45**, **46**).

Scheme 3.^a

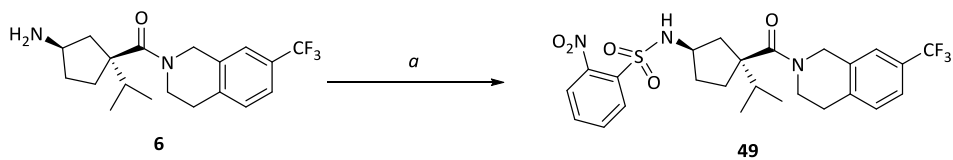
^aReagents and conditions: a) TBDMS-Cl, DBU, 0 °C → room temperature, 99%; b) i) LDA, 1 h, -78 °C → -35 °C, → -78 °C, 1 h, corresponding alkyl iodide; ii) 12 M HCl, 82%.

The racemic (1*S*)-5-bromo-3-methyl-2,3-dihydro-1*H*-indanol (**47**) and racemic (1*R*)-5-bromo-3-methyl-2,3-dihydro-1*H*-indanol (**48**) were prepared via catalytic enantioselective reduction of racemic 5-bromo-3-methyl-2,3-dihydro-1*H*-indanone (**42**) using the (*R*)-methyl-CBS-oxazaborolidine and (*S*)-methyl-CBS-oxazaborolidine catalysts, respectively, with *N,N*-diethylaniline borane as reducing agent providing excellent enantioselectivity (Scheme 4).¹⁴

Scheme 4.^a

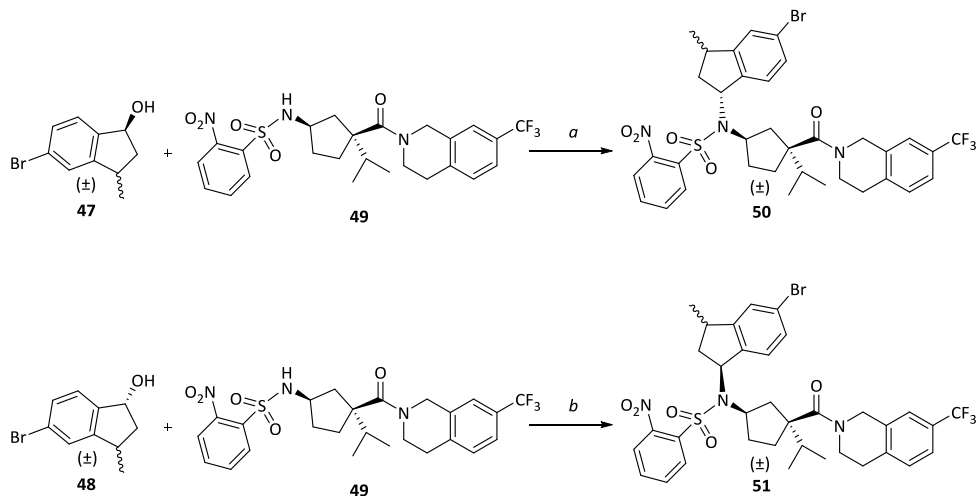
^aReagents and conditions: a) (*R*)-(+)-2-methyl-CBS-oxazaborolidine catalyst, *N,N*, diethylaniline borane, toluene, 3 h, room temperature, 97 %. b) (*S*)-(+)-2-methyl-CBS-oxazaborolidine catalyst, *N,N*, diethylaniline borane, toluene, 3 h, room temperature, 99 %.

To prepare for the subsequent coupling, amine **6** was protected as the 2-nitrobenzenesulfonamide (**49**) (Scheme 5).¹⁵

Scheme 5.^a

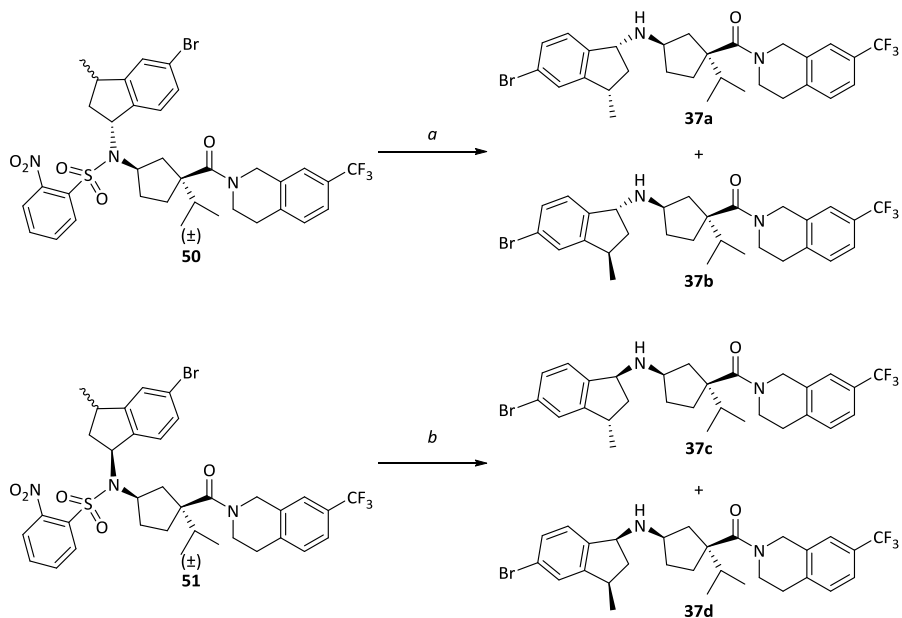
^aReagents and conditions: a) 2-nitrobenzenesulfonyl chloride, DIPEA, CH_2Cl_2 , 1 h, room temperature, 98 %.

The respective racemic alcohols (**47**) and (**48**) when treated with (**49**) under Fukuyama–Mitsunobu conditions, resulted in *N*-alkylation to afford the 2-nitrobenzenesulfonamides (**50**) and (**51**) (scheme 6).

Scheme 6.^a

^aReagents and conditions: *a* and *b*) DEAD, PPh₃, THF, -78 °C to room temperature.

Selective deprotection of the 2-nitrobenzenesulfonamides (**50**) and (**51**) with thiophenol and K₂CO₃ gave the desired diastereomers **37a**, **37b**, **37c** and **37d** (Scheme 7).

Scheme 7.^a

^aReagents and conditions: *a* and *b*) PhSH, K₂CO₃, DMF, room temperature.

Biology

To determine their binding affinity all compounds were tested in a ^{125}I -CCL2 radioligand displacement assay on U2OS-CCR2 membrane preparations as described previously by our group.¹⁶ Compounds with affinities lower than or equal to 100 nM were subsequently screened in a [^3H]INCB3344 dual point competition association assay on U2OS-CCR2 membrane preparations to determine their kinetic-rate-index (KRI), which served as an indicator for the magnitude of the RT. Compounds with a KRI >1 were finally tested in the full competition association assay to determine the RT, as described previously by our group.¹⁰

Structure–Affinity Relationships and Structure–Kinetics Relationships

In the past few years several distinctly different amide groups have been disclosed for the general CCR2 scaffold of 3-amino-1-isopropylcyclopentanecarboxamides, with many final compounds displaying high and often very similar affinities (Figure 1).¹⁷⁻¹⁹

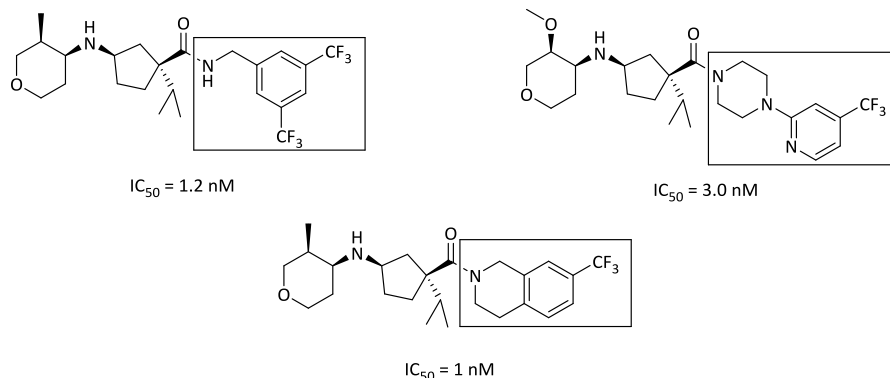
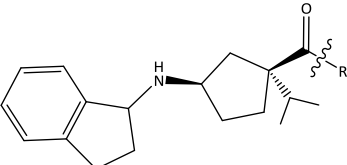
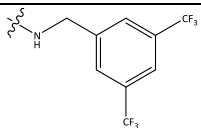
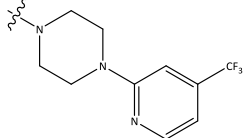
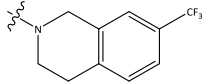


Figure 1. CCR2 antagonists from Merck and Pfizer based on a 3-amino-1-isopropylcyclopentanecarboxamide scaffold with different amide groups.¹⁷⁻¹⁹

In the current study we decided to keep the 3-((inden-1-yl)amino)-1-isopropyl-cyclopentane-1-carboxamide scaffold that was central in our previous report,¹⁰ and investigated the effect on affinity and RT of three different amide groups (Table 1). When we changed the 3,5-bis(trifluoromethyl)benzyl group (compound **1**) to a 1-(4-(trifluoromethyl)pyridin-2-yl)piperazine group (compound **7**) the affinity was improved 3-fold, while a rigidification of

the benzyl group into the 7-(trifluoromethyl)-1,2,3,4-tetrahydroisoquinoline group (compound **8**) yielded an even higher, 20-fold increase in affinity (compounds **1**, **7** and **8**; $K_i = 50$ nM, 15 nM and 2.2 nM, respectively).

Table 1. Binding Affinities, KRI and Residence Time of compounds **1**; **7** and **8**

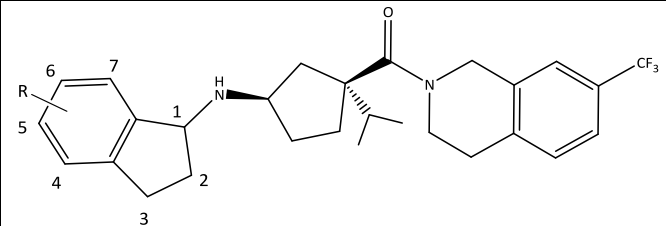
				
Nr.	R	K_i (nM) \pm SEM ($n=3$)	KRI ($n=2$)	RT (min)
1		50 ± 8	0.8 (0.7/0.8)	9.1 ± 1.7
7		15 ± 1	0.5 (0.5/0.5)	8.3 ± 2.8
8		2.2 ± 0.6	1.0 (0.9/1.0)	21 ± 3

In kinetic tests of these compounds (kinetic rate index (KRI)²⁰ and RT) we learned that for longer receptor occupancy smaller and less flexible groups are preferred (KRI = 0.8, 0.5 and 1.0; RT = 9.1, 8.3 and 21 min, for **1**, **7** and **8**, respectively).

Encouraged by these results we decided to continue with compound **8** and investigate different substituents on the indenyl group (Table 2). The rigidification of the right-hand side of the structure improved the affinity in general, while the order of substituents on the indenyl group was hardly affected when compared to our previous findings on the 3,5-bis(trifluoromethyl)benzylamide derivatives (compound **1**).¹⁰ Substitution on the 4-position decreased the affinity. Introduction of 4-Me (compound **9**) led to a 15-fold decrease. However, more polar groups were better tolerated. The 4-NH₂ substituent (compound **10**) led

to a 2-fold decrease only, while 4-CN and 4-OH groups caused a 7- and 10-fold decrease (compounds **11** and **12**; $K_i = 15$ and 21 nM, respectively).

Table 2. Binding Affinities, KRI and Residence Time of compounds **8–22**



Nr.	R	K_i (nM) \pm SEM ($n=3$)	KRI ($n=2$)	RT (min)
8	H	2.2 ± 0.6	1.0 (0.9/1.0)	21 ± 3
9	4-Me	31 ± 2	0.7 (0.7/0.7)	-
10	4-NH ₂	4.6 ± 1.0	0.7 (0.7/0.8)	-
11	4-CN	15 ± 5	0.6 (0.6/0.6)	-
12	4-OH	21 ± 3	0.7 (0.7/0.7)	-
13	5-F	4.9 ± 1.6	0.9 (0.9/0.9)	55 ± 6
14	5-Cl	1.6 ± 0.7	1.2 (1.0/1.3)	100 ± 20
15	5-Br	2.3 ± 0.6	1.3 (1.3/1.3)	213 ± 32
16	5-I	4.4 ± 0.9	1.3 (1.3/1.2)	103 ± 9
17a	5-CF ₃	13 ± 5	1.4 (1.5/1.3)	667 ± 222
18	6-Me	23 ± 6	0.6 (0.6/0.5)	-
19	6-CN	13 ± 8	0.6 (0.6/0.7)	-
20	6-Cl	7.9 ± 2.0	0.6 (0.6/0.6)	-
21	5;6-di-OMe	1.2 ± 0.3	1.0 (1.1/0.9)	63 ± 5
22	4,7-di OMe	49 ± 7	0.8 (0.8/0.8)	-

Substituents on the 5 position had little effect on affinity. 5-F (compound **13**) led to a 2-fold decrease, but with an increase in the size of the halogen, 5-Cl and 5-Br, the affinity was regained (compounds **14** and **15**). However, 5-I (compound **16**) apparently was too big and led to a 2-fold decrease. An even bigger decrease was observed with the introduction of a CF₃ group (compound **17a**) often considered as a bioisostere of chlorine. However, this substitution pattern resulted in an 8-fold decrease compared to the chloro compound. On the 6 position neither an electron donating group (compound **18**), nor a strongly electron withdrawing group (compound **19**) was tolerated, while the 6-Cl substituent (compound **20**) led to a small decrease in affinity. However, the highest affinity compound **21** was obtained by double substitution on the 5 and 6 positions with methoxy groups. The corresponding

regioisomer with 4,7-di-OMe (compound **22**) displayed a 40-fold decrease in affinity compared to compound **21**.

Testing these compounds in the high-throughput dual-point competition association assay showed that the abovementioned rigidification on the right-hand side of the molecule affects RT only for 5-substituted indenyl derivatives, with most of them having KRI values higher than unity. These compounds were tested in a full competition association assay and the highest affinity compound **21** had a RT of 63 min. Halogen substituents had size-dependent effects on KRI values. When tested for RT, indeed, increasing size correlated with longer residence times except for 5-I **16** where we observed a decrease in RT, as was the case for its affinity. However, compound **17a** (single diastereomer) displayed a more than 6-fold increase in RT compared to the 5-Cl compound (**14**). This indicates that affinity does not correlate with the residence time in this series of compounds. All other compounds showed KRI values below unity and thus showed a behavior comparable to the benzyl derivatives reported earlier.¹⁰

Next, we explored the 5 position by incorporating an additional aromatic system. Previously Xue et al²¹ had shown this approach to be successful in a pyrrolidine series of CCR2 antagonists. However, for our structures, an added unsubstituted phenyl ring (compound **23**) resulted in a dramatic decrease of affinity (Table 3). Adding a 2-Me group (compound **24**) yielded a small increase while 3-Me (compound **25**) did not improve the affinity compared to unsubstituted **23**. Incorporation of a cyano group on the 3 or 4 position (compounds **26** and **27**) resulted in a regain of affinity into the nanomolar range. The same effect was observed with a methoxy group (compounds **29** and **30**). However, 2-OMe (compound **28**) was detrimental for affinity.

Table 3. Binding Affinities, KRI and Residence Time of compounds **23–30**

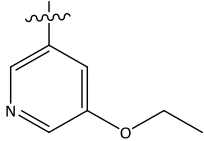
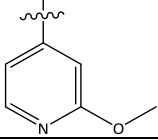
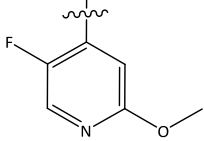
Nr.	R	K_i (nM) \pm SEM ($n=3$)	KRI ($n=2$)
23	H	28% ^a	-
24	2-Me	46% ^a	-
25	3-Me	24% ^a	-
26	3-CN	55 \pm 14	0.7 (0.7/0.7)
27	4-CN	11 \pm 4.7	0.9 (0.8/1.0)
28	2-OMe	2% ^a	-
29	3-OMe	39 \pm 6	0.8 (0.8/0.8)
30	4-OMe	75 \pm 23	0.9 (0.9/0.9)

^aPercent displacement at 1 μ M ¹²⁵I-CCL2

These findings suggest that the space filling and hydrogen-accepting properties are more important for binding than the electronic properties of the substituents. Possible hydrogen bonding may also play a role when the phenyl ring was exchanged for 3-pyridine (compound **31**; K_i = 10 nM) (Table 4).

Table 4. Binding Affinities, KRI and Residence Time of compounds **31–35**

Nr.	R	K_i (nM) \pm SEM ($n=3$)	KRI ($n=2$)
31		10 \pm 4.5	0.7 (0.6/0.7)
32		41 \pm 8	0.8 (0.7/0.8)

33		10 ± 4	0.5 (0.4/0.6)
34		23 ± 7	0.6 (0.6/0.6)
35		12 ± 1	0.8 (0.8/0.8)

Incorporation of a 2-OMe group (compound **32**) resulted in a decrease of affinity, with an affinity comparable to its phenyl analogue **29**. Extending the substituent to an ethoxy group (compound **33**) is in accordance with the idea of space filling properties, as it yielded a gain in affinity compared to **32**. Changing the location of the nitrogen atom in the pyridine ring to the 4-position (compound **34**) improved the affinity by 2-fold vs **32**. An additional gain in affinity was reached by incorporating a fluorine atom on the 5 position (compound **35**). In general, this series of compounds suggests there is enough space in the binding pocket to accommodate another aromatic ring with preferably hydrogen bond accepting properties. However, when these compounds were tested in the dual-point competition association assay none of them showed KRI values above 1.

Another approach to investigate SAR and SKR in more detail was based on the superimposition of structure **8** with the structure of MK-0483, which has been reported as a CCR2 antagonist with a receptor dissociation time ($T_{1/2}$) of over 9 h (Figure 2).²²

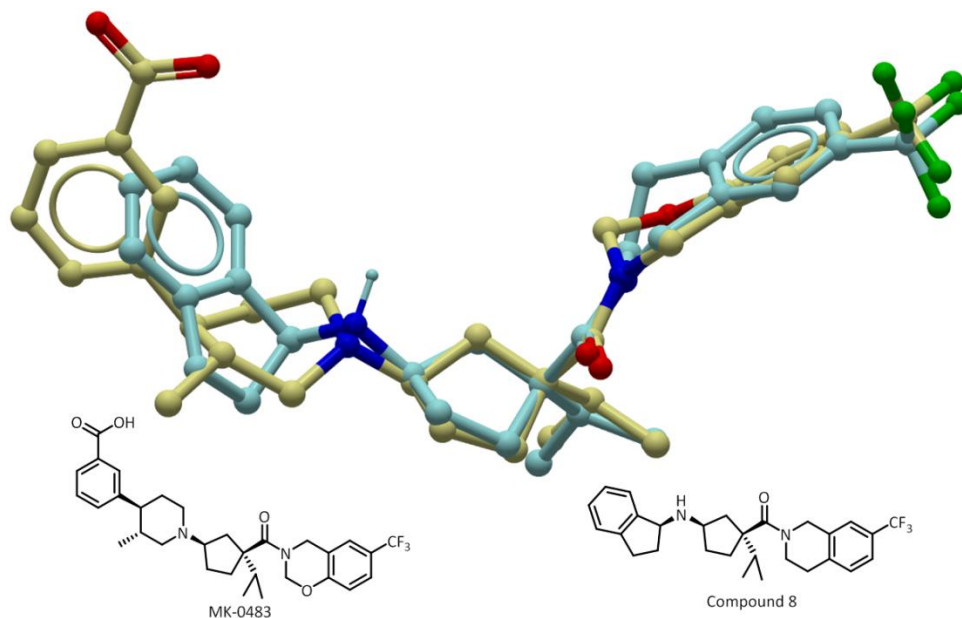


Figure 2. Superimposition of MK-0483 (yellow) with compound **8** (cyan) using “ICM-Pro 3.7b, Molsoft LLC”.

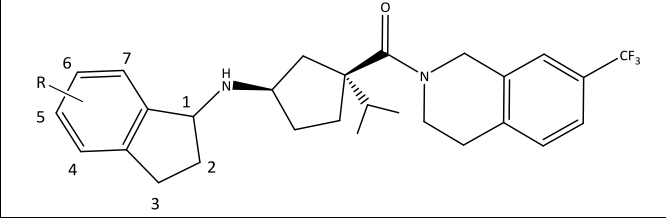
In the superimposition the 3-position of the indane ring of compound **8** overlaps with the 3 position of the piperidine ring of MK-0483. So we decided to incorporate a methyl group on the 3 position of the indenyl system to yield compound **36** (Table 5).

Table 5. Binding Affinities, KRI and Residence Time of compounds **36–40**.

Nr.	R	K_i (nM) \pm SEM ($n=3$)	KRI ($n=2$)	RT (min)
36	3-Me	3.4 ± 0.5	0.7 (0.6/0.7)	-
37	5-Br, 3-Me	2.0 ± 0.2	1.3 (1.3/1.2)	345 ± 48
38	5-Br, 6-OMe	4.5 ± 1.0	1.3 (1.3/1.2)	323 ± 10
39	5-Br, 3-Me, 6-OMe	13 ± 4	1.5 (1.6/1.3)	238 ± 11
40	5-Br, 3-Et, 6-OMe	83 ± 5	1.3 (1.3/1.3)	179 ± 10

This had a minor effect on the affinity, but caused a significant decrease in KRI value. However, the combination of a 3-Me and 5-Br substituent (compound **37**) yielded an increase in RT while affinity remained unchanged. This is an indication that the 3-Me group *per se* is not in direct contact with the receptor binding site. However, it could play an important role in shielding of a sub-pocket in combination with 5-Br; a similar idea was put forward by Schmidtke et al.²³ in calculations on hydrogen bond shielding. Intrigued by our findings, we decided to combine the substituents of the long RT compound **15** (5-Br) and highest affinity compound **21** (6-OMe) in one structure **38**. This combination prolonged the RT, but the affinity was decreased by 2-fold. Our next step was to make a hybrid of compounds **37** and **38** to incorporate 3-Me; 5-Br; 6-OMe substituents on the indenyl group in one compound **39**. Next to this, we also extended the methyl group into an ethyl group (compound **40**). Unfortunately, these changes yielded 5- and 40-fold decreases in affinity, respectively, however, their RT was not affected when compared to 5-Br (compound **15**).

We then decided to separate compound **15** into diastereomers (Table 6) by preparative supercritical fluid chromatography (SFC). Similar to our previous findings¹⁰ the first compound to elute also showed a higher affinity. However, the difference in affinity between the diastereomers was only 10-fold in the case of compounds **15a** and **15b**. In addition, compound **37** was resynthesized using a different method to yield all four diastereomers, which were separated (**37a-d**). *R*-diastereomers **37a** and **37b** retained high affinity, while *S*-diastereomers **37c** and **37d** had only sub-micromolar affinity values ($K_i = 1.7, 4.6, 199$ and 137 nM, respectively).

Table 6. Binding Affinities, KRI and Residence Time of Separated Diastereomers. (**15**, **15a**, **15b**, **37**, **37a-d**)


Nr.	R	K_i (nM) \pm SEM (n=3)	KRI (n=2)	RT (min)
15	5-Br	2.3 ± 0.6	1.3 (1.3/1.3)	213 ± 32
15a	5-Br	2.4 ± 1.2	1.7 (1.7/1.7)	714 ± 153
15b	5-Br	24 ± 9	0.8 (0.7/0.9)	15 ± 4
37	5-Br, 3-Me	2.0 ± 0.2	1.3 (1.3/1.2)	345 ± 48
37a	5-Br, 3-Me	1.7 ± 0.1	1.4 (1.4/1.4)	588 ± 208
37b	5-Br, 3-Me	4.6 ± 0.1	1.2 (1.2/1.1)	208 ± 35
37c	5-Br, 3-Me	199 ± 47	-	-
37d	5-Br, 3-Me	137 ± 15	-	-

In the RT measurements, a distinct difference was observed for the different diastereomers in the case of 7-(trifluoromethyl)-1,2,3,4-tetrahydroisoquinoline compounds on the amide part, quite the opposite of our previous findings for the flexible benzylamide derivatives.¹⁰ The diastereomers of compound **15** had very different dissociation rate constants while the association rate constants were similar (Table 7).

Table 7. Kinetic data of **15a**, **b**, **17a** and **37a**, **b** compounds

Nr.	K_i (nM) \pm SEM (n=3)	k_{on} (nM ⁻¹ min ⁻¹)	k_{off} (min ⁻¹)	RT (min)
15a	2.4 ± 1.2	0.0080 ± 0.0011	0.0014 ± 0.0003	714 ± 153
15b	24 ± 9	0.0059 ± 0.001	0.066 ± 0.017	15 ± 4
17a	13 ± 5	0.0032 ± 0.0004	0.0015 ± 0.0005	667 ± 222
37a	1.7 ± 0.1	0.0044 ± 0.0003	0.0017 ± 0.0006	588 ± 208
37b	4.6 ± 0.1	0.0026 ± 0.0006	0.0048 ± 0.0008	208 ± 35

We succeeded in crystalizing compound **15a** for single-crystal X-ray diffraction analysis. Based on the crystallographic analysis, the absolute configuration of compound **15a** was the *R*-isomer (Figure 3). Apparently, the rigidification stabilizes specific interactions of the *R*-isomer in the binding site of the CCR2, which results in smaller dissociation rate constants. This is also in accordance with **37a** and **37b**, however, the additional methyl group on the indane ring

should be positioned in the 3*R*-conformation (**37a**) resulting in an almost 3-fold longer RT than the 3*S*-diastereomer (**37b**).

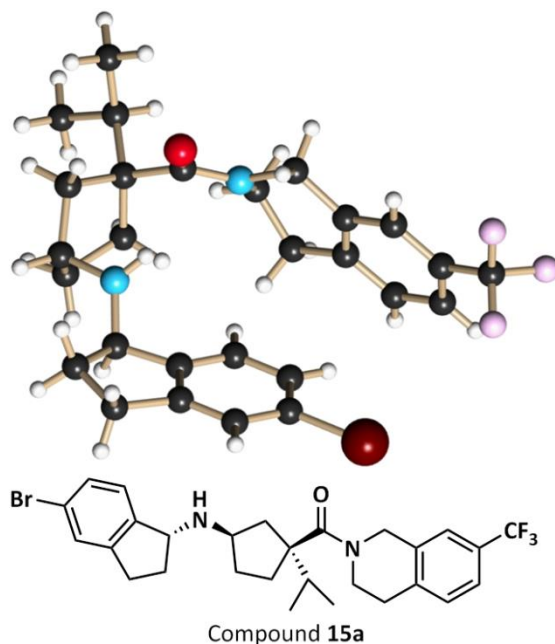


Figure 3. X-ray structure of ((1*S*,3*R*)-3-(((*R*)-5-bromo-2,3-dihydro-1*H*-inden-1-yl)amino)-1-isopropylcyclopentyl)(7-(trifluoromethyl)-3,4-dihydroisoquinolin-2(1*H*)-yl)methanone (**15a**).

CONCLUSION

We have evaluated the SAR and SKR of 3-((inden-1-yl)amino)-1-isopropyl-cyclopentane-1-carboxamide derivatives as CCR2 antagonists. On the right-hand side of the molecule the 7-(trifluoromethyl)-1,2,3,4-tetrahydroisoquinoline group is optimal to increase residence time. On the left-hand side, the indane ring can accommodate very different substituents, as many compounds maintain nanomolar affinity. However, lipophilic and electron-withdrawing substituents (e.g. Cl, Br, I, CF₃) on the 5-position of the indane ring are crucial for long residence time. Moreover, compound **17a** (5-CF₃) having a modest (compared to other compounds in the series) affinity of 13 nM and a long residence time (RT = 667 min) is a good example that affinity and residence time do not necessarily. It also stresses the importance of additional screening for residence time in the early stages of drug discovery. In addition, small

changes of the structure can have a big impact on residence time, e.g., the incorporation of a 5-Br (**15a**) substituent yielded a more than 30-fold increase in residence time (714 min). From this perspective compound **15a** should be evaluated in CCR2-related disease animal models to assess the usefulness of prolonged inhibition of CCR2. In general, this work provides methodology to retrieve the kinetic parameters from the vast number of high affinity compounds in the early stages of the drug discovery, which could help to provide better drug candidates for the later stages of drug development.

EXPERIMENTAL SECTION

Chemistry

All solvents and reagents were purchased from commercial sources and were of analytical grade. Demineralized water is simply referred to as H₂O, because it was used in all cases, unless stated otherwise (i.e., brine). ¹H and ¹³C NMR spectra were recorded on a Bruker AV 400 liquid spectrometer (¹H NMR, 400 MHz; ¹³C NMR, 100 MHz) or on a Bruker 500 MHz Avance III NMR spectrometer (compounds **15a**, **b** and **37a – d**) at ambient temperature. Chemical shifts are reported in parts per million (ppm), are designated by δ , and are downfield to the internal standard tetramethylsilane (TMS). Coupling constants are reported in hertz and are designated as *J*. Analytical purity of the final compounds was determined by high-performance liquid chromatography (HPLC) with a Phenomenex Gemini 3 μ m C18 110A column (50 \times 4.6 mm, 3 μ m), measuring UV absorbance at 254 nm. The sample preparation and HPLC method for compounds **8**; **14 – 16** and **36 – 40** were as follows: 0.3–0.8 mg of compound was dissolved in 1 mL of a 1:1:1 mixture of CH₃CN/H₂O/*t*-BuOH and eluted from the column within 15 min at a flow rate of 1.3 mL/min. The elution method was set up as follows: 1–4 min isocratic system of H₂O/CH₃CN/1% TFA in H₂O, 80:10:10, from the 4th min, a gradient was applied from 80:10:10 to 0:90:10 within 9 min, followed by 1 min of equilibration at 0:90:10 and 1 min at 80:10:10. All compounds showed a single peak at the designated retention time and are at least 95% pure. Enantiomeric excess was accomplished using chiral SFC. For **47** and **48** the column was Chiralpak AD-H (250 \times 4.6mm), 5 μ m. The mobile phase condition of 10% MeOH with 20 mM NH₃ and 90% CO₂ was applied at a flow rate of 3.0 mL/min at 254 nm. For **37a** and **37b** the column was Phenomenex Lux-4 (250 \times 4.6 mm), 5 μ m. The mobile phase condition of 20% *i*-propanol (IPA) with 1.0% DEA and 80% CO₂ was applied at a flow rate of 3.0 mL/min at 254 nm. For **37c** and **37d** the column was Regis RR-Whelko (250 \times 4.6 mm), 5 μ m. The mobile phase condition of 25% IPA with 1.0% diethylamine (DEA) and 75% CO₂ was applied at a flow rate of 3.0 mL/min at 254 nm. High-resolution mass spectral analyses (HRMS) were performed on LTQ-Orbitrap FTMS operated in a positive ionization mode with an electrospray ionization (ESI) source, with the following conditions: mobile phase A, 0.1% formic acid in water; mobile phase B, 0.08% formic acid in CH₃CN; gradient, 10–80% B in 26 min; and flow rate, 0.4 mL/min. Preparative HPLC (for compounds **7**; **9 – 13** and **18 – 35**) was performed on a Waters Auto Purification HPLC-ultraviolet (UV) system with a diode array detector using a Luna C18 Phenomenex column (75 \times 30 mm, 5 μ m), and a linear gradient from 1 to 99% of mobile phase B was applied. Mobile phase A consisted of 5 mM HCl solution, and mobile phase B consisted of acetonitrile. The flow rate was 50 mL/min. Liquid chromatography–mass spectrometry (LC–MS) analyses were performed using an Onyx C18 monolithic column (50 \times 4.6 mm, 5 μ m), and a linear gradient from 1 to 99% mobile phase B was

applied. Mobile phase A consisted of 0.05% TFA in water, and mobile phase B consisted of 0.035% TFA in acetonitrile. The flow rate was 1.2 mL/min. Separations of enantiomers were accomplished using chiral SFC. The column was Phenomenex Lux-4 (250 × 10 mm, 5 μm). The mobile phase condition of 10% MeOH with 20 mM NH₃ and 90% CO₂ was applied at a flow rate of 10 mL/min. Optical rotations were measured in ethanol at 20 °C on a Perkin-Elmer polarimeter (Wavelength = 589 nm). The single crystal X-ray diffraction studies were carried out on a Bruker Kappa APEX-II CCD diffractometer equipped with Mo K_α radiation (λ = 0.71073 Å). Thin-layer chromatography (TLC) was routinely consulted to monitor the progress of reactions, using aluminum-coated Merck silica gel F²⁵⁴ plates. Purification by column chromatography was achieved by use of Grace Davison Davisil silica column material (LC60A, 30–200 μm). The procedure for a series of similar compounds is given as a general procedure for all within that series, annotated by the numbers of the compounds.

Synthesis of (1*S*,3*R*)-3-(tert-butoxycarbonylamino)-1-isopropylcyclopentanecarboxylic acid (**2**) was achieved following the synthetic approach reported earlier by our group.¹⁰

General Procedure for the Synthesis of Compounds 3 and 4.

Compound **2** (1 equiv) was dissolved in 25 ml DCM. To this mixture the corresponding amine (1 equiv) was added and subsequently DiPEA (3 equiv), PyBrOP (1 equiv) and DMAP (0.8 equiv). The reaction mixture was stirred for 24 hours at room temperature. The product was partitioned between DCM and 1 M citric acid solution in water and then with DCM/1M NaOH. The organic layer was dried with MgSO₄ and evaporated. The product was purified by column chromatography (0–100% ethyl acetate in DCM).

tert-Butyl ((1*R*,3*S*)-3-isopropyl-3-(4-(4-(trifluoromethyl)pyridin-2-yl)piperazine-1-carbonyl)cyclopentyl)carbamate (**3**).¹⁸ Yield = 90%. ¹H NMR (400 MHz, CDCl₃) δ: 8.22 (d, *J* = 4.8 Hz, 1H), 6.77–6.72 (m, 2H), 4.94 (br s, 1H), 3.82 (br s, 1H), 3.70–3.61 (m, 4H), 3.59–3.45 (m, 4H), 2.11–1.90 (m, 3H), 1.80–1.61 (m, 4H), 1.31 (s, 9H), 0.81–0.72 (m, 6H).

tert-Butyl ((1*R*,3*S*)-3-isopropyl-3-(7-(trifluoromethyl)-1,2,3,4-tetrahydroisoquinoline-2-carbonyl)cyclopentyl)carbamate (**4**).²⁴ Yield = 82%. ¹H NMR (400 MHz, CDCl₃) δ: 7.45 (d, *J* = 7.6 Hz, 1H), 7.40 (s, 1H), 7.28 (d, *J* = 7.6, 1H), 4.97–4.61 (m, 3H), 4.00–3.73 (m, 3H), 2.94 (br s, 2H), 2.30–2.05 (m, 3H), 1.88–1.67 (m, 3H), 1.59 (br s, 1H), 1.42 (s, 9H), 0.91–0.84 (m, 6H).

((1*S*,3*R*)-3-Amino-1-isopropylcyclopentyl)(4-(4-(trifluoromethyl)pyridin-2-yl)piperazin-1-yl)methanone (**5**).¹⁸ Trifluoroacetic acid (4 mL) was added to a solution of compound **3** (1.20 g, 2.48 mmol) in 10 mL of DCM. The reaction mixture was stirred for 2 h at room temperature. The reaction mixture was neutralized with 1 M NaOH and extracted with DCM. The organic layer was dried with MgSO₄, filtered, and evaporated to give the product as yellow crystals (0.86 g, 90%). ¹H NMR (400 MHz, CDCl₃) δ: 8.20 (d, *J* = 4.8 Hz, 1H), 6.77–6.72 (m, 2H), 3.72–3.38 (m, 8H), 3.20–3.10 (m, 1H), 2.45–2.30 (m, 1H), 2.07–1.90 (m, 2H), 1.80–1.35 (m, 4H), 0.83–0.70 (m, 6H).

((1*S*,3*R*)-3-Amino-1-isopropylcyclopentyl)(7-(trifluoromethyl)-3,4-dihydroisoquinolin-2(1*H*)-yl)methanone (**6**).²⁴ Trifluoroacetic acid (10 mL) was added to a solution of compound **4** (3.27 g, 7.2 mmol) in 10 mL of DCM. The reaction mixture was stirred for 1 h at room temperature. The reaction mixture was neutralized with 1 M NaOH and extracted with DCM. The organic layer was dried with MgSO₄, filtered, and evaporated to give the product as yellow crystals (2.50 g, 98%). ¹H NMR (400 MHz, CDCl₃) δ: 7.40 (d, *J* = 7.6 Hz, 1H), 7.36 (s, 1H), 7.24 (d, *J* = 7.6, 1H), 4.76 (s, 2H), 3.81 (br s, 2H), 3.32–3.22 (m, 1H), 2.91 (br s, 2H), 2.53–2.45 (m, 1H), 2.18–1.73 (m, 4H), 1.69–1.60 (m, 1H), 1.40–1.35 (m, 1H), 0.91–0.84 (m, 6H).

General Procedure for the Synthesis of Compounds 7, 9 – 13 and 18 – 23.

To a series of 1.5 mL glass tubes was added amine **5** or **6** in NMP (0.95 M, 0.095 mmol), followed by solutions of different indanones (0.5 M, 0.1 mmol) in NMP, and these mixtures were subsequently treated with acetic acid (0.1 mmol), followed by 5-ethyl-2-methyl-pyridine borane (PEMB) (0.2 mmol). The reaction mixture was heated at 65 °C on a reaction block for 24 h. The reaction mixtures were purified directly using an automated mass-guided reverse-phase HPLC, and product containing fractions

were concentrated to give final products of >90% purity as judged by LC-MS (average of 220 and 254 nm traces).

((1*S*,3*R*)-3-((2,3-dihydro-1*H*-inden-1-yl)amino)-1-isopropylcyclopentyl)(4-(4-(trifluoromethyl)pyridin-2-yl)piperazin-1-yl)methanone (**7**). Purity (Average of 220 and 254 nm) = 95.4, LC-MS = 501⁺, *t*_R = 1.75 min.

Table 8. Purity, M⁺ and Retention Times of Compounds **9-13**, **18-22**.

Nr.	R	% Purity (Average of 220 and 254 nm)	Mol wt	M ⁺	Retention time (min)
9	4-Me	97.3	484.3	485.4	1.70
10	4-NH ₂	99.3	485.3	486.4	1.39
11	4-CN	97.4	495.3	496.3	1.57
12	4-OH	92.5	486.3	487.3	1.56
13	5-F	92.5	488.3	489.4	1.67
18	6-Me	97.9	484.3	485.2	1.72
19	6-CN	95.1	495.3	496.3	1.62
20	6-Cl	98.9	504.2	505.3	1.71
21	5;6-di OMe	96.1	530.3	531.3	1.58
22	4;7-di OMe	92.3	530.3	531.3	1.74

General Procedure for the Synthesis of Compounds **8, **14** – **16** and **36** – **40**.**

In a 5 mL glass tube, amine **6** (1 equiv) dissolved in 1 mL of dry THF, and the corresponding indanone (1.2 equiv) dissolved in 1 mL of dry THF were loaded. Mixture was flushed with nitrogen gas and the tube was capped. Through the septa Ti(O-*i*Pr)₄ (3 equiv) was added and the reaction mixture was stirred for 48 h at room temperature. Then the tube was decapped and NaBH₄ (5 equiv) and 0.5 mL of absolute EtOH were added, and stirred for 16 h. The reaction mixture was quenched with H₂O and resulting inorganic precipitate was filtered off and washed with DCM. The filtrate was extracted with DCM/H₂O. The organic layer was dried with MgSO₄ and evaporated. The product was purified by column chromatography (40% ethyl acetate in DCM).

((1*S*,3*R*)-3-((2,3-dihydro-1*H*-inden-1-yl)amino)-1-isopropylcyclopentyl)(7-(trifluoromethyl)-3,4-dihydroisoquinolin-2(1*H*)-yl)methanone (**8**). Yield = 34%. ¹H NMR (400 MHz, CDCl₃) δ: 7.57–7.37 (m, 2H), 7.37–7.10 (m, 5H), 4.91–4.75 (m, 2H), 4.37–4.20 (m, 1H), 3.85 (s, 2H), 3.36–3.20 (m, 1H), 3.09–2.88 (m, 3H), 2.88–2.74 (m, 1H), 2.58 (br s, 1H), 2.49–2.33 (m, 1H), 2.25–1.87 (m, 4H), 1.87–1.72 (m, 2H), 1.72–1.56 (m, 1H), 1.48–1.35 (m, 1H), 1.01–0.79 (m, 6H). LC-MS: 471⁺; *t*_R: 9.79 min.

((1*S*,3*R*)-3-((5-chloro-2,3-dihydro-1*H*-inden-1-yl)amino)-1-isopropylcyclopentyl)(7-(trifluoromethyl)-3,4-dihydroisoquinolin-2(1*H*)-yl)methanone (**14**). Yield = 32%. ¹H NMR (400 MHz, CDCl₃) δ: 7.53–7.34 (m, 2H), 7.30–7.18 (m, 4H), 4.90–4.70 (m, 2H), 4.30–4.13 (m, 1H), 3.90–3.75 (m, 2H), 3.30–3.14 (m, 1H), 3.02–2.84 (m, 3H), 2.82–2.69 (m, 1H), 2.62–2.34 (m, 2H), 2.20–1.54 (m, 7H), 1.38 (br.s, 1H), 0.98–0.76 (m, 6H). LC-MS: 505⁺; *t*_R: 9.82 min.

((1*S*,3*R*)-3-((5-bromo-2,3-dihydro-1*H*-inden-1-yl)amino)-1-isopropylcyclopentyl)(7-(trifluoromethyl)-3,4-dihydroisoquinolin-2(1*H*)-yl)methanone (**15**). Yield = 14%. ¹H NMR (400 MHz, CDCl₃) δ: 7.81–7.04 (m, 6H), 4.79 (br s, 2H), 4.21 (dd, *J* = 15.3, 8.7 Hz, 1H), 3.85 (br s, 2H), 3.23 (d, *J* = 6.5 Hz, 1H), 2.94 (d, *J* = 4.3 Hz, 2H), 2.89–2.71 (m, 2H), 2.69–2.40 (m, 2H), 2.34–1.20 (m, 8H), 1.19–0.73 (m, 6H). LC–MS: 549⁺; *t*_R: 10.19 min.

((1*S*,3*R*)-3-(((*R*)-5-bromo-2,3-dihydro-1*H*-inden-1-yl)amino)-1-isopropylcyclopentyl)(7-(trifluoromethyl)-3,4-dihydroisoquinolin-2(1*H*)-yl)methanone (**15a**). ¹H NMR (500 MHz, DMSO-*d*₆) δ: 9.05 (br s, 1H), 7.70 (br s, 1H), 7.61 (br s, 2H), 7.54 (d, *J* = 8.1 Hz, 1H), 7.52 (d, *J* = 8.1 Hz, 1H), 7.41 (d, *J* = 8.1 Hz, 1H), 4.85–4.68 (m, 3H), 3.85–3.70 (m, 2H), 3.20–3.10 (m, 1H), 3.00–2.82 (m, 3H), 2.60–2.32 (m, 4H), 2.30–2.03 (m, 4H), 1.70–1.50 (m, 2H), 0.90 (d, *J* = 6.1 Hz, 3H) 0.65 (d, *J* = 6.1 Hz, 3H),

¹³C NMR (125 MHz, DMSO-*d*₆) δ: 174.6, 148.3, 148.3, 137.7, 135.3, 129.9, 129.5, 128.5 (d, *J*_{C-F} = 11.65 Hz), 128.4, 128.1, 126.7 (q, *J*_{C-F} = 222.65 Hz), 123.9, 123.7, 123.2, 60.9, 60.9, 57.3, 57.2, 56.2, 35.3, 32.9, 30.1, 29.9, 28.8, 28.8, 28.2, 18.3, 18.3.

HRMS calcd for (C₂₈H₃₃BrF₃N₂O) [M + H]⁺ 549.1723, found 549.1708.

SFC chiral purity: 100 % ee.

15a = [α]_D²⁰ = - 5.1 (*c* = 0.65, EtOH).

((1*S*,3*R*)-3-(((*S*)-5-bromo-2,3-dihydro-1*H*-inden-1-yl)amino)-1-isopropylcyclopentyl)(7-(trifluoromethyl)-3,4-dihydroisoquinolin-2(1*H*)-yl)methanone (**15b**). ¹H NMR (500 MHz, DMSO-*d*₆) δ: 9.61 (br s, 1H), 7.70 (br s, 1H), 7.66 (br s, 2H), 7.54 (d, *J* = 8.1 Hz, 1H), 7.52 (d, *J* = 8.1 Hz, 1H), 7.41 (d, *J* = 8.1 Hz, 1H), 4.85–4.68 (m, 3H), 3.85–3.70 (m, 2H), 3.20–2.86 (m, 1H), 3.00–2.82 (m, 3H), 2.46–2.32 (m, 4H), 2.30–2.03 (m, 4H), 1.70–1.50 (m, 2H), 0.90 (d, *J* = 6.1 Hz, 3H) 0.65 (d, *J* = 6.1 Hz, 3H),

¹³C NMR (125 MHz, DMSO-*d*₆) δ: ppm 174.5, 148.3, 148.3, 137.7, 137.7, 130.3, 129.9, 128.5 (d, *J*_{C-F} = 11.65 Hz), 128.4, 128.4, 126.7 (q, *J*_{C-F} = 222.65 Hz), 123.9, 123.6, 123.3, 60.9, 60.9, 57.3, 57.2, 56.2, 35.4, 32.9, 30.1, 29.9, 28.8, 28.8, 28.2, 18.3, 18.3.

HRMS calcd for (C₂₈H₃₃BrF₃N₂O) [M + H]⁺ 549.1723, found 549.1718.

SFC chiral purity: 97.4 % ee.

15b = [α]_D²⁰ = -0.9 (*c* = 0.68, EtOH)

((1*S*,3*R*)-3-((5-iodo-2,3-dihydro-1*H*-inden-1-yl)amino)-1-isopropylcyclopentyl)(7-(trifluoromethyl)-3,4-dihydroisoquinolin-2(1*H*)-yl)methanone (**16**). Yield = 28%. ¹H NMR (400 MHz, CDCl₃) δ: 7.55 (s, 1H), 7.48–7.40 (m, 3H), 7.28 (s, 1H), 7.05 (d, *J* = 7.9 Hz, 0.5H^{*a*}), 6.99 (d, *J* = 7.9 Hz, 0.5H^{*b*}), 4.79 (s, 2H), 4.24–4.16 (m, 1H), 3.84 (br s, 2H), 3.22 (q, *J* = 6.0 Hz, 1H), 2.93 (s, 3H), 2.82–2.72 (m, 1H), 2.53 (br s, 1H), 2.43–2.34 (m, 1H), 2.16–1.82 (m, 4H), 1.80–1.60 (m, 3H), 1.38 (br s, 1H), 0.93 (d, *J* = 5.7 Hz, 3H^{*a*}); 0.87 (d, *J* = 5.7 Hz, 3H^{*b*}). *a* and *b* are indicated for different diastereomers. LC–MS: 597⁺; *t*_R: 10.06 min.

((1*S*,3*R*)-1-isopropyl-3-((3-methyl-2,3-dihydro-1*H*-inden-1-yl)amino)cyclopentyl)(7-(trifluoromethyl)-3,4-dihydroisoquinolin-2(1*H*)-yl)methanone (**36**). Yield = 41%. ¹H NMR (400 MHz, CDCl₃) δ: 7.58–7.05 (m, 7H), 4.79 (d, *J* = 16.5 Hz, 2H), 4.35–4.11 (m, 1H), 3.87 (s, 2H), 3.27 (s, 1H), 3.03 (dd, *J* = 17.9, 15.0 Hz, 1H), 2.96 (s, 2H), 2.73–2.61 (m, 2H), 2.32–1.84 (m, 4H), 1.67 (dd, *J* = 17.8, 11.2 Hz, 2H), 1.55–1.20 (m, 5H), 1.11–0.75 (m, 6H). LC–MS: 485⁺; *t*_R: 10.08 min.

((1*S*,3*R*)-3-((5-bromo-3-methyl-2,3-dihydro-1*H*-inden-1-yl)amino)-1-isopropylcyclopentyl)(7-(trifluoromethyl)-3,4-dihydroisoquinolin-2(1*H*)-yl)methanone (**37**). Yield = 8%. ¹H NMR (400 MHz, CDCl₃) δ: 7.52–7.34 (m, 2H), 7.34–7.17 (m, 3H), 7.14 (d, *J* = 7.8 Hz, 1Ha), 7.08 (d, *J* = 8.0 Hz, 1Hb), 4.90–4.70 (m, 2H), 4.20–4.00 (m, 1H), 3.86 (s, 2H), 3.32–3.25 (m, 1H), 3.13–2.84 (m, 3H), 2.81–2.61 (m, 1H), 2.54 (br s, 1H), 2.28–2.05 (m, 2H), 1.94–1.58 (m, 4H), 1.50–1.16 (m, 5H), 1.03–0.79 (m, 6H). LC–MS: 563⁺, 565⁺; *t*_R: 10.00 min.

((1*S*,3*R*)-3-((5-bromo-6-methoxy-2,3-dihydro-1*H*-inden-1-yl)amino)-1-isopropylcyclopentyl)(7-(trifluoromethyl)-3,4-dihydroisoquinolin-2(1*H*)-yl)methanone (**38**). Yield = 27%. ¹H NMR (400 MHz, CDCl₃) δ: 7.54–7.18 (m, 4H), 6.92 (s, 1H^a); 6.84 (s, 1H^b), 4.90–4.70 (m, 2H), 4.30–4.20 (m, 1H), 3.98–3.66 (m, 5H), 3.36–3.13 (m, 1H), 3.01–2.81 (m, 3H), 2.80–2.66 (m, 1H), 2.44 (br s, 2H), 2.32–1.98 (m, 4H), 1.98–1.56 (m, 3H), 1.40 (m, 1H), 0.93 (d, *J* = 5.7 Hz, 3H^a); 0.87 (d, *J* = 5.7 Hz, 3H^b). *a* and *b* are indicated for different diastereomers. LC–MS: 579⁺, 581⁺; *t*_R: 10.06 min.

((1*S*,3*R*)-3-((5-bromo-6-methoxy-3-methyl-2,3-dihydro-1*H*-inden-1-yl)amino)-1-isopropylcyclopentyl)(7-(trifluoromethyl)-3,4-dihydroisoquinolin-2(1*H*)-yl)methanone (**39**). Yield = 20%. ¹H NMR (400 MHz, CDCl₃) δ: 7.54–7.35 (m, 2H), 7.35–7.20 (m, 2H), 6.91 (s, 0.25H^a), 6.84 (s, 0.75H^b), 4.95–4.68 (m, 2H), 4.24–4.03 (m, 1H), 3.88–3.79 (m, 5H), 3.35–3.16 (m, 1H), 3.07–2.85 (m, 3H), 2.81–2.64 (m, 1H), 2.56 (s, 1H), 2.20–2.05 (m, 3H), 1.92–1.85 (m, 2H), 1.69–1.64 (m, 1H), 1.55–1.37 (m, 1H), 1.36–1.18 (m, 4H), 1.02–0.78 (m, 6H). *a* and *b* are indicated for different diastereomers. LC–MS: 593⁺, 595⁺; *t*_R: 9.35 min.

((1*S*,3*R*)-3-((5-bromo-3-ethyl-6-methoxy-2,3-dihydro-1*H*-inden-1-yl)amino)-1-isopropylcyclopentyl)(7-(trifluoromethyl)-3,4-dihydroisoquinolin-2(1*H*)-yl)methanone (**40**). Yield = 17%. ¹H NMR (400 MHz, CDCl₃) δ: 7.67–7.44 (m, 2H), 7.44–7.34 (m, 1H), 7.30 (s, 1H), 7.14 (s, 1H), 6.46 (s, 2H), 5.01–4.76 (m, 2H), 4.70 (d, *J* = 7.3 Hz, 1H), 4.09–3.71 (m, 6H), 3.19–2.64 (m, 4H), 2.51–2.14 (m, 4H), 2.13–1.70 (m, 5H), 1.56–1.39 (m, 1H), 1.16–0.77 (m, 9H). LC–MS: 607⁺, 609⁺; *t*_R: 9.60 min.

((1*S*,3*R*)-1-isopropyl-3-((5-(trifluoromethyl)-2,3-dihydro-1*H*-inden-1-yl)amino)cyclopentyl)(7-(trifluoromethyl)-3,4-dihydroisoquinolin-2(1*H*)-yl)methanone (**17a**). In a 50 mL round-bottom flask, to a solution of 1 equivalent of amine **6** in anhydrous methanol was added 1 equivalent of 5-(trifluoromethyl)-2,3-dihydro-1*H*-inden-1-one which was subsequently treated with 2 equivalents of acetic acid, followed by 4 equivalents of 5-ethyl-2-methyl-pyridine borane (PEMB). The reaction mixture was heated at 65°C for 24 h. Reaction mixture was monitored by reverse phase UPLC (*t*_R : 0.53) and was carefully quenched with concentrated HCl, then water was added to the reaction mixture and extracted with dichloromethane. The combined organic layer was washed with brine, dried over Na₂SO₄, and concentrated in vacuo. Reaction mixture was purified by flash chromatography (0–20 % CH₂Cl₂/MeOH) to afford product **17** (mixture of diastereomers). Further purification by reverse-phase HPLC using a gradient from 1 to 99% mobile phase B (mobile phase A = 0.1% HCl in water, mobile phase B = 0.1% HCl in CH₃CN) resulted in the separation of the two diastereomers **17 a** and **17 b** as HCl salt. Yield: **17a** = 19.5 %, 96% purity, UPLC-MS: 539⁺; *t*_R: 1.45 min and **17b** = 8.0%, 83% purity, UPLC-MS: 539⁺; *t*_R: 1.48 min. **17a** : ¹H NMR (400 MHz, CDCl₃) δ 10.09 (s, 1H), 9.24 (s, 1H), 7.85 (d, *J* = 8.0 Hz, 1H), 7.57 (s, 1H), 7.50 (d, *J* = 7.7 Hz, 1H), 7.46–7.38 (m, 1H), 7.35 (s, 1H), 7.29–7.20 (m, 1H), 4.90–4.62 (m, 3H), 3.84 (s, 1H), 3.68 (t, *J* = 8.7 Hz, 1H), 3.48 (q, *J* = 7.8, 7.0 Hz, 1H), 2.93 (ddt, *J* = 19.3, 11.4, 5.0 Hz, 3H), 2.68 (d, *J* = 14.1 Hz, 1H), 2.64–2.37 (m, 3H), 2.18–1.97 (m, 3H), 1.92 (dd, *J* = 14.2, 7.4 Hz, 1H), 1.80 (s, 1H), 1.68 (d, *J* = 12.1 Hz, 1H), 0.84 (dd, *J* = 20.0, 6.6 Hz, 6H).

General Procedure for the Synthesis of Compounds **23** – **35**.

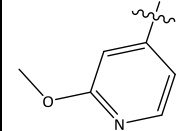
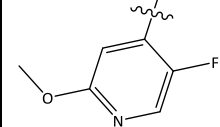
To a series of 1.5 mL glass tubes was added **15** in toluene (0.1 mmol) followed by solutions of different aryl boronic acids (0.5 M, 0.2 mmol) in NMP and these mixtures were subsequently treated with Na₂CO₃ solution (1 M, 0.2 mmol) followed by Pd(PPh₃)₄ in toluene (0.05 eq, 0.005 mmol). The reaction mixtures (0.15 M) were capped and heated at 80°C on a reaction block overnight. The reaction mixtures were purified directly using an automated mass-guided reverse phase-HPLC, and product containing fractions were concentrated to give final products >90% purity as judged by LC-MS (average of 220 nm and 254 nm traces).

Table 9. Purity, M⁺ and retention times of compounds **23–30**.

Nr.	R	% Purity (Average of 220 and 254 nm)	Mol wt	M ⁺	Retention time (min)
23	H	96.8	546.29	547.2	1.92
24	2-Me	91.5	560.3	561.3	1.92
25	3-Me	99.5	560.3	561.3	1.96
26	3-CN	99.38	571.3	572.3	1.77
27	4-CN	99.5	571.3	572.2	1.76
28	2-OMe	92.9	576.3	577.3	1.89
29	3-OMe	97.7	576.3	577.3	1.66
30	4-OMe	99.0	576.3	577.3	1.83

Table 10. Purity, M⁺ and retention times of compounds **31-35**.

Nr.	R	% Purity (Average of 220 and 254 nm)	Mol wt	M ⁺	Retention time (min)
31		99.9	547.3	548.2	1.40
32		99.9	577.3	578.3	1.45
33		99.9	591.3	592.3	1.43

34		93.7	577.3	578.3	1.66
35		96.8	595.3	596.3	1.79

(1*S*,3*R*)-*N*-(3,5-bis(trifluoromethyl)benzyl)-3-(((1*S*,3*R*)-5-bromo-3-methyl-2,3-dihydro-1*H*-inden-1-yl)amino)-1-isopropylcyclopentanecarboxamide (**37a**) and (1*S*,3*R*)-*N*-(3,5-bis(trifluoromethyl)benzyl)-3-(((1*S*,3*S*)-5-bromo-3-methyl-2,3-dihydro-1*H*-inden-1-yl)amino)-1-isopropylcyclopentanecarboxamide (**37b**). In a 20 mL scintillation vial, to a solution of **50** (1.00 g, 1.34 mmol) in DMF (10 mL) was added K₂CO₃ (0.55 g, 4.01 mmol) and benzenethiol (274.4 μL, 2.67 mmol), and the reaction mixture was stirred at room temperature for 30 min. The reaction was monitored by reverse phase UPLC (*t_R*: 0.73 and 0.74). To the reaction mixture was added water (20 mL) followed by extraction with CH₂Cl₂ (4 × 100 mL). The combined organic layer was washed with water, brine, dried over Na₂SO₄, and concentrated *in vacuo*. The brown residue was purified by flash chromatography (0-10% CH₂Cl₂/MeOH) to afford **37a** (0.10 g) and **37b** (0.10 g) with 80% diastereomeric excess purity by SFC analysis. Further purification was carried out by reverse-phase preparatory HPLC-UV with a gradient from 1 to 99% mobile phase B (mobile phase A = 0.1% HCl in water, mobile phase B = 0.1% HCl in CH₃CN) resulting in pure **37a** HCl salt and **37b** HCl salt as a white solid. Yield: **37a** = 14.7 mg, 1.8%, UPLC-MS: 563⁺, 565⁺; *t_R*: 2.45 min. ¹H NMR (500 MHz, DMSO-*d*₆) δ: 9.06 (br s, 1 H), 7.66 (bs, 1 H), 7.60 (m, 1 H), 7.52 (d, *J* = 8.1 Hz, 1 H), 7.50 (m, 1 H), 7.47 (m, 1 H), 7.41 (d, *J* = 8.1 Hz, 1 H), 4.70 (m, 2 H), 4.69 (dd, *J* = 15.7, 7.3 Hz, 1 H), 3.77 (m, 2 H), 3.51 (s, 1 H), 3.16 (dt, *J* = 14.3, 7.0 Hz, 1 H), 2.91 (m, 2 H), 2.76–1.68 (m, 2 H), 2.39–2.24 (m, 2 H), 2.17–1.59 (m, 2 H), 2.12 (m, 1 H), 1.64 (m, 2 H), 1.33 (d, *J* = 6.8 Hz, 3 H), 0.89–0.75 (d, *J* = 6.1 Hz, 6 H). ¹³C NMR (125 MHz, DMSO-*d*₆) δ: 175.3, 150.9, 144.6, 139.3, 135.0, 130.3, 129.9, 128.6 (d, *J*_{C-F} = 11.65 Hz), 126.9, 126.4 (q, *J*_{C-F} = 222.65 Hz), 126.9, 123.6, 123.3, 120.1, 60.0, 55.7, 57.7, 47.8, 42.8, 38.5, 37.2, 36.6, 32.9, 29.9, 28.8, 28.8, 19.9, 18.3, 18.3. ROESY (NOE) (500 MHz, DMSO-*d*₆) δ ppm 7.50 [1.33 (H-30)], 4.69 [2.76 (H-6), 1.68 (H-6 weak), 2.17 (H-12), 3.16 (H-7)]. HRMS calcd for (C₂₉H₃₄BrF₃N₂O) [M + H]⁺ 563.1879, found 563.1883. SFC chiral purity: 99.1% ee. **37a** = [α]_D²⁰ = + 12.2 (*c* = 0.43, EtOH)

37b = 17.3 mg, 2.1%, UPLC-MS: 563⁺, 565⁺; *t_R*: 2.49 min. ¹H NMR (500 MHz, DMSO-*d*₆) δ: 9.06 (bs, 1 H), 7.66 (bs, 1 H), 7.60 (m, 1 H), 7.52 (d, *J* = 8.1 Hz, 1 H), 7.50 (m, 1 H), 7.47 (m, 1 H), 7.41 (d, *J* = 8.1 Hz, 1 H), 4.70 (m, 2 H), 4.69 (dd, *J* = 15.7, 7.3 Hz, 1 H), 3.77 (m, 2 H), 3.52 (m, 1 H), 3.41 (s, 1 H), 2.91 (m, 2 H), 2.91 (m, 2 H), 2.50–1.98 (m, 2 H), 2.39–2.24 (m, 2 H), 2.17–1.59 (m, 2 H), 2.12 (m, 1 H), 1.64 (m, 2 H), 1.25 (d, *J* = 6.8 Hz, 3 H), 0.89–0.75 (d, *J* = 6.1 Hz, 6 H).

^{13}C NMR (125 MHz, DMSO- d_6) δ : 175.3, 150.9, 144.6, 139.3, 135.0, 130.3, 129.9, 128.6 (d, $J_{\text{C-F}}$ = 11.65 Hz), 126.9, 126.9, 126.4 (q, $J_{\text{C-F}}$ = 222.65 Hz), 123.6, 123.3, 120.1, 59.89, 57.7, 55.7, 47.8, 42.8, 38.0, 37.4, 36.6, 32.9, 29.9, 28.8, 28.8, 19.9, 18.3, 18.3

ROESY (NOE) (500 MHz, DMSO- d_6) δ : ppm 7.50 [3.52 (H-7)], 1.25 (H-30 weak)], 4.69 [2.50 (H-6), 1.98 (H-6 weak)].

HRMS calcd for (C₂₉H₃₄BrF₃N₂O) [M + H]⁺ 563.1879, found 563.1883.

SFC chiral purity: 95.2% ee.

37b = $[\alpha]_{\text{D}}^{20}$ = + 13.9 (c = 0.50, EtOH)

(1*S*,3*R*)-*N*-(3,5-bis(trifluoromethyl)benzyl)-3-(((1*R*,3*R*)-5-bromo-3-methyl-2,3-dihydro-1*H*-inden-1-yl)amino)-1-isopropylcyclopentanecarboxamide (**37c**) and (1*S*,3*R*)-*N*-(3,5-bis(trifluoromethyl)benzyl)-3-(((1*R*,3*S*)-5-bromo-3-methyl-2,3-dihydro-1*H*-inden-1-yl)amino)-1-isopropylcyclopentanecarboxamide (**37d**). In a 20 mL scintillation vial, to a solution of **51** (1.00 g, 1.34 mmol) in DMF (10 mL) was added K₂CO₃ (0.55 g, 4.01 mmol) and benzenethiol (274.4 μL , 2.67 mmol), and the reaction mixture was stirred at room temperature for 30 min. The reaction was monitored by reverse phase UPLC (t_{R} : 0.76). To the reaction mixture was added water (20 mL) followed by extraction with CH₂Cl₂ (4 \times 100 mL). The combined organic layer was washed with water, brine, dried over Na₂SO₄, and concentrated *in vacuo*. The brown residue was purified by flash chromatography (0-10% CH₂Cl₂/MeOH) to afford **37c** (50 mg) and **37d** (90 mg) both with 50% diastereomeric excess purity. Further purification was carried out by reverse-phase preparatory HPLC-UV with a gradient from 1 to 99% mobile phase B (mobile phase A = 0.1% HCl in water, mobile phase B = 0.1% HCl in CH₃CN) resulting in **37c** HCl salt and **37d** HCl salt as a white solid, both again with 70% diastereomeric excess purity. Therefore further purification was carried out on a Gilson purification instrument with a normal phase silica column and a diode array detector using a Luna Phenomenex column (50mm \times 21mm, 5 μm), and a linear gradient from 1 to 10% (CH₂Cl₂/MeOH) of mobile phase was applied. Mobile phase A consisted of CH₂Cl₂ and mobile phase B consisted of 10% MeOH/CH₂Cl₂. Yield: **37c** = 13.1 mg, 1.7%, UPLC-MS: 563⁺, 565⁺; t_{R} : 2.52 min. ^1H NMR (500 MHz, DMSO- d_6) δ : 7.66 (bs, 1 H), 7.60 (m, 1 H), 7.52 (d, J = 8.1 Hz, 1 H), 7.41 (d, J = 8.1 Hz, 1 H), 7.38 (m, 1 H), 7.30 (m, 1 H), 4.70 (m, 2 H), 4.01 (m, 1 H), 3.77 (m, 2 H), 3.51 (s, 1 H), 3.14 (m, 1 H), 2.91 (m, 2 H), 2.57–1.20 (m, 2 H), 2.39–2.24 (m, 2 H), 2.17–1.59 (m, 2 H), 2.12 (m, 1 H), 1.64 (m, 2 H), 1.24 (d, J = 6.8 Hz, 3 H), 0.89–0.75 (d, J = 6.1 Hz, 6 H).

^{13}C NMR (125 MHz, DMSO- d_6) δ : 175.3, 150.9, 144.6, 139.3, 135.0, 130.3, 129.9, 128.6 (d, $J_{\text{C-F}}$ = 11.65 Hz), 126.9, 126.4 (q, $J_{\text{C-F}}$ = 222.65 Hz), 123.6, 123.4, 123.3, 120.1, 60.0, 58.4, 57.7, 55.7, 47.8, 44.8, 42.8, 36.6, 32.9, 29.9, 28.8, 28.8, 19.9, 18.3, 18.3

HRMS calcd for (C₂₉H₃₄BrF₃N₂O) [M + H]⁺ 563.1879, found 563.1883.

SFC chiral purity: 95.0% ee.

37c = $[\alpha]_{\text{D}}^{20}$ = + 1.9 (c = 1.9, EtOH).

37d = 12.7 mg, 1.7%, UPLC-MS: 563⁺, 565⁺; t_{R} : 2.52 min. ^1H NMR (500 MHz, DMSO- d_6) δ : 9.06 (bs, 1 H), 7.66 (bs, 1 H), 7.60 (m, 1 H), 7.52 (d, J = 8.1 Hz, 1 H), 7.50 (m, 1 H), 7.47 (m, 1 H), 7.41 (d, J = 8.1 Hz, 1 H), 4.70 (m, 2 H), 4.12 (dd, J = 15.7, 7.3 Hz, 1 H), 3.77 (m, 2 H), 3.51 (s, 1 H), 3.23 (dt, J = 14.3, 7.0 Hz, 1 H), 2.91 (m, 2 H), 2.76–1.68 (m, 2 H), 2.39–2.24 (m, 2 H), 2.17–1.59 (m, 2 H), 2.12 (m, 1 H), 1.64 (m, 2 H), 1.16 (d, J = 6.8 Hz, 3 H), 0.89–0.75 (d, J = 6.1 Hz, 6 H).

^{13}C NMR (125 MHz, DMSO- d_6) δ : 175.3, 150.9, 144.6, 139.3, 135.0, 130.3, 129.9, 128.6(d, $J_{\text{C-F}} = 11.65$ Hz), 126.9, 126.9, 126.4 (q, $J_{\text{C-F}} = 222.65$ Hz), 123.6, 123.3, 120.1, 60.0, 57.7, 55.7, 47.8, 42.8, 38.5, 37.2, 36.6, 32.9, 29.9, 28.8, 28.8, 20.9, 18.3, 18.3

HRMS calcd for ($\text{C}_{29}\text{H}_{34}\text{BrF}_3\text{N}_2\text{O}$) [$\text{M} + \text{H}$] $^+$ 563.1879, found 563.1857.

SFC chiral purity: 95.3% ee.

37d = $[\alpha]_{\text{D}}^{20} = -0.9$ ($c = 0.9$, EtOH).

5-bromo-3-methyl-2,3-dihydro-1H-inden-1-one (**42**).¹³ In a 50 mL round-bottom flask NaCl (3.7 g, 63.0 mmol) and AlCl_3 (15.0 g, 115 mmol) were loaded and heated at 130 °C until completely melted. Next, 4-bromo-4-chloro-butyrophenone (**41**) (3.0 g, 11.5 mmol) was added and the reaction mixture was heated at 180 °C for 30 min. After cooling to room temperature, the reaction mixture was slowly poured on an ice/1N HCl mixture – an exothermic reaction was observed. The reaction mixture was extracted with DCM, dried with MgSO_4 and the organic solvent was evaporated to yield 2.35 g (yield 91%, with 90% purity) of light brown crystals which were used in the next step without purification. ^1H NMR (400 MHz, CDCl_3) δ : 7.70 (s, 1H), 7.61 (d, $J = 8.4$ Hz, 1H), 7.54 (d, $J = 8.4$ Hz, 1H), 3.50–3.40 (m, 1H), 2.96 (ABX, $J = 19.2$ Hz a , $J = 7.6$ Hz b , 1H), 2.30 (ABX, $J = 18.8$ Hz a , $J = 3.6$ Hz b , 1H), 1.43 (d, $J = 7.2$ Hz, 3H).

((6-bromo-5-methoxy-1H-inden-3-yl)oxy)(tert-butyl)dimethylsilane (**44**). In a 25 mL round-bottom flask 5-bromo-6-methoxy-2,3-dihydro-1H-inden-1-one (**43**) (0.96 g, 4.0 mmol) was dissolved in 8 mL of toluene and cooled to 0 °C. TBDMS-Cl solution in toluene (1.95 mL, 6.5 mmol) was added, followed by dropwise addition of DBU (1.12 mL, 7.5 mmol). The reaction mixture was stirred at 0 °C for 10 min and continued to be stirred at room temperature for 7 days. The reaction mixture was extracted with $\text{Et}_2\text{O}/\text{H}_2\text{O}$, dried with MgSO_4 , and evaporated. Yield = 1.40 g (98%), which was used in the next step without purification. ^1H NMR (400 MHz, CDCl_3) δ : 7.55 (s, 1H), 6.94 (s, 1H), 5.47 (t, $J = 2.4$ Hz, 1H), 3.96 (s, 3H), 3.22 (d, $J = 2.4$ Hz, 2H), 1.05 (s, 9H), 0.29 (s, 6H).

5-bromo-6-methoxy-3-methyl-2,3-dihydro-1H-inden-1-one (**45**). In a 20 mL reaction tube a 2 M solution of LDA (0.6 mL, 1.2 mmol) in THF/heptane/ethylbenzene was mixed with 5 mL of dry THF. The reaction mixture was cooled down to –78 °C and compound **44** (0.35 g, 1 mmol) (dissolved in 1 mL of dry THF) was added. The reaction mixture was warmed to –35 °C during 1 h and then cooled back to –78 °C. Methyl iodide (0.08 mL, 1.3 mmol) was added and the reaction mixture was warmed to room temperature over 2 h and left stirring overnight. 37% HCl in water (0.27 mL, 3.2 mmol) was added and this mixture was stirred for 3 h. The reaction mixture was extracted with $\text{DCM}/\text{H}_2\text{O}$, dried with MgSO_4 , and evaporated. The product was purified by column chromatography with DCM as eluent. Yield = 0.21 g (82%). ^1H NMR (400 MHz, CDCl_3) δ : 7.61 (s, 1H), 7.03 (s, 1H), 3.83 (s, 3H), 3.35 – 3.25 (m, 1H), 2.85 (ABX, $J = 18.8$ Hz a , $J = 7.6$ Hz b , 1H), 2.18 (ABX, $J = 19.2$ Hz a , $J = 3.2$ Hz b , 1H), 1.29 (d, $J = 7.2$ Hz, 3H).

5-bromo-6-methoxy-3-ethyl-2,3-dihydro-1H-inden-1-one (**46**). In a 20 mL reaction tube a 2 M solution of LDA (0.6 mL, 1.2 mmol) was dissolved in 5 mL of dry THF. The reaction mixture was cooled down to –78 °C and compound **44** (0.35 g, 1 mmol) (dissolved in 1 mL of dry THF) was added. The reaction mixture was warmed to –35 °C during 1 h and then cooled back to –78 °C. Ethyl iodide (0.10 mL, 1.3 mmol) was added and the reaction mixture was warmed to room temperature during 2 h and left stirring overnight. 37% HCl in water (0.27 mL, 3.2 mmol) was added and stirred for 3 h. The reaction mixture was extracted with $\text{DCM}/\text{H}_2\text{O}$, dried with MgSO_4 , and evaporated. The product was purified by column chromatography with DCM as eluent. Yield = 0.24 g (89%). ^1H NMR (400 MHz, CDCl_3) δ : 7.67 (s, 1H), 7.11 (s, 1H), 3.88 (s, 3H), 3.35–3.25 (m, 1H), 2.81 (ABX, $J = 19.2$ Hz a , $J = 7.2$ Hz b , 1H), 2.32 (ABX, $J = 19.2$ Hz a , $J = 3.2$ Hz b , 1H), 1.95–1.85 (m, 1H), 1.55–1.45 (m, 1H), 0.93 (t, $J = 7.2$ Hz, 3H).

(1S)-5-bromo-3-methyl-2,3-dihydro-1H-inden-1-ol (**47**). In a 50 mL round bottom flask under N_2 atmosphere, (*R*)-(+)-2-methyl-CBS-oxazaborolidine catalyst (73.9 mg, 0.27 mmol, 1 M in toluene) in anhydrous toluene (5 mL) was added to *N,N*-diethylaniline borane (1.58 mL, 8.88 mmol) at room temperature (25 °C). To this solution **42** (0.50 g, 2.22 mmol) in toluene (20 mL) was added dropwise over

5 h, and the resulting mixture was stirred overnight at room temperature (25°C). Reaction was monitored by reverse phase UPLC (t_R : 0.59). The reaction mixture was carefully quenched with methanol (5 mL) and 1 M HCl (1 mL) and extracted with ethyl acetate (4 × 50 mL). The combined organic layer was washed with brine, dried over Na_2SO_4 , and concentrated *in vacuo*. The white residue was purified by flash chromatography (0-30 % ethyl acetate/hexanes) to afford the white crystalline solid **47** as a racemic mixture of diastereomers in a ratio 3:5. Yield = 0.49 g, 2.16 mmol (97%). ^1H NMR (400 MHz, CDCl_3) δ : 7.41–7.32 (m, 3H), 7.29–7.22 (m, 3H), 5.20 (dd, J = 6.4, 3.1 Hz, 1H), 5.16–5.08 (m, 1H), 3.43 (h, J = 7.0 Hz, 1H), 3.05 (h, J = 7.1 Hz, 1H), 2.76 (dt, J = 12.7, 7.1 Hz, 1H), 2.25 (ddd, J = 13.6, 7.4, 3.1 Hz, 1H), 1.98 (dt, J = 13.4, 6.6 Hz, 1H), 1.49 (ddd, J = 12.7, 8.9, 7.6 Hz, 1H), 1.34 (d, J = 6.8 Hz, 3H), 1.26 (dd, J = 7.1, 2.4 Hz, 2H). HPLC (Chiralpak AD-H column, 10% MeOH with 20 nM NH_3 , 90% CO_2 , 3.0 mL/min, 254 nm, ee = 95.8%. UPLC-MS: 209⁺, 211⁺; t_R : 1.91 min.

(1*R*)-5-bromo-3-methyl-2,3-dihydro-1*H*-inden-1-ol (**48**). In a 50 mL round bottom flask under N_2 , (S)-(+)-2-methyl-CBS-oxazaborolidine catalyst (73.9 mg, 0.27 mmol, 1 M in toluene) in anhydrous toluene (5 mL) was added to *N,N*-diethylaniline borane (1.58 mL, 8.88 mmol) at room temperature (25°C). To this solution **42** (0.50 g, 2.22 mmol) in toluene (20 mL) was added dropwise over 5 h, and the resulting mixture was stirred overnight at room temperature (25°C). The reaction was monitored by reverse phase UPLC (t_R : 0.58). The reaction mixture was carefully quenched with methanol (5 mL) and 1 N HCl (1 mL) and then extracted with ethyl acetate (4 × 50 mL). The combined organic layer washed with brine, dried over Na_2SO_4 , and concentrated *in vacuo*. The white residue was purified by flash chromatography (0-30 % ethyl acetate/hexanes) to afford the white crystalline solid **48** as a racemic mixture in a ratio (3:5). Yield = 0.50 g, 2.20 mmol (99%). ^1H NMR (400 MHz, CDCl_3) δ : 7.37 (dddt, J = 8.4, 5.6, 2.8, 1.2 Hz, 4H), 7.28–7.22 (m, 2H), 5.20 (dd, J = 6.4, 3.1 Hz, 1H), 5.12 (t, J = 7.3 Hz, 1H), 3.43 (h, J = 7.0 Hz, 1H), 3.12–2.97 (m, 1H), 2.76 (dt, J = 12.7, 7.1 Hz, 1H), 2.25 (ddd, J = 13.6, 7.4, 3.1 Hz, 1H), 1.98 (dt, J = 13.4, 6.6 Hz, 1H), 1.49 (ddd, J = 12.7, 8.9, 7.7 Hz, 1H), 1.34 (d, J = 6.8 Hz, 3H), 1.26 (d, J = 7.0 Hz, 2H). HPLC (Chiralpak AD-H column, 10% MeOH with 20 nM NH_3 , 90% CO_2 , 3.0 mL/min, 254 nm, ee = 96.2%. UPLC-MS: 209⁺, 211⁺; t_R : 1.92, 1.95 min.

N-((1*R*,3*S*)-3-isopropyl-3-(7-(trifluoromethyl)-1,2,3,4-tetrahydroisoquinoline-2-carbonyl)cyclopentyl)-2-nitrobenzenesulfonamide (**49**). In a 50 mL round bottom flask, to a solution of amine **6** (1.00 g, 2.82 mmol) in anhydrous CH_2Cl_2 (10 mL) was added 2-nitrobenzenesulfonyl chloride (0.75 mg, 3.38 mmol) followed by DIPEA (1.70 mL, 9.73 mmol) and stirred at room temperature (25°C) for 1 h. The reaction was monitored by reverse phase UPLC (t_R : 0.77). The reaction mixture was concentrated *in vacuo* to obtain the crude product (yellow oil). The product was purified by flash chromatography (40-80 % ethyl acetate/hexanes) to afford the light yellow foamy solid **49**. Yield = 1.50 g (98%). ^1H NMR (400 MHz, CDCl_3) δ : 8.16–8.09 (m, 1H), 7.82–7.75 (m, 1H), 7.75–7.64 (m, 2H), 7.48–7.40 (m, 1H), 7.36 (s, 1H), 7.27 (d, J = 4.9 Hz, 1H), 6.05 (s, 1H), 4.81 (s, 1H), 4.71 (d, J = 16.4 Hz, 1H), 3.94 (d, J = 16.7 Hz, 1H), 3.81 (dq, J = 8.7, 4.3 Hz, 1H), 3.76–3.64 (m, 1H), 2.90 (tt, J = 16.6, 6.4 Hz, 2H), 2.40 (d, J = 12.9 Hz, 1H), 2.14 (pent., J = 6.7 Hz, 1H), 1.82 (d, J = 16.1 Hz, 3H), 1.67 (dd, J = 8.6, 4.5 Hz, 1H), 1.58–1.40 (m, 1H), 0.87 (d, J = 6.7 Hz, 3H), 0.76 (d, J = 6.7 Hz, 3H). UPLC-MS: 540⁺; t_R : 2.85 min.

N-((1*R*)-5-bromo-3-methyl-2,3-dihydro-1*H*-inden-1-yl)-*N*-((1*R*,3*S*)-3-isopropyl-3-(7-(trifluoromethyl)-1,2,3,4-tetrahydroisoquinoline-2-carbonyl)cyclopentyl)-2-nitrobenzenesulfonamide (**50**). In a 100 mL round-bottom flask, to a cooled solution (–78 °C, acetone/dry ice bath) of PPh_3 (1.23 g, 4.69 mmol) in anhydrous THF (20 mL) was added DEAD (0.82 g, 4.69 mmol) and stirred for 30 min, followed by addition of **47** (0.40 g, 1.76 mmol). The pink colored reaction mixture was allowed to stir for 30 min maintaining the temperature at –78 °C. To this solution, **49** (0.63 g, 1.17 mmol) was added. The reaction mixture was stirred for 6 h at –78 °C and allowed to warm up to room temperature overnight. The

reaction was monitored by reverse phase UPLC (t_R : 0.93). The reaction mixture was concentrated *in vacuo* to obtain a pink-colored residue. The crude residue was purified by flash chromatography (0-10 % $\text{CH}_2\text{Cl}_2/\text{MeOH}$) to afford the light pink foamy solid **50** (purity 80%). Yield = 1.00 g (<100%). UPLC-MS: 540⁺; t_R : 3.53 min. Without further purification, **50** was taken forward in the following deprotection step.

N-((1*S*)-5-bromo-3-methyl-2,3-dihydro-1*H*-inden-1-yl)-*N*-((1*R*,3*S*)-3-isopropyl-3-(7-(trifluoromethyl)-1,2,3,4-tetrahydroisoquinoline-2-carbonyl)cyclopentyl)-2-nitrobenzenesulfonamide (**51**). In a 100 mL round-bottom flask, to a cooled solution (−78 °C, acetone/ dry ice bath) of PPh_3 (1.23 g, 4.69 mmol) in anhydrous THF (20 mL) was added DEAD (0.82 g, 4.69 mmol) and stirred for 30 min, followed by addition of **48** (0.40 g, 1.76 mmol). The pink colored reaction mixture was allowed to stir for 30 min maintaining the temperature at −78 °C. To this solution, **49** (0.63 g, 1.17 mmol) was added. The reaction mixture was stirred for 6 h at −78 °C and allowed to warm up to room temperature overnight. The reaction was monitored by reverse phase UPLC (t_R : 0.93). The reaction mixture was concentrated *in vacuo* to obtain a pink color residue. The crude residue was purified by flash chromatography (0-10 % $\text{CH}_2\text{Cl}_2/\text{MeOH}$) to afford the light pink foamy solid **55** (purity 80%). Yield = 1.00 g (<100%). UPLC-MS: 540⁺; t_R : 3.53 min. Without further purification, **51** was taken forward in the following deprotection step.

X-Ray Data

Experimental Summary for (15a)

The single crystal X-ray diffraction studies were carried out on a Bruker Kappa APEX-II CCD diffractometer equipped with Mo K_α radiation ($\lambda = 0.71073 \text{ \AA}$). A 0.30 x 0.25 x 0.20 mm colorless block was mounted on a Cryoloop with Paratone oil. Data were collected in a nitrogen gas stream at 100(2) K using ϕ and ω scans. Crystal-to-detector distance was 40 mm and exposure time was 5 seconds per frame using a scan width of 0.5°. Data collection was 98.6% complete to 25.00° in θ . A total of 6816 reflections were collected covering the indices, $-7 \leq h \leq 4$, $-12 \leq k \leq 19$, $-30 \leq l \leq 25$. 4615 reflections were found to be symmetry independent, with a R_{int} of 0.0235. Indexing and unit cell refinement indicated a primitive, orthorhombic lattice. The space group was found to be $P2_12_12_1$. The data were integrated using the Bruker SAINT software program and scaled using the SADABS software program. Solution by direct methods (SHELXS) produced a complete phasing model consistent with the proposed structure. All nonhydrogen atoms were refined anisotropically by full-matrix least-squares (SHELXL-97). All hydrogen atoms were placed using a riding model. Their positions were constrained relative to their parent atom using the appropriate HFIX command in SHELXL-97.

Biology

Chemicals and reagents. ^{125}I -CCL2 (2200 Ci/mmol) was purchased from Perkin-Elmer (Waltham, MA). INCB3344 was synthesized as described previously.^{25, 26} [^3H]INCB3344 (specific activity 32 Ci mmol^{-1}) was custom-labeled by Vitrox (Placentia, CA) for which a dehydrogenated precursor of INCB3344 was provided. TangoTM CCR2-*bla* U2OS cells stably expressing human CCR2 were obtained from Invitrogen (Carlsbad, CA).

Cell culture and membrane preparation. U2OS cells stably expressing the human CCR2 receptor (Invitrogen, Carlsbad, CA) were cultured in McCoy5a medium supplemented with 10% fetal calf serum, 2 mM glutamine, 0.1 mM non-essential amino acids (NEAA), 25 mM HEPES, 1 mM sodium pyruvate, 100

IU/ml penicillin, 100 µg/ml streptomycin, 100 µg/ml G418, 50 µg/ml hygromycin and 125 µg/ml zeocin in a humidified atmosphere at 37°C and 5% CO₂. Cell culture and membrane preparation were performed as described previously.¹⁶

¹²⁵I-CCL2 displacement assay. Binding assays were performed as described previously.¹⁶

[³H]INCB3344 dual point competition association assay. Kinetic rate index (KRI) values of unlabeled ligands were determined using the dual-point competition association assay as described previously.¹⁰

[³H]INCB3344 competition association assay. The kinetic parameters of unlabeled ligands were determined using the competition association assay described earlier by our group.¹⁰

Data Analysis. All experiments were analyzed using the nonlinear regression curve fitting program Prism 5 (GraphPad, San Diego, CA). For radioligand displacement data K_i values were calculated from IC₅₀ values using the Cheng and Prusoff equation.²⁷

Abbreviations

Boc, tert-butyloxycarbonyl; CCL2, chemokine ligand 2; CCR2, chemokine receptor 2; CHAPS, 3-[(3-cholamidopropyl)dimethylammonio]-1-propanesulfonate; DBU, 1,8-diazabicycloundec-7-ene; DEA, diethylamine; DEAD, Diethyl azodicarboxylate; DCM, dichloromethane; DiPEA, N,N-diisopropylethylamine; DMAP, N,N-dimethylaminopyridine; DMF, dimethylformamide; DPM, disintegrations per minute; ESI, electrospray ionisation; FTMS, fourier transform mass spectrometer; HEPES, 4-(2-hydroxyethyl)piperazine-1-ethanesulfonic acid; hERG, human Ether-à-go-go-Related Gene; HPLC, high-performance liquid chromatography; HRMS, high resolution mass spectral analyses; IPA, isopropanol; KRI, kinetic rate index; LDA, lithium diisopropylamide; LC-MS, liquid chromatography – mass spectrometer; NEAA, non-essential amino acids; NMP, N-methylpyrrolidone; NMR, nuclear magnetic resonance; PEI, polyethylenimine; PEMB, 5-ethyl-2-methylpyridine borane; PyBrOP, bromo-trispyrrolidino phosphoniumhexafluorophosphate; RT, residence time; SAR, structure-affinity relationships; SFC, supercritical fluid chromatography; SKR, structure-kinetic relationships; TBDMS-Cl, tert-butyldimethylsilyl chloride; TFA, trifluoroacetic acid; THF, tetrahydrofuran; TLC, thin layer chromatography; TMS, tetramethylsilane; Tris, tris(hydroxymethyl)aminomethane; U2OS, human bone osteosarcoma cells; UPLC, ultra performance liquid chromatography; UV, ultraviolet.

ACKNOWLEDGEMENT

This study was financially supported by the Dutch Top Institute Pharma, project number D1-301. We thank Dr. Julien Louvel and Jacobus van Veldhoven for their input in analytical data analysis and helpful comments. We acknowledge Dong Guo and Prof. Dr. Martine Smit (Vrije Universiteit, Amsterdam, The Netherlands) for helpful comments and suggestions.

REFERENCES

1. D'Ambrosio, D.; Panina-Bordignon, P.; Sinigaglia, F. Chemokine receptors in inflammation: an overview. *Journal of immunological methods* **2003**, *273*, 3-13.
2. Kang, Y. S.; Cha, J. J.; Hyun, Y. Y.; Cha, D. R. Novel C-C chemokine receptor 2 antagonists in metabolic disease: a review of recent developments. *Expert Opin Inv Drug* **2011**, *20*, 745-56.
3. Charo, I. F.; Ransohoff, R. M. The many roles of chemokines and chemokine receptors in inflammation. *The New England journal of medicine* **2006**, *354*, 610-21.
4. Feria, M.; Diaz-Gonzalez, F. The CCR2 receptor as a therapeutic target. *Expert Opin Ther Pat* **2006**, *16*, 49-57.
5. Struthers, M.; Pasternak, A. CCR2 antagonists. *Current topics in medicinal chemistry* **2010**, *10*, 1278-98.

6. Kalliomaki, J.; Attal, N.; Jonzon, B.; Bach, F. W.; Huizar, K.; Ratcliffe, S.; Eriksson, B.; Janecki, M.; Danilov, A.; Bouhassira, D. A randomized, double-blind, placebo-controlled trial of a chemokine receptor 2 (CCR2) antagonist in posttraumatic neuralgia. *Pain* **2013**, *154*, 761-7.
7. Kalinowska, A.; Losy, J. Investigational C-C chemokine receptor 2 antagonists for the treatment of autoimmune diseases. *Expert Opin Inv Drug* **2008**, *17*, 1267-79.
8. Vergunst, C. E.; Gerlag, D. M.; Lopatinskaya, L.; Klareskog, L.; Smith, M. D.; van den Bosch, F.; Dinant, H. J.; Lee, Y.; Wyant, T.; Jacobson, E. W.; Baeten, D.; Tak, P. P. Modulation of CCR2 in rheumatoid arthritis: a double-blind, randomized, placebo-controlled clinical trial. *Arthritis Rheum-Us* **2008**, *58*, 1931-9.
9. Gilbert, J.; Lekstrom-Himes, J.; Donaldson, D.; Lee, Y.; Hu, M. X.; Xu, J.; Wyant, T.; Davidson, M.; Grp, M. S. Effect of CC Chemokine Receptor 2 CCR2 Blockade on Serum C-Reactive Protein in Individuals at Atherosclerotic Risk and With a Single Nucleotide Polymorphism of the Monocyte Chemoattractant Protein-1 Promoter Region. *American Journal of Cardiology* **2011**, *107*, 906-911.
10. Vilums, M.; Zweemer, A. J.; Yu, Z.; de Vries, H.; Hillger, J. M.; Wapenaar, H.; Bollen, I. A.; Barmare, F.; Gross, R.; Clemens, J.; Krenitsky, P.; Brussee, J.; Stamos, D.; Saunders, J.; Heitman, L. H.; Ijzerman, A. P. Structure-Kinetic Relationships-An Overlooked Parameter in Hit-to-Lead Optimization: A Case of Cyclopentylamines as Chemokine Receptor 2 Antagonists. *Journal of Medicinal Chemistry* **2013**, *56*, 7706-7714.
11. Frerot, E.; Coste, J.; Pantaloni, A.; Dufour, M. N.; Jouin, P. Pybop and Pybrop - 2 Reagents for the Difficult Coupling of the Alpha,Alpha-Dialkyl Amino-Acid, Aib. *Tetrahedron* **1991**, *47*, 259-270.
12. Burkhardt, E. R.; Coleridge, B. M. Reductive amination with 5-ethyl-2-methylpyridine borane. *Tetrahedron Lett* **2008**, *49*, 5152-5155.
13. Zhang, P.; Kern, J. C.; Terefenko, E. A.; Trybulski, E. J. 5-Aryl-indan-1-ol and analogs useful as progesterone receptor modulators. *Patent US2007066628*, **2007**.
14. Lee, S. H.; Kim, I. S.; Li, Q. R.; Dong, G. R.; Jeong, L. S.; Jung, Y. H. Stereoselective Amination of Chiral Benzylic Ethers Using Chlorosulfonyl Isocyanate: Total Synthesis of (+)-Sertraline. *Journal of Organic Chemistry* **2011**, *76*, 10011-10019.
15. Fukuyama, T.; Cheung, M.; Jow, C. K.; Hidai, Y.; Kan, T. 2,4-dinitrobenzenesulfonamides: A simple and practical method for the preparation of a variety of secondary amines and diamines. *Tetrahedron Lett* **1997**, *38*, 5831-5834.
16. Zweemer, A. J. M.; Nederpelt, I.; Vrieling, H.; Hafith, S.; Doornbos, M. L. J.; de Vries, H.; Abt, J.; Gross, R.; Stamos, D.; Saunders, J.; Smit, M. J.; Ijzerman, A. P.; Heitman, L. H. Multiple binding sites for small molecule antagonists at the chemokine receptor CCR2. *Mol. Pharmacol.* **2013** Oct;*84*(4):551-61.
17. Kothandaraman, S.; Donnelly, K. L.; Butora, G.; Jiao, R.; Pasternak, A.; Morriello, G. J.; Goble, S. D.; Zhou, C.; Mills, S. G.; Maccoss, M.; Vicario, P. P.; Ayala, J. M.; Demartino, J. A.; Struthers, M.; Cascieri, M. A.; Yang, L. Design, synthesis, and structure-activity relationship of novel CCR2 antagonists. *Bioorganic & Medicinal Chemistry Letters* **2009**, *19*, 1830-4.
18. Zheng, C.; Cao, G.; Xia, M.; Feng, H.; Glenn, J.; Anand, R.; Zhang, K.; Huang, T.; Wang, A.; Kong, L.; Li, M.; Galya, L.; Hughes, R. O.; Devraj, R.; Morton, P. A.; Rogier, D. J.; Covington, M.; Baribaud, F.; Shin, N.; Scherle, P.; Diamond, S.; Yeleswaram, S.; Vaddi, K.; Newton, R.; Hollis, G.; Friedman, S.; Metcalf, B.; Xue, C. B. Discovery of INCB10820/PF-4178903, a potent, selective, and orally bioavailable dual CCR2 and CCR5 antagonist. *Bioorganic & Medicinal Chemistry Letters* **2011**, *21*, 1442-6.
19. Jiao, R.; Goble, S. D.; Mills, S. G.; Morriello, G.; Pasternak, A.; Yang, L.; Zhou, C.; Butora, G.; Kothandaraman, S.; Guaideen, D.; Moyes, C. Tetrahydropyranyl cyclopentyl tetrahydropyridopyridine modulators of chemokine receptor activity. *Patent WO03093231*, November 13, **2003**.
20. Guo, D.; van Dorp, E. J. H.; Mulder-Krieger, T.; van Veldhoven, J. P. D.; Brussee, J.; Ijzerman, A. P.; Heitman, L. H. Dual-Point Competition Association Assay: A Fast and High-Throughput Kinetic Screening Method for Assessing Ligand-Receptor Binding Kinetics. *Journal of Biomolecular Screening* **2013**, *18*, 309-320.
21. Xue, C. B.; Wang, A. L.; Han, Q.; Zhang, Y. X.; Cao, G. F.; Feng, H.; Huang, T. S.; Zheng, C. S.; Xia, M.; Zhang, K.; Kong, L. Q.; Glenn, J.; Anand, R.; Meloni, D.; Robinson, D. J.; Shao, L. X.; Storace, L.; Li, M.; Hughes, R. O.; Devraj, R.; Morton, P. A.; Rogier, D. J.; Covington, M.; Scherle, P.; Diamond, S.; Emm, T.; Yeleswaram, S.; Contel, N.; Vaddi, K.; Newton, R.; Hollis, G.; Metcalf, B. Discovery of INCB8761/PF-4136309, a Potent, Selective, and Orally Bioavailable CCR2 Antagonist. *Acs Med Chem Lett* **2011**, *2*, 913-918.
22. Pasternak, A.; Goble, S. D.; Struthers, M.; Vicario, P. P.; Ayala, J. M.; Di Salvo, J.; Kilburn, R.; Wisniewski, T.; Demartino, J. A.; Mills, G. S.; Yang, L. Discovery of a potent orally bioavailable CCR2 and CCR5 dual antagonist. *Medicinal Chemistry Letters* **2010**, *1*, 14-18.

23. Schmidtke, P.; Luque, F. J.; Murray, J. B.; Barril, X. Shielded Hydrogen Bonds as Structural Determinants of Binding Kinetics: Application in Drug Design. *Journal of the American Chemical Society* **2011**, *133*, 18903-18910.
24. Butora, G.; Goble, S. D.; Pasternak, A.; Yang, L.; Zhou, C.; Moyes, C. R. Heterocyclic Cyclopentyl Tetrahydroisoquinoline And Tetrahydropyridopyridine Modulators Of Chemokine Receptor Activity. *US Patent US7598243*, **2004**.
25. Xue, C. M., B.; Feng, H.; Cao, G.; Huang, T.; Zheng, C.; Robinson, D. J.; Han, A. 3-Aminopyrrolidine derivatives as modulators of chemokine receptors. *Patent WO2004050024*, **2004**.
26. Brodmerkel, C. M.; Huber, R.; Covington, M.; Diamond, S.; Hall, L.; Collins, R.; Leffet, L.; Gallagher, K.; Feldman, P.; Collier, P.; Stow, M.; Gu, X.; Baribaud, F.; Shin, N.; Thomas, B.; Burn, T.; Hollis, G.; Yeleswaram, S.; Solomon, K.; Friedman, S.; Wang, A.; Xue, C. B.; Newton, R. C.; Scherle, P.; Vaddi, K. Discovery and pharmacological characterization of a novel rodent-active CCR2 antagonist, INCB3344. *Journal of immunology* **2005**, *175*, 5370-8.
27. Cheng, Y.; Prusoff, W. H. Relationship between Inhibition Constant (K1) and Concentration of Inhibitor Which Causes 50 Per Cent Inhibition (I50) of an Enzymatic-Reaction. *Biochem Pharmacol* **1973**, *22*, 3099-3108.

CHAPTER 5

EVALUATION OF (4-ARYLPYPERIDIN-1- YL)CYCLOPENTANECARBOXAMIDES AS HIGH AFFINITY AND LONG RESIDENCE TIME ANTAGONISTS FOR THE CCR2 RECEPTOR

This chapter was based upon:

M. Vilums, A.J.M. Zweemer, A. Dilanchian, J.P.D. van Veldhoven, H. de Vries, J. Brussee, D. Stamos, J. Saunders, L.H. Heitman, A.P. IJzerman.

(manuscript in preparation)

ABSTRACT

Preclinical animal models suggest that the CCL2/CCR2 axis plays an important role in the development and maintenance of inflammatory disease states (e.g., multiple sclerosis, atherosclerosis, asthma, diabetes, and neuropathic pain), which could be treated through inhibition of the CCR2 receptor. However, until now all high-affinity CCR2 antagonists that were advanced into clinical trials have failed due to the lack of efficacy. We have previously described a new approach for the design of CCR2 antagonists by the use of structure-kinetics relationships (SKR). Here we report new findings on the SAR and SKR of the reference compound MK-0483, its diastereomers, and structural analogues of it as CCR2 antagonists. On the “right-hand” side of the molecules the 7-(trifluoromethyl)-1,2,3,4-tetrahydroisoquinoline group generally yields better affinity and longer drug-target residence time (RT). On the “left-hand” side SAR of the phenyl ring suggests that lipophilic hydrogen bond accepting substituents on the 3-position are favourable. However, SKR suggests that a lipophilic group with a certain size is desired (e.g. 3-Br, 3-*i*-Pr), as present in compounds **21** and **22** ($K_i = 2.8$ and 3.6 nM, RT = 243 and 266 min, respectively). Alternatively a shielded hydrogen bond can also prolong the residence time; this was most prominently observed in MK-0483 ($K_i = 1.2$ nM, RT = 724 min) and its close analogue **26** ($K_i = 7.8$ nM) with a short residence time.

INTRODUCTION

Chemotactic cytokines (chemokines) play a vital role in the activation and regulation of leukocyte trafficking¹ and are involved in immunomodulation and host-defence mechanisms.^{2,3} Their chemoattractant activity is mediated through activation of cell-surface seven-transmembrane spanning G protein-coupled receptors (GPCRs). It seems that most of the chemokines are promiscuous in their actions since they can bind to numerous receptors.⁴ However, monocyte chemoattractant protein-1 (MCP-1/CCL2) only binds and activates the CC-chemokine receptor 2 (CCR2) and the axis of CCL2/CCR2 has been suggested to be involved in various autoimmune and inflammation-associated diseases (e.g. multiple sclerosis, atherosclerosis, asthma, diabetes, and neuropathic pain).⁵⁻⁹

As a consequence there has been an increasing interest in advancing CCR2 receptor antagonists into clinical studies. However, thus far, high-affinity CCR2 antagonists have failed to show efficacy in phase 2 clinical trials. Recently several reviews¹⁰⁻¹² have suggested to incorporate an additional parameter coined “drug-target residence time (RT)” in the early drug discovery process. RT is thought to be correlated to drug efficacy, and could serve as an early criterion to diminish the attrition rate in later stages of drug development. We have previously described how the implementation of this additional parameter in the hit-to-lead optimization process helped us to distinguish between different structures for optimization.¹³ Instead of proceeding with the highest affinity hit (**1**) (Figure 1) having a very short RT (a close analogue of MK-0812, which failed to show efficacy in clinical trials) we continued with a structure having moderate affinity only but with longer RT on the CCR2 receptor.

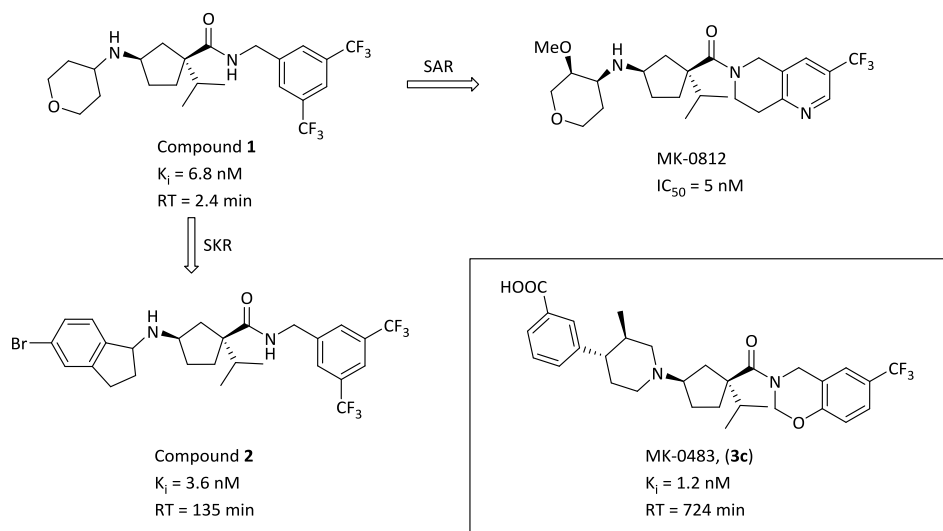


Figure 1. Structures of CCR2 antagonists **1**, **2**,¹³ MK-0812 (Merck's clinical candidate)¹⁴ and MK0483 (Merck's back-up clinical candidate).¹⁵

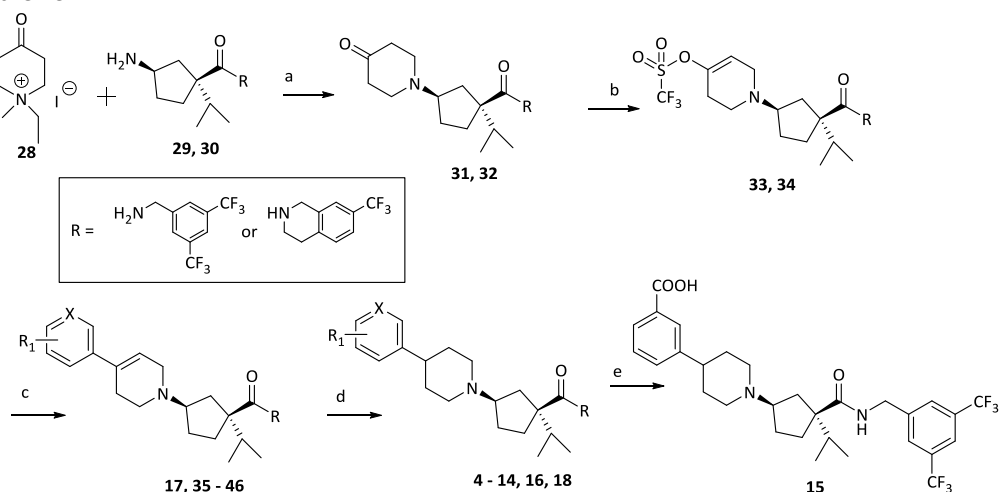
In the optimization process we improved both parameters simultaneously yielding a high-affinity and long RT CCR2 antagonist (**2**). However, the Merck research group has also reported on the discovery of MK-0483 (**3c**) a potent and orally bioavailable CCR2 and CCR5 dual antagonist, having a very slow dissociation half-life from the CCR2 receptor ($T_{1/2} > 9 \text{ h}$).¹⁵ Struthers and Pasternak¹⁴ described MK-0483 (**3c**) as the backup compound of the clinical candidate MK-0812, however, after the failure of MK-0812 in the clinical trials there is no information on further advancement of MK-0483 (**3c**) despite its slow dissociation kinetics.

In this study, we used the knowledge from our previous findings¹³ to evaluate the binding kinetics of MK-0483 (**3c**), its diastereomers (**3a**, **b**, **d**) and structural analogues that we synthesized (**4 - 27**) and to determine the structure-kinetics relationships (SKR) on the CCR2 receptor for this class of compounds. In a step-by-step manner we classified substituents on the 4 position of the piperidine ring to assess their importance in binding kinetics. In addition, we evaluated different amide substituents on the right-hand side of the molecule for the same purpose.

RESULTS AND DISCUSSION

Chemistry

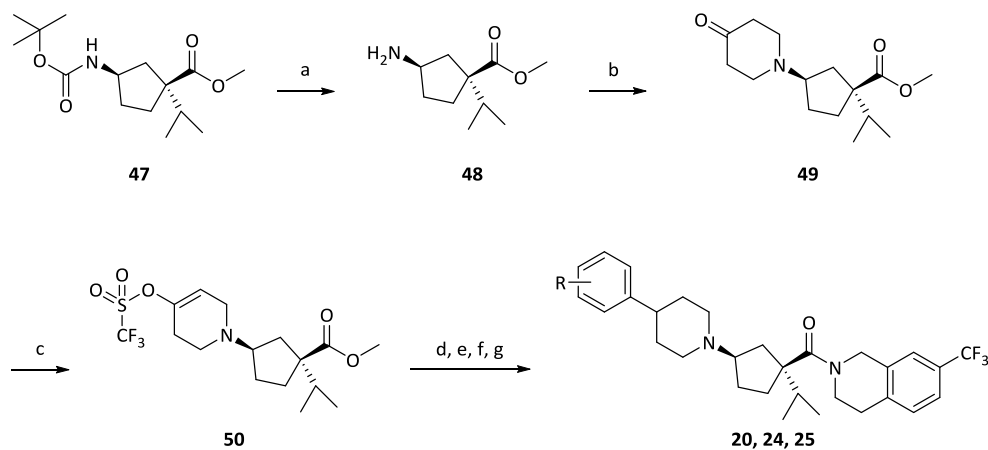
Synthesis of MK-0483 (**3c**) and its diastereomers (**3a**, **b**, **d**) was achieved following the synthetic approach reported by Pasternak et al.¹⁵ For the synthesis of MK-0483 analogues (**4** - **18**) we designed a new synthetic route, which allowed us to incorporate different substituents directly on the *cis*-cyclopentane isomer in the one before last step of the synthesis (Scheme 1).

Scheme 1.^a

^aReagents and conditions: a) K_2CO_3 , EtOH/ H_2O (3:1), reflux, 5 h, (25-72%); b) i) LDA, dry THF, $-78^\circ\text{C} \rightarrow -20^\circ\text{C}$; ii) *N*-phenyl-bis(trifluoromethanesulfonyl)imide, $-78^\circ\text{C} \rightarrow$ room temperature, (21-42%); c) corresponding arylboronic acid, LiCl, 2 M $\text{Na}_2\text{CO}_3(\text{aq})$, Pd(PPh_3)₄, DME, 90°C , 3.5 h, (20-99%); d) Pd/C, Pd(OAc)₂, H_2 1 atm, MeOH or THF, (9-70%); e) ester **16**, 4 M LiOH_(aq), $\text{H}_2\text{O}/\text{EtOH}$, 50°C , 1.5 h, (53%). For designation of R₁, see Table 2 and 3.

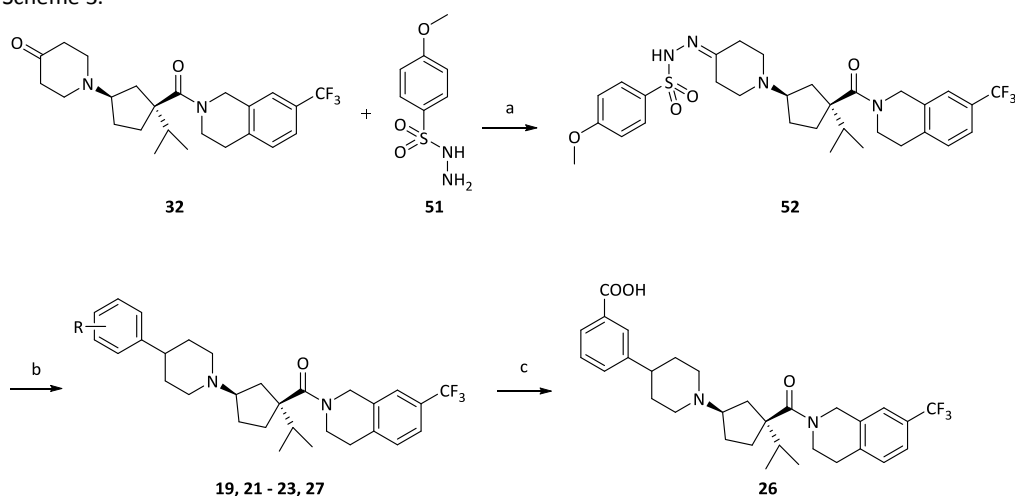
We started with a sequenced Hoffman elimination and conjugated addition¹⁶ of *N,N*-ethylmethyl-4-oxo-piperidinium iodide¹⁷ (**28**) to amines **29** and **30**, which were obtained following the synthetic approaches described earlier by our group.¹⁸ Piperidones **31** and **32** were deprotonated with lithium diisopropylamide (LDA) and subsequently treated with *N*-phenyl-bis(trifluoromethanesulfonyl)imide to generate triflates **33** and **34**. These triflates were used in a Suzuki-coupling with different arylboronic acids, and subsequent hydrogenation of the

formed olefins (**17**, **35** - **46**) resulted in the final compounds (**4** - **14**, **16**, **18**) with the desired groups on the 4 position of the piperidine ring. Additional saponification of compound **16** yielded benzoic acid **15**. Any attempts to introduce halogen substituents on the aryl group using this synthetic route resulted in dehalogenation products during the hydrogenation step. We argued that the hydrogenation could be more selective if less bulky structures were used. Therefore we decided to reverse the synthetic route and modify the left-hand side of the molecules prior to peptide coupling on the right-hand side (Scheme 2). The synthesis of (1*S*,3*R*)-methyl-3-((*tert*-butoxycarbonyl)amino)-1-isopropylcyclopentanecarboxylate **47** was achieved following the synthetic approach reported by Kothandaraman et al.¹⁹ The TFA mediated *N*-Boc deprotection yielded amine **48**, which was used in a coupling reaction with the piperidone salt **28**. The coupling was performed in several smaller batches in parallel as big scale reactions resulted in poor yields. Subsequently the triflate **50** was generated from the piperidone **49** under the same conditions as for compounds **33** and **34**. The triflate **50** was coupled with corresponding boronic acids and the obtained olefins were hydrogenated using PtO₂. In this case only traces of the dehalogenated products were observed.

Scheme 2.^a

^aReagents and conditions: a) TFA, DCM, 2 h, room temperature (98%); b) K₂CO₃, EtOH/H₂O (3:1), reflux, 3 h (56%); c) i) LDA, dry THF, -100 °C → -40 °C; ii) *N*-phenyl-bis(trifluoromethanesulfonylimide), -80 °C → room temperature (67%); d) corresponding arylboronic acid, LiCl, 2 M Na₂CO_{3(aq)}, Pd(PPh₃)₄, DME, 90 °C, 3.5 h; e) PtO₂, H₂ 2 atm, THF, room temperature, 10-15 min; f) 4 M LiOH_(aq), H₂O/EtOH, reflux, 3 h; g) 7-(trifluoromethyl)-1,2,3,4-tetrahydroisoquinoline hydrochloride, PyBrOP, DIPEA, DMAP, DCM, room temperature, 48 h, (yield in four steps = 0.8-9%). For designation of R, see Table 3.

Next, a saponification of the esters and peptide coupling under bromo-tris-pyrrolidino phosphoniumhexafluorophosphate (PyBroP) conditions yielded final compounds **20**, **24**, and **25**. However, this approach gave poor overall yields and was abandoned for further synthesis. Recently, Allwood et al.²⁰ described a new, metal-free reductive coupling of saturated heterocyclic sulfonylhydrazones with boronic acids as an alternative to the tedious step-by-step route depicted in scheme 1. Analogous to the method described by Allwood et al., the tosylhydrazone **52** was obtained in a quantitative yield from piperidone intermediate **32** and sulfonylhydrazide **51** (Scheme 3).²⁰ Subsequently, the reductive coupling of the corresponding arylboronic acids and the tosylhydrazone **52** resulted in the desired products, which were purified by preparative HPLC yielding the final compounds **19**, **21 – 23**, **27** as TFA salts. The methylester **27** was saponified to give the carboxylic acid derivative **26** as a white HCl salt.

Scheme 3.^a

^aReagents and conditions: a) MeOH, room temperature, 4 h (100%); b) corresponding boronic acid, Cs₂CO₃, dry 1,4-dioxane, 100 °C, 18 h, (8-23%); c) ester **27**, 4 M LiOH_(aq), H₂O/EtOH, 50 °C, 2 h, (65%). For designation of R, see Table 3.

Biology

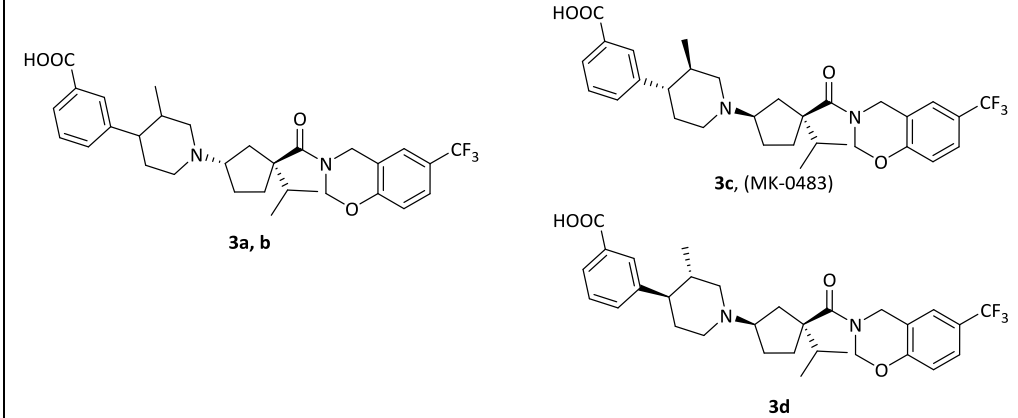
To determine their binding affinity all compounds were tested in a ¹²⁵I-CCL2 radioligand displacement assay on U2OS-CCR2 membrane preparations as described previously by our group.²¹ Next to all four MK-0483 diastereomers compounds with affinities lower than or

equal to 100 nM were subsequently screened in a [³H]INCB3344 dual point competition association assay on U2OS–CCR2 membrane preparations to determine their kinetic–rate–index (KRI), which served as an indicator for the magnitude of the RT. Compounds with a KRI >1 were finally tested in the full competition association assay to determine the RT, as described previously by our group.¹⁸

Structure–Affinity Relationships and Structure–Kinetics Relationships

The 3-piperidinylcyclopentanecarboxamide scaffold has been extensively evaluated by the Merck research group for CCR2 receptor binding.²²⁻²⁴ All these efforts resulted in the discovery of MK-0483, which, upon tritiation, served as a radioligand. This [³H]–MK-0483 bound to monocytes and appeared to have very slow receptor dissociation kinetics.¹⁵ We decided to resynthesize MK-0483 and its diastereomers and to evaluate these four compounds in our various binding assays on the CCR2 receptor to determine the structural components responsible for both the high affinity and the long RT of MK-0483. Following the synthetic approach reported by Pasternak et.al.¹⁵ we were able to generate the same four diastereomers and assigned them **3a-d** according to the sequence of elution from the preparative chiral HPLC, respectively. First, we determined their affinity in a ¹²⁵I–CCL2 competition displacement assay in which the *trans*-cyclopentane isomers (**3a** and **3b**) showed only moderate affinity (K_i = 59 and 383 nM, respectively) (Table 1). However, the *cis*-cyclopentane isomers (**3c** and **3d**) had high affinity for the CCR2 receptor (K_i = 1.2 and 11 nM, respectively) which is in accordance with the reported values.¹⁵ Next, we evaluated all four diastereomers in the competition–association assay as this could help us to understand the importance of 3D conformation for SKR.

Table 1. Binding affinities, association and dissociation rate constants, and residence times of MK-0483 and its diastereomers



Nr.	K_i (nM) \pm SEM ($n = 3$)	k_{on} (nM ⁻¹ min ⁻¹)	k_{off} (min ⁻¹)	RT (min)
3a	59 \pm 2	0.00044 \pm 0.0004	0.0028 \pm 0.0004	357 \pm 51
3b	383 \pm 19	0.000058 \pm 0.000007	0.0037 \pm 0.0007	270 \pm 51
3c, (MK-0483)	1.2 \pm 0.1	0.020 \pm 0.002	0.0014 \pm 0.00004	724 \pm 20
3d	11 \pm 2.6	0.013 \pm 0.001	0.018 \pm 0.002	56 \pm 6

Surprisingly, both *trans*-isomers (**3a** and **3b**), despite their moderate affinity, had similar and very slow dissociation characteristics translating in residence times longer than 4 hours (RT = 357 and 270 min, respectively) (Table 1), whereas the association rate constants displayed a 7-fold difference ($k_{on} = 0.00044$ and 0.000058 nM⁻¹ min⁻¹, respectively) causing also the difference in affinity. The opposite was observed in the case of *cis*-isomers **3c** and **3d**. For these compounds, the association rate constants were similar and the dissociation rate constants showed a more than 12-fold difference, yielding residence times of 724 (**3c**) and 56 min (**3d**), respectively, which is also in line with the reported half-life value for MK-0483 (**3c**) by the Merck researchers.¹⁵ Apparently, the *cis*-isomers have the best conformation for the eventual binding state on the receptor (affinity), reach that state quickly as can be gauged from their relatively fast k_{on} values, and stay there for prolonged times (Table 1). The only difference for the *trans*-isomers is their relatively slow association rate, but still they are capable of binding to the CCR2 receptor, and display long residence times as well.

Bis(trifluoromethyl)benzyl Derivatives 4-16

From the above we chose to continue with *cis*-analogues of MK-0483 and decided to synthesize several new analogues of MK-0483 and a small number of known^{15, 24} compounds to describe the SAR and SKR for the CCR2 receptor in this series of structures. In the first array we generated the more flexible (on the right-hand side) bis(trifluoromethyl)benzyl derivatives with different substituents on the aromatic ring connected to the piperidine (**4-16**) (Table 2). The unsubstituted phenyl compound (**4**) had an affinity of 1.5 nM for CCR2, which was best in class. However, in the dual-point competition-association assay it yielded a KRI below unity (KRI = 0.7), indicative of a short RT. Incorporation of the 2-methoxy group (compound **5**) resulted in a decrease of both the affinity and the KRI value ($K_i = 28$ nM, KRI = 0.6). The 3-methoxy group (compound **6**) yielded a small regain in the affinity (correlating with the reported values)²⁴ and the KRI value ($K_i = 5.9$ nM, KRI = 0.7). However, the 4-methoxy derivative (**7**), despite its moderate affinity ($K_i = 29$ nM), had a KRI value of 0.8. The double substitution of 3,4-di-methoxy (compound **8**) resulted in a big decrease in both the affinity and the KRI value. Closing the methoxy groups to yield a benzo[1,3]dioxole ring (compound **9**) yielded a minor improvement in affinity, however, it did not enhance the KRI value (KRI = 0.6). Lipophilic groups on the 4 position (e.g. 4-OCF₃, 4-*t*-Bu) resulted in an even bigger decrease of the affinity (compound **10**, 4-OCF₃) or a complete loss of the affinity (compound **11**, 4-*t*-Bu). The hydrophilic 4-hydroxy group (compound **12**) boosted affinity somewhat but still had a lower KRI value compared to the 4-methoxy derivative (**7**).

Table 2. Binding affinities and KRI values of compounds **4-16**.

Nr.	R	K_i (nM) \pm SEM ($n = 3$)	KRI ($n=2$)
4	H	1.5 \pm 0.1	0.7 (0.6/0.7)
5	2-OMe	28 \pm 2	0.6 (0.5/0.7)
6	3-OMe	5.9 \pm 1.7	0.7 (0.6/0.8)
7	4-OMe	29 \pm 2	0.8 (0.7/0.9)
8	3,4-di-OMe	48 \pm 1	0.6 (0.5/0.6)

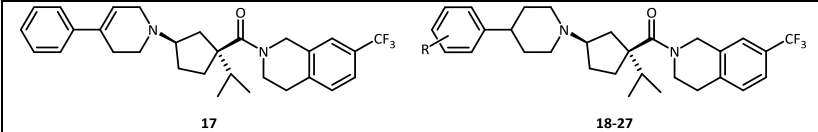
9	3,4-OCH ₂ O-	17 ± 3	0.6 (0.6/0.7)
10	4-OCF ₃	122 ± 20	-
11	4-tBu	7% ^a	-
12	4-OH	17 ± 2	0.6 (0.6/0.6)
13	H	5.4 ± 0.9	0.6 (0.6/0.6)
14	4-OMe	76 ± 14	0.5 0.5/0.6)
15	3-COOH	22 ± 6	0.8 (0.8/0.8)
16	3-COOMe	7.9 ± 1.6	0.6 (0.5/0.7)

^aPercent displacement at 1 μM ¹²⁵I-CCL2.

Comparing the 3-pyridine (**13**) with phenyl ring (**4**) also resulted in a minor decrease in affinity (correlating with the reported values)²⁴ and the KRI value ($K_i = 5.4$ nM, KRI = 0.6). The combination of 4-methoxy and 3-pyridine (compound **14**) yielded a 50-fold decrease in affinity compared to **4** and the smallest KRI value observed in this study (KRI = 0.5). Apparently, any substitution on the phenyl ring is not favorable and results in a decrease in affinity compared to the unsubstituted phenyl ring (**4**), although the 3-substituents are tolerated more than others. The evaluation of direct analogues of MK-0483, such as the 3-carboxylic acid (compound **15**), resulted in a 14-fold decrease in affinity ($K_i = 22$ nM, in agreement with the reported values)²⁴ compared to **4**, however, the KRI value increased to 0.8, whereas the methyl ester (**16**) had better affinity than the acid ($K_i = 7.9$ nM), but a smaller KRI value.

7-(Trifluoromethyl)-1,2,3,4-tetrahydroisoquinoline Derivatives 17-27

The rigidification on the right-hand side into the 7-(trifluoromethyl)-1,2,3,4-tetrahydroisoquinoline group provided compounds **17-27**. The unsubstituted phenyl intermediate (olefin **17**) had a 14-fold lower affinity than its saturated analogue **18** and two-fold shorter RT (Table 3) indicating that the phenyl ring should be positioned in an angle to the piperidine ring for optimal binding.

Table 3. Binding affinities, KRI values and residence times of compounds **17-27**.


Nr.	R	K_i (nM) \pm SEM (n = 3)	KRI (n=2)	RT (min)
17	-	70 \pm 25	1.1 (1.1/1.0)	38 \pm 4
18	H	4.4 \pm 0.7	1.1 (1.2/1.0)	91 \pm 25
19	3-OMe	0.95 \pm 0.22	0.9 (0.8/0.9)	-
20	3-Cl	2.6 \pm 0.3	1.0 (0.9/1.2)	200 \pm 29
21	3-Br	2.8 \pm 0.2	1.0 (1.0/1.1)	243 \pm 45
22	3- <i>i</i> Pr	3.6 \pm 0.4	1.0 (1.0/0.9)	266 \pm 48
23	3-CF ₃	5.3 \pm 0.3	1.0 (0.9/1.1)	158 \pm 35
24	4-Cl	2.0 \pm 0.3	0.8 (0.8/0.8)	-
25	4-CF ₃	7.2 \pm 0.2	0.8 (0.8/0.9)	-
26	3-COOH	7.8 \pm 1.4	0.7 (0.7/0.7)	-
27	3-COOMe	0.91 \pm 0.25	0.8 (0.8/0.8)	-

From the bis(trifluoromethyl)benzyl series (Table 2) we learned that substituents on the 3 position were better tolerated so therefore we focused on this position in this array of compounds. The 3-methoxy derivative (**19**) had excellent affinity ($K_i = 0.95$ nM), but the KRI was below unity. Changing from 3-methoxy to 3-chloro (**20**) resulted in a small decrease in affinity, but an increase in RT. The 3-bromo derivative (**21**) had similar affinity as 3-chloro, but a longer RT. We have previously reported a similar correlation in another series of CCR2 antagonists where the methoxy substituents yielded the best affinity compounds, while the halogen derivatives had a longer RT.¹³ The 3-isopropyl substituent (**22**) being similar in size to the bromine but having electron donating properties yielded only a minor decrease in the affinity and a minor increase in the RT, thus suggesting the importance of the space-filling properties of the substituents. The 3-trifluoromethyl derivative (**23**) (bioisoster of chlorine) showed similar results as **20** (3-Cl). In our effort to increase the RT we also explored the 4 position by introducing the lipophilic 4-chloro (**24**) and 4-trifluoromethyl (**25**) groups. However, despite the good affinity, both compounds had KRI values below unity (KRI = 0.8 for both).

A direct analogue of MK-0483 with an acid group on the 3 position (**26**) resulted in a minor decrease in affinity (comparable to the reported values),¹⁵ but we noticed a substantial

decrease in RT (KRI = 0.7). Apparently, either the additional methyl group on the 3 position of the piperidine ring, the oxygen atom in the 3,4-dihydro-2*H*-benzo[e][1,3]oxazine ring or the combination of both is responsible for the long residence time of MK-0483. The compound with a corresponding methyl ester (**27**) yielded the best affinity in this study, although it had a short RT ($K_i = 0.91$ nM, KRI = 0.8).

CONCLUSIONS

We have evaluated the SAR and SKR of MK-0483 (**3c**), its diastereomers (**3a**, **b**, **d**) and structural analogues (**4** - **27**) as CCR2 antagonists. On the right-hand side of the molecules a rigid 7-(trifluoromethyl)-1,2,3,4-tetrahydroisoquinoline moiety yields better affinity than the more flexible bis(trifluoromethyl)benzyl substituent and generally prolongs the drug-target residence time. On the left-hand side SAR of the phenyl ring suggests that lipophilic hydrogen bond accepting substituents on the 3 position (e.g. 3-OMe (**19**), 3-COOMe (**27**)) are vital for improved affinity. However, the SKR suggests that to have long RT a lipophilic group with a certain size is desired (e.g. 3-Br (**21**), 3-*i*-Pr (**22**)) or alternatively (in the case of MK-0483 (**3c**)) a carboxylic acid group can be used. However, the acid group *per se* does not provide the long RT for these structures. Possibly the additional methyl group on the piperidine ring (as seen in MK-0483 (**3c**)) provides shielding of a hydrogen bond formed between the acid group and the receptor. We have reported similar observations on shielding in another series of CCR2 antagonists, moreover, a similar idea was put forward by Schmidtke et al.²⁵ in calculations on hydrogen bond shielding. Likewise, the additional oxygen atom in the 3,4-dihydro-2*H*-benzo[e][1,3]oxazine ring of MK-0483 (**3c**) could make an additional hydrogen bond and cause its long RT as the hydrogen bond would be shielded by the ring system itself. In conclusion, this study contributes to one of the first detailed structure-kinetics relationships for CCR2 antagonists which can help to develop better drug candidates. Moreover, the value of the long RT drugs has already been proven on other targets, although only in retrospect.¹⁰ From this perspective, MK-0483 (**3c**) would be a suitable candidate to be deliberately advanced into clinical studies due to its long RT. If it failed due to lack of efficacy one could

argue that blockade of CCR2 (alone) is not sufficient to treat the many immunological disorders that were mentioned in the Introduction.

EXPERIMENTAL SECTION

Chemistry

All solvents and reagents were purchased from commercial sources and were of analytical grade. Demineralized water is simply referred to as H₂O, because it was used in all cases, unless stated otherwise (i.e., brine). ¹H and ¹³C NMR spectra were recorded on a Bruker AV 400 liquid spectrometer (¹H NMR, 400 MHz; ¹³C NMR, 100 MHz) at ambient temperature. Chemical shifts are reported in parts per million (ppm), are designated by δ , and are downfield to the internal standard tetramethylsilane (TMS). Coupling constants are reported in hertz and are designated as *J*. Analytical purity of the final compounds was determined by high-performance liquid chromatography (HPLC) with a Phenomenex Gemini 3 μ m C18 110A column (50 \times 4.6 mm, 3 μ m), measuring UV absorbance at 254 nm. The sample preparation and HPLC method was as follows: 0.3–0.8 mg of compound was dissolved in 1 mL of a 1:1:1 mixture of CH₃CN/H₂O/*t*-BuOH and eluted from the column within 15 min at a flow rate of 1.3 mL/min. The elution method was set up as follows: 1–4 min isocratic system of H₂O/CH₃CN/1% TFA in H₂O, 80:10:10, from the 4th min, a gradient was applied from 80:10:10 to 0:90:10 within 9 min, followed by 1 min of equilibration at 0:90:10 and 1 min at 80:10:10. All compounds showed a single peak at the designated retention time and are at least 95% pure. Preparative HPLC was performed on a Schimatzu HPLC–ultraviolet (UV) system using a Gemini C18 Phenomenex column (100 \times 10 mm, 5 μ m), and a linear gradient from 10 to 90% of mobile phase B was applied, keeping mobile phase C constant at 10%. Mobile phase A consisted of H₂O, mobile phase B consisted of acetonitrile, and mobile phase C consisted of 1% TFA solution in H₂O. The flow rate was 5 mL/min. Liquid chromatography–mass spectrometry (LC–MS) analyses were performed using Thermo Finnigan Surveyor - LCQ Advantage Max LC–MS system and a Gemini C18 Phenomenex column (50 \times 4.6 mm, 3 μ m). The elution method was set up as follows: 1–4 min isocratic system of H₂O/CH₃CN/1% TFA in H₂O, 80:10:10, from the 4th min, a gradient was applied from 80:10:10 to 0:90:10 within 9 min, followed by 1 min of equilibration at 0:90:10 and 1 min at 80:10:10. Microwave reactions were done using Biotage Initiator microwave synthesizer. Thin-layer chromatography (TLC) was routinely consulted to monitor the progress of reactions, using aluminum-coated Merck silica gel F²⁵⁴ plates. Purification by column chromatography was achieved by use of Grace Davison Davisil silica column material (LC60A, 30–200 μ m). The procedure for a series of similar compounds is given as a general procedure for all within that series, annotated by the numbers of the compounds.

General procedure for the synthesis of compounds 4 – 14, 16.

In a round-bottom flask a mixture of the corresponding olefin (**35 – 46**), Pd/C 5% wt (5 mol%) and palladium acetate (1.5 mol %) were dissolved in MeOH and stirred overnight with a hydrogen balloon. The reaction mixture was filtered through Celite and purified by preparative HPLC purification system.

(1S,3R)-N-(3,5-bis(trifluoromethyl)benzyl)-1-isopropyl-3-(4-phenylpiperidin-1-yl)cyclopentane-1-carboxamide (TFA salt) (4). Yield = 69%, ¹H NMR (400 MHz, CDCl₃) δ : 10.62 (s, 1H), 7.76–7.74 (m, 3H), 7.60 (s, 1H), 7.37–7.17 (m, 5H), 4.60–4.43 (m, 2H), 3.76–3.65 (m, 2H), 3.43 (s, 1H), 2.92–2.71 (m, 3H), 2.61–2.56 (m, 1H), 2.29–2.01 (m, 8H), 2.92–2.85 (m, 1H), 1.81–7.23 (m, 1H), 0.88–0.87 (m, 6H); ¹³C NMR (101 MHz, CDCl₃) δ : 176.8, 161.5, 161.2, 142.6, 141.7, 131.9, 131.6, 129.2, 129.0, 127.9, 127.4, 126.6, 124.7, 122.0, 117.5, 67.5, 57.3, 52.9, 51.8, 43.3, 40.3, 34.8, 32.5, 31.9, 30.5, 27.9, 18.6, 17.8; MS peak: 541⁺[H⁺]; HPLC: t_r = 8.9 min.

(1*S*,3*R*)-*N*-(3,5-bis(Trifluoromethyl)benzyl)-1-isopropyl-3-(4-(2-methoxyphenyl)piperidin-1-yl)cyclopentane-1-carboxamide (TFA salt) (**5**). Yield = 64%, ¹H NMR (400 MHz, CD₃CN) δ: 8.77 (br s, 1H), 7.92 (s, 3H), 7.46 (t, *J* = 4.8 Hz, 1H), 7.27 (t, *J* = 20.0 Hz, 1H), 7.16 (dd, *J*¹=*J*²= 1.2 Hz, 1H), 7.01–6.97 (m, 2H), 4.58–4.53 (m, 2H), 3.84 (s, 3H), 3.74 (d, *J* = 12.0 Hz, 1H), 3.60–3.51 (m, 2H), 3.24–3.15 (m, 1H), 3.04–2.95 (m, 2H), 2.45 (dd, *J*¹ = 7.6 Hz, *J*² = 6.8 Hz, 1H), 2.19–1.97 (m, 7H), 1.84–1.67 (m, 2H), 0.90–0.86 (m, 6H). ¹³C NMR (101 MHz, CD₃CN) δ: 157.1, 142.9, 131.3, 128.1, 126.9, 126.4, 121.0, 117.4, 114.7, 111.0, 66.9, 57.3, 55.2, 55.0, 51.6, 42.5, 33.7, 33.4, 32.3, 31.5, 29.0, 27.8, 18.0, 16.9; MS peak : 571⁺ [H⁺]; HPLC t_r = 8.9 min.

(1*S*,3*R*)-*N*-(3,5-bis(Trifluoromethyl)benzyl)-1-isopropyl-3-(4-(3-methoxyphenyl)piperidin-1-yl)cyclopentane-1-carboxamide (TFA salt) (**6**). Yield = 16%, ¹H NMR (400 MHz, CDCl₃) δ: 11.74 (s, 1H), 7.79–7.77 (m, 3H), 7.60 (s, 1H), 7.25–7.11 (m, 2H), 6.83–6.18 (m, 2H), 4.65–4.46 (m, 2H), 3.85–3.83 (m, 4H), 3.45–3.21 (m, 4H), 2.89–2.72 (m, 4H), 2.33–1.97 (m, 8H), 1.72 (s, 1H), 0.91–0.89 (m, 6H); ¹³C NMR (101 MHz, CDCl₃) δ: 176.9, 160.0, 144.2, 141.8, 131.8, 129.9, 127.9, 124.6, 118.3, 112.7, 112.2, 99.9, 67.6, 56.9, 55.6, 55.2, 52.9, 52.1, 43.1, 40.6, 35.0, 30.2, 30.1, 28.1, 18.7, 17.8; MS peak: 571⁺ [H⁺]; HPLC: t_r = 8.9 min.

(1*S*,3*R*)-*N*-(3,5-bis(Trifluoromethyl)benzyl)-1-isopropyl-3-(4-(4-methoxyphenyl)piperidin-1-yl)cyclopentane-1-carboxamide (TFA salt) (**7**). Yield = 9%, ¹H NMR (400 MHz, CDCl₃) δ: 11.72 (s, 1H), 7.77–7.75 (m, 3H), 7.0 (s, 1H), 7.12 (d, *J* = 8.8 Hz, 2H), 6.87 (d, *J* = 8.8 Hz, 2H), 4.65–4.41 (m, 2H), 3.81 (s, 3H), 3.79–3.68 (m, 2H), 3.33 (s, 1H), 2.82–2.63 (m, 4H), 2.32–2.25 (m, 9H), 1.96–1.93 (m, 1H), 0.88–0.87 (m, 6H); ¹³C NMR (101 MHz, CDCl₃) δ: 142.0, 135.0, 128.1, 127.8, 121.3, 114.5, 67.8, 57.2, 55.5, 53.2, 52.4, 43.4, 39.9, 35.2, 32.3, 30.7, 30.6, 28.3, 18.9, 18.0; MS peak: 571⁺ [H⁺]; HPLC: t_r = 9.1 min.

(1*S*,3*R*)-*N*-(3,5-bis(Trifluoromethyl)benzyl)-3-(4-(3,4-dimethoxyphenyl)piperidin-1-yl)-1-isopropylcyclopentane-1-carboxamide (TFA salt) (**8**). Yield = 37%, ¹H NMR (400 MHz, CDCl₃) δ: 11.48 (s, 1H), 7.77–7.75 (m, 3H), 7.59 (s, 1H), 6.81 (d, *J* = 8.4 Hz, 1H), 6.74 (d, *J* = 7.2 Hz, 2H), 4.64–4.43 (m, 2H), 3.89–3.86 (m, 6H), 3.76–3.68 (m, 2H), 3.36 (s, 1H), 2.83–2.67 (m, 4H), 2.32–1.94 (m, 9H), 1.72–1.66 (m, 1H), 0.89–0.87 (m, 6H); ¹³C NMR (101 MHz, CDCl₃) δ: 149.4, 148.3, 141.9, 135.5, 131.9, 131.6, 128.0, 121.2, 112.0, 111.5, 109.7, 67.7, 57, 2, 43.3, 40.3, 35.1, 32.6, 32.2, 30.6, 30.5, 28.2, 18.8, 18.0; MS peak: 601⁺ [H⁺]; HPLC: t_r = 8.7 min.

(1*S*,3*R*)-3-(4-(Benzo[d][1,3]dioxol-5-yl)piperidin-1-yl)-*N*-(3,5-bis(trifluoromethyl)benzyl)-1-isopropylcyclopentane-1-carboxamide (TFA salt) (**9**). Yield = 38%, ¹H NMR (400 MHz, CDCl₃) δ: 11.72 (s, 1H), 7.76–7.75 (m, 3H), 7.57 (s, 1H), 6.78 (d, *J* = 10.0 Hz, 1H), 6.67 (d, *J* = 10.4 Hz, 1H), 6.63 (s, 1H), 5.93 (s, 2H), 4.63–5.51 (m, 2H), 3.76–3.67 (m, 2H), 3.35 (s, 1H) 2.83–2.70 (m, 2H), 2.69–2.61 (m, 2H), 2.31–1.86 (m, 8H), 1.72–1.64 (m, 1H), 0.88–0.86 (m, 6H); ¹³C NMR (101 MHz, CDCl₃) δ: 176.2, 148.1, 146.8, 141.9, 136.7, 131.9, 131.6, 128.0, 121.2, 119.7, 108.7, 107.2, 101.2, 67.7, 57.1, 52.9, 52.1, 43.3, 40.4, 35.1, 32.4, 32.2, 30.6, 28.1, 18.8, 17.9; MS peak: 585⁺ [H⁺]; HPLC: t_r = 8.9 min.

(1*S*,3*R*)-*N*-(3,5-bis(Trifluoromethyl)benzyl)-1-isopropyl-3-(4-(4-(trifluoromethoxy)phenyl)piperidin-1-yl)cyclopentane-1-carboxamide (TFA salt) (**10**). Yield = 32%, ¹H NMR (400 MHz, CDCl₃) δ: 11.06, (s, 1H), 7.76, (s, 3H), 7.35 (s, 1H), 2.23–2.17 (m, 4H), 4.64–4.43 (m, 2H), 3.79–3.70 (m, 2H), 3.42 (s, 2H), 2.88–2.72 (m, 3H), 2.66–2.60 (m, 1H), 2.34–1.86 (m, 9H), 1.75–1.61 (m, 1H), 0.91–0.89 (m, 6H); ¹³C NMR (101 MHz, CDCl₃) δ: 176.3, 148.5, 141.6, 141.2, 132.1, 131.7, 128.1, 124.8, 12.0, 121.6, 121.4, 67.7, 57.2, 52.9, 51.8, 43.3, 39.9, 35.2, 32.7, 31.9, 30.4, 30.3, 27.9, 18.7, 18.0; MS peak: 625⁺ [H⁺]; HPLC: t_r = 9.4 min.

(1*S*,3*R*)-*N*-(3,5-bis(Trifluoromethyl)benzyl)-3-(4-(4-(*tert*-butyl)phenyl)piperidin-1-yl)-1-isopropylcyclopentane-1-carboxamide (TFA salt) (**11**). Yield = 17%, ¹H NMR (400 MHz, CDCl₃) δ: 11.76 (s, 1H), 9.12 (s, 1H), 7.83–7.78 (m, 4H), 7.63 (d, *J* = 8.4 Hz, 2H), 7.38 (d, *J* = 8.4 Hz, 0.5 H^a), 7.17 (d, *J* = 8.4 Hz, 0.5 H^b), 4.63–4.47 (m, 2H), 3.83–3.37 (m, 6H), 2.87–1.73 (m, 11H), 1.41 (s, 4.5 H^a), 1.35 (s, 4.5 H^b), 0.95–0.93 (m, 6H); ¹³C NMR (101 MHz, CDCl₃) δ: 177.2, 156.9, 156.8, 143.5, 141.8, 141.6, 139.6, 130.4, 127.6, 126.3, 124.4, 121.2, 70.1, 67.6, 59.2, 56.9, 52.9, 43.3, 43.1, 39.9, 34.5, 32.3, 31.1, 30.3, 18.9, 18.7, 17.8, 17.7; MS peak: 597⁺ [H⁺]; HPLC: t_r = 9.8 min. *a* and *b* for different rotamers.

(1*S*,3*R*)-*N*-(3,5-bis(trifluoromethyl)benzyl)-3-(4-(4-hydroxyphenyl)piperidin-1-yl)-1-isopropylcyclopentane-1-carboxamide (TFA salt) (**12**). Yield = 31%, ¹H NMR (400 MHz, CDCl₃) δ: 10.63 (s, 1H), 7.92 (s, 3H), 7.52 (s, 1H), 7.09 (d, *J* = 8.0 Hz, 2H), 6.79 (d, *J* = 8.0 Hz, 2H), 4.51–4.50 (m, 2H), 3.62–3.46 (m, 3H), 2.95–2.75 (m, 3H), 2.45–1.97 (m, 10H), 1.80–1.70 (m, 2H), 0.89–0.86 (m, 6H); ¹³C NMR (101 MHz, CDCl₃) δ: 155.9, 143.2, 135.3, 128.3, 127.7, 120.8, 117.4, 115.4, 66.6, 56.8, 42.2, 51.5, 42.5, 38.6, 34.4, 33.0, 30.5, 27.6, 17.7, 17.2; MS peak: 557⁺ [H⁺]; HPLC: t_r = 8.5 min.

(1*S*,3*R*)-*N*-(3,5-bis(trifluoromethyl)benzyl)-1-isopropyl-3-(4-(pyridin-3-yl)piperidin-1-yl)cyclopentane-1-carboxamide (TFA salt) (**13**). Yield = 55%, ¹H NMR (400 MHz, CDCl₃) δ: 12.11 (s, 1H), 8.94 (s, 1H), 8.65 (d, *J* = 5.2 Hz, 1H), 8.43 (d, *J* = 8.0 Hz, 1H), 7.86 (t, *J* = 5.6 Hz, 1H), 7.76–7.74 (m, 3H), 7.52 (s, 1H), 4.64–4.47 (m, 2H), 3.82–3.74 (m, 2H), 3.43–3.39 (m, 1H), 2.68–2.47 (m, 3H), 2.17–1.69 (m, 8H), 1.23 (s, 2H), 0.91–0.87 (m, 6H); ¹³C NMR (101 MHz, CDCl₃) δ: 178.45, 148.73, 147.8, 142.5, 140.7, 133.9, 132.0, 131.9, 131.7, 131.6, 131.3, 127.7, 124.7, 123.6, 121.9, 121.1, 65.9, 57.1, 53.4, 52.9, 51.3, 50.0, 47.4, 44.2, 42.8, 39.7, 38.5, 38.2, 35.5, 35.1, 33.9, 33.2, 32.9, 29.7, 29.1, 28.3, 26.2, 23.8, 19.3, 19.2, 17.5; MS peak: 542⁺ [H⁺]; HPLC: t_r = 7.9 min.

(1*S*,3*R*)-*N*-(3,5-bis(trifluoromethyl)benzyl)-1-isopropyl-3-(4-(6-methoxypyridin-3-yl)piperidin-1-yl)cyclopentane-1-carboxamide (TFA salt) (**14**). Yield = 70%, ¹H NMR (400 MHz, CDCl₃) δ: 11.18 (s, 1H), 8.25 (s, 1H), 7.84 (d, *J* = 8.8 Hz, 1H), 7.35 (s, 1H), 7.30–7.25 (m, 3H), 6.95 (d, *J* = 8.8 Hz, 1H), 4.63–4.46 (m, 2H), 4.03 (s, 3H), 3.78–3.69 (m, 2H), 3.41–3.39 (m, 1H), 2.95–2.89 (m, 3H), 2.62–2.56 (m, 1H), 2.30–1.67 (m, 10H), 0.80–0.86 (m, 6H); ¹³C NMR (101 MHz, CDCl₃) δ: 176.4, 162.5, 161.9, 161.5, 161.2, 160.8, 142.5, 141.7, 140.6, 132.3, 132.0, 131.7, 131.3, 128.0, 124.7, 122.0, 121.4, 121.3, 117.3, 114.5, 111.3, 67.6, 57.3, 44.6, 52.6, 51.6, 43.3, 36.8, 34.9, 32.6, 31.9, 30.0, 29.9, 28.1, 18.7, 17.9; MS peak: 572⁺ [H⁺]; HPLC: t_r = 8.0 min.

3-(1-((1*R*,3*S*)-3-((3,5-bis(trifluoromethyl)benzyl)carbamoyl)-3-isopropylcyclopentyl)piperidin-4-yl)benzoic acid (**15**). In a 50 mL round-bottom flask compound **16** (0.058 g, 0.128 mmol) was dissolved in EtOH (10 mL). Subsequently, 4 M LiOH (0.3 mL, 1.2 mmol) in H₂O was added and the reaction mixture was stirred for 1.5 hours at 50 °C. EtOH was evaporated in vacuum. The reaction mixture was partitioned between brine and chloroform and the pH was adjusted to 7 with 1 M HCl (aq.). The organic layer was collected, dried over MgSO₄ and concentrated in vacuum, yielding compound **15** as a HCl salt (0.042 g, 53 %). ¹H NMR (400 MHz, CDCl₃) δ: 9.34 (s, 1H), 8.04 (s, 1H), 7.76–7.75 (m, 3H), 7.64 (s, 1H), 7.22–7.20 (m, 2H), 4.64–4.58 (m, 1H), 4.27–4.22 (m, 1H), 3.88 (d, *J* = 11.2 Hz, 1H), 3.78 (d, *J* = 11.2 Hz, 1H), 3.49–3.42 (m, 1H), 3.14–3.12 (m, 1H), 2.90–2.65 (m, 4H), 2.36–2.32 (m, 1H), 2.19–1.96 (m, 5H), 1.93–1.88 (m, 2H), 1.69–1.68 (m, 1H), 0.93–0.89 (m, 6H); ¹³C NMR (101 MHz, CDCl₃) δ: 176.3, 173.1, 142.9, 142.5, 136.6, 131.4, 131.2, 131.0, 128.2, 128.0, 127.9, 125.2, 124.7, 122.0, 120.6, 68.1, 57.6, 53.5, 52.7, 43.2, 40.2, 35.2, 34.3, 32.8, 30.6, 29.4, 26.9, 19.3, 17.8; MS peak: 585⁺ [H⁺]; HPLC: t_r = 9.2 min.

Methyl 3-(1-((1*R*,3*S*)-3-((3,5-bis(trifluoromethyl)benzyl)carbamoyl)-3-isopropylcyclopentyl)piperidin-4-yl)benzoate (TFA salt) (**16**). Yield = 69%, ¹H NMR (400 MHz, CDCl₃) δ: 8.66 (s, 1H), 7.85 (s, 1H), 7.78–7.76 (m, 3H), 7.36 (t, *J* = 7.7 Hz, 1H), 7.26 (d, *J* = 7.7 Hz, 1H), 4.57 (d, *J* = 5.6 Hz, 2H), 3.91 (s, 3H), 3.26 (d, *J* = 11.0 Hz, 1H), 3.12 (d, *J* = 11.0 Hz, 1H), 2.75 (s, 1H), 2.65–2.49 (m, 1H), 2.32–2.27 (m, 1H), 2.18–1.93 (m, 4H), 1.93–1.76 (m, 4H), 1.76–1.63 (m, 2H), 1.60–1.30 (m, 2H), 0.94–0.89 (m, 6H); ¹³C NMR (101 MHz, CDCl₃) δ: 178.7, 167.1, 145.8, 142.5, 131.8, 131.5, 131.0, 128.5, 127.9, 127.5, 124.6, 121.9, 121.0, 65.7, 56.9, 53.5, 52.1, 51.1, 42.6, 41.9, 35.4, 33.6, 33.3, 29.9, 19.3, 17.3; MS peak: 599⁺ [H⁺]; HPLC: t_r = 9.7 min.

((1*S*,3*R*)-1-isopropyl-3-(4-phenyl-3,6-dihydropyridin-1(2*H*)-yl)cyclopentyl)(7-(trifluoromethyl)-3,4-dihydroisoquinolin-2(1*H*)-yl)methanone (**17**). In a 5 mL microwave tube a mixture of triflate **34** (0.06 g, 0.1 mmol), phenylboronic acid (0.018 g, 1.5 mmol), LiCl (0.012 g, 0.3 mmol), 2 M Na₂CO₃ in H₂O (0.15 mL, 0.3 mmol) and tetrakis(triphenylphosphine)palladium(0) (5 mol%) was dissolved in DME (1 mL) under a nitrogen atmosphere. The reaction mixture was heated under microwave irradiation at 90 °C for 5.5 hours. The reaction mixture was partitioned between DCM and H₂O. The organic layer was dried with

MgSO₄ and concentrated in vacuum. The product was purified by preparative HPLC system, yielding compound **17** as TFA salt (0.014 g, 23%). ¹H NMR (400 MHz, CD₃CN) δ: 7.50–7.28 (m, 8H), 6.00 (s, 1H), 4.90–4.60 (m, 3H), 4.30 (d, *J* = 16.0 Hz, 0.5H^a), 4.20 (d, *J* = 16.0 Hz, 0.5H^b), 3.90–3.55 (m, 4H), 3.34 (br s, 0.5H^a), 3.20–2.90 (m, 3.5H), 2.80–2.65 (m, 3H), 2.40–1.95 (m, 4H), 1.72 (br s, 1H), 0.93 (d, *J* = 6.4 Hz, 3H^a), 0.86 (d, *J* = 6.4 Hz, 3H^b); MS peak: 497⁺ [H⁺]; HPLC: t_r = 8.7 min. *a* and *b* indicating different rotamers.

((1*S*,3*R*)-1-isopropyl-3-(4-phenylpiperidin-1-yl)cyclopentyl)(7-(trifluoromethyl)-3,4-dihydroisoquinolin-2(1*H*)-yl)methanone (**18**). In a 10 mL round-bottom flask compound **17** (6.6 mg, 0.011 mmol) was dissolved in 5 mL of THF. To the reaction mixture Pd/C 5% wt (5 mol%) and palladium acetate (1.5 mol %) were added. The reaction mixture was flushed with hydrogen and kept under hydrogen atmosphere with a hydrogen balloon. The reaction mixture was heated at 50 °C for 30 seconds and stirring continued at room temperature for 2 hours. After the reaction was finished the mixture was filtered over celite and the product was purified by preparative HPLC system, yielding compound **18** as TFA salt (4.5 mg, 67%). ¹H NMR (400 MHz, CD₃CN) δ: 7.45–7.18 (m, 8H), 4.85–4.68 (m, 2H), 3.90–3.60 (m, 3H), 3.40 (br s, 1H), 3.00–1.80 (m, 17H), 1.64 (br s, 1H), 0.91 (d, *J* = 6.4 Hz, 3H), 0.82 (d, *J* = 6.4 Hz, 3H); MS peak: 499⁺ [H⁺]; HPLC: t_r = 8.7 min.

General procedure for the synthesis of compounds 19, 21 – 23 and 27.

Into an oven dried glass tube were added the tosylhydrazone **52** (140 mg, 0.23 mmol, 1 equiv.), the corresponding boronic acid (0.34 mmol, 1.5 equiv.), Cs₂CO₃ (110 mg, 0.34 mmol, 1.5 equiv. dried at 100 °C overnight) and then sealed with a crimp top with septum. High vacuum was applied for 30 minutes after which it was backfilled with nitrogen and 1 mL of dry 1,4-dioxane was added. Subsequently, the mixture was degassed 4 times by applying a vacuum and a nitrogen atmosphere sequentially. The reaction mixture was heated at 100 °C for 18 hours. TLC showed full conversion of the tosylhydrazone (EtOAc, KMnO₄ spray to visualize). The cooled reaction mixture was quenched with 2 mL of an aqueous saturated NaHCO₃ solution, extracted 3 times with DCM, dried over MgSO₄ and concentrated in vacuum. The crude yellow oil was pre-purified by column chromatography followed by preparative HPLC purification to give the final compounds **19**, **21 – 23** and **27** as TFA salts as colorless solidified oils.

1-((1*R*,3*S*)-3-isopropyl-3-(7-(trifluoromethyl)-1,2,3,4-tetrahydroisoquinoline-2-carbonyl)cyclopentyl)-4-(3-methoxyphenyl)piperidin-1-ium 2,2,2-trifluoroacetate (**19**). Yield = 10%. ¹H NMR (400 MHz, CD₃CN) δ: 10.66 (br s, 1H, NH), 7.53 (s, 1H), 7.47 (d, *J* = 8.4 Hz, 1H), 7.33 (d, *J* = 8.0 Hz, 1H), 7.23 (td, *J* = 7.2, 2.0 Hz, 1H), 6.82–6.70 (m, 3H), 4.78–4.68 (m, 2H), 3.78–3.65 (m, 6H), 3.60 (d, *J* = 12.0 Hz, 1H), 3.40–3.28 (m, 1H), 2.95–2.86 (m, 4H), 2.81–2.74 (m, 1H), 2.57–2.52 (m, 1H), 2.48–2.35 (m, 2H), 2.11–1.98 (m, 6H), 1.72–1.56 (m, 2H), 0.89 (d, *J* = 6.4 Hz, 3H), 0.75 (d, *J* = 6.4 Hz, 3H). LC-MS: 529⁺ [H⁺]; HPLC t_r: 8.09 min.

4-(3-Bromophenyl)-1-((1*R*,3*S*)-3-isopropyl-3-(7-(trifluoromethyl)-1,2,3,4-tetrahydroisoquinoline-2-carbonyl)cyclopentyl)piperidin-1-ium 2,2,2-trifluoroacetate (**21**). Yield = 8%. ¹H NMR (400 MHz, CD₃CN) δ: 10.84 (br s, 1H, NH), 7.52 (s, 1H), 7.47 (d, *J* = 8.0 Hz, 1H), 7.42–7.37 (m, 2H), 7.33 (d, *J* = 8.0 Hz, 1H), 7.27–7.21 (m, 2H), 4.78–4.68 (m, 2H), 3.85–3.65 (m, 3H), 3.60 (d, *J* = 12.6 Hz, 1H), 3.40–3.28 (m, 1H), 2.96–2.77 (m, 5H), 2.57–2.52 (m, 1H), 2.48–2.35 (m, 2H), 2.16–1.98 (m, 6H), 1.68–1.56 (m, 2H), 0.89 (d, *J* = 6.4 Hz, 3H), 0.75 (d, *J* = 6.4 Hz, 3H). ¹³C NMR (101 MHz, CD₃CN) δ: 147.0, 134.8, 130.6, 129.9, 129.8, 129.6, 125.7, 123.3, 123.0, 122.2, 56.4, 56.0, 52.3, 51.6, 39.1, 34.7, 32.6, 29.9, 28.1, 27.7, 17.4, 17.1. LC-MS: 578⁺ [H⁺]; t_r: 8.87 min.

1-((1*R*,3*S*)-3-isopropyl-3-(7-(trifluoromethyl)-1,2,3,4-tetrahydroisoquinoline-2-carbonyl)cyclopentyl)-4-(3-isopropylphenyl)piperidin-1-ium 2,2,2-trifluoroacetate (**22**). Yield = 23%. ¹H NMR (400 MHz, CD₃CN) δ: 9.25 (br s, 1H, NH), 7.54 (s, 1H), 7.48 (d, *J* = 8.0 Hz, 1H), 7.35 (d, *J* = 8.0 Hz, 1H), 7.24 (t, *J* = 7.6 Hz, 1H), 7.14–7.10 (m, 2H), 7.03 (d, *J* = 7.6 Hz, 1H), 4.82–4.71 (m, 2H), 3.90–3.69 (m, 3H), 3.60 (d, *J* = 12.2 Hz, 1H), 3.42–3.31 (m, 1H), 3.00–2.78 (m, 5H), 2.54–2.32 (m, 3H), 2.22–2.08 (m, 2H), 2.07–1.96 (m, 4H), 1.67–1.59 (m, 2H), 1.20 (d, *J* = 7.0 Hz, 6H), 0.88 (d, *J* = 6.4 Hz, 3H), 0.79 (d, *J* = 6.4 Hz, 3H). ¹³C NMR (101 MHz,

CD₃CN) δ : 149.4, 144.1, 134.7, 129.7, 128.7, 127.7, 124.9, 124.0, 123.3, 67.3, 56.5, 52.8, 51.9, 39.3, 34.0, 32.3, 30.4, 30.3, 28.3, 17.4, 17.2. LC–MS: 541⁺ [H⁺]; t_R : 9.22 min.

1-((1*R*,3*S*)-3-Isopropyl-3-(7-(trifluoromethyl)-1,2,3,4-tetrahydroisoquinoline-2-carbonyl)cyclopentyl)-4-(3-(trifluoromethyl)phenyl)piperidin-1-ium 2,2,2-trifluoroacetate (**23**). Yield = 9%. ¹H NMR (400 MHz, CD₃CN) δ : 10.80 (br s, 1H, NH), 7.60–7.49 (m, 5H), 7.47 (d, J = 8.4 Hz, 1H), 7.33 (d, J = 8.0 Hz, 1H), 4.81–4.66 (m, 2H), 3.94–3.69 (m, 3H), 3.62 (d, J = 12.0 Hz, 1H), 3.42–3.30 (m, 1H), 3.02–2.83 (m, 5H), 2.61–2.40 (m, 3H), 2.14–1.98 (m, 6H), 1.72–1.55 (m, 2H), 0.89 (d, J = 6.4 Hz, 3H), 0.75 (d, J = 6.4 Hz, 3H). ¹³C NMR (101 MHz, CD₃CN) δ : 146.5, 135.7, 131.7, 130.5, 124.5, 124.3, 68.3, 57.0, 53.2, 52.6, 40.1, 35.7, 33.6, 30.9, 29.1, 18.4, 18.1. LC–MS: 567⁺ [H⁺]; t_R : 8.88 min.

1-((1*R*,3*S*)-3-Isopropyl-3-(7-(trifluoromethyl)-1,2,3,4-tetrahydroisoquinoline-2-carbonyl)cyclopentyl)-4-(3-(methoxycarbonyl)phenyl)piperidin-1-ium 2,2,2-trifluoroacetate (**27**). Yield = 14%. ¹H NMR (400 MHz, CD₃CN) δ : 10.94 (br s, 1H, NH), 7.86–7.84 (m, 2H), 7.52 (s, 1H), 7.50–7.41 (m, 3H), 7.33 (d, J = 8.0 Hz, 1H), 4.81–4.66 (m, 2H), 3.92–3.65 (m, 5H), 3.62 (d, J = 12.1 Hz, 1H), 3.42–3.30 (m, 1H), 3.02–2.82 (m, 5H), 2.60–2.40 (m, 3H), 2.17–1.96 (m, 6H), 1.72–1.55 (m, 2H), 0.89 (d, J = 6.4 Hz, 3H), 0.74 (d, J = 6.2 Hz, 3H). ¹³C NMR (101 MHz, CD₃CN) δ : 166.7, 144.9, 134.8, 131.5, 130.6, 129.6, 129.0, 127.8, 127.6, 123.3, 67.4, 56.0, 52.3, 51.8, 51.7, 39.2, 34.8, 32.6, 30.0, 28.1, 17.4, 17.1. LC–MS: 557⁺ [H⁺]; t_R : 8.49 min.

General procedure for synthesis of compounds 20, 24, 25.

In a 5 mL microwave tube a solution of compound **50** (0.5 mmol, 1 equiv.) in 3 mL of DME was mixed with corresponding arylboronic acid (0.65 mmol, 1.3 equiv), LiCl (1.5 mmol, 3 equiv), 2 M Na₂CO₃ (1.5 mmol, 3 equiv) solution in H₂O and Pd(PPh₃)₄ (5 mol%). The reaction mixture was heated under microwave irradiation at 90 °C for 30 min – 2.5 hours. The reaction mixture was partitioned between DCM/H₂O. The organic layer was dried with MgSO₄ and concentrated in vacuum. The product was purified by column chromatography on silica gel with an eluent system consisting of DCM and increasing amounts of EtOAc (0–50%). The corresponding olefin was dissolved in THF and transferred to a 20 mL microwave tube. To the reaction mixture PtO₂ (20 wt%) and acetic acid (3 equiv) were added. The tube was capped, flushed with H₂ gas, and additionally pressurized with 20 mL of H₂ gas using a 20 mL syringe. The reaction was monitored using TLC/MS. The reaction was complete after 10 to 15 min. In the case of halogen substituents, if longer reaction times were used a de-halogenation was observed. Next, the corresponding esters were dissolved in EtOH and transferred to a 50 mL round-bottom flask. To the reaction mixture 4 M LiOH (10 equiv) in H₂O was added and the reaction mixture was refluxed for 3 hours. EtOH was evaporated in vacuum. The reaction mixture was acidified with 1 M HCl and the product was extracted with DCM. The organic layer was dried with MgSO₄ and concentrated in vacuum. The corresponding acid was dissolved in DCM and transferred to a 10 mL round-bottom flask. To the reaction mixture 7-trifluoromethyl-1,2,3,4-tetrahydroisoquinoline HCl salt (2 equiv) was added followed by the addition of DIPEA (12 equiv), PyBrOP (3 equiv), DMAP (1.5 equiv), and several beads of 4 Å molecular sieves. The reaction mixture was stirred for 48 hours at room temperature. The reaction mixture was extracted with DCM/H₂O, dried with MgSO₄ and concentrated in vacuum. The product was purified by preparative HPLC. All intermediates were checked by MS and were advanced to the next step without further analysis.

((1*S*,3*R*)-3-(4-(3-chlorophenyl)piperidin-1-yl)-1-isopropylcyclopentyl)(7-(trifluoromethyl)-3,4-dihydroisoquinolin-2(1*H*)-yl)methanone TFA salt (**20**). Overall yield = 9%, ¹H NMR (400 MHz, CD₃CN) δ : 8.51 (br s, 1H), 7.50–7.40 (m, 2H), 7.30–7.16 (m, 4H), 7.09 (d, J = 6.8 Hz, 1H), 4.81 (br s, 2H), 4.00–3.65 (m, 4H), 3.52 (br s, 1H), 3.15–2.75 (m, 5H), 2.60–2.40 (m, 2H), 2.35–2.00 (m, 7H), 1.79 (br s, 1H), 0.89 (br s, 6H). MS peak: 533⁺ [H⁺]; HPLC: t_R = 8.82 min.

((1*S*,3*R*)-3-(4-(4-Chlorophenyl)piperidin-1-yl)-1-isopropylcyclopentyl)(7-(trifluoromethyl)-3,4-dihydroisoquinolin-2(1*H*)-yl)methanone TFA salt (**24**). Overall yield = 0.8%, ¹H NMR (400 MHz, CD₃CN) δ : 10.81 (br s, 1H), 7.50–7.24 (m, 5H), 7.15 (d, J = 8.4 Hz, 2H), 4.40–4.20 (m, 2H), 3.86 (d, J = 11.6 Hz, 2H),

3.72 (d, $J = 11.2$ Hz, 2H), 3.52 (br s, 1H), 3.10–2.60 (m, 7H), 2.35–2.05 (m, 7H), 1.95–1.80 (m, 1H), 1.75–1.62 (m, 1H), 0.95–0.83 (m, 6H). MS peak: 533^+ [H^+]; HPLC: $t_r = 8.96$ min.

((1S,3R)-1-Isopropyl-3-(4-(4-(trifluoromethyl)phenyl)piperidin-1-yl)cyclopentyl)(7-(trifluoromethyl)-3,4-dihydroisoquinolin-2(1H)-yl)methanone TFA salt (25). Overall yield = 2%, 1H NMR (400 MHz, CD_3CN) δ : 9.43 (br s, 1H), 7.70–7.29 (m, 7H), 4.81 (s, 2H), 3.95–3.74 (m, 4H), 3.53 (br s, 1H), 3.10–2.85 (m, 5H), 2.65–2.45 (m, 2H), 2.30–2.10 (m, 7H), 1.95–1.70 (m, 2H), 0.95–0.83 (m, 6H). MS peak: 567^+ [H^+]; HPLC: $t_r = 9.07$ min.

4-(3-carboxyphenyl)-1-((1R,3S)-3-isopropyl-3-(7-(trifluoromethyl)-1,2,3,4-tetrahydroisoquinoline-2-carbonyl)cyclopentyl)piperidin-1-ium chloride (26). Ester **27** (25 mg, 0.045 mmol, 1.0 equiv.) was dissolved in a mixture of EtOH (5 mL), water (2 mL) and an 4M LiOH (aq.) (113 μ L, 0.45 mmol, 10.0 equiv.) was added. After 2 hours at 50 °C all of **27** was consumed as shown by TLC (EtOAc, $KMnO_4$ spray to visualize). The ethanol was evaporated and the pH was adjusted to pH = 1 with a 3M HCl (aq.) solution. The white precipitate was filtered off, rinsed with water and dried in vacuum to yield compound **26** as HCl salt. Yield = 17 mg, 65%. 1H NMR (400 MHz, CD_3CN) δ : 7.88–7.84 (m, 2H), 7.52 (s, 1H), 7.50–7.45 (m, 2H), 7.42 (t, $J = 7.6$ Hz, 1H), 7.33 (d, $J = 8.0$ Hz, 1H), 4.80–4.70 (m, 2H), 3.90–3.63 (m, 3H), 3.58 (d, $J = 12.8$ Hz, 1H), 3.40–3.29 (m, 1H), 3.01–2.85 (m, 5H), 2.70–2.40 (m, 3H and water), 2.24–2.05 (m, 6H), 1.82–1.75 (m, 1H), 1.67–1.59 (m, 1H), 0.88 (d, $J = 6.4$ Hz, 3H), 0.76 (d, $J = 6.4$ Hz, 3H). LC-MS: 543^+ [H^+]; HPLC t_r : 8.10 min.

1-Ethyl-1-methyl-4-oxo-piperidin-1-ium iodide (28). In a 20 mL microwave tube a solution of 1-methyl-4-piperidone (2.2 mL, 17.9 mmol) in acetone (15 mL) was mixed with ethyl iodide (1.43 mL, 17.9 mmol) under nitrogen atmosphere. The reaction mixture was stirred in the microwave at 60 °C for 5 hours forming yellow solids. The solids were filtered, washed with acetone and dried under vacuum to yield yellow salt **28** (4.35 g, 90%). The compound was used in next step as is.

Synthesis of (1S,3R)-3-amino-N-(3,5-bis(trifluoromethyl)benzyl)-1-isopropylcyclopentane-1-carboxamide (29) was achieved following the synthetic approach reported by our group earlier.¹⁸

Synthesis of ((1S,3R)-3-amino-1-isopropylcyclopentyl)(7-(trifluoromethyl)-3,4-dihydroisoquinolin-2(1H)-yl)methanone (30) was achieved following the synthetic approach reported earlier by our group.

(1S,3R)-N-(3,5-bis(trifluoromethyl)benzyl)-1-isopropyl-3-(4-oxopiperidin-1-yl)cyclopentane-1-carboxamide (31). In 250 mL round-bottom flask a solution of amine **29** (2.0 g, 5.0 mmol) dissolved in ethanol (75 mL) and H_2O (25 mL) was stirred at 40 °C. Compound **28** (2.02 g, 7.5 mmol) was dissolved in H_2O (30 mL) and added dropwise within 5 minutes to the reaction mixture. Then K_2CO_3 (1.4 g, 10 mmol) was added and the reaction mixture was refluxed for 5 hours, followed by an additional 12 hour stirring at room temperature. Ethanol was removed in vacuum and the reaction mixture was partitioned between DCM/ H_2O . The organic layer was dried over $MgSO_4$ and concentrated in vacuum. Compound **31** was purified by column chromatography on silica gel with an eluent system consisting of DCM and increasing amounts of EtOAc (50-100%). Yield = 1.7 g, (72%). 1H NMR (400 MHz, $CDCl_3$) δ : 7.77–7.70 (m, 3H), 7.49 (s, 1H), 4.56 (d, $J = 5.6$ Hz, 2H), 2.83–2.76 (m, 5H), 2.38–2.27 (m, 4H), 2.19–1.90 (m, 5H), 1.70–1.53 (m, 2H), 1.15 (s, 1H), 0.92–0.89 (m, 6H)

1-((1R,3S)-3-isopropyl-3-(7-(trifluoromethyl)-1,2,3,4-tetrahydroisoquinoline-2-carbonyl)cyclopentyl)piperidin-4-one (32). In a 20 mL microwave tube a solution of amine **30** (0.71 g, 2.0 mmol) in ethanol (10 mL) and H_2O (3 mL) was stirred at 40 °C. Compound **28** (0.81 g, 3 mmol) was dissolved in H_2O (3 mL) and added dropwise during 5 minutes to the reaction mixture. Then K_2CO_3 (0.56 g, 4 mmol) was added and the reaction mixture was heated under microwave irradiation at 100 °C for 3 hours. Ethanol was removed in vacuum and the reaction mixture was extracted with DCM/ 1M NaOH solution in H_2O . The organic layer was dried over $MgSO_4$ and concentrated in vacuum. Compound **32** was purified by column chromatography on silica gel with an eluent system consisting of DCM and increasing amounts of EtOAc (50-100%). Yield = 0.22 g, (25%). 1H NMR (400 MHz, $CDCl_3$) δ : 7.40–7.30 (m, 2H), 7.21 (d, $J = 8$ Hz, 1H), 4.80–4.60 (m, 2H), 3.77 (br s, 2H), 2.88 (br s, 2H), 2.72 (br s, 3H), 2.63–2.53

(m, 2H), 2.41–2.38 (m, 3H), 2.24–2.18 (m, 1H), 2.05–1.80 (m, 4H), 1.60–1.30 (m, 3H), 0.89 (d, $J = 6.8$ Hz, 3H), 0.73 (d, $J = 6.8$ Hz, 3H).

1-((1R,3S)-3-((3,5-bis(trifluoromethyl)benzyl)carbamoyl)-3-isopropylcyclopentyl)-1,2,3,6-tetrahydropyridin-4-yl trifluoromethanesulfonate (33). In a 100 mL round-bottom flask a solution of LDA (2M in heptanes, 2.2 mL, 2.88 mmol) in dry THF (20 mL) was cooled down to -78 °C under a nitrogen atmosphere. The ketone compound **31** (0.55 g, 1.15 mmol) was dissolved in dry THF (15 mL) and added dropwise to the reaction mixture. Vigorous stirring was necessary. The reaction mixture was stirred for 1 hour at -78 °C. After 1 hour, the reaction mixture was slowly warmed to -20 °C and kept at this temperature for 1 hour. Subsequently the reaction mixture was cooled down to -78 °C and *N*-phenyl-bis(trifluoromethanesulfonimide) (0.65 g, 2.3 mmol) dissolved in dry THF (8 mL) was added dropwise to the reaction mixture. After the addition was complete, the reaction mixture was slowly brought to room temperature and stirred overnight. The reaction mixture was quenched with EtOH, concentrated in vacuum and partitioned between DCM/H₂O. The organic layer was dried with MgSO₄ and concentrated in vacuum. The product was purified by column chromatography on silica gel with an eluent system consisting of DCM and increasing amounts of EtOAc (0-30%), yielding the triflate compound **33** (0.3 g, 42%). ¹H NMR (400 MHz, CDCl₃) δ : 8.08 (t, $J = 5.6$ Hz, 1H), 7.76–7.72 (m, 3H), 5.68 (s, 1H), 4.49 (d, $J = 5.6$ Hz, 2H), 3.20–3.06 (m, 2H), 2.89–2.82 (m, 2H), 2.67–2.60 (m, 1H), 2.40–2.20 (m, 3H), 2.04–1.79 (m, 4H), 1.73–1.59 (m, 2H), 0.91(d, $J = 6.8$ Hz, 3H), 0.88 (d, $J = 6.8$ Hz, 3H).

1-((1R,3S)-3-((3,5-bis(trifluoromethyl)benzyl)carbamoyl)-3-isopropylcyclopentyl)-1,2,3,6-tetrahydropyridin-4-yl trifluoromethanesulfonate (34). In a 20 mL microwave tube a solution of LDA (2M in heptanes, 0.33 mL, 0.65 mmol) in THF (5 mL) was cooled down to -78 °C under nitrogen atmosphere. The ketone compound **32** (0.22 g, 0.5 mmol) was dissolved in dry THF (5 mL) and added dropwise to the reaction mixture. Vigorous stirring was necessary. The reaction mixture was stirred for 1 hour at -78 °C. After 1 hour, the reaction mixture was slowly warmed to -20 °C and kept at this temperature for 1.5 hours. Subsequently the reaction mixture was cooled down to -78 °C and *N*-phenyl-bis(trifluoromethanesulfonimide) (0.23 g, 0.65 mmol) dissolved in THF (5 mL) was added dropwise to the reaction mixture. After the addition was complete, the reaction mixture was slowly brought to room temperature and stirred overnight. The reaction mixture was quenched with EtOH, concentrated in vacuum and partitioned between DCM/H₂O. The organic layer was dried with MgSO₄ and concentrated in vacuum. The product was purified by column chromatography on silica gel with an eluent system consisting of DCM and increasing amounts of EtOAc (0-20%), yielding the triflate compound **34** (0.06 g, 21%). ¹H NMR (400 MHz, CDCl₃) δ : 7.44 (d, $J = 8$ Hz, 1H), 7.38 (s, 1H), 7.27 (d, $J = 8.0$ Hz, 1H), 5.71 (s, 1H), 4.90–4.57 (m, 2H), 3.82 (br s, 2H), 3.17 (s, 2H), 2.93 (d, $J = 5.2$ Hz, 2H), 2.80–2.60 (m, 4H), 2.43 (br s, 2H), 2.25–2.15 (m, 1H), 2.08–1.82 (m, 3H), 1.60–1.38 (m, 2H), 0.95 (d, $J = 6.4$ Hz, 3H), 0.80 (d, $J = 6.4$ Hz, 3H).

General synthesis of compounds **35** – **46**.

In a 5 mL microwave tube a mixture of triflate **33** (0.25 mmol, 1 equiv.), corresponding arylboronic acid (0.35 mmol, 1.4 equiv.), LiCl (0.75 mmol, 3 equiv.), 2 M Na₂CO₃ in H₂O (0.75 mmol, 3 equiv.) and tetrakis(triphenylphosphine)palladium(0) (5 mol%) was dissolved in DME (4 mL) under a nitrogen atmosphere. The reaction was heated under microwave irradiation at 90 °C for 3.5 hours. DME was evaporated in vacuum and the reaction mixture was partitioned between 2 M Na₂CO₃/DCM. The organic layer was dried with MgSO₄ and concentrated in vacuum. The products were purified by column chromatography on silica gel with an eluent system consisting of DCM and increasing amounts of EtOAc (0-50%). LC–MS was used for confirmation of the products before using them in the next step.

(1S,3R)-N-(3,5-bis(trifluoromethyl)benzyl)-1-isopropyl-3-(4-phenyl-3,6-dihydropyridin-1(2H)-yl)cyclopentane-1-carboxamide (35). Yield = 40 %, MS peak: 539⁺ [H⁺].

(1S,3R)-N-(3,5-bis(Trifluoromethyl)benzyl)-1-isopropyl-3-(4-(2-methoxyphenyl)-3,6-dihydropyridin-1(2H)-yl)cyclopentane-1-carboxamide (36). Yield = 21%, MS peak: 569⁺ [H⁺].

(1*S*,3*R*)-*N*-(3,5-bis(trifluoromethyl)benzyl)-1-isopropyl-3-(4-(3-methoxyphenyl)-3,6-dihydropyridin-1(2*H*)-yl)cyclopentane-1-carboxamide (**37**). Yield = 20%, MS peak: 569⁺ [H⁺].

(1*S*,3*R*)-*N*-(3,5-bis(trifluoromethyl)benzyl)-1-isopropyl-3-(4-(4-methoxyphenyl)-3,6-dihydropyridin-1(2*H*)-yl)cyclopentane-1-carboxamide (**38**). Yield = 99% (without purification), MS peak: 569⁺ [H⁺].

(1*S*,3*R*)-*N*-(3,5-bis(trifluoromethyl)benzyl)-3-(4-(3,4-dimethoxyphenyl)-3,6-dihydropyridin-1(2*H*)-yl)-1-isopropylcyclopentane-1-carboxamide (**39**). Yield = 30%, MS peak: 599⁺ [H⁺].

(1*S*,3*R*)-3-(4-(Benzo[d][1,3]dioxol-5-yl)-3,6-dihydropyridin-1(2*H*)-yl)-*N*-(3,5-bis(trifluoromethyl)benzyl)-1-isopropylcyclopentane-1-carboxamide (**40**). Yield = 41%, MS peak: 583⁺ [H⁺].

(1*S*,3*R*)-*N*-(3,5-bis(trifluoromethyl)benzyl)-1-isopropyl-3-(4-(4-(trifluoromethoxy)phenyl)-3,6-dihydropyridin-1(2*H*)-yl)cyclopentane-1-carboxamide (**41**). Yield = 51%, MS peak: 623⁺ [H⁺].

(1*S*,3*R*)-*N*-(3,5-bis(trifluoromethyl)benzyl)-3-(4-(4-(*tert*-butyl)phenyl)-3,6-dihydropyridin-1(2*H*)-yl)-1-isopropylcyclopentane-1-carboxamide (**42**). Yield = 32%, MS peak: 595⁺ [H⁺].

(1*S*,3*R*)-*N*-(3,5-bis(trifluoromethyl)benzyl)-3-(4-(4-hydroxyphenyl)-3,6-dihydropyridin-1(2*H*)-yl)-1-isopropylcyclopentane-1-carboxamide (**43**). Yield = 25%, MS peak: 555⁺ [H⁺].

(1*S*,3*R*)-*N*-(3,5-bis(trifluoromethyl)benzyl)-3-(3',6'-dihydro-[3,4'-bipyridin]-1'(2'*H*)-yl)-1-isopropylcyclopentane-1-carboxamide (**44**). Yield = 55%, MS peak: 540⁺ [H⁺].

(1*S*,3*R*)-*N*-(3,5-bis(trifluoromethyl)benzyl)-1-isopropyl-3-(6-methoxy-3',6'-dihydro-[3,4'-bipyridin]-1'(2'*H*)-yl)cyclopentane-1-carboxamide (**45**). Yield = 59%, MS peak: 570⁺ [H⁺].

Methyl 3-(1-((1*R*,3*S*)-3-((3,5-bis(trifluoromethyl)benzyl)carbonyl)-3-isopropylcyclopentyl)-1,2,3,6-tetrahydropyridin-4-yl)benzoate (**46**). Yield = 53%, MS peak: 597⁺ [H⁺].

Synthesis of (1*S*,3*R*)-methyl-3-((*tert*-butoxycarbonyl)amino)-1-isopropylcyclopentanecarboxylate (**47**) was achieved following the synthetic approach reported by Kothandaraman S. et al.¹⁹

Methyl (1*S*,3*R*)-3-amino-1-isopropylcyclopentane-1-carboxylate (**48**). In a 100 mL round-bottom flask compound **47** (11.4 g, 40 mmol) was dissolved in a mixture of DCM (30 mL) and TFA (20 mL). The reaction mixture was stirred at room temperature for 2 hours. After completion, the reaction mixture was basified to pH 14 with 2 M NaOH solution in H₂O and extracted with DCM. The organic layer was dried with MgSO₄ and concentrated in vacuum. Yield = 7.3 g (98%). The crude product was used in the next step without further purification. ¹H NMR (400 MHz, CDCl₃) δ: 3.57 (s, 3H), 3.25–3.18 (m, 1H), 2.20–2.12 (m, 1H), 1.90–1.70 (m, 4H), 1.48–1.35 (m, 2H), 1.28–1.15 (m, 2H), 0.80–0.71 (m, 6H).

Methyl (1*S*,3*R*)-1-isopropyl-3-(4-oxopiperidin-1-yl)cyclopentane-1-carboxylate (**49**). In 7 separate batches of 100 mL round-bottom flasks a solution of amine **48** (0.74 g, 4.0 mmol) dissolved in ethanol (20 mL) and H₂O (8 mL) was stirred at 40 °C. Compound **28** (1.61 g, 6 mmol) was dissolved in H₂O (8 mL) and added dropwise during 5 minutes to the reaction mixture. Then K₂CO₃ (1.12 g, 8 mmol) was added and the reaction mixture was refluxed for 3 hours. All batches were combined and ethanol was removed in vacuum and the reaction mixture was partitioned between DCM/H₂O. The organic layer was dried over MgSO₄ and concentrated in vacuum. The product was purified by column chromatography on silica gel with an eluent system consisting of DCM and increasing amounts of EtOAc (0-100%). Combined yield = 4.19 g, (56%). ¹H NMR (400 MHz, CDCl₃) δ: 3.55 (s, 3H), 2.63 (t, *J* = 6.4 Hz, 4H), 2.59–2.50 (m, 1H), 2.29 (t, *J* = 6.4 Hz, 4H), 2.16–2.12 (m, 1H), 2.01–1.95 (m, 1H), 1.87–1.74 (m, 3H), 1.37 (t, *J* = 4.8 Hz, 2H), 0.74 (d, *J* = 6.8 Hz, 3H), 0.71 (d, *J* = 6.8 Hz, 3H).

Methyl (1*S*,3*R*)-1-isopropyl-3-(4-(((trifluoromethyl)sulfonyl)oxy)-3,6-dihydropyridin-1(2*H*)-yl)cyclopentane-1-carboxylate (**50**). In a 250 mL round-bottom flask a solution of LDA (2M in heptanes, 11 mL, 22 mmol) in dry THF (100 mL) was cooled down to –100 °C under a nitrogen atmosphere. The ketone compound **49** (4.19 g, 15.6 mmol) was dissolved in dry THF (20 mL) and added dropwise to the reaction mixture keeping the temperature below –78 °C. Vigorous stirring was necessary. The reaction mixture was stirred for 3 hours, slowly rising the temperature to –40 °C. Subsequently, the reaction mixture was cooled down to –80 °C and *N*-phenyl-bis(trifluoromethanesulfonylimide) (7.86 g, 22 mmol) dissolved in dry THF (10 mL) was added dropwise to the reaction mixture keeping the temperature of

the reaction below $-80\text{ }^{\circ}\text{C}$. After the addition was complete, the reaction mixture was slowly brought to room temperature and stirred overnight. The reaction mixture was quenched with EtOH, concentrated in vacuum and partitioned between DCM/H₂O. The organic layer was dried with MgSO₄ and concentrated in vacuum. The product was purified by column chromatography on silica gel with an eluent system consisting of DCM and increasing amounts of EtOAc (0-10%), yielding the triflate compound **50** (4.2 g, 67%). ¹H NMR (400 MHz, CDCl₃) δ : 5.73 (s, 1H), 3.70 (s, 3H), 3.25–3.12 (m, 2H), 2.80–2.67 (m, 3H), 2.46 (br s, 2H), 2.35–2.25 (m, 1H), 2.13–1.85 (m, 4H), 1.60–1.48 (m, 2H), 0.89 (d, $J = 6.4\text{ Hz}$, 3H), 0.86 (d, $J = 6.4\text{ Hz}$, 3H).

N'-(1-((1*R*,3*S*)-3-isopropyl-3-(7-(trifluoromethyl)-1,2,3,4-tetrahydroisoquinoline-2-carbonyl)cyclopentyl)piperidin-4-ylidene)-4-methoxybenzenesulfonylhydrazide (**52**). Sulfonylhydrazide **51** (365 mg, 1.80 mmol, 1.05 equiv.) was slurried in 3,5 mL of MeOH and piperidone **32** (750 mg, 1.72 mmol, 1.00 equiv.) was added at room temperature, resulting in a homogeneous reaction mixture. After 4 hours all of the piperidone was consumed shown by TLC (1/1 EtOAc/Pet. Ether). Methanol was removed in vacuum and the solidified oil (1.06 g, yield 100%) was used in the next reactions without purification. ¹H NMR (400 MHz, CDCl₃) δ : 7.88 (d, $J = 8.0\text{ Hz}$, 2H), 7.42 (d, $J = 8.0\text{ Hz}$, 1H), 7.36 (s, 1H), 4.90–4.60 (m, 2H), 3.87 (s, 3H), 3.85–3.60 (m, 2H), 3.46 (s, 1H), 2.90 (s, 2H), 2.60–2.41 (m, 6H), 2.33 (br s, 3H), 2.19–2.14 (m, 1H), 2.00 (br s, 1H), 1.88–1.78 (m, 2H), 1.54–1.43 (m, 1H), 1.36–1.25 (m, 1H), 0.92 (d, $J = 6.4\text{ Hz}$, 3H), 0.75 (d, $J = 6.4\text{ Hz}$, 3H).

Abbreviations

Boc, *tert*-butyloxycarbonyl; CCL2, chemokine ligand 2; CCR2, chemokine receptor 2; CCR5, chemokine receptor 5; DCM, dichloromethane; DiPEA, *N,N*-diisopropylethylamine; DMAP, *N,N*-dimethylaminopyridine; DME, dimethoxyethane; EtOAc, ethylacetate; EtOH, ethanol; HPLC, high-performance liquid chromatography; ¹²⁵I-CCL2, ¹²⁵I-labelled chemokine ligand 2; KRI, kinetic rate index; LDA, lithium diisopropylamide; LC-MS, liquid chromatography – mass spectrometer; MCP-1, monocyte chemoattractant protein-1; MeOH, methanol; NMR, nuclear magnetic resonance; PyBrOP, bromo-tris-pyrrolidino phosphoniumhexafluorophosphate; RT, residence time; SAR, structure–affinity relationships; SKR, structure–kinetic relationships; TFA, trifluoroacetic acid; THF, tetrahydrofuran; TLC, thin layer chromatography; TMS, tetramethylsilane; U2OS, human bone osteosarcoma cells; UV, ultraviolet.

ACKNOWLEDGEMENTS

This study was financially supported by the Dutch Top Institute Pharma, project number D1-301. We thank Dr. Julien Louvel for the helpful comments and suggestions on the synthesis and his input in analytical data analysis. We acknowledge Prof. Dr. Martine Smit (Vrije Universiteit, Amsterdam, The Netherlands) for helpful comments and suggestions.

REFERENCES.

1. Baggiolini, M. Chemokines and leukocyte traffic. *Nature* **1998**, 392, 565-568.
2. Bachmann, M. F.; Kopf, M.; Marsland, B. J. Chemokines: more than just road signs. *Nat Rev Immunol* **2006**, 6, 159-164.
3. Onuffer, J. J.; Horuk, R. Chemokines, chemokine receptors and small-molecule antagonists: recent developments. *Trends in Pharmacological Sciences* **2002**, 23, 459-467.
4. Tarrant, T. K.; Patel, D. D. Chemokines and leukocyte trafficking in rheumatoid arthritis. *Pathophysiology : the official journal of the International Society for Pathophysiology / ISP* **2006**, 13, 1-14.
5. Fife, B. T.; Huffnagle, G. B.; Kuziel, W. A.; Karpus, W. J. CC chemokine receptor 2 is critical for induction of experimental autoimmune encephalomyelitis. *The Journal of experimental medicine* **2000**, 192, 899-905.

6. Dawson, T. C.; Kuziel, W. A.; Osahar, T. A.; Maeda, N. Absence of CC chemokine receptor-2 reduces atherosclerosis in apolipoprotein E-deficient mice. *Atherosclerosis* **1999**, *143*, 205-11.
7. Kanda, H.; Tateya, S.; Tamori, Y.; Kotani, K.; Hiasa, K.; Kitazawa, R.; Kitazawa, S.; Miyachi, H.; Maeda, S.; Egashira, K.; Kasuga, M. MCP-1 contributes to macrophage infiltration into adipose tissue, insulin resistance, and hepatic steatosis in obesity. *The Journal of clinical investigation* **2006**, *116*, 1494-505.
8. Kim, Y. K.; Oh, H. B.; Lee, E. Y.; Gho, Y. S.; Lee, J. E.; Kim, Y. Y. Association between a genetic variation of CC chemokine receptor-2 and atopic asthma. *Allergy* **2007**, *62*, 208-9.
9. White, F. A.; Feldman, P.; Miller, R. J. Chemokine Signaling and the Management of Neuropathic Pain. *Molecular Interventions* **2009**, *9*, 188-195.
10. Guo, D.; Hillger, J. M.; Ijzerman, A. P.; Heitman, L. H. Drug-Target Residence Time-A Case for G Protein-Coupled Receptors. *Medicinal Research Reviews* **2014**, Jul;34(4):856-92.
11. Swinney, D. C. Biochemical mechanisms of drug action: what does it take for success? *Nature Reviews Drug Discovery* **2004**, *3*, 801-808.
12. Copeland, R. A.; Pompliano, D. L.; Meek, T. D. Drug-target residence time and its implications for lead optimization. *Nat Rev Drug Discov* **2006**, *5*, 730-9.
13. Vilums, M.; Zweemer, A. J. M.; Yu, Z. Y.; de Vries, H.; Hillger, J. M.; Wapenaar, H.; Bollen, I. A. E.; Barmare, F.; Gross, R.; Clemens, J.; Krenitsky, P.; Brussee, J.; Stamos, D.; Saunders, J.; Heitman, L. H.; Ijzerman, A. P. Structure-Kinetic Relationships-An Overlooked Parameter in Hit-to-Lead Optimization: A Case of Cyclopentylamines as Chemokine Receptor 2 Antagonists. *Journal of Medicinal Chemistry* **2013**, *56*, 7706-7714.
14. Struthers, M.; Pasternak, A. CCR2 antagonists. *Current topics in medicinal chemistry* **2010**, *10*, 1278-98.
15. Pasternak, A.; Goble, S. D.; Struthers, M.; Vicario, P. P.; Ayala, J. M.; Di Salvo, J.; Kilburn, R.; Wisniewski, T.; Demartino, J. A.; Mills, G. S.; Yang, L. Discovery of a potent orally bioavailable CCR2 and CCR5 dual antagonist. *Medicinal Chemistry Letters* **2010**, *1*, 14-18.
16. Kuehne, M. E.; Muth, R. S. Total Syntheses of Yohimbe Alkaloids, with Stereoselection for the Normal, Allo, and 3-Epiallo Series, Based on Annelations of 4-Methoxy-1,2-Dihydropyridones. *Journal of Organic Chemistry* **1991**, *56*, 2701-2712.
17. Crawford, J. B.; Chen, G.; Carpenter, B.; Wilson, T.; Ji, J.; Skerlj, R. T.; Bridger, G. J. Practical Convergent Laboratory-Scale Synthesis of a CCR5 Receptor Antagonist. *Org Process Res Dev* **2012**, *16*, 109-116.
18. Vilums, M.; Zweemer, A. J.; Yu, Z.; de Vries, H.; Hillger, J. M.; Wapenaar, H.; Bollen, I. A.; Barmare, F.; Gross, R.; Clemens, J.; Krenitsky, P.; Brussee, J.; Stamos, D.; Saunders, J.; Heitman, L. H.; Ijzerman, A. P. Structure-Kinetic Relationships-An Overlooked Parameter in Hit-to-Lead Optimization: A Case of Cyclopentylamines as Chemokine Receptor 2 Antagonists. *Journal of Medicinal Chemistry* **2013**, *56*, 7706-7714.
19. Kothandaraman, S.; Donnelly, K. L.; Butora, G.; Jiao, R.; Pasternak, A.; Morriello, G. J.; Goble, S. D.; Zhou, C.; Mills, S. G.; Maccoss, M.; Vicario, P. P.; Ayala, J. M.; Demartino, J. A.; Struthers, M.; Cascieri, M. A.; Yang, L. Design, synthesis, and structure-activity relationship of novel CCR2 antagonists. *Bioorganic & Medicinal Chemistry Letters* **2009**, *19*, 1830-4.
20. Allwood, D. M.; Blakemore, D. C.; Brown, A. D.; Ley, S. V. Metal-Free Coupling of Saturated Heterocyclic Sulfonylhydrazones with Boronic Acids. *Journal of Organic Chemistry* **2014**, *79*, 328-338.
21. Zweemer, A. J. M.; Nederpelt, I.; Vrieling, H.; Hafith, S.; Doornbos, M. L. J.; de Vries, H.; Abt, J.; Gross, R.; Stamos, D.; Saunders, J.; Smit, M. J.; Ijzerman, A. P.; Heitman, L. H. Multiple binding sites for small molecule antagonists at the chemokine receptor CCR2. *Mol. Pharmacol.* **2013** Oct;84(4):551-61.
22. Yang, L.; Butora, G.; Jiao, R. X.; Pasternak, A.; Zhou, C.; Parsons, W. H.; Mills, S. G.; Vicario, P. P.; Ayala, J. M.; Cascieri, M. A.; MacCoss, M. Discovery of 3-piperidinyl-1-cyclopentanecarboxamide as a novel scaffold for highly potent CC chemokine receptor 2 antagonists. *Journal of Medicinal Chemistry* **2007**, *50*, 2609-11.
23. Butora, G.; Jiao, R.; Parsons, W. H.; Vicario, P. P.; Jin, H.; Ayala, J. M.; Cascieri, M. A.; Yang, L. 3-Amino-1-alkyl-cyclopentane carboxamides as small molecule antagonists of the human and murine CC chemokine receptor 2. *Bioorganic & Medicinal Chemistry Letters* **2007**, *17*, 3636-41.
24. Pasternak, A.; Goble, S. D.; Vicario, P. P.; Di Salvo, J.; Ayala, J. M.; Struthers, M.; DeMartino, J. A.; Mills, S. G.; Yang, L. Potent heteroarylpyperidine and carboxyphenylpyperidine 1-alkyl-cyclopentane carboxamide CCR2 antagonists. *Bioorganic & Medicinal Chemistry Letters* **2008**, *18*, 994-8.
25. Schmidtke, P.; Luque, F. J.; Murray, J. B.; Barril, X. Shielded Hydrogen Bonds as Structural Determinants of Binding Kinetics: Application in Drug Design. *Journal of the American Chemical Society* **2011**, *133*, 18903-18910.

CHAPTER 6

DESIGN AND SYNTHESIS OF NOVEL SMALL MOLECULE CCR2 ANTAGONISTS: EVALUATION OF 4-AMINOPIPERIDINE DERIVATIVES

This chapter was based upon:

M. Vilums, A.J.M. Zweemer, S. Dekkers, Y. Askar, H. de Vries, J. Saunders, D. Stamos, J. Brussee, L.H. Heitman, A.P. IJzerman.

(manuscript in preparation)

ABSTRACT

A novel *N*-(2-oxo-2-(piperidin-4-ylamino)ethyl)-3-(trifluoromethyl)benzamide series of human CCR2 chemokine receptor antagonists was identified. With a pharmacophore model based on known CCR2 antagonists a new core scaffold was designed, analogues of it synthesized and structure–affinity relationship studies derived yielding a new high affinity CCR2 antagonist *N*-(2-((1-(4-(3-methoxyphenyl)cyclohexyl)piperidin-4-yl)amino)-2-oxoethyl)-3-(trifluoromethyl)benzamide.

The CC chemokine CCL2, through its interaction with the CCR2 G protein-coupled receptor, plays an important role in the recruitment of monocytes, natural killer cells, dendritic cells and T-lymphocytes.¹ Research on CCL2 knockout (KO) and CCR2 KO mice suggests that inhibition of the CCL2/CCR2 axis may be beneficial in the treatment of inflammatory diseases.² The pair is thought to be involved in atherosclerosis,³ insulin resistance,⁴ multiple sclerosis,⁵ neuropathic pain⁶ and asthma.⁷ Different *in vitro* and *in vivo* models have shown the usefulness of small molecule CCR2 antagonists to inhibit the chemotactic response of CCL2.⁸⁻¹⁰ Consequently, the pharmaceutical industry has devoted considerable efforts to the development of CCR2 antagonists to combat these diseases. A vast number of different scaffolds used in the design of CCR2 antagonists has been described.^{11, 12}

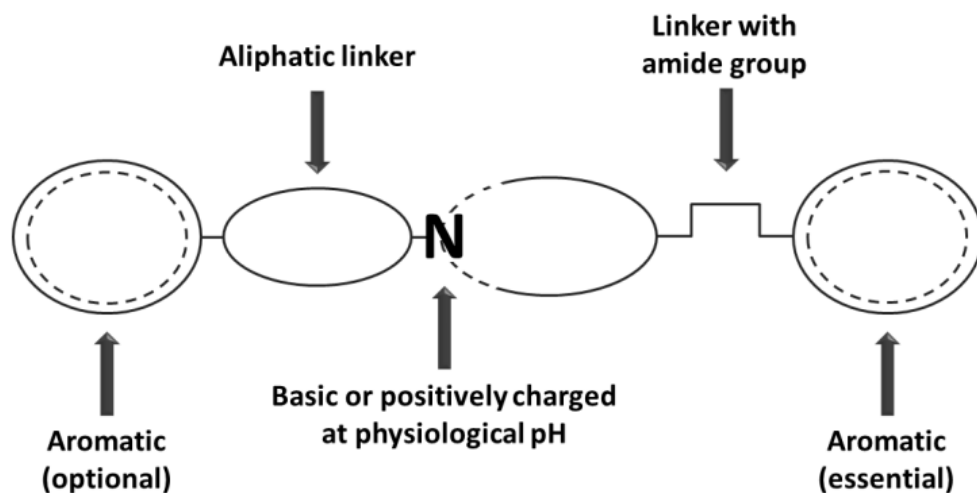


Figure 1. Pharmacophore of CCR2 antagonists.

However, the bulk of these antagonists share the same structural motifs: a basic nitrogen atom in the center, flanked by two aromatic rings of which one is connected to the nitrogen atom with an amide containing linker and the other with an aliphatic linker (Figure 1). In some cases the latter aromatic ring is missing and only the aliphatic group is left on one side.¹² Usually, the central nitrogen is part of an aliphatic heterocycle (e.g. piperidine, **1**,¹³ pyrrolidine, **2**¹⁴ and INCB3344^{14, 15} or azetidine, JNJ lead¹⁶) (Figure 2).

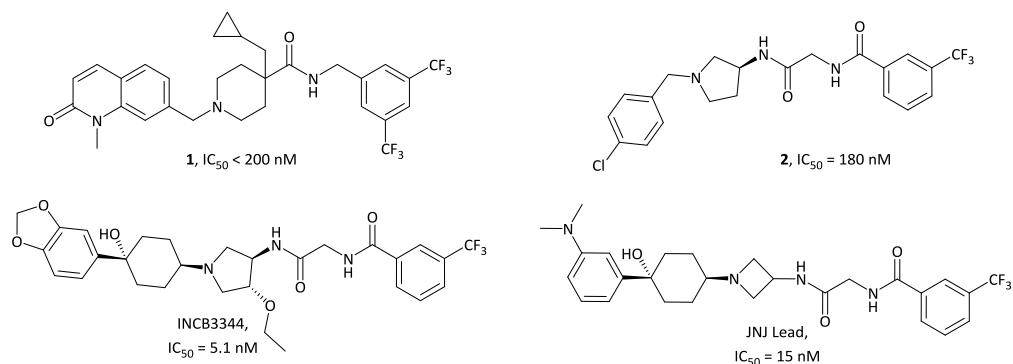
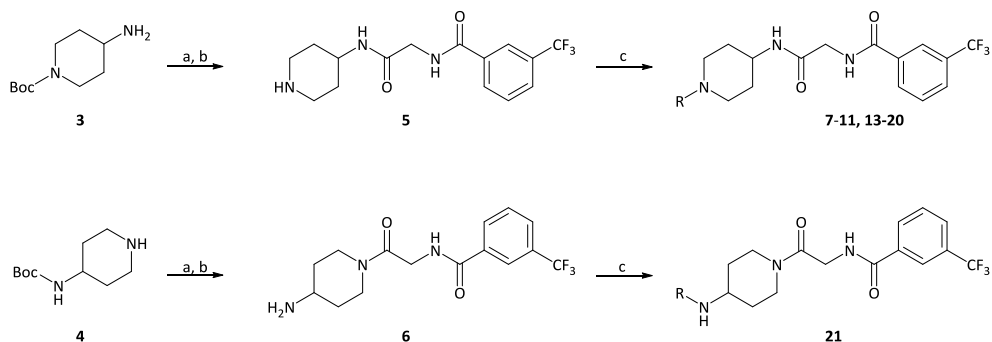


Figure 2. Known CCR2 antagonists.

In this paper, we describe our efforts towards the identification of a new class of CCR2 receptor antagonists. Using the structural knowledge of CCR2 antagonists as in figure 2 we generated hybrid scaffolds based on a piperidine ring. We explored different linkers between the basic nitrogen and aromatic groups as well as different substituents on the aromatic group. All compounds were evaluated in a ^{125}I -CCL2 displacement assay on a human bone osteosarcoma (U2OS) cell membrane preparation expressing CCR2 as described previously by our group.¹⁷

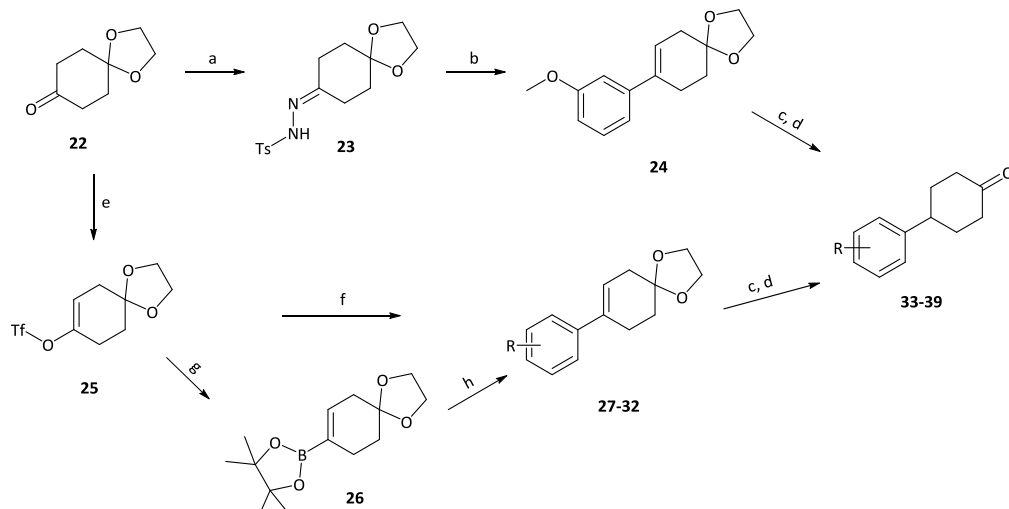
Scheme 1.^a

^aReagents and conditions: a) PyBrOP, DIPEA, DMAP, *N*-(3-(trifluoromethyl)benzoyl)glycine, DCM, MS 4 Å, room temperature; b) dry 3 M HCl in MeOH, room temperature, yield in two steps: 57-89%; c) corresponding aldehyde or ketone, NaBH(OAc)₃, AcOH, DCE, room temperature, (2-64%).

The synthetic methods to arrive at these compounds are depicted in schemes 1, 2 and 3. The commercially available *N*-Boc-protected piperidineamines **3** and **4** were used in a peptide-coupling reaction with *N*-(3-(trifluoromethyl)benzoyl)glycine under bromo-tris-pyrrolidino

phosphoniumhexafluorophosphate (PyBroP) conditions.¹⁸ Subsequent removal of the Boc-protecting group with dry HCl in methanol produced the free amines **5** and **6**. These amines were used in reductive amination reactions with different aldehydes and ketones to yield the desired products **7-11**, **13-21** (Scheme 1).

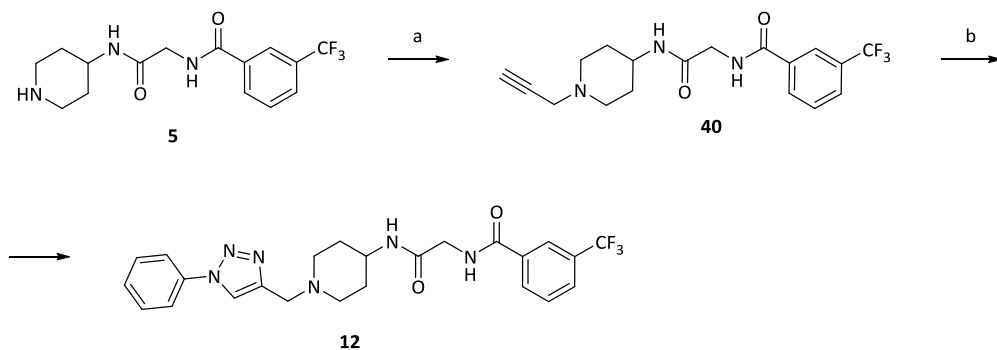
For the synthesis of the desired ketones we first used a synthetic route via hydrazone intermediates (Scheme 2) under conditions described by Barluenga et al.¹⁹ Commercially available ketone **22** was reacted with tosylhydrazide to generate hydrazone **23**, which was used subsequently in a Pd-catalyzed cross-coupling reaction to generate **24** with moderate yield.

Scheme 2.^a

^aReagents and conditions: a) *p*-toluenesulfonylhydrazide, dioxane, 130 °C, 45 minutes, MW, (65%); b) Pd₂(dba)₃, XPhos, Li^t-BuO 1.0 M in hexanes, dioxane, 110 °C, 2 h, MW, (24%); c) Pd/C 10% wt, Pd(OAc)₂, MeOH, H₂, room temperature, 4-12 h, (85-99%); d) FeCl₃•6H₂O, acetone, DCM, 5-12 h, room temperature, (42-99%); e) i) 1.3 eq. LDA, THF, under N₂, -78 °C → -25 °C, 2 h, cool down to -78 °C; ii) *N*-phenyl-bis(trifluoromethanesulfonyl)hydrazide, -78 °C → room temperature, 24 h, (80%); f) 3,4-(methylenedioxy)phenylboronic acid, KF, Pd(dppf)Cl₂, room temperature overnight, (58%); g) PdCl₂, PPh₃, bis(pinacolato)diboron, KOPh, toluene, under N₂, 4 h at 50 °C, 24 h at room temperature, (59%); h) Pd(PPh₃)₄, corresponding arylhalogen, Na₂CO₃ 2 M in H₂O, dioxane, under N₂, 80 °C, 5 h, MW, (80-99%).

However, attempts to use this method with other substituents on the phenyl ring resulted in very poor yields or no product at all. Another synthetic route was therefore chosen to yield the desired ketones. The acetal protected cyclohexanone **22** was deprotected with

lithiumdiisopropylamide (LDA) and reacted with *N*-phenyl-bis(trifluoromethanesulfonimide) to generate triflate **25**. This compound was used directly in a Suzuki–coupling with 3,4-methylenedioxyphenylboronic acid, however, to introduce other substituents we decided to transform the triflate in boronic ester **26** with bis(pinacolato)diboron. This allowed us to use a wider range of arylhalogens as coupling partners in the Suzuki–coupling to eventually generate the desired intermediates with good overall yields. Subsequently, reduction of the double bond and removal of the acetal protecting group yielded the desired ketones **33–39**, which were used in reductive amination reactions to yield the final compounds.

Scheme 3.^a

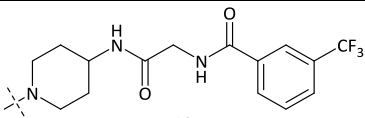
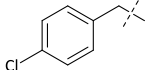
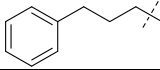
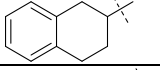
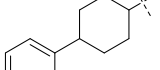
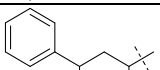
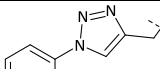
^aReagents and conditions: a) propargyl bromide, K₂CO₃, acetone, reflux overnight, (99%); b) iodobenzene, proline, Na₂CO₃, NaN₃, ascorbic acid, CuSO₄•5H₂O, DMSO/H₂O 3:1, 80 °C, 48 h, (4%).

To explore the influence of a methylenetriazole group as a linker between the piperidine and phenyl moieties we used click chemistry (Scheme 3). First, we alkylated the piperidine of compound **5** with propargyl bromide to generate compound **40**, which was used in a further reaction with sodium azide and iodobenzene in the presence of proline, ascorbic acid and CuSO₄ as described by Feldman et al.²⁰

As mentioned before we combined the different scaffolds from two known CCR2 antagonists (compound **1** of Epix Delaware;¹³ compound **2** from Tejin¹⁴) to generate a hybrid scaffold by transfecting the *N*-(3-(trifluoromethyl)benzoyl)glycine part onto the piperidine ring. We argued that the expansion of the central ring to piperidine (compared to INCB3344 and JNJ Lead) might have a minor effect only on the configuration of the molecule. However, the 4-

chlorobenzyl group (compound **7**) which had yielded good affinity in combination with the pyrrolidine scaffold¹⁴ (compound **2**), provided no affinity in the case of piperidine (Table 1).

Table 1. CCR2 affinities of compounds **7-12**.

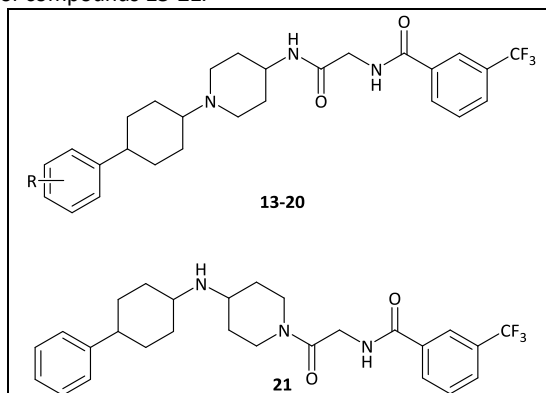
 7 - 12		
R	Nr.	K_i , (nM) \pm SEM (n = 3) ^a
	7	0%
	8	6%
	9	24%
	10	74 \pm 9
	11	10%
	12	12%

^aHuman CCR2 binding affinity in [¹²⁵I]CCL2 assay or % displ. at 1 μ M of [¹²⁵I]CCL2 binding

Extending the linker to propyl (compound **8**) had a minor effect on the affinity and the rigidification of the linker into tetrahydronaphthalene (compound **9**) yielded negligible improvement (displacement at 1 μ M concentration of 6% and 24%, respectively). However, separation of the rings into a 4-phenylcyclohexyl group (compound **10**) resulted in a boost of affinity (K_i = 74 nM). To explore the correct location of the phenyl ring we moved it to the 3 position on the cyclohexane ring (compound **11**), which resulted in a complete loss of affinity. In addition, the cyclohexane's exchange to methylenetriazole as a linker (compound **12**) did not yield any affinity either. Apparently, the distance, 3D orientation and lipophilicity provided by the cyclohexane moiety is just right for the binding of these molecules to the

CCR2 receptor and any deviation from it results in complete loss of affinity. This could also be the reason why the 4-aryl-cyclohexane motif is used in so many pyrrolidine^{15, 21} and azetidine^{16, 22} derivatives (e.g. INCB3344, JNJ Lead, see figure 2). We continued the SAR studies with different substituents on the phenyl ring of the 4-phenyl-cyclohexyl group. Introduction of a methyl group on different positions indicated that substitution on the 2 and 4 positions (compounds **13** and **15**) decreased the affinity (Table 2).

Table 2. CCR2 affinities of compounds **13-21**.



Nr.	R	K_i , (nM) \pm SEM (n = 3) ^a
13	2-Me	26%
14	3-Me	270 \pm 20
15	4-Me	38%
16	3-OMe	66 \pm 12
17	3,5-di-OMe	41%
18	2,6-di-OMe	42%
19	4-OH	139 \pm 35
20	3,4-OCH ₂ O-	90 \pm 18
21	-	31%

^aHuman CCR2 binding affinity in [¹²⁵I]CCL2 assay or % displ. at 1 μ M of [¹²⁵I]CCL2 binding

The 3 position can tolerate substitution, albeit with a slight decrease in affinity (**14**, K_i = 270 nM). Changing the methyl to methoxy resulted in a regain of the affinity (compound **16**, K_i = 66 nM) pointing to a possible H-bond formation in the receptor binding pocket. However, insertion of two methoxy groups on either the 3,5 or 2,6 positions (compounds **17**, **18**) yielded a decrease in affinity (displacement of 41% and 42%, respectively). Inserting a hydroxyl group on the 4 position (compound **19**) was tolerated with a twofold affinity

decrease compared to **10**. Combining substituents of **16** and **19** into a 3,4-methylenedioxy group retained the affinity (compound **20**, $K_i = 90$ nM) which is in accordance with observations from the pyrrolidine¹⁵ and azetidine¹⁶ series. Finally, we wanted to explore the possibility of reversing the piperidine ring (compound **21**) in the same fashion as it was described for pyrrolidines²³ where it had only minimal effect on the binding affinity. However, in our case of the piperidine moiety such reversal substantially decreased the affinity for the CCR2 receptor.

In conclusion, we have synthesized a novel series of *N*-(2-oxo-2-(piperidin-4-ylamino)ethyl)-3-(trifluoromethyl)benzamide derivatives and compounds substituted with 4-arylcyclohexanes were identified as good hits for CCR2 antagonism and might be considered for further optimization.

EXPERIMENTAL SECTION

Chemistry

All solvents and reagents were purchased from commercial sources and were of analytical grade. Demineralized water is simply referred to as H₂O, because it was used in all cases, unless stated otherwise (i.e., brine). ¹H and ¹³C NMR spectra were recorded on a Bruker AV 400 liquid spectrometer (¹H NMR, 400 MHz; ¹³C NMR, 101 MHz). Chemical shifts are reported in parts per million (ppm), are designated by δ , and are downfield to the internal standard tetramethylsilane (TMS). Coupling constants are reported in hertz and are designated as *J*, *a* and *b* indicating different diastereomers. Analytical purity of the final compounds was determined by high-performance liquid chromatography (HPLC) with a Phenomenex Gemini 3 μ m C18 110A column (50 \times 4.6 mm, 3 μ m), measuring UV absorbance at 254 nm. The sample preparation and HPLC method for compounds were as follows: 0.3–0.8 mg of compound was dissolved in 1 mL of a 1:1:1 mixture of CH₃CN/H₂O/*t*-BuOH and eluted from the column within 15 min at a flow rate of 1.3 mL/min. The elution method was set up as follows: 1–4 min isocratic system of H₂O/CH₃CN/1% TFA in H₂O, 80:10:10, from the 4th min, a gradient was applied from 80:10:10 to 0:90:10 within 9 min, followed by 1 min of equilibration at 0:90:10 and 1 min at 80:10:10. All compounds showed a single peak at the designated retention time and are at least 95% pure. Microwave reactions were done using Biotage Initiator microwave synthesizer. Thin-layer chromatography (TLC) was routinely consulted to monitor the progress of reactions, using aluminum-coated Merck silica gel F²⁵⁴ plates. Purification by column chromatography was achieved by use of Grace Davison Davisil silica column material (LC60A, 30–200 μ m). The procedure for a series of similar compounds is given as a general procedure for all within that series, annotated by the numbers of the compounds.

N-(2-oxo-2-(piperidin-4-ylamino)ethyl)-3-(trifluoromethyl)benzamide (**5**). To 2 g, 10 mmol (1 equiv.) of 4-amino-1-boc-piperidine (**3**) dissolved in 30 mL DCM was added 2.47 g, 10 mmol (1 equiv.) of *N*-(3-(trifluoromethyl)benzoyl)glycine, 4.66 g, 10 mmol (1 equiv.) of PyBroP, 1 g, 8 mmol (0.8 equiv.) of 4-dimethylaminopyridine, 5.10 mL, 30 mmol (3 equiv.) of *N,N*-diisopropylethylamine and molecular sieves

4 Å. The reaction mixture was stirred for 24 h at room temperature. The product was partitioned between DCM/1M NaOH. The organic layer was washed with brine, dried over MgSO_4 and evaporated. The intermediate was purified by column chromatography (50/50 EtOAc in DCM). ^1H NMR (400 MHz, CDCl_3) δ : 8.11 (s, 1H), 8.00 (d, $J = 8.0$ Hz, 2H), 7.76 (d, $J = 7.6$ Hz, 1H), 7.54 (t, $J = 8.0$ Hz, 1H), 7.14 (d, $J = 7.6$ Hz, 1H), 4.17 (d, $J = 4.8$ Hz, 2H), 4.00–3.92 (m, 3H), 2.89 (t, $J = 11.6$ Hz, 2H), 1.91 (d, $J = 2.8$ Hz, 2H), 1.45–1.37 (m, 11H). Subsequently, *tert*-butyl 4-(2-(3-(trifluoromethyl)benzamido)acetamido)piperidine-1-carboxylate was added to a dry solution of 3M HCl in MeOH. The reaction was stirred at room temperature for 2.5 hours. Upon completion, the reaction was neutralized with 1M NaOH (aq.) to pH = 10 and the methanol was evaporated. Extraction with DCM and subsequent drying over MgSO_4 and evaporation yielded the product. Overall yield = 57%. ^1H NMR (400 MHz, CDCl_3) δ : 8.80 (s, 1H), 8.61 (d, $J = 8.0$ Hz, 2H), 7.76 (d, $J = 7.6$ Hz, 1H), 6.54 (s, 1H), 4.86 (d, $J = 7.6$ Hz, 2H), 3.92–3.87 (m, 3H), 2.63 (t, $J = 10.2$ Hz, 2H), 1.89–1.86 (m, 2H), 1.32–1.30 (m, 2H).

N-(2-oxo-2-(piperidin-4-ylamino)ethyl)-3-(trifluoromethyl)benzamide (**6**). To 1 equivalent of *tert*-butyl piperidin-4-ylcarbamate (**4**) dissolved in DCM was added 1 equivalent of *N*-(3-(trifluoromethyl)benzoyl)glycine, 1 equivalent of PyBroP, 0.8 equivalents of 4-dimethylaminopyridine, 3 equivalents of *N,N*-diisopropylethylamine and molecular sieves 4 Å. The reaction mixture was stirred for 24 h at room temperature. The product was extracted with DCM/ 1 M NaOH. The organic layer was washed with brine, dried over MgSO_4 and evaporated. The intermediate was purified by column chromatography (50/50 EtOAc in DCM). ^1H NMR (400 MHz, CDCl_3) δ : 8.13 (s, 1H), 8.01 (d, $J = 8.0$ Hz, 1H), 7.78 (d, $J = 8.0$ Hz, 1H), 7.59 (t, $J = 8.0$ Hz, 1H), 7.47 (br s, 1H), 4.65–4.50 (m, 2H), 4.70 (dd, $J = 22.4$, 3.6 Hz, 2H), 3.82–3.72 (m, 2H), 3.23–3.15 (m, 1H), 2.88 (t, $J = 12.0$ Hz, 1H), 2.15–2.00 (m, 2H), 1.47 (s, 9H), 1.41–1.30 (m, 2H). *tert*-butyl (1-((3-(trifluoromethyl)benzoyl)glycyl)piperidin-4-yl)carbamate was added to a dry solution of 3M HCl in MeOH. The reaction was stirred at room temperature for 2.5 hours. Upon completion, the reaction was neutralized with 1M NaOH (aq.) to pH = 10 and the methanol was evaporated. Extraction with DCM and subsequent drying on MgSO_4 and evaporation yielded the product. Overall yield = 89%. ^1H NMR (400 MHz, CDCl_3) δ : 8.00 (s, 1H), 7.88 (d, $J = 8.0$ Hz, 2H), 7.59 (d, $J = 7.6$ Hz, 1H), 7.40 (t, $J = 8.0$ Hz, 1H), 4.31 (d, $J = 12.0$ Hz, 2H), 4.40–4.10 (m, 2H), 3.68 (d, $J = 12.0$ Hz, 1H), 3.10–2.65 (m, 4H), 1.83–1.70 (m, 2H), 1.28–1.14 (m, 2H).

General procedure for the preparation of compounds **7**, **10**, **16** and **19**.

A round-bottom flask was purged with N_2 gas before adding DCM. *N*-(2-oxo-2-(piperidin-4-ylamino)ethyl)-3-(trifluoromethyl)benzamide (**5**) was added together with the corresponding aldehyde or ketone in a 1:1 ratio. In the case of ketones, 1 equivalent of acetic acid was added. 2 equivalents of $\text{NaBH}(\text{OAc})_3$ were added and the reaction mixture was stirred with 4 Å MS for 48 hours at room temperature. The reaction was quenched with 1M NaOH (aq.) and extracted with DCM. The organics were washed with brine and dried over MgSO_4 . Purification by column chromatography was performed using an eluent system of 90:9:1 DCM:MeOH: NH_4OH .

N-(2-((1-(4-chlorobenzyl)piperidin-4-yl)amino)-2-oxoethyl)-3-(trifluoromethyl)benzamide (**7**). The product was obtained in a yield of 62%. ^1H NMR (400 MHz, Acetone- d_6) δ : 8.35–8.20 (m, 3H), 7.90 (d, $J = 7.6$ Hz, 1H), 7.75 (t, $J = 7.6$ Hz, 1H), 7.25–7.42 (m, 5H), 4.06 (d, $J = 5.6$ Hz, 2H), 3.70–3.80 (m, 1H), 3.49 (s, 2H), 2.80 (d, $J = 11.6$ Hz, 2H), 2.16–2.05 (m, 2H), 1.88–1.80 (m, 2H), 1.58–1.47 (m, 2H). ^{13}C NMR (101Hz, Acetone- d_6) δ : 168.0, 165.3, 138.0, 135.4, 132.0, 131.1, 130.4, 130.0, 129.5, 128.1, 127.8, 127.8, 125.5, 124.1, 124.1, 61.6, 52.1, 46.6, 43.1, 31.8. LC/MS mass found: 454⁺, 456⁺ [H^+]. Purity: 96.9 %.

N-(2-oxo-2-((1-(4-phenylcyclohexyl)piperidin-4-yl)amino)ethyl)-3-(trifluoromethyl)benzamide (**10**). The product was obtained with a yield of 43%. ^1H NMR (400 MHz, CDCl_3) δ : 8.17 (s, 1H), 8.10–8.00 (m, 2H), 7.76 (d, $J = 8.0$ Hz, 1H), 7.55 (t, $J = 7.6$ Hz, 1H), 7.35–7.18 (m, 5H), 7.08 (d, $J = 8.0$ Hz, 0.3H),^o 7.00 (d, $J = 8.0$ Hz, 0.7H),^b 4.20 (d, $J = 5.2$ Hz, 2H), 3.88–3.76 (m, 1H), 3.10–2.90 (m, 2H), 2.77–2.69 (m, 1H), 2.50–2.38 (m, 1H), 2.30 (br s, 1H), 2.11 (t, $J = 10.6$ Hz, 1H), 2.05–1.88 (m, 6H), 1.68–1.40 (m, 6H). ^{13}C NMR (101Hz, CDCl_3) δ : 168.5,^o 168.5,^b 166.4, 146.8,^o 146.8,^b 134.2, 131.3, 130.9, 130.4, 129.2, 128.4, 128.3,

127.1, 126.8, 126.0, 125.7, 125.0, 124.5, 122.3, 63.4, 59.2, 48.6, 47.8, 47.3, 44.2, 44.1, 42.2, 33.6, 32.3, 28.7, 28.5, 27.9. LC/MS mass found: 488⁺ [H⁺]. Purity: 99.0 %. *a* and *b* are indicated for different diastereomers.

N-(2-((1-(4-(3-methoxyphenyl)cyclohexyl)piperidin-4-yl)amino)-2-oxoethyl)-3-(trifluoromethyl)benzamide (**16**). This final compound was obtained with a yield of 6%. ¹H NMR (400 MHz, CDCl₃ + drop of MeOD) δ: 8.13 (s, 1H), 8.03 (d, *J* = 7.6 Hz, 1H), 7.76 (d, *J* = 7.6 Hz, 1H), 7.64–7.55 (m, 2H), 7.24–7.19 (m, 1H), 6.87 (d, *J* = 8.4 Hz, 1H), 6.74–6.72 (m, 1H), 6.63 (s, NH), 4.15 (d, *J* = 4.8 Hz, 2H), 3.80 (s, 3H), 3.02 (t, *J* = 13.2 Hz, 2H), 2.71 (t, *J* = 4.4 Hz, 1H), 2.62–2.45 (m, 2H), 2.18 (s, 1H), 2.11–1.86 (m, 6H), 1.74–1.43 (m, 6H). ¹³C NMR (400 MHz, CDCl₃ + drop of MeOD) δ: 168.2, 166.4, 134.5, 130.5, 129.5, 129.4, 124.5, 119.7, 119.3, 113.6, 112.9, 111.2, 110.5, 77.5, 77.2, 76.8, 55.3, 48.6, 44.1, 43.9, 33.4, 28.6. LC/MS mass found: 518⁺ [H⁺]. Purity: 97.1 %.

N-(2-((1-(4-(4-hydroxyphenyl)cyclohexyl)piperidin-4-yl)amino)-2-oxoethyl)-3-(trifluoromethyl)benzamide (**19**). The product was obtained with a yield of 40%. ¹H NMR (400 MHz, CDCl₃ + drop of MeOD) δ: 8.13 (s, 1H), 8.03 (d, *J* = 7.6 Hz, 1H), 7.76 (d, *J* = 7.6 Hz, 1H), 7.56 (t, *J* = 8.0 Hz, 1H), 7.11 (d, *J* = 8.4 Hz, 1H), 7.01 (d, *J* = 8.4 Hz, 1H), 6.76 (dd, *J*¹ = 4.8 Hz, *J*² = 4.4 Hz, 2H), 4.07 (s, 2H), 3.77 (q, *J* = 4.0 Hz, 1H), 2.94 (d, *J* = 9.2 Hz, 2H), 2.71 (s, 1H), 2.40–2.52 (m, 3H), 2.12 (t, *J* = 10.8 Hz, 1H), 1.98–1.88 (m, 5H), 1.75 (d, *J* = 4.8 Hz, 1H), 1.65–1.49 (m, 4H), 1.41 (t, *J* = 10.4 Hz, 2H). ¹³C NMR (400 MHz, CDCl₃ + drop of MeOD) δ: 168.3, 154.7, 154.3, 138.2, 134.4, 131.0, 130.6, 129.3, 128.5, 128.2, 127.7, 124.4, 115.3, 115.2, 63.6, 48.6, 48.0, 47.0, 43.5, 43.2, 33.8, 31.8, 31.7, 29.0, 28.5, 26.8. LC/MS mass found: 504⁺ [H⁺]. Purity: 96.3 %.

General procedure for the preparation of the final compounds 8, 9, 11, 13, 14, 18, 20 and 21.

A 5 mL vial was loaded with 0.5 mmol (1 equiv.) of the corresponding aldehyde or ketone together with 0.5 mmol (1 equiv.) of piperidine **5** or **6**. In the case of ketones 1.25 mmol (2.5 equiv.) of acetic acid were added. 1 mL of MeOH was added and left to stir at room temperature for 30 minutes. 1 mmol (2 equiv.) of PEMB were added, dropwise. The reaction mixture heated at 60 °C overnight. The crude reaction mixture was directly poured onto a column and purified using the eluent system of 97:2:1 DCM:MeOH:NH₄OH.

N-(2-oxo-2-((1-(3-phenylpropyl)piperidin-4-yl)amino)ethyl)-3-(trifluoromethyl)benzamide (**8**). Yield = 10%, ¹H NMR (400 MHz, MeOD-d₄) δ: 8.18 (s, 1H), 8.12 (d, *J* = 7.6 Hz, 1H), 7.84 (d, *J* = 8.0 Hz, 1H), 7.67 (t, *J* = 8.0 Hz, 1H), 7.26 (t, *J* = 8.0 Hz, 2H), 7.19–7.14 (m, 3H), 4.0 (s, 2H), 3.82–3.77 (m, 1H), 3.15 (d, *J* = 12.4 Hz, 2H), 2.66 (q, *J* = 6.8 Hz, 4H), 2.47 (t, *J* = 11.2 Hz, 2H), 1.97–1.88 (m, 4H), 1.66 (q, *J* = 11.2 Hz, 2H). LC/MS: 448⁺ [H⁺]. Purity: 96.7%.

N-(2-oxo-2-((1-(1,2,3,4-tetrahydronaphthalen-2-yl)piperidin-4-yl)amino)ethyl)-3-(trifluoromethyl)benzamide (**9**). Yield = 77%, ¹H NMR (400 MHz, CDCl₃) δ: 9.01 (t, *J* = 5.6 Hz, 1H), 8.22 (s, 1H), 8.19 (d, *J* = 7.6 Hz, 1H), 7.94–7.90 (m, 2H), 7.76 (t, *J* = 7.6 Hz, 1H), 7.05 (s, 4H), 3.88 (d, *J* = 5.6 Hz, 2H), 3.58–3.50 (m, 1H), 3.34–2.67 (m, 7H), 2.89–2.25 (m, 2H), 1.97 (d, *J* = 12.0 Hz, 1H), 1.75 (d, *J* = 11.6 Hz, 2H), 1.57–1.53 (m, 1H), 1.45 (q, *J* = 10.8 Hz, 2H). LC/MS: 460⁺ [H⁺]. Purity: 99.0%.

N-(2-oxo-2-((1-(3-phenylcyclohexyl)piperidin-4-yl)amino)ethyl)-3-(trifluoromethyl)benzamide (**11**). Yield = 3%, ¹H NMR (400 MHz, CDCl₃) δ: 11.23 (s, 1H), 8.10 (s, 1H), 8.02 (d, *J* = 7.2 Hz, 1H), 7.75 (dd, *J*¹ = 8.0 Hz, *J*² = 7.6 Hz, 2H), 7.54 (t, *J* = 15.6 Hz, 1H), 7.34–7.12 (m, 4H), 7.20 (d, *J* = 4.8 Hz, 2H), 3.98 (s, 1H), 3.47 (d, *J* = 7.2 Hz, 1H), 3.35 (s, 1H), 3.15 (m, 1H), 2.92–2.86 (m, 4H), 2.56 (d, *J* = 11.6 Hz, 1H), 2.30–2.05 (m, 4H), 2.05–1.98 (m, 2H), 1.96–1.93 (m, 2H), 1.74 (t, *J* = 10.8 Hz, 1H), 1.65–1.60 (m, 1H). LC/MS: 488⁺ [H⁺]. Purity: 99.0%.

N-(2-oxo-2-((1-(4-(2-methoxyphenyl)cyclohexyl)piperidin-4-yl)amino)ethyl)-3-(trifluoromethyl)benzamide (**13**). The product was obtained with a yield of 13%. ¹H NMR (400 MHz, CDCl₃) δ: 8.15 (s, 1H), 8.05–8.00 (m, 2H), 7.74 (d, *J* = 7.6 Hz, 1H), 7.54 (t, *J* = 7.6 Hz, 1H), 7.17–7.07 (m, 3H), 6.91 (d, *J* = 7.6 Hz, 1H), 4.19 (d, *J* = 4.8 Hz, 2H), 3.82–3.80 (m, 1H), 3.02–2.79 (m, 3H), 2.47–2.36 (m, 1H), 2.33 (s, 3H), 2.25 (s, 1H), 2.07–1.95 (m, 5H), 1.89–1.79 (m, 2H), 1.57–1.47 (m, 6H). ¹³C NMR (400 MHz, CDCl₃) δ: 168.4, 166.5,

145.7, 144.8, 135.3, 134.4, 131.2, 130.4, 129.3, 128.5, 126.2, 125.7, 125.2, 124.5, 122.4, 63.6, 58.0, 48.9, 47.9, 47.4, 44.2, 39.8, 32.7, 29.2, 27.5, 19.5. LC/MS: 502⁺ [H⁺]. Purity: 95.3%.

N-(2-oxo-2-((1-(4-(3-methyl-phenyl)cyclohexyl)piperidin-4-yl)amino)ethyl)-3-(trifluoromethyl)benzamide (**14**). The product was obtained with a yield of 12%. ¹H NMR (400 MHz, CDCl₃) δ: 8.13 (s, 1H), 8.03 (d, *J* = 7.6 Hz, 1H), 7.96 (d, *J* = 4.8 Hz, 1H), 7.74 (d, *J* = 7.6 Hz, 1H), 7.54 (t, *J* = 8.0 Hz, 1H), 7.18 (t, *J* = 8.0 Hz, 1H), 7.07 (s, 1H), 6.99 (d, *J* = 9.6 Hz, 2H), 6.92 (d, *J* = 8.0 Hz, ½H^a), 6.85 (d, *J* = 7.6 Hz, ½H^b), 4.16 (d, *J* = 4.8 Hz, 2H), 3.90–3.70 (m, 1H), 2.96–2.88 (m, 2H), 2.66–2.62 (m, 1H), 2.44–2.26 (m, 5H), 2.11–2.05 (m, 1H), 2.00–1.85 (m, 6H), 1.62–1.35 (m, 6H). ¹³C NMR (400 MHz, CDCl₃) δ: 168.4, 166.5, 147.0, 137.9, 134.4, 131.1, 130.5, 129.3, 128.5, 128.3, 127.8, 125.1, 124.5, 124.1, 123.8, 63.5, 59.2, 48.7, 47.9, 47.4, 44.3, 44.1, 42.4, 33.7, 32.5, 28.7, 28.1, 21.6. LC/MS: 502⁺ [H⁺]. Purity: 98.6%.

N-(2-((1-(4-(2,6-dimethoxyphenyl)cyclohexyl)piperidin-4-yl)amino)-2-oxoethyl)-3-(trifluoromethyl)benzamide (**18**). The product was obtained with a yield of 30%. ¹H NMR (400 MHz, CDCl₃) δ: 8.15 (s, 1H), 8.05 (d, *J* = 7.6 Hz, 1H), 7.99 (s, 1H), 7.75 (d, *J* = 7.6 Hz, 1H), 7.55 (t, *J* = 7.6 Hz, 1H), 7.12–7.07 (m, 1H), 6.85 (s, 1H), 6.53 (d, *J* = 7.6 Hz, 2H), 4.18–4.13 (m, 2H), 3.83–3.78 (m, 1H), 3.77 (s, 6H), 3.32–3.26 (m, 1H), 3.02–2.96 (m, 2H), 2.46–2.36 (m, 2H), 2.26 (s, 1H), 2.15–1.93 (m, 6H), 1.66–1.53 (m, 2H), 1.49–1.39 (m, 2H), 1.25 (d, *J* = 6.8 Hz, 2H). ¹³C NMR (400 MHz, CDCl₃) δ: 168.4, 166.5, 158.8, 134.4, 131.1, 129.3, 128.5, 126.9, 125.1, 124.5, 123.8, 122.4, 104.8, 57.8, 55.9, 51.5, 47.5, 44.1, 40.5, 34.6, 33.9, 32.7, 32.0, 29.6, 29.0, 24.2. LC/MS: 548⁺ [H⁺]. Purity: 96.7%.

N-(2-((1-(4-(benzo[d][1,3]dioxol-5-yl)cyclohexyl)piperidin-4-yl)amino)-2-oxoethyl)-3-(trifluoromethyl)benzamide (**20**). The product was obtained with a yield of 24%. ¹H NMR (400 MHz, CDCl₃ + drop of MeOD) δ: 8.13 (s, 1H), 8.03 (d, *J* = 8.0 Hz, 1H), 7.77–7.73 (m, 2H), 7.56 (t, *J* = 8.0 Hz, 1H), 6.76–6.63 (m, 4H), 5.91 (s, 2H), 4.16 (d, *J* = 4.8 Hz, 2H), 3.84–3.76 (m, 1H), 2.93 (t, *J* = 12.4 Hz, 2H), 2.60 (s, 1H), 2.49–2.33 (m, 2H), 2.27 (s, 1H), 2.09 (t, *J* = 11.2 Hz, 1H), 1.98–1.84 (m, 6H), 1.60–1.44 (m, 4H), 1.42–1.38 (m, 2H). ¹³C NMR (400 MHz, CDCl₃ + drop of MeOD) δ: 168.2, 166.5, 147.6, 145.6, 141.1, 134.4, 131.3, 130.5, 129.3, 128.5, 124.5, 119.7, 108.2, 107.7, 107.3, 100.9, 63.5, 59.2, 48.7, 47.9, 47.3, 44.1, 42.3, 34.0, 32.4, 28.8, 28.0. LC/MS: 532⁺ [H⁺]. Purity: 95.5%.

N-(2-oxo-2-4-[(4-phenylcyclohexyl)amino]piperidin-1-ylethyl)-3-(trifluoromethyl)benzamide (**21**). Yield = 2%, ¹H NMR (400 MHz, MeOH-d₄) δ: 8.21 (s, 1H), 8.15 (d, *J* = 7.5 Hz, 1H), 7.88 (d, *J* = 7.6 Hz, 1H), 7.70 (t, *J* = 7.6 Hz, 1H), 7.30–7.16 (m, 5H), 4.69 (d, *J* = 13.6 Hz, 1H), 4.45 (d, *J* = 16.4 Hz, 1H), 4.21–4.15 (m, 2H), 3.65–3.58 (m, 1H), 3.52 (s, 2H), 3.39–3.36 (m, 1H), 3.26–3.23 (m, 1H), 2.79 (t, *J* = 12.4 Hz, 1H), 2.59 (t, *J* = 11.6 Hz, 1H), 2.28–2.15 (m, 4H), 2.04–2.01 (m, 2H), 1.73–1.49 (m, 6H). LC/MS: 488⁺ [H⁺]. Purity: 99.6%.

N-(2-oxo-2-((1-(1-phenyl-1*H*-1,2,3-triazol-4-yl)methyl)piperidin-4-yl)amino)ethyl)-3-(trifluoromethyl)benzamide (**12**). To a 50 mL round-bottom flask equipped with magnetic stirrer 0.72 mmol (1 equiv.) of iodobenzene, 0.8 mmol (1.1 equiv.) of *N*-(2-oxo-2-((1-(prop-2-yn-1-yl)piperidin-4-yl)amino)ethyl)-3-(trifluoromethyl)benzamide (**40**), 0.16 mmol (0.25 equiv.) of proline, 0.10 mmol (0.14 equiv.) of Na₂CO₃, 0.96 mmol (1.3 equiv.) of NaN₃ and 0.08 mmol (0.12 equiv.) of ascorbic acid were added and dissolved in a mixture of DMSO and H₂O (3:1). Then, 0.08 mmol (0.12 equiv.) of CuSO₄•5H₂O were added and the reaction was heated at 80 °C for 48h. The mixture was quenched with 3% NH₄OH, extracted 5 times with 10 mL EtOAc, washed with brine, dried over MgSO₄, filtered and concentrated *in vacuo*. Solids were recrystallized from a mixture of H₂O / Acetone = 1:1 and washed with petroleum ether. Yield = 4%. ¹H NMR (400 MHz, Acetone-d₆) δ: 8.43 (s, 1H), 8.23–8.20 (m, 2H), 7.92–7.90 (m, 2H), 7.76 (t, *J* = 7.6 Hz, 1H), 7.61 (t, *J* = 7.6 Hz, 1H), 7.48 (m, 1H), 7.47 (t, *J* = 7.2 Hz, 1H), 7.32 (d, *J* = 6.4 Hz, 1H), 4.04 (d, *J* = 5.2 Hz, 2H), 3.69 (s, 2H), 2.22 (t, *J* = 11.2 Hz, 2H) 2.16 (s, 1H), 2.14 (s, 1H), 1.95 (s, 1H), 1.85 (m, 2H), 1.54 (q, *J* = 8.4 Hz, 1H), 1.21 (d, *J* = 4.8 Hz, 2H). LC/MS: 487⁺ [H⁺]. Purity: 95.7%.

General procedure for the preparation compounds 15 and 17.

A round-bottom flask was loaded with 0.25 mmol (1 equiv.) of *N*-(2-oxo-2-(piperidin-4-ylamino)ethyl)-3-(trifluoromethyl)benzamide (**5**) and 0.25 mmol (1 equiv.) of the corresponding ketone. 40 mL of benzene together with 10 mol% *p*-toluenesulfonic acid and 4 Å MS were added. The reaction mixture was left to

reflux with a Dean-Stark setup for 48 hours. Then, to the cooled mixture 2.5 mmol (10 equiv.) sodium borohydride were added portionwise and the reaction was left to stir at room temperature for 24 h. The reaction mixture was quenched with 1M NaOH and extracted with DCM. The organic layer was washed with brine, dried over MgSO_4 and evaporated. The product was purified by column chromatography (90:9:1 DCM:MeOH: NH_4OH).

N-(2-oxo-2-((1-(4-(*p*-tolyl)cyclohexyl)piperidin-4-yl)amino)ethyl)-3-(trifluoromethyl)benzamide (**15**). The product was obtained with a yield of 10%. ^1H NMR (400 MHz, CDCl_3 + drop of MeOD) δ : 8.10 (s, 1H), 8.02 (s, 1H), 7.90 (s, 1H), 7.70 (d, $J = 7.2$ Hz, 1H), 7.53–7.52 (m, 1H), 7.17–7.02 (m, 4H), 4.09 (s, 2H), 3.94 (s, 1H), 3.47–3.21 (m, 3H), 2.98 (s, 1H), 2.84 (s, 2H), 2.46–2.40 (m, 1H), 2.31 (m, 4H), 2.17 (s, 1H), 2.09–2.01 (m, 4H), 1.85–1.78 (m, 2H), 1.70–1.51 (m, 3H). ^{13}C NMR (400 MHz, CDCl_3 + drop of MeOD) δ : 141.9, 139.3, 136.3, 135.8, 134.6, 130.9, 130.7, 129.4, 128.4, 127.0, 126.6, 125.2, 124.5, 122.5, 65.5, 48.5, 44.8, 43.5, 42.7, 36.0, 32.5, 28.6, 26.9, 22.9, 21.1. LC/MS: 502^+ [H^+]. Purity: 98.9%.

N-(2-((1-(4-(3,5-dimethoxyphenyl)cyclohexyl)piperidin-4-yl)amino)-2-oxoethyl)-3-(trifluoromethyl)benzamide (**17**). The product was obtained with a yield of 2%. ^1H NMR (400 MHz, CDCl_3 + drop of MeOD) δ : 8.10 (s, 1H), 8.02 (d, $J = 7.6$ Hz, 1H), 7.77 (d, $J = 8.0$ Hz, 1H), 7.58 (t, $J = 8.0$ Hz, 1H), 7.30 (s, 1H), 7.17 (d, $J = 7.6$ Hz, 1H), 6.44 (d, $J = 2.0$ Hz, 1H), 6.32 (d, $J = 2.4$ Hz, 1H), 4.12 (t, $J = 5.2$ Hz, 2H), 4.05–3.97 (m, 1H), 3.78 (s, 6H), 3.55 (d, $J = 10.4$ Hz, 1H), 3.43 (d, $J = 12.0$ Hz, 1H), 3.25 (t, $J = 10.4$ Hz, 1H), 2.99 (s, 1H), 2.92 (s, 2H), 2.38 (d, $J = 12.0$ Hz, 2H), 2.25–2.02 (m, 5H), 1.94–1.85 (m, 2H), 1.69–1.56 (m, 1H). ^{13}C NMR (400 MHz, CDCl_3 + drop of MeOD) δ : 161.3, 144.8, 134.6, 130.6, 129.4, 124.5, 105.8, 105.0, 97.5, 65.5, 55.4, 48.6, 44.6, 43.5, 28.5, 22.9. LC/MS: 548^+ [H^+]. Purity: 97.7%.

Synthesis of 4-methyl-N'-(1,4-dioxaspiro[4.5]decan-8-ylidene)benzenesulfonohydrazone (23). In a microwave tube 3.2 mmol (1 equiv.) of 1,4-dioxaspiro[4.5]decan-8-one (**22**) was dissolved in 5 mL of dioxane and 3.5 mmol (1.1 equiv.) of tosylhydrazide was added. The reaction mixture was heated at 130 °C in the microwave for 1 h. Product crystallized upon cooling and was collected by filtration. Yield = 65%. ^1H NMR (CDCl_3) δ : 7.84 (d, $J = 7.6$ Hz, 2H), 7.61 (s, 1H), 7.31 (d, $J = 7.6$ Hz, 2H), 3.95 (s, 4H), 2.44–2.32 (m, 7H), 1.82–1.71 (m, 4H).

Synthesis of 8-(3-methoxyphenyl)-1,4-dioxaspiro[4.5]dec-7-ene (24). In a 20 mL microwave tube 2.0 mmol (1 equiv.) of 4-methyl-*N'*-(1,4-dioxaspiro[4.5]decan-8-ylidene)benzenesulfonohydrazone (**23**) is dissolved in 7 mL of dioxane and flushed with nitrogen gas. Next, 2 mol% of $\text{Pd}_2(\text{dba})_3$, 4 mol% of 2-dicyclohexylphosphino-2',4',6'-triisopropylbiphenyl (Xphos) and 2.8 equivalents of 1 M $\text{Li}^t\text{-BuO}$ in hexanes were added. The reaction mixture was stirred for 1 minute and 2.2 mmol (1.1 equiv.) of 3-bromoanisole was added. Reaction mixture was heated at 110 °C in the microwave for 24 h. Reaction mixture was quenched with saturated solution of NaHCO_3 in water and extracted with DCM. The organic layer was washed with brine and dried over MgSO_4 . The product was purified by column chromatography (2:8 EtOAc/DCM). Yield = 24%. ^1H NMR (CDCl_3) δ : 7.21 (t, $J = 8$ Hz, 1H), 6.98 (d, $J = 7.6$ Hz, 1H), 6.93 (s, 1H), 6.77 (d, $J = 8.4$ Hz, 1H), 5.98 (s, 1H), 4.01 (s, 4H), 3.80 (s, 3H), 2.65 (br s, 2H), 2.46 (br s, 2H), 1.91 (t, $J = 6.4$ Hz, 2H).

1,4-dioxaspiro[4.5]dec-7-en-8-yl trifluoromethanesulfonate (25). An oven-dried round-bottom flask was flushed with N_2 gas and filled with 5 mL of dry THF. 3.9 mmol (1.3 equiv.) of 2 M solution of LDA in ethylbenzene was added. The reaction mixture was cooled to -78 °C. 3 mmol (1 equiv.) of ketone **22** was dissolved in 10 mL of dry THF and slowly added to the reaction mixture. The reaction mixture was stirred for 1 hour at -78 °C, half an hour at -25 °C and then cooled again to -78 °C. Next, 3.9 mmol (1.3 equiv.) of the *N*-phenyl-bis(trifluoromethanesulfonimide) was added to the reaction and the mixture was stirred for 4 hours at -78 °C after which it was stirred at room temperature overnight. The reaction mixture was quenched with H_2O and extracted with EtOAc. The organic layer was washed with brine (3x) and dried over MgSO_4 . The product was purified by column chromatography (1:4 diethylether / petroleum ether). Yield = 80%. ^1H NMR (400 MHz, CDCl_3) δ : 6.20 (t, $J = 4.2$ Hz, 1H), 4.04 (s, 4H), 2.81–2.75 (m, 1H), 2.48 (d, $J = 7.6$ Hz, 2H), 1.90 (t, $J = 6.4$ Hz, 2H).

4,4,5,5-tetramethyl-2-(1,4-dioxaspiro[4.5]dec-7-en-8-yl)-1,3,2-dioxaborolane (26). In a round-bottom flask 1.1 mmol (1.1 equiv.) of bis(pinacolato)diboron was dissolved in 50 mL of toluene and PdCl₂(PPh₃)₂ (0.03 equiv), triphenylphosphine (0.06 equiv) and potassium phenolate (1.5 equiv) were added. The reaction mixture was flushed with N₂ gas and 1 mmol (1 equiv.) of triflate **25** was added. The mixture was stirred at 50 °C under a nitrogen atmosphere. After 4 hours the heat source was removed and the reaction was stirred for 24 hours at room temperature. The reaction mixture was partitioned between H₂O/EtOAc and the organic layer was washed with brine and dried over MgSO₄. Column chromatography was performed using a gradient of 0-10% EtOAc in DCM as eluent. Yield = 59%. ¹H NMR (400 MHz, CDCl₃) δ: 6.47 (s, 1H), 3.98 (s, 4H), 2.39–2.36 (m, 4H), 1.73 (t, *J* = 6.4 Hz, 2H), 1.25 (s, 12H). ¹³C NMR (100 MHz, CDCl₃) δ: 139.7, 108.0, 83.4, 64.5, 37.2, 31.2, 25.9, 25.0.

Synthesis of 8-(2H-1,3-benzodioxol-5-yl)-1,4-dioxaspiro[4.5]dec-7-ene (27). 0.7 mmol (1 equiv.) of triflate **25** was dissolved in 10 mL of dry THF. To the reaction mixture 0.77 mmol (1.1 equiv.) of 3,4-(methylenedioxy)phenylboronic acid, 2.31 mmol (3.3 equiv.) of potassium fluoride and 10 mol% of Pd(dppf)Cl₂ were added. The reaction mixture was stirred at room temperature overnight. Next, the reaction mixture was filtered over celite and purified with column chromatography (DCM). Yield = 58%. ¹H NMR δ: (CDCl₃): 6.89 (s, 1H), 6.85 (d, *J* = 8.0 Hz, 1H), 6.73 (d, *J* = 8.0 Hz, 1H), 5.93 (s, 2H), 5.86 (t, *J* = 4.0 Hz, 1H), 4.01 (s, 4H), 2.60 (br s, 2H), 2.44 (s, 2H), 1.90 (t, *J* = 6.4 Hz, 2H).

General procedure for the synthesis of compounds 28-32.

In a 20 mL microwave tube 0.75 mmol (1 equiv.) of the boron ester **26** was dissolved in 10 mL of dioxane and 5 mol% of Pd(PPh₃)₄ was added along with 0.75 mmol (1 equiv.) of the corresponding arylbromide. Next, 8 equivalents of 2 M Na₂CO₃ in H₂O solution was added and the reaction mixture was flushed with N₂ gas and capped. The reaction mixture was heated in the microwave for 10 hours at 80 °C. Upon completion, the reaction mixture was partitioned between DCM/H₂O and the organic layer was dried over MgSO₄. Column chromatography was performed with DCM as eluent.

8-(2-methyl-phenyl)-1,4-dioxaspiro[4.5]dec-7-ene (28). Yield = 90%, ¹H NMR (CDCl₃) δ: 7.16–7.06 (m, 4H), 5.44 (s, 1H), 4.01 (s, 4H), 2.45 (br s, 4H), 2.29 (s, 3H), 1.89 (t, *J* = 7.2 Hz, 2H).

8-(3-methyl-phenyl)-1,4-dioxaspiro[4.5]dec-7-ene (29). Yield = 99%, ¹H NMR (CDCl₃) δ: 7.23–7.16 (m, 3H), 7.03 (br s, 1H), 5.95 (s, 1H), 4.00 (s, 4H), 2.65 (br s, 2H), 2.46 (br s, 2H), 2.33 (s, 3H), 1.91 (t, *J* = 6.4 Hz, 2H).

8-(4-methyl-phenyl)-1,4-dioxaspiro[4.5]dec-7-ene (30). Yield = 84%, ¹H NMR (CDCl₃) δ: 7.26 (d, *J* = 6.8 Hz, 2H), 7.10 (d, *J* = 6.8 Hz, 2H), 5.94 (s, 1H), 4.02 (s, 4H), 2.64 (br s, 2H), 2.46 (br s, 2H), 2.33 (s, 3H), 1.92 (t, *J* = 6.4 Hz, 2H).

8-(3,5-dimethoxyphenyl)-1,4-dioxaspiro[4.5]dec-7-ene (31). Yield = 80%, ¹H NMR (CDCl₃) δ: 6.54 (d, *J* = 2 Hz, 2H), 6.35 (t, *J* = 2.2 Hz, 1H), 5.97 (t, *J* = 4.0 Hz, 1H), 4.01 (s, 4H), 3.78 (s, 6H), 2.63 (br s, 2H), 2.46 (br s, 2H), 1.92 (t, *J* = 6.4 Hz, 2H).

8-(2,6-dimethoxyphenyl)-1,4-dioxaspiro[4.5]dec-7-ene (32). Yield = 90%, ¹H NMR (CDCl₃) δ: 7.15 (t, *J* = 8.4 Hz, 1H), 6.54 (d, *J* = 8.4 Hz, 2H), 5.47 (s, 1H), 4.01 (s, 4H), 3.78 (s, 6H), 2.47–2.40 (m, 4H), 1.90 (t, *J* = 6.4 Hz, 2H).

General procedure for the hydrogenation of the double bond of compounds 24, 27-32.

A round-bottom flask was purged with hydrogen gas and the corresponding cyclohexene was added. 4 wt% of Pd/C (10% wt) was added together with 2 mol% Pd(OAc)₂ and MeOH was added and hydrogen balloon. The reaction mixture was flushed with hydrogen and stirred overnight under hydrogen atmosphere. When the reaction was finished, the reaction mixture was filtered through celite. Column chromatography was performed if necessary, using 100% DCM as eluent. The obtained yields were 85-99%. All products showed correct mass in TLC/MS.

General procedure for the synthesis of compounds 33-39. To a round-bottom flask was added 1 equivalent of the corresponding acetal. Mixture of DCM and acetone (4:1) was added. Finally 3.5 equivalents of FeCl₃·6H₂O were added and the reaction mixture was stirred at room temperature for 3.5

hours. The reaction mixture was quenched with saturated aqueous NaHCO₃ and extracted with DCM, the organic layer was washed with brine and dried over MgSO₄. The product was purified by column chromatography (DCM).

4-(2-methylphenyl)cyclohexan-1-one (33). This compound was obtained in 99% yield. ¹H NMR (400 MHz, CDCl₃) δ: 7.25–7.10 (m, 4H), 3.26–3.19 (m, 1H), 2.58–2.50 (m, 4H), 2.41 (s, 3H), 2.17–2.13 (m, 2H), 1.97–1.79 (m, 2H). ¹³C NMR (100 MHz, CDCl₃) δ: 211.2, 142.9, 135.2, 130.6, 126.5, 125.0, 41.8, 38.5, 33.2, 19.5.

4-(3-methylphenyl)cyclohexan-1-one (34). This compound was obtained in 99% yield. ¹H NMR (400 MHz, CDCl₃) δ: 7.25–7.19 (m, 1H), 7.04 (d, *J* = 8.0 Hz, 3H), 3.02–2.94 (m, 1H), 2.55–2.47 (m, 4H), 2.32 (s, 3H), 2.22–2.17 (m, 2H), 2.17–1.88 (m, 2H). ¹³C NMR (100 MHz, CDCl₃) δ: 211.3, 144.9, 138.2, 128.6, 127.5, 123.8, 42.8, 41.5, 34.1, 21.5.

4-(4-methylphenyl)cyclohexan-1-one (35). This compound was obtained in 90% yield. ¹H NMR (400 MHz, CDCl₃) δ: 7.18 (s, 4H), 3.08–3.00 (m, 1H), 2.60–2.50 (m, 4H), 2.36 (s, 3H), 2.26–2.21 (m, 2H), 2.02–1.96 (m, 2H). ¹³C NMR (100 MHz, CDCl₃) δ: 211.3, 141.9, 136.2, 129.1, 126.6, 42.4, 41.5, 34.1, 21.1.

4-(3-methoxyphenyl)cyclohexan-1-one (36). This compound was obtained in 95% yield. ¹H NMR (400 MHz, CDCl₃) δ: 7.27–7.23 (m, 1H), 6.84 (d, *J* = 7.6 Hz, 1H), 6.77 (s, 1H), 6.78 (s, 1H), 3.80 (s, 3H), 3.04–2.97 (m, 1H), 2.53–2.49 (m, 4H), 2.25–2.20 (m, 2H), 1.11–1.88 (m, 2H).

4-(3,5-dimethoxyphenyl)cyclohexan-1-one (37). This compound was obtained in 98% yield. ¹H NMR (400 MHz, CDCl₃) δ: 6.40 (s, 2H), 6.34 (s, 1H), 3.78 (s, 6H), 2.99–2.93 (m, 1H), 2.51 (d, *J* = 4.4 Hz, 2H), 2.47 (d, *J* = 4.4 Hz, 2H), 2.23–2.20 (m, 2H), 1.98–1.93 (m, 2H). ¹³C NMR (100 MHz, CDCl₃) δ: 211.2, 161.0, 147.4, 105.1, 98.2, 55.4, 43.2, 41.4, 33.9.

4-(2,6-dimethoxyphenyl)cyclohexan-1-one (38). This product was obtained in 42% yield. ¹H NMR (400 MHz, CDCl₃) δ: 7.25–7.08 (m, 1H), 6.53 (q, *J* = 6.0 Hz, 2H), 3.80 (s, 6H), 2.57–2.47 (m, 5H), 1.91–1.87 (m, 2H), 1.80–1.65 (m, 2H). ¹³C NMR (100 MHz, CDCl₃) δ: 213.2, 158.6, 127.4, 126.9, 120.5, 109.1, 104.4, 55.8, 42.1, 35.8, 33.9, 29.7, 27.3.

4-(2H-1,3-benzodioxol-5-yl)cyclohexan-1-one (39). This product was obtained in 87% yield. ¹H NMR (400 MHz, CDCl₃) δ: 6.77–6.69 (m, 3H), 5.91 (s, 2H), 2.99–2.92 (m, 1H), 2.54–2.47 (m, 4H), 2.20–2.16 (m, 2H), 1.93–1.82 (m, 2H). ¹³C NMR (100 MHz, CDCl₃) δ: 211.2, 147.9, 146.2, 138.9, 119.6, 108.4, 107.2, 101.0, 42.7, 41.4, 34.3.

***N*-(2-oxo-2-((1-(prop-2-yn-1-yl)piperidin-4-yl)amino)ethyl)-3-(trifluoromethyl)benzamide (40).** In a 50 mL round-bottom flask 1.1 mmol (1.1 equiv.) of *N*-(2-oxo-2-(piperidin-4-ylamino)ethyl)-3-(trifluoromethyl)benzamide (**5**) was dissolved in 15 mL of acetone. Subsequently, 1.1 mmol (1.1 equiv.) of K₂CO₃ and 1 mmol (1 equiv.) of propargyl bromide were added. The mixture was refluxed overnight. The product precipitated from the reaction mixture and was collected by filtration. Yield = 99%. ¹H NMR (400 MHz, CDCl₃) δ: 8.21–8.18 (m, 2H), 7.76 (d, *J* = 8.0 Hz, 1H), 7.61–7.57 (m, 1H), 4.71 (s, 2H), 4.54 (s, 2H), 4.19–4.15 (m, 3H), 3.98–3.95 (m, 2H), 3.83–3.81 (m, 2H), 3.07 (s, 2H), 1.26 (s, 1H).

Abbreviations

AcOH, acetic acid; Boc, *tert*-butyloxycarbonyl; CCL2, chemokine ligand 2; CCR2, chemokine receptor 2; DCE, dichloroethane; DCM, dichloromethane; DiPEA, *N,N*-diisopropylethylamine; DMAP, *N,N*-dimethylaminopyridine; DMSO, dimethylsulfoxide; INCB3344, *N*-(2-((3S,4S)-1-(4-(benzo[d][1,3]dioxol-5-yl)-4-hydroxycyclohexyl)-4-ethoxypropylidino-3-yl)amino)-2-oxoethyl)-3-(trifluoromethyl)benzamide; JNJ Lead, *N*-(2-((1-(1*R*,4*R*)-4-(3-(dimethylamino)phenyl)-4-hydroxycyclohexyl)azetidino-3-yl)amino)-2-oxoethyl)-3-(trifluoromethyl)benzamide; KO, knock-out; KOPh, potassium phenolate; LDA, lithium diisopropylamide; Li^t-BuO, lithium *tert*-butoxide; MeOH, methanol; MW, microwave; MS, molecular sieves; Pd₂(dba)₃, tris(dibenzylideneacetone)dipalladium(0); Pd(dppf)Cl₂, [1,1'-bis(diphenylphosphino)ferrocene]dichloropalladium(II), complex with dichloromethane; Pd(OAc)₂, palladium acetate; Pd(PPh₃)₄, tetrakis(triphenylphosphine)palladium(0); PEMB, 5-ethyl-2-methyl-

pyridine borane; PPh₃, triphenylphosphine; PyBrOP, bromo-tris-pyrrolidino phosphoniumhexafluorophosphate; SAR, structure–affinity relationships; TFA, trifluoroacetic acid; THF, tetrahydrofuran; U2OS, Human Bone Osteosarcoma Cells; XPhos, 2-dicyclohexylphosphino-2',4',6'-triisopropylbiphenyl.

ACKNOWLEDGEMENTS

This study was financially supported by the Dutch Top Institute Pharma, project number D1-301. We thank Dr. Julien Louvel and Jacobus van Veldhoven for their input in analytical data analysis. We acknowledge Prof. Dr. Martine Smit (Vrije Universiteit, Amsterdam, The Netherlands) for helpful comments and suggestions.

REFERENCES

1. Deshmane, S. L.; Kremlev, S.; Amini, S.; Sawaya, B. E. Monocyte Chemoattractant Protein-1 (MCP-1): An Overview. *Journal of Interferon and Cytokine Research* **2009**, *29*, 313-326.
2. Daly, C.; Rollins, B. J. Monocyte chemoattractant protein-1 (CCL2) in inflammatory disease and adaptive immunity: therapeutic opportunities and controversies. *Microcirculation* **2003**, *10*, 247-57.
3. Dawson, T. C.; Kuziel, W. A.; Osahar, T. A.; Maeda, N. Absence of CC chemokine receptor-2 reduces atherosclerosis in apolipoprotein E-deficient mice. *Atherosclerosis* **1999**, *143*, 205-11.
4. Kamei, N.; Tobe, K.; Suzuki, R.; Ohsugi, M.; Watanabe, T.; Kubota, N.; Ohtsuka-Kowatari, N.; Kumagai, K.; Sakamoto, K.; Kobayashi, M.; Yamauchi, T.; Ueki, K.; Oishi, Y.; Nishimura, S.; Manabe, I.; Hashimoto, H.; Ohnishi, Y.; Ogata, H.; Tokuyama, K.; Tsunoda, M.; Ide, T.; Murakami, K.; Nagai, R.; Kadowaki, T. Overexpression of monocyte chemoattractant protein-1 in adipose tissues causes macrophage recruitment and insulin resistance. *Journal of Biological Chemistry* **2006**, *281*, 26602-26614.
5. Fife, B. T.; Huffnagle, G. B.; Kuziel, W. A.; Karpus, W. J. CC chemokine receptor 2 is critical for induction of experimental autoimmune encephalomyelitis. *The Journal of Experimental Medicine* **2000**, *192*, 899-905.
6. White, F. A.; Feldman, P.; Miller, R. J. Chemokine Signaling and the Management of Neuropathic Pain. *Molecular Interventions* **2009**, *9*, 188-195.
7. Kim, Y. K.; Oh, H. B.; Lee, E. Y.; Gho, Y. S.; Lee, J. E.; Kim, Y. Y. Association between a genetic variation of CC chemokine receptor-2 and atopic asthma. *Allergy* **2007**, *62*, 208-9.
8. Xia, M.; Sui, Z. Recent developments in CCR2 antagonists. *Expert Opinion on Therapeutic Patents* **2009**, *19*, 295-303.
9. Xia, M.; Hou, C.; DeMong, D. E.; Pollack, S. R.; Pan, M.; Brackley, J. A.; Jain, N.; Gerchak, C.; Singer, M.; Malaviya, R.; Matheis, M.; Olini, G.; Cavender, D.; Wachter, M. Synthesis, structure-activity relationship and in vivo antiinflammatory efficacy of substituted dipiperidines as CCR2 antagonists. *Journal of Medicinal Chemistry* **2007**, *50*, 5561-3.
10. Pease, J. E.; Horuk, R. Chemokine receptor antagonists: Part 1. *Expert Opinion on Therapeutic Patents* **2009**, *19*, 39-58.
11. Struthers, M.; Pasternak, A. CCR2 antagonists. *Current Topics in Medicinal Chemistry* **2010**, *10*, 1278-98.
12. Carter, P. H. Progress in the discovery of CC chemokine receptor 2 antagonists, 2009 - 2012. *Expert Opinion on Therapeutic Patents* **2013**, *23*, 549-68.
13. Ben-Zeev, E.; Chen, D.; Fichman, M.; Ghosh, S.; Koerner, S. i.; Marantz, Y.; Melendez, R.; Mohanty, P.; Shacham, S.; Zhang, Z. Carboxamide compounds and their use as antagonists of the chemokine ccr2 receptor. *Patent WO2009076404*, **2009**.
14. Moree, W. J.; Kataoka, K.; Ramirez-Weinhouse, M. M.; Shiota, T.; Imai, M.; Sudo, M.; Tsutsumi, T.; Endo, N.; Muroga, Y.; Hada, T.; Tanaka, H.; Morita, T.; Greene, J.; Barnum, D.; Saunders, J.; Kato, Y.; Myers, P. L.; Tarby, C. M. Small molecule antagonists of the CCR2b receptor. Part 2: Discovery process and initial structure-activity relationships of diamine derivatives. *Bioorganic & Medicinal Chemistry Letters* **2004**, *14*, 5413-5416.
15. Xue, C. B.; Wang, A.; Meloni, D.; Zhang, K.; Kong, L.; Feng, H.; Glenn, J.; Huang, T.; Zhang, Y.; Cao, G.; Anand, R.; Zheng, C.; Xia, M.; Han, Q.; Robinson, D. J.; Storace, L.; Shao, L.; Li, M.; Brodmerkel, C. M.; Covington, M.

- Scherle, P.; Diamond, S.; Yeleswaram, S.; Vaddi, K.; Newton, R.; Hollis, G.; Friedman, S.; Metcalf, B. Discovery of INCB3344, a potent, selective and orally bioavailable antagonist of human and murine CCR2. *Bioorganic & Medicinal Chemistry Letters* **2010**, *20*, 7473-8.
16. Zhang, X.; Hufnagel, H.; Markotan, T.; Lanter, J.; Cai, C.; Hou, C.; Singer, M.; Opas, E.; McKenney, S.; Crysler, C.; Johnson, D.; Sui, Z. Overcoming hERG activity in the discovery of a series of 4-azetidyl-1-aryl-cyclohexanes as CCR2 antagonists. *Bioorganic & Medicinal Chemistry Letters* **2011**, *21*, 5577-82.
17. Vilums, M.; Zweemer, A. J. M.; Yu, Z. Y.; de Vries, H.; Hillger, J. M.; Wapenaar, H.; Bollen, I. A. E.; Barmare, F.; Gross, R.; Clemens, J.; Krenitsky, P.; Brussee, J.; Stamos, D.; Saunders, J.; Heitman, L. H.; IJzerman, A. P. Structure-Kinetic Relationships-An Overlooked Parameter in Hit-to-Lead Optimization: A Case of Cyclopentylamines as Chemokine Receptor 2 Antagonists. *Journal of Medicinal Chemistry* **2013**, *56*, 7706-7714.
18. Frerot, E.; Coste, J.; Pantaloni, A.; Dufour, M. N.; Jouin, P. Pybop and Pybrop - 2 Reagents for the Difficult Coupling of the Alpha,Alpha-Dialkyl Amino-Acid, Aib. *Tetrahedron* **1991**, *47*, 259-270.
19. Barluenga, J.; Quinones, N.; Cabal, M. P.; Aznar, F.; Valdes, C. Tosylhydrazide-Promoted Palladium-Catalyzed Reaction of beta-Aminoketones with o-Dihaloarenes: Combining Organocatalysis and Transition-Metal Catalysis. *Angewandte Chemie-International Edition* **2011**, *50*, 2350-2353.
20. Feldman, A. K.; Colasson, B.; Fokin, V. V. One-pot synthesis of 1,4-disubstituted 1,2,3-triazoles from in situ generated azides. *Organic Letters* **2004**, *6*, 3897-3899.
21. Xue, C. B.; Feng, H.; Cao, G. F.; Huang, T. S.; Glenn, J.; Anand, R.; Meloni, D.; Zhang, K.; Kong, L. Q.; Wang, A. L.; Zhang, Y. X.; Zheng, C. S.; Xia, M.; Chen, L. H.; Tanaka, H.; Han, Q.; Robinson, D. J.; Modi, D.; Storace, L.; Shao, L. X.; Sharief, V.; Li, M.; Galya, L. G.; Covington, M.; Scherle, P.; Diamond, S.; Emm, T.; Yeleswaram, S.; Contel, N.; Vaddi, K.; Newton, R.; Hollis, G.; Friedman, S.; Metcalf, B. Discovery of INCB3284, a Potent, Selective, and Orally Bioavailable hCCR2 Antagonist. *Acs Medicinal Chemistry Letters* **2011**, *2*, 450-454.
22. Zhang, X. Q.; Hou, C. F.; Hufnagel, H.; Singer, M.; Opas, E.; McKenney, S.; Johnson, D.; Sui, Z. H. Discovery of a 4-Azetidyl-1-thiazoyl-cyclohexane CCR2 Antagonist as a Development Candidate. *Acs Medicinal Chemistry Letters* **2012**, *3*, 1039-1044.
23. Xue, C. B.; Wang, A. L.; Han, Q.; Zhang, Y. X.; Cao, G. F.; Feng, H.; Huang, T. S.; Zheng, C. S.; Xia, M.; Zhang, K.; Kong, L. Q.; Glenn, J.; Anand, R.; Meloni, D.; Robinson, D. J.; Shao, L. X.; Storace, L.; Li, M.; Hughes, R. O.; Devraj, R.; Morton, P. A.; Rogier, D. J.; Covington, M.; Scherle, P.; Diamond, S.; Emm, T.; Yeleswaram, S.; Contel, N.; Vaddi, K.; Newton, R.; Hollis, G.; Metcalf, B. Discovery of INCB8761/PF-4136309, a Potent, Selective, and Orally Bioavailable CCR2 Antagonist. *Acs Medicinal Chemistry Letters* **2011**, *2*, 913-918.

CHAPTER 7

CONCLUSIONS AND FUTURE PERSPECTIVES

Inhibition of the CC chemokine 2 receptor (CCR2), the subject of my thesis, is an attractive strategy to combat inflammatory conditions. Hence, the pharmaceutical industry, both smaller and bigger actors, has paid considerable attention to this and related chemokine receptors. Currently, there are more than 45 different chemical classes known as CCR2 antagonists. However, despite the big diversity of antagonists and all the efforts in (pre)clinical pharmacology in the CCR2 research field there are still no marketed drugs targeting this receptor. In fact, all clinical trials targeting CCR2 have failed to show efficacy, which would suggest that CCR2 is the “wrong” target. However, the research described in this thesis provides a better understanding of the small-molecule antagonist interactions with the CCR2 receptor and might help to improve the efficacy of CCR2 antagonists in the future, and to resurrect CCR2 as a potential target for the treatment of various inflammatory diseases.

DEVELOPMENT OF NEW CCR2 ANTAGONISTS

All small-molecule CCR2 antagonists can be divided into two distinct classes based on their binding site in the CCR2 receptor. The bulk of antagonists bind to the same orthosteric binding site located at the interface between transmembrane domains and extracellular side of the receptor, where they are directly competing with the endogenous ligand CCL2. Recently we discovered another (allosteric) binding site, which is located on the intracellular side of the receptor. Until now, only a few scaffolds are known to bind to this intracellular binding site (unpublished data).

PHARMACOPHORES OF CCR2 ANTAGONISTS

Despite the substantial chemical diversity in the structures of the antagonists, the majority of the orthosteric ligands correspond to the same pharmacophore (Figure 1). In the pharmacophore one of the general features is the presence of a basic nitrogen in the center of the molecule. Although Bristol-Meyers Squibb developed BMS22¹ – a high affinity CCR2 antagonist without basic nitrogen -, a subsequent incorporation of an additional amine yielded a strong boost in affinity.² This is also in accordance with mutagenesis studies, which

suggest that the nitrogen atom, positively charged at physiological pH, forms a salt-bridge interaction with the receptor's glutamic acid E291. Another crucial feature is an aromatic ring on one side of the molecule connected via an amide-containing linker to the central nitrogen atom.

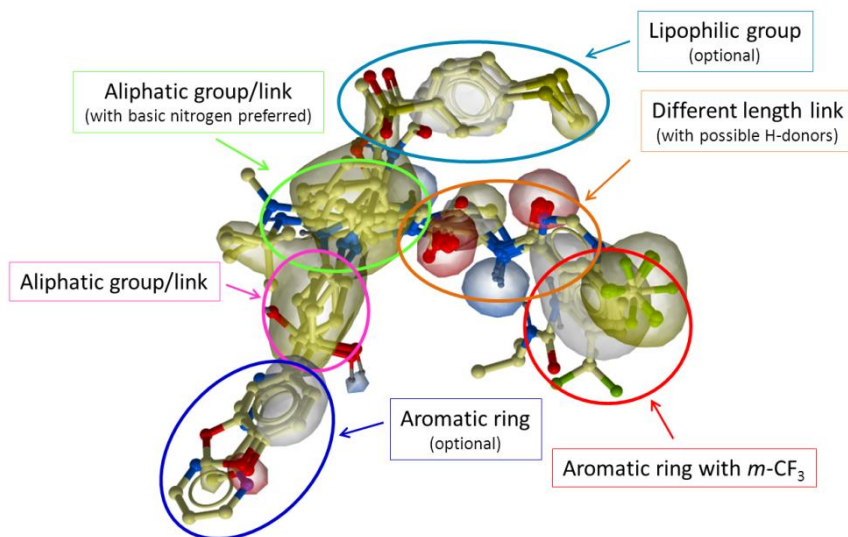


Figure 1. Pharmacophore based on superimposition of 7 CCR2 small-molecule antagonists. Important groups are indicated by the circles: aromatic ring with *m*-CF₃ group (red), amide containing linker (orange), aliphatic group/link with basic nitrogen (green), lipophilic group (light blue), aliphatic link (pink) between basic nitrogen and aromatic ring (blue).

Usually this aromatic ring is furnished with lipophilic, electron-withdrawing groups (preferentially CF₃) on the *meta* position. Interestingly, in the case of cyclopentylamines in the center of the molecule (see also **chapter 3**) any attempt to alter the location or characteristics of the substituent on this aromatic ring completely abolished affinity (unpublished data). The other side of the molecule is more versatile and can bear a wide range of different substituents as long as they fit the pharmacophore. Nevertheless, several criteria should be met before reasonable affinities can be achieved. This was evaluated in more detail with a piperidinediamide scaffold (**chapter 6**). This moiety is based on both pyrrolidine and azetidine scaffolds^{3, 4} by expanding the central aliphatic ring to piperidine. Despite that this scaffold still

fits the pharmacophore, substituents that were very well tolerated in the pyrrolidine series⁵ caused a complete loss of affinity. After extensive SAR studies it was concluded that, similarly to the azetidine series, a 4-aryl-cyclohexyl group is the preferred substituent for this scaffold.

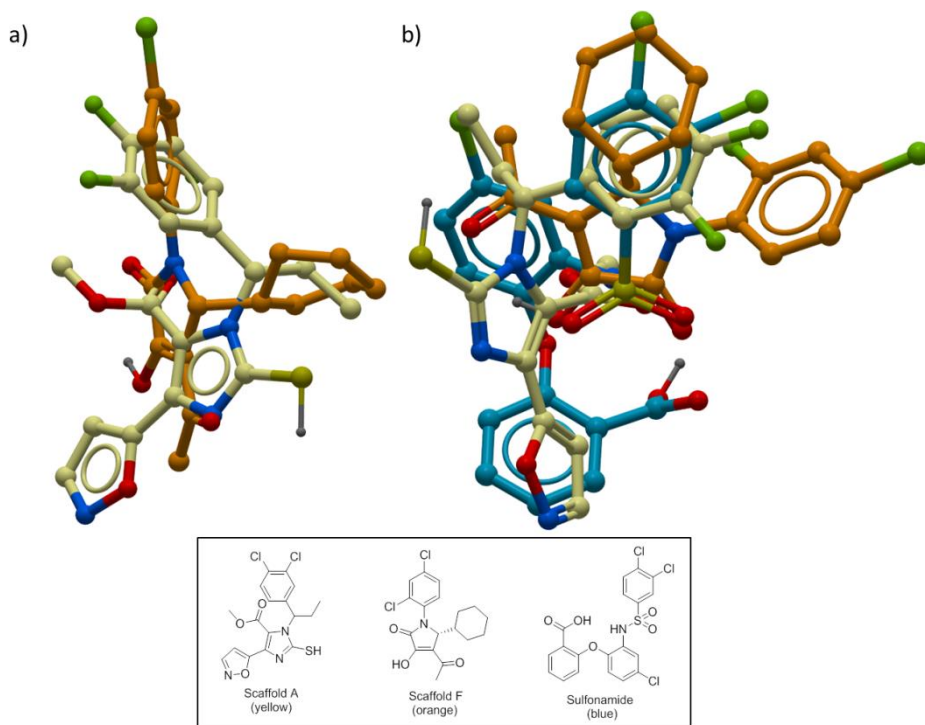


Figure 2. a) superimposition of allosteric CCR2 antagonists: Scaffold A (yellow) and Scaffold F (orange), which did not yield high affinity compounds; b) superimposition of docking poses (based on mutagenesis studies) of allosteric CCR2 antagonists: Scaffold A (yellow), Scaffold F (orange) and Sulfonamide (blue).

Structures of the allosteric (intracellular) binders (Scaffold A and Scaffold F) are similar and can be superimposed to generate another pharmacophore (Figure 2a). However, the new scaffolds (Figure 3) that were designed based on such a pharmacophore failed to yield compounds with better affinity than 10 μ M towards the CCR2 receptor (unpublished data).

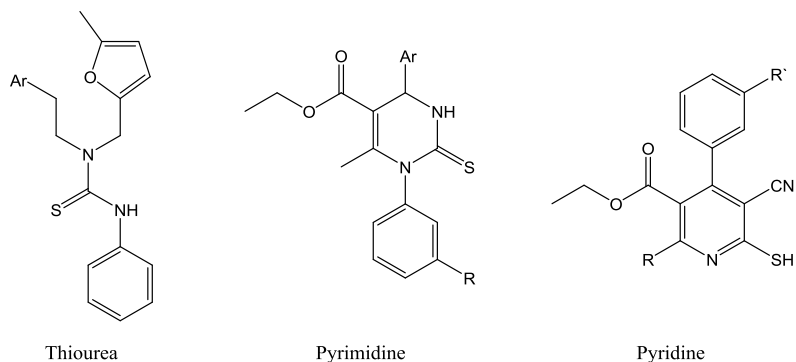


Figure 3. New core structures (thiourea, pyrimidine and pyridine) designed based on superimposition of scaffolds A and F (Figure 2a).

These failures suggested that there must be differences between the binding modes of the known allosteric antagonists. Later mutagenesis studies showed that, despite the structural similarity of the ligands (scaffold A and F), they only partially overlap in the binding site and this was also proposed by further docking studies (Figure 2b). To generate a valid pharmacophore of the allosteric binders I would suggest combining the knowledge of mutagenesis and docking studies with the SAR studies performed on known allosteric antagonists (Figure 2b). This could potentially reveal unexplored sub-pockets for interaction in the allosteric binding site and generate new CCR2 antagonists.

STRUCTURE-AFFINITY RELATIONSHIPS AND/OR STRUCTURE-KINETICS RELATIONSHIPS

Despite the big diversity and substantial amount of already known CCR2 antagonists and irrespective of all failures in clinical trials targeting CCR2, the same pharmaceutical companies file further patents almost on a yearly basis disclosing new chemical entities as potential drugs for the treatment of CCR2-related diseases.⁶ Apparently, the general idea of “*if something doesn't work, try something else*” also applies to drug discovery and development. Apparently it is tempting to generate huge amounts of structurally diverse compounds and to hope that one will eventually have the necessary properties in one compound to become an efficacious treatment. However, a more elaborate reevaluation of known hits may reveal important factors that were previously overlooked. Until now, the development of CCR2

antagonists has been based primarily on improving CCR2 affinity but it failed to yield efficacious medication. As described in the introduction of this thesis, for a CCR2 antagonist to exert its effect it should block its target for as long as possible. To be able to do this, first it needs to bind to the target (good affinity) and second it must stay bound to the target (long residence time) thus continuing to block it. In this thesis I describe the first attempts to use both properties (affinity and residence time) for the design of new high affinity and long residence time CCR2 antagonists. **Chapter 3** is a reflection of how the combined knowledge of structure-affinity relationships (SAR) and the drug-target residence time, which can be analyzed as structure-kinetics relationships (SKR), helped to reinvigorate a chemical structure that was previously discarded by other scientists due to its moderate affinity for the CCR2 receptor.^{7, 8} Based on this structure, we designed and synthesized high affinity and long residence time antagonists. **Chapter 4** reports the follow-up on these structures and defines more detailed SAR and SKR through interrogation of the binding site of the CCR2 receptor by applying small changes to the ligand molecule in a step-by-step manner.⁹ As I see it, this approach can already be utilized at the very beginning of the drug discovery cycle thus potentially improving the success rate of drug candidates while decreasing the expenses for the development of new drugs.

However, it will take time before principle of binding kinetics advocated in this thesis will become part of routine tests in early drug discovery. Until now, a possible correlation of binding kinetics with the efficacy of a drug has been shown only in hindsight. I hope the work described in this thesis and similar research will form the basis for the pharmaceutical industry to use binding kinetics in a more prospective manner. A next step would be to test the long residence time compounds in *in vivo* models and compare their efficacy with structurally similar high affinity, but short residence time CCR2 antagonists. Maybe the best choice for *in vivo* tests would be one of the derivatives of MK-0483 described in **chapter 5**. MK-0483 itself, stemming from the Merck Research Laboratories, is a high affinity dual CCR2/CCR5 antagonist and was developed as a potential clinical candidate with a good PK/PD profile and very slow binding kinetics at CCR2.¹⁰ Despite the excellent properties of this compound, Merck decided to continue clinical trials with MK-0812 (thought to have fast

kinetics) while MK-0483 was kept as a backup candidate.¹¹ After the clinical failure of MK-0812 mentioned previously, the long residence time CCR2 antagonist MK-0483 never got a chance to enter clinical trials. However, if Merck would restore the CCR2 program in their pipeline, the best option for proof-of-concept would be to use MK-0483, due to its long residence time and dual antagonism (the value of dual antagonism will be discussed later).

SPECIFICITY, DUAL ANTAGONISM OR FUNCTIONAL SELECTIVITY – WHAT DO WE NEED?

To develop a new drug and get it to the market as an effective treatment, it must fulfill many requirements, one of which is being selective to avoid potential adverse effects via off-target binding. Usually, during the early stages of the drug discovery process, a counterscreen against a panel of different off-targets is used to determine the selectivity of a lead compound before advancing it into *in vivo* studies. However, in some cases, lack of selectivity over some targets can be tolerated or it can even be beneficial. Orthosteric CCR2 antagonists often have affinity for the CCR5 receptor too and are called dual antagonists, like the above-mentioned MK-0483. According to Pasternak et al.¹⁰ it is unlikely that CCR5 blockade is a treatment liability for CCR2-related diseases. Zhao et al.¹² even suggested that BMS-A (a dual CCR2/CCR5 antagonist) offers a novel oral therapy for the treatment of autoimmune diseases. Additionally, CCR2/CCR5 dual inhibition could be beneficial in the treatment of Crohn's disease and atherosclerosis.¹³ However, in the case of rheumatoid arthritis (RA), Lebre et al. recently described that even dual antagonism of CCR2/CCR5 does not prevent monocyte migration when induced by synovial fluid (taken from RA patients), which contains many different chemokines.¹⁴ Only the blockade of the CCR1 receptor in this assay resulted in inhibition of chemotaxis; however, CCR1 antagonists failed to show effect in clinical trials.¹⁵ Apparently, the chemokine system in RA pathology is very versatile and one could argue that selective inhibition is doomed for failure as described above. To tackle this multi-level system, one should combine the separate benefits (observed in numerous *in vitro* studies) of the inhibition of CCR1, CCR2 and CCR5 in one treatment. This could potentially be achieved by a combination of an allosteric dual CCR1/CCR2 antagonist (such as the sulfonamide in Figure

2b)¹⁶ with an orthosteric dual CCR2/CCR5 antagonist (e.g., MK-0483). Moreover, in radioligand binding studies it was observed that allosteric and orthosteric CCR2 antagonists enhance each other's binding.¹⁷ Another possibility would be to develop an "all-in-one" antagonist, which most probably would be an allosteric binder as the intracellular binding site is more conserved between the different chemokine receptors. A good starting point could be the sulfonamide core (Figure 2b), which already has high affinity for CCR1/2 and sub-micromolar affinity for CCR4/5 receptors.¹⁶

Another peculiarity that should be taken into account when developing drugs that target the chemokine system is its intricate complexity. For example, the CCR2 receptor can be activated by multiple chemokines (e.g. CCL2, CCL7, CCL8, CCL11 and CCL13), while all these chemokines, except CCL2, can bind to multiple other chemokine receptors. Moreover, such receptor-ligand interchangeability is observed between almost all chemokine receptors and their ligands, rendering the whole chemokine system promiscuous. However, the distinct tissue expression of different chemokines points out that they are part of specific and fine-tuned immune system.¹⁸ For example, the CCL2/CCR2 axis is important for monocyte migration from the bone marrow to the blood under normal homeostatic conditions. During inflammation, however, also CCL7, next to CCL2, plays an essential role in monocyte recruitment to the inflamed tissue.¹⁹ Additionally, Berchiche et al. reported that CCR2 shows a degree of biased signaling when activated by different chemokines.²⁰ Although not entirely understood, this intricacy of the chemokine system must be taken into consideration when developing new ligands. For instance, lead compounds should not only be tested against the "primary" endogenous ligand but also all other endogenous ligands as they could bind differently and continue to activate the receptor.

HERG K⁺ CHANNEL AS AN OFF-TARGET OF CCR2 ANTAGONISTS

Next to the challenge of developing efficacious drugs, they must be also safe. One of the major safety concerns for the pharmaceutical industry has become the human ether-à-go-go-related gene (hERG) potassium (K⁺) channel. Blockade of the hERG K⁺ channel can affect heart

rhythm by prolonging the QT interval, thereby increasing the risk of ventricular arrhythmias and fibrillation, potentially leading to torsades de pointes and sudden death.²¹ Due to their binding to this off-target, many drugs have been withdrawn from the market or labeled with a 'black box' warning. Nowadays, screening for hERG K⁺ channel interaction is an FDA prerequisite and a routine procedure in the drug discovery and development cycle. One of the reasons why so many drugs bind to this channel is the broad tolerance of the hERG binding pocket. In general, if a molecule contains a charged or basic nitrogen that can be protonated at physiological pH, linked to an aromatic group on one side of the molecule, and to a lipophilic group on the other, it is a potential binder to the hERG channel. Such description fits a considerable variety of molecules including the orthosteric CCR2 antagonists (Figure 1). However, medicinal chemists have developed different ways to synthesize out hERG affinity from lead compounds. One of the well-known methods is the introduction of an acidic group in the molecule. This approach was used in the development of MK-0483, where the introduction of a carboxylic acid moiety resulted in a 600-fold decrease in affinity for the hERG channel compared to its parent compound.¹⁰ Another approach is to alter the pharmacophore by decreasing the pK_a of the basic nitrogen²² or by exchanging an aromatic group to an aliphatic one.²³ However, such interventions often result in an affinity decrease for the primary target too, thus requiring additional lead optimization if possible. Redfern et al. have proposed a 30-fold margin be a minimum between free plasma concentration of the drug and its IC₅₀ value for the hERG channel.²⁴ However, pharmaceutical companies should consider increasing this safety margin especially for drugs intended for non-debilitating diseases. Next to the affinity also binding kinetics to and binding configuration (i.e. binding to either the open or closed state of the channel) of the hERG channel should be taken into account. Recently, Veroli et al.²⁵ described that hERG inhibitors with similar affinities but different binding kinetics do not hold the same pro-arrhythmic risk. However, binding configuration (especially the closed state of the channel) had a much bigger influence on QT interval prolongation than binding kinetics, suggesting the need for additional screening for hERG binding configurations rather than potency alone.

FINAL NOTE

Drug discovery has come a long way in its evolution. Mankind journeyed from the prehistoric times when healers found and used medicinal herbs by trial and error of consumption of the local flora, throughout the birth of scientific understanding of chemistry and pharmacology in the 19th century, to current more rational design approaches in drug discovery. Throughout this journey, drug discovery and development have become more effective, safer and more complex and all these improvements have happened in evolutionary jumps. Usually these jumps accrued after discovering new methods, new relationships, or testing and proving new ideas that led to new understandings and paradigm changes. However, such breakthroughs usually came after facing a crisis and at the moment the pharmaceutical industry is thought to face a productivity crisis.²⁶ At the same time there is an increasing awareness that drug discovery cannot be successfully done anymore in ‘splendid isolation’. Public-private partnerships, such as the Innovative Medicines Initiative of the EU and the Dutch TIPharma program (that made this thesis possible) are examples how the ideas and knowledge of academia come together with the practical expertise of the industry and in synergy can provide possible solutions to overcome the aforementioned crisis. This joint collaboration and awareness provides room for a further exploration of novel concepts in drug discovery, for which time was often lacking in industry alone. This is certainly true for the subject of my thesis, i.e. another paradigm shift in drug discovery – from “SAR” to “SAR/SKR”, and I am happy that I could play a role in it.

REFERENCES

1. Cherney, R. J.; Mo, R. W.; Meyer, D. T.; Nelson, D. J.; Lo, Y. C.; Yang, G.; Scherle, P. A.; Mandlekar, S.; Wasserman, Z. R.; Jezak, H.; Solomon, K. A.; Tebben, A. J.; Carter, P. H.; Decicco, C. P. Discovery of disubstituted cyclohexanes as a new class of CC chemokine receptor 2 antagonists. *Journal of Medicinal Chemistry* **2008**, 51, 721-724.
2. Cherney, R. J.; Brogan, J. B.; Mo, R.; Lo, Y. C.; Yang, G.; Miller, P. B.; Scherle, P. A.; Molino, B. F.; Carter, P. H.; Decicco, C. P. Discovery of trisubstituted cyclohexanes as potent CC chemokine receptor 2 (CCR2) antagonists. *Bioorganic & Medicinal Chemistry Letters* **2009**, 19, 597-601.
3. Xue, C. B.; Wang, A.; Meloni, D.; Zhang, K.; Kong, L.; Feng, H.; Glenn, J.; Huang, T.; Zhang, Y.; Cao, G.; Anand, R.; Zheng, C.; Xia, M.; Han, Q.; Robinson, D. J.; Storace, L.; Shao, L.; Li, M.; Brodmerkel, C. M.; Covington, M.; Scherle, P.; Diamond, S.; Yeleswaram, S.; Vaddi, K.; Newton, R.; Hollis, G.; Friedman, S.; Metcalf, B. Discovery of INCB3344, a potent, selective and orally bioavailable antagonist of human and murine CCR2. *Bioorganic & Medicinal Chemistry Letters* **2010**, 20, 7473-8.

4. Zhang, X.; Hufnagel, H.; Markotan, T.; Lanter, J.; Cai, C.; Hou, C.; Singer, M.; Opas, E.; McKenney, S.; Crysler, C.; Johnson, D.; Sui, Z. Overcoming hERG activity in the discovery of a series of 4-azetidyl-1-aryl-cyclohexanes as CCR2 antagonists. *Bioorganic & Medicinal Chemistry Letters* **2011**, *21*, 5577-82.
5. Moree, W. J.; Kataoka, K.; Ramirez-Weinhouse, M. M.; Shiota, T.; Imai, M.; Sudo, M.; Tsutsumi, T.; Endo, N.; Muroga, Y.; Hada, T.; Tanaka, H.; Morita, T.; Greene, J.; Barnum, D.; Saunders, J.; Kato, Y.; Myers, P. L.; Tarby, C. M. Small molecule antagonists of the CCR2b receptor. Part 2: Discovery process and initial structure-activity relationships of diamine derivatives. *Bioorganic & Medicinal Chemistry Letters* **2004**, *14*, 5413-5416.
6. Carter, P. H. Progress in the discovery of CC chemokine receptor 2 antagonists, 2009 - 2012. *Expert Opin Ther Pat* **2013**, *23*, 549-68.
7. Vilums, M.; Zweemer, A. J.; Yu, Z.; de Vries, H.; Hillger, J. M.; Wapenaar, H.; Bollen, I. A.; Barmare, F.; Gross, R.; Clemens, J.; Krenitsky, P.; Brussee, J.; Stamos, D.; Saunders, J.; Heitman, L. H.; IJzerman, A. P. Structure-Kinetic Relationships-An Overlooked Parameter in Hit-to-Lead Optimization: A Case of Cyclopentylamines as Chemokine Receptor 2 Antagonists. *Journal of Medicinal Chemistry* **2013**, *56*, 7706-7714.
8. Kothandaraman, S.; Donnelly, K. L.; Butora, G.; Jiao, R.; Pasternak, A.; Morriello, G. J.; Goble, S. D.; Zhou, C.; Mills, S. G.; Maccoss, M.; Vicario, P. P.; Ayala, J. M.; Demartino, J. A.; Struthers, M.; Cascieri, M. A.; Yang, L. Design, synthesis, and structure-activity relationship of novel CCR2 antagonists. *Bioorganic & Medicinal Chemistry Letters* **2009**, *19*, 1830-4.
9. Vilums, M.; Zweemer, A. J. M.; Barmare, F.; Gracht, A. M. F.; Bleeker, D. C. T.; Yu, Z.; Vries, H.; Gross, R.; Clemens, J.; Krenitsky, P.; Brussee, J.; Stamos, D.; Saunders, J.; Heitman, L. H.; IJzerman, A. P. When Structure-Affinity Relationships Meet Structure-Kinetics Relationships: An Example of 3-((Inden-1-yl)amino)-1-isopropyl-cyclopentane-1-carboxamides as CCR2 Antagonists. *Prepared Manuscript*.
10. Pasternak, A.; Goble, S. D.; Struthers, M.; Vicario, P. P.; Ayala, J. M.; Di Salvo, J.; Kilburn, R.; Wisniewski, T.; Demartino, J. A.; Mills, G. S.; Yang, L. Discovery of a potent orally bioavailable CCR2 and CCR5 dual antagonist. *Medicinal Chemistry Letters* **2010**, *1*, 14-18.
11. Struthers, M.; Pasternak, A. CCR2 antagonists. *Current Topics in Medicinal Chemistry* **2010**, *10*, 1278-98.
12. Zhao, Q. H.; Pang, J.; McIntyre, K.; Gillooly, K.; Townsend, R.; Postelnek, J.; Grafstrom, R.; He, B.; Ford, G.; Conarello, S.; Xie, J.; Davies, P.; Barrish, J.; Trzaskos, J.; Cid, L. S.; Mckinnon, M.; Mandlekar, S.; Carter, P. A CCR2/CCR5-dual antagonist, BMS-A, offers a potential novel oral therapy for the treatment of autoimmune disease *The Journal of Immunology* **2009**, *182*, 92.6.
13. Zhao, Q. H. Dual targeting of CCR2 and CCR5: therapeutic potential for immunologic and cardiovascular diseases. *J Leukocyte Biol* **2010**, *88*, 41-55.
14. Lebre, M. C.; Vergunst, C. E.; Choi, I. Y. K.; Aarrass, S.; Oliveira, A. S. F.; Wyant, T.; Horuk, R.; Reedquist, K. A.; Tak, P. P. Why CCR2 and CCR5 Blockade Failed and Why CCR1 Blockade Might Still Be Effective in the Treatment of Rheumatoid Arthritis. *PLoS One* **2011**, *6*.
15. Vergunst, C. E.; Gerlag, D. M.; von Moltke, L.; Karol, M.; Wyant, T.; Chi, X. D.; Matzkin, E.; Leach, T.; Tak, P. P. MLN3897 Plus Methotrexate in Patients With Rheumatoid Arthritis Safety, Efficacy, Pharmacokinetics, and Pharmacodynamics of an Oral CCR1 Antagonist in a Phase IIa, Double-Blind, Placebo-Controlled, Randomized, Proof-of-Concept Study. *Arthritis Rheum-Us* **2009**, *60*, 3572-3581.
16. Peace, S.; Philp, J.; Brooks, C.; Piercy, V.; Moores, K.; Smethurst, C.; Watson, S.; Gaines, S.; Zippoli, M.; Mookherjee, C.; Ife, R. Identification of a sulfonamide series of CCR2 antagonists. *Bioorganic & Medicinal Chemistry Letters* **2010**, *20*, 3961-4.
17. Zweemer, A. J. M.; Nederpelt, I.; Vrieling, H.; Hafith, S.; Doornbos, M. L. J.; de Vries, H.; Abt, J.; Gross, R.; Stamos, D.; Saunders, J.; Smit, M. J.; IJzerman, A. P.; Heitman, L. H. Multiple Binding Sites for Small-Molecule Antagonists at the CC Chemokine Receptor 2. *Molecular Pharmacology* **2013**, *84*, 551-561.
18. Zlotnik, A.; Yoshie, O. The Chemokine Superfamily Revisited. *Immunity* **2012**, *36*, 705-716.
19. Tsou, C. L.; Peters, W.; Si, Y.; Slaymaker, S.; Aslanian, A. M.; Weisberg, S. P.; Mack, M.; Charo, I. F. Critical roles for CCR2 and MCP-3 in monocyte mobilization from bone marrow and recruitment to inflammatory sites. *Journal of Clinical Investigation* **2007**, *117*, 902-909.
20. Berchiche, Y. A.; Gravel, S.; Pelletier, M. E.; St-Onge, G.; Heveker, N. Different Effects of the Different Natural CC Chemokine Receptor 2b Ligands on beta-Arrestin Recruitment, G alpha(i) Signaling, and Receptor Internalization. *Molecular Pharmacology* **2011**, *79*, 488-498.
21. Sanguinetti, M. C.; Tristani-Firouzi, M. hERG potassium channels and cardiac arrhythmia. *Nature* **2006**, *440*, 463-9.

22. Vilums, M.; Overman, J.; Klaasse, E.; Scheel, O.; Brussee, J.; Ilzerman, A. P. Understanding of Molecular Substructures that Contribute to hERG K⁺ Channel Blockade: Synthesis and Biological Evaluation of E-4031 Analogues. *ChemMedChem* **2012**, *7*, 107-113.
23. Trujillo, J. I.; Huang, W.; Hughes, R. O.; Rogier, D. J.; Turner, S. R.; Devraj, R.; Morton, P. A.; Xue, C. B.; Chao, G.; Covington, M. B.; Newton, R. C.; Metcalf, B. Design and synthesis of novel CCR2 antagonists: investigation of non-aryl/heteroaryl binding motifs. *Bioorganic & Medicinal Chemistry Letters* **2011**, *21*, 1827-31.
24. Redfern, W. S.; Carlsson, L.; Davis, A. S.; Lynch, W. G.; MacKenzie, I.; Palethorpe, S.; Siegl, P. K. S.; Strang, I.; Sullivan, A. T.; Wallis, R.; Camm, A. J.; Hammond, T. G. Relationships between preclinical cardiac electrophysiology, clinical QT interval prolongation and torsade de pointes for a broad range of drugs: evidence for a provisional safety margin in drug development. *Cardiovascular Research* **2003**, *58*, 32-45.
25. GY, D. I. V.; Davies, M. R.; Zhang, H.; Abi-Gerges, N.; Boyett, M. R. hERG Inhibitors With Similar Potency But Different Binding Kinetics Do Not Pose the Same Proarrhythmic Risk: Implications for Drug Safety Assessment. *J Cardiovasc Electrophysiol* **2013**.
26. Pammolli, F.; Magazzini, L.; Riccaboni, M. The productivity crisis in pharmaceutical R&D. *Nature Reviews Drug Discovery* **2011**, *10*, 428-438.

SUMMARY

This thesis starts with a brief description of the evolution of drug discovery from the “trial and error experiments” to the complex “rational drug design” transforming development of new drugs into the multi-disciplinary field as we know it today (**chapter 1**). However, despite all the developments and gained knowledge, it is still very difficult to develop effective and safe drugs. Recently, a paradigm shift has been proposed that instead of structure–affinity relationship (SAR) based drug discovery one should use both SAR and structure–kinetic relationships (SKR). This could result in the next evolutionary jump of drug discovery and development. To test this rationale a G protein-coupled receptor (GPCR) family member – chemotactic chemokine receptor 2 (CCR2) was chosen as the target of interest. At the time of beginning of this thesis the literature already described a “graveyard” of failed CCR2 ligands whose development was based on SAR only. However, several chemical structures showed potential to improve their binding kinetics especially when an indane moiety was incorporated (described in this thesis).

The indane (2,3-dihydro-1*H*-indene) ring system *per se* is an appealing scaffold for biologically active compounds and is reviewed in **chapter 2**. It provides a wide range of possibilities to incorporate specific substituents in different directionalities, thus being an attractive template structure for medicinal chemists. Notably, many indane-based compounds are being used in the clinic to treat various diseases, such as indinavir, an HIV-1 protease inhibitor, indantadol, a potent MAO-inhibitor, the amine uptake inhibitor indatraline, and the ultra-long-acting β -adrenoceptor agonist indacaterol. Given the diversity of targets these drugs act on, one could argue that the indane ring system is a privileged substructure, just like indole, the nitrogen atom containing unsaturated version of it.

Chapter 3 describes the development of a competition association assay for CCR2 and the primary investigation on the relation of the structure of the ligand and its receptor residence time [i.e. SKR] next to a traditional SAR. This approach resulted in the discovery of a new 5-

bromo-indane derivative with high affinity (3.6 nM) as CCR2 antagonist with a residence time of 135 min.

Chapter 4 contains the report on our findings on both SAR and SKR studies for a series of 3-((inden-1-yl)amino)-1-isopropyl-cyclopentane-1-carboxamides as CCR2 antagonists. SAR studies showed that this class of compounds tolerates a vast diversity of substituents on the indenyl ring with only small changes in affinity. However, the SKR is affected greatly by minor modifications of the structure. The combination of SAR and SKR in the hit-to-lead process resulted in the discovery of a new high-affinity and long-residence-time CCR2 antagonist (K_i = 2.4 nM; RT = 714 min).

In **chapter 5** we report new findings on the SAR and SKR of the reference compound MK-0483, its diastereomers, and structural analogues of it as CCR2 antagonists. On the “right-hand” side of the molecules the 7-(trifluoromethyl)-1,2,3,4-tetrahydroisoquinoline group generally yields better affinity and longer drug-target residence time (RT). On the “left-hand” side SAR of the phenyl ring suggests that lipophilic hydrogen bond accepting substituents on the 3-position are favourable. However, SKR suggests that a lipophilic group with a certain size is desired (e.g. 3-Br, 3-*i*Pr). Alternatively a shielded hydrogen bond can also prolong the residence time; this was most prominently observed in MK-0483 itself (K_i = 1.2 nM, RT = 724 min).

Next to the SKR studies outlined above, we also developed a novel *N*-(2-oxo-2-(piperidin-4-ylamino)ethyl)-3-(trifluoromethyl)benzamide series of human CCR2 chemokine receptor antagonists described in **chapter 6**. With a pharmacophore model based on known CCR2 antagonists a new core scaffold was designed, analogues of it synthesized and SAR studies derived yielding a new high affinity CCR2 antagonist *N*-(2-((1-(4-(3-methoxyphenyl)cyclohexyl)piperidin-4-yl)amino)-2-oxoethyl)-3-(trifluoromethyl)benzamide.

Finally, general conclusions about the research described in this thesis are outlined. This is also supplemented with future perspectives of CCR2 antagonists based upon the knowledge and results obtained from this work (**chapter 7**).

SAMENVATTING

Dit proefschrift begint met een korte beschrijving van de evolutie van de drug discovery van "trial and error experimenten" naar het complexe "rational drug design" en de transformatie van de ontwikkeling van nieuwe geneesmiddelen in het multi-disciplinaire gebied zoals we dat nu kennen (**hoofdstuk 1**). Ondanks alle ontwikkelingen en opgedane kennis, is het nog steeds erg moeilijk om effectieve en veilige geneesmiddelen te ontwikkelen. Onlangs is een paradigmaverschuiving voorgesteld waarbij men in plaats van structuur–affiniteit relatie (SAR) gebaseerd geneesmiddelenonderzoek, zowel de SAR als de structuur–kinetiek relatie (SKR) zou moeten gebruiken. Dit kan resulteren in de volgende evolutionaire sprong van drug discovery en ontwikkeling. Om dit rationaal te testen werd een G eiwit gekoppelde receptor (GPCR) familielid - chemokine receptor 2 (CCR2) - gekozen als doelwit. Ten tijde van de start van dit project omschreef de literatuur een "begraafplaats" van mislukte CCR2 liganden die ontwikkeld waren enkel gebaseerd op de SAR. Echter, verschillende chemische structuren toonden potentieel om hun bindingskinetiek te verbeteren, vooral wanneer een indaan groep werd opgenomen in de structuur (beschreven in dit proefschrift).

Een indaan (2,3-dihydro-1H-indene) ringsysteem is een aantrekkelijke steiger voor biologisch actieve verbindingen en wordt nader beschreven in **hoofdstuk 2**. Het biedt een breed scala aan mogelijkheden om specifieke substituenten in verschillende richtingen op te nemen, en daarom is het een aantrekkelijk sjabloonstructuur voor chemici. Op indaan gebaseerde verbindingen worden met name veel gebruikt in de kliniek om verschillende ziekten te behandelen, zoals indinavir, een HIV-1 protease remmer, indantadol, een sterke MAO - remmer, de amine opname remmer indatraline, en de ultra - langwerkende β -adrenoceptor agonist indacaterol. Gezien de diversiteit van de receptoren waar deze medicijnen via werken, zou men kunnen stellen dat het indaan ringsysteem een bevoorrechte substructuur is, net als indole, de stikstofatoom bevattende onverzadigde versie van indaan.

Hoofdstuk 3 beschrijft de ontwikkeling van een competitie associatie assay voor CCR2, en het onderzoek naar de verhouding van de structuur van het ligand en zijn receptor verblijftijd [SKR] naast detraditionele SAR. Deze benadering resulteerde in de ontdekking van een nieuw 5-bromo-indaan derivaat als CCR2 antagonist, met hoge affiniteit (3.6 nM) en een verblijftijd van 135 minuten.

Hoofdstuk 4 rapporteert onze bevindingen in zowel SAR en SKR studies voor een serie van 3-((inden-1-yl)amino)-1-isopropyl-cyclopentane-1-carboxamides als CCR2 antagonisten. SAR studies toonden aan dat deze klasse van verbindingen een grote verscheidenheid aan substituenten op de indenylring tolereert met slechts kleine veranderingen in affiniteit. Anderzijds wordt de SKR sterk beïnvloed door kleine wijzigingen in de structuur. De combinatie van SAR en SKR in het hit-to-lead proces heeft geleid tot de ontdekking van een nieuwe CCR2 antagonist met hoge-affiniteit en een lange verblijftijd ($K_i = 2.4$ nM, RT = 714 min).

In **hoofdstuk 5** beschrijven we nieuwe bevindingen over de SAR en SKR van de referentie-verbinding MK-0483, zijn diastereomeren, en zijn structurele analogen als CCR2 antagonisten. Op de "rechter" kant van de moleculen geeft de 7-(trifluormethyl)-1,2,3,4-tetrahydroisochinoline groep over het algemeen een betere affiniteit en langere verblijftijd (RT). Op de "linker" zijde geeft de SAR van de phenylring aan dat lipofiele waterstof brug accepterende substituenten op de 3-positie gunstig zijn. Echter, de SKR suggereert dat een lipofiele groep met een bepaalde grootte is gewenst (bijvoorbeeld 3-Br, 3-*i*Pr). Als alternatief kan een afgeschermd waterstofbrug ook de verblijftijd verlengen. Dit was het meest prominent waargenomen in MK-0483 zelf ($K_i = 1.2$ nM, RT = 724 min).

Naast de SKR studies beschreven hierboven ontwikkelden we een nieuwe N-(2-oxo-2-(piperidin-4-ylamino)ethyl)-3-(trifluormethyl)benzamide serie van CCR2 chemokine-receptor antagonisten, beschreven in **hoofdstuk 6**. Een nieuwe kernstructuur werd ontworpen met behulp van een farmacofoommodel op basis van een bekende CCR2 antagonist. Vervolgens werden analogen gesynthetiseerd en SAR studies uitgevoerd waardoor een nieuwe hoge

affiniteit CCR2 antagonist, N-(2-((1-(4-(3-methoxyphenyl)cyclohexyl)piperidin-4-yl)amino)-2-oxoethyl)-3-(trifluoromethyl)benzamide, werd gevonden.

Tot slot worden de algemene conclusies over het onderzoek in dit proefschrift beschreven in **hoofdstuk 7**. Dit wordt aangevuld met toekomstperspectieven van CCR2 antagonisten gebaseerd op de kennis en de resultaten die zijn verkregen uit dit werk.

LIST OF PUBLICATIONS

M. Vilums, A.J.M. Zweemer, S. Dekkers, Y. Askar, H. de Vries, J. Saunders, D. Stamos, J. Brussee, L.H. Heitman, A.P. IJzerman. Design and Synthesis of Novel Small Molecule CCR2 Antagonists: Evaluation of 4-Aminopiperidine Derivatives. In preparation.

M. Vilums, A.J.M. Zweemer, A. Dilanchian, J.P.D. van Veldhoven, H. de Vries, J. Brussee, D. Stamos, J. Saunders, L.H. Heitman, A.P. IJzerman. Evaluation of (4-Arylpiperidin-1-yl)cyclopentanecarboxamides as High Affinity and Long Residence Time Antagonists for the CCR2 Receptor. In preparation.

M. Vilums, A.J.M. Zweemer, F. Barmare, A.M.F. van der Gracht, D.C.T. Bleeker, Z. Yu, H. de Vries, R. Gross, J. Clemens, P. Krenitsky, J. Brussee, D. Stamos, J. Saunders, L.H. Heitman, A. P. IJzerman. When Structure-Affinity Relationships Meet Structure-Kinetics Relationships: 3-((Inden-1-yl)amino)-1-isopropyl-cyclopentane-1-carboxamides as CCR2 Antagonists. In preparation.

M. Vilums, J. Heuberger, L.H. Heitman, A.P. IJzerman. Indanes – Properties, Preparation, and Presence in Ligands for G Protein-Coupled Receptors. *Med Res Rev*. Submitted.

A.J. Zweemer, J. Bunnik, M. Veenhuizen, F. Miraglia, E.B. Lenselink, **M. Vilums**, H. de Vries, A. Gibert, S. Thiele, M.M. Rosenkilde, A.P. IJzerman, L.H. Heitman. Discovery and Mapping of an Intracellular Antagonist Binding Site at the Chemokine Receptor CCR2. *Mol Pharmacol*. 2014 Oct;86(4):358-68

M. Vilums, A. J. M. Zweemer, Z. Yu, H. de Vries, J. M. Hillger, H. Wapenaar, I. A. E. Bollen, F. Barmare, R. Gross, J. Clemens, P. Krenitsky, J. Brussee, D. Stamos, J. Saunders, L. H. Heitman, A. P. IJzerman. Structure–Kinetic Relationships –An Overlooked Parameter in Hit-to-Lead Optimization: A Case of Cyclopentylamines as Chemokine Receptor 2 Antagonists. *J. Med. Chem*. 2013, 56, 7706–7714

M. Vilums, J. Overman, E. Klaasse, O. Scheel, J. Brussee, A. P. IJzerman. Understanding of Molecular Substructures that Contribute to hERG K⁺ Channel Blockade: Synthesis and Biological Evaluation of E-4031 Analogues. *ChemMedChem* 2012, 7, 107 – 113

M.van der Steen, **M. Vilums**, C. V. Stevens. Synthesis of novel urethanes from a castor oil derived C22-acyloin. *Arkivoc* 2011, (ix), 261-271.

A. Krauze, E. Liepins, **M. Vilums**, G. Duburs. A new regioselective synthesis of 2-methoxymethyl-3-oxo-2,3-di-hydro-7H-thiazolo[3,2-a]pyridine-8-carboxylic acid methylamide. *Chem. of Heterocyc. Comp.*, 2009, Nr 2, 250-252.

H. Kazoka, A. Krauze, **M. Vilums**, L. Chernova, L. Sile and G. Duburs. Synthesis of 6'-carbamoylmethylthio-5'-cyano-1',4'-dihydro-3,4'-bipyridine-3'-carboxylic and 6'-carbamoylmethylthio-5'-cyano-1',4'-dihydro-4,4'-bipyridine-3'-carboxylic esters and investigation of their stability. 2. Esters of 6'-carbamoylmethyl-thio-5'-cyano-1',4'-dihydro-4,4'-bipyridine-3-carboxylic acids. *Chem. of Heterocyc. Comp.*, 2007, Nr 6, 708-714.

A. Krauze, **M. Vilums**, L. Sile, G. Duburs. Alternative products in one-pot reaction of benzylidenemalononitrile, N-methyl-2-thiocarbamoylacetamide, and ω-bromoacetophenone. *Chem. of Heterocyc. Comp.*, 2007, Nr 5, 653-657.

H. Kazoka, A. Krauze, **M. Vilums**, L. Chernova, L. Sile and G. Duburs. Synthesis and investigation of the stability of esters of 6'-carbamoylmethylthio-5'-cyano-1',4'-dihydro-3,4'-and-4,4'-bipyridine-3'-carboxylic acids 1. Esters of 6'-carbamoylmethylthio-5'-cyano-1',4'-dihydro-3,4'-bipyridine-3'-carboxylic acids. *Chem. of Heterocyc. Comp.*, 2007, 43, 1, 50-57.

A. Krauze, R. Danne, **M. Vilums**, Z. Kalme, L. Chernova, L. Sile, G. Duburs. Synthesis of new partially hydrogenated 6-alkylthio-2,4-diaryl-3-ethoxycarbonylpyridine-5-carbonitriles. (in Latvian) *Latv. Kim.Z.*, 2007, 2, 3.

A. Krauze, L. Chernova, **M. Vilums**, L. Sile, G. Duburs. Green one-pot multicomponent synthesis of 4-aryl-6-carbamoylmethylthio-5-cyano-2-methyl-1,4-dihydropyridine-3- carboxylic acid methyl esters. *Heterocycl. Commun.*, 2006, 12, 3/4, 281-286.

A. Krauze, L. Baumanė, L. Sīle, L. Chernova, **M. Vilums**, R. Vitolina, G. Duburs, J. Stradins. Synthesis, cardiovascular activity, and electrochemical oxidation of nitriles of 5-ethoxycarbonyl-2-methyl-thio-1,4-dihydropyridine-3-carboxylic acid. *Chem. of Heterocyc. Comp.*, 2004, Vol. 40, No. 7, pp.876-887

AFTERWORD

Always keep your mind open and continue learning...

From my supervisors – Hans, John, Dean, Laura and Ad

“Efficiency is doing things right. Effectiveness is doing the right things”

From my colleagues:

Leiden University – Annelien, Arnault, Bart, Clara, Dennis, Dong, Elaine, Ellen, Elisabeth, Gerard, Henk, Indira, Jaco, Joao, Joey, Julien, Lence, Miriam, Maarten, Patricia, Rob, Rongfang and Thea

Vertex Pharmaceuticals Inc. – Farhana, Paul, Raymond, Jeremy, Mike and Silvia

“Growth is never by mere chance; it is the result of forces working together”

James Cash Penney

From my students – Jeroen, Julia, Hannah, Guido, Joleen, Arthur, Jules, Sebastian, Arien, Yousry, and all the minors

“Supervision is an opportunity to bring someone back to their own mind, to show them how good they can be”

Nancy Kline, ‘Time to Think’

From my very first real chemistry teacher – Erika

“Just come and have a try...”